

HIGH-TURNOVER C-H BORYLATION OF ARENES WITH (POCOP) IRIDIUM
COMPLEXES, THE SYNTHESIS OF GROUP 9/10 (POCS) COMPLEXES AND THE
STUDY OF TRIFLYLOXY-SUBSTITUTED CARBORANES

A Dissertation

by

LOREN PAUL PRESS

Submitted to the Office of Graduate and Professional Studies of
Texas A&M University
in partial fulfillment of the requirements for the degree of

DOCTOR OF PHILOSOPHY

Chair of Committee,	Oleg V. Ozerov
Committee Members,	Donald J. Darensbourg
	Michael B. Hall
	Jodie L. Lutkenhaus
Head of Department,	Simon W. North

August 2016

Major Subject: Chemistry

Copyright 2016 Loren P. Press

ABSTRACT

Over the last century, transition metal-catalyzed C-H functionalization has emerged as one of the most important topics in synthetic chemistry. One type of C-H functionalization, known as C-H borylation, generates organoboron reagents directly from hydrocarbon substrates. The synthetic utility of organoboron compounds is well established and numerous systems have been developed for the catalytic C-H borylation of alkyl and aromatic substrates since the reaction was first conceived over 20 years ago, yet catalysts that support high TONs remain limited to a handful of examples. Here we present highly active POCOP iridium complexes for the catalytic C-H borylation of arenes. In favorable cases, TONs exceeding 10,000 have been observed. The synthesis and isolation of multiple complexes potentially relevant to catalysis permitted examination of several key elementary reactions. We found C-H activation at Ir(I) here is in contrast to the olefin-free catalysis with state-of-the-art Ir complexes supported by neutral bidentate ligands, where the C-H activating step is understood to involve trivalent Ir-boryl intermediates.

Next, we investigated the stoichiometric reactivity of a (POCOP)Ir(boryl)₂ complex with various small molecules under thermolytic conditions. Transition metal-boryl complexes are ubiquitous in the literature and have been identified as key intermediates in several critical chemical transformations including C-H borylation and hydroborylation chemistries. The (POCOP)Ir(boryl)₂ complex was found to undergo

several stoichiometric transformations including reduction of CO₂ to CO, 1,2-diborylation of ethylene and the selective protonation of one boryl ligand.

The synthesis and characterization of novel POCS pincer complexes of nickel, palladium and iridium are described. The modular design of the POCS pincer ligand allowed the exploration of monomeric and bridging ligand designs akin to PNN and PCN complexes.

The selective B-H functionalization of the mono-anionic carborane [HCB₁₁H₁₁]⁻ with one or three triflyloxy (OTf) groups is described. The mono-triflyloxy substituted carborane can be halogenated to give pentabromo and decachloro derivatives with preservation of the B-OTf linkage. The use of [HCB₁₁Cl₁₀OTf]⁻ as a weakly coordinating anion is demonstrated.

DEDICATION

To my Mom, Dad and Grammy Rose.

ACKNOWLEDGEMENTS

I would like to thank my committee chair and research advisor Prof. Oleg Ozerov for his guidance and patience during my time at Texas A&M University. He has taught me an approach to synthetic chemistry that is world-class. I would also like to thank my committee members, Prof. Michael Hall, Prof. Don Darensbourg and Prof. Jodie Lutkenhaus.

I want to give a special thanks to Dr. Rita Silbernagel for her friendship and support. I want to thank Billy McCulloch for his companionship and for helping me think outside of the box. I would also like to acknowledge: Dr. Jessica DeMott, Dr. Morgan MacInnis, Dr. Rodrigo Ramirez, Dr. Dan Smith and Chris Pell. Thank you for the good times. To all of the members of the Ozerov group that I had the privilege to work with, it has been a pleasure. I want to recognize Dr. Weixing Gu and Dr. David Herbert, among others, for helping me throughout my formative years as a synthetic chemist.

I also want to extend my gratitude to Dr. Yohannes Rezenom at the Laboratory for Biological Mass Spectrometry as well as the Texas A&M Chemistry Department NMR staff and instrumentation.

I would like to thank the lovely Miss Martha Todd for all that she has done for me. Above all, I want to thank to my Mom, Dad and family for their encouragement and support through thick and thin.

NOMENCLATURE

FG	functional group
DG	directing group
EAS	electrophilic aromatic substitution
py	pyridine
bpy	2,2'-bipyridine
dtbpy	4,4'-di- <i>tert</i> -butyl-2,2'-dipyridyl
DMAP	4-dimethylaminopyridine
TMS	trimethylsilyl
OEt ₂	diethyl ether
ⁱ Pr	isopropyl
^t Bu	<i>tert</i> -butyl
Et	ethyl
Me	methyl
Cp*	pentamethylcyclopentadienyl
Ind	indenyl
COD	cyclooctadiene
COE	cyclooctene
COA	cyclooctane
TBE	3,3-dimethyl-1-butene
TBA	2,2-dimethylbutane

Ar	aryl
Ph	phenyl
OAc	acetate
THF	tetrahydrofuran
L	ligand
Bpin	4,4,5,5-tetramethyl-1,3,2-dioxaboranyl ligand
HBpin	4,4,5,5-tetramethyl-1,3,2-dioxaborolane
B ₂ pin ₂	4,4,4',4',5,5,5',5'-octamethyl-2,2'-bi-1,3,2-dioxaborolane
HOTf	trifluoromethanesulfonic acid
OTf	trifluoromethanesulfonate
TON	turnover number
TOF	turnover frequency
DHBTA	dehydrogenative borylation of terminal alkynes
HDF	hydrodefluorination
rt	room temperature
dmpe	1,2-bis(dimethylphosphino)ethane
dppe	1,2-bis(diphenylphosphino)ethane
NMR	nuclear magnetic resonance

TABLE OF CONTENTS

	Page
ABSTRACT	ii
DEDICATION	iv
ACKNOWLEDGEMENTS	v
NOMENCLATURE	vi
TABLE OF CONTENTS	viii
LIST OF SCHEMES	xi
LIST OF FIGURES	xv
LIST OF TABLES	xix
CHAPTER I INTRODUCTION AND LITERATURE REVIEW	1
1.1 Introduction	1
1.2 Types of C-H bond functionalization	3
1.3 Early examples of C-H activation and functionalization	7
1.4 Directed C-H functionalizations	9
1.5 Transition metal catalyzed arene C-H bond borylation	12
1.5.1 Introduction to transition metal catalyzed arene C-H bond borylation	12
1.5.2 Mechanism of $L_2Ir(Bpin)_3$ catalyzed C-H borylation	14
1.5.3 Selectivity in Ir catalyzed arene C-H borylation	16
1.6 Homogeneous transition metal-catalyzed alkane dehydrogenation	20
1.6.1 Alkane dehydrogenation background	20
1.6.2 Ir pincer complexes for alkane dehydrogenation	21
1.6.3 Recent advances in alkane dehydrogenation catalyzed by Ir pincer complexes	24
1.6.4 Synthesis of alkanes and aromatics using Ir pincer catalysts	29
1.7 Introduction to carboranes	31
1.7.1 Carborane functionalization	34
CHAPTER II HIGH-TURNOVER AROMATIC C-H BORYLATION CATALYZED BY POCOP-TYPE PINCER COMPLEXES OF IRIDIUM	36

2.1 Introduction	36
2.2 Results and discussion.....	39
2.2.1 Synthesis of (POCOP)Ir(H)(Cl) and (POCOP)Ir(olefin) precatalysts	39
2.2.2 Catalytic arene borylation studies with (POCOP)Ir pre-catalysts.....	42
2.2.3 Preparative scale catalytic arene borylation using (POCOP)Ir precatalysts ...	45
2.2.4 Comparison with the ITHM arene borylation system	48
2.2.5 Synthesis of relevant (POCOP)Ir compounds.....	49
2.2.6 XRD and NMR characterization of Ir hydrido-boryl complexes.....	55
2.2.7 C-H borylation mechanistic analysis.....	59
2.3 Conclusion.....	66
2.4 Experimental	68
2.4.1 General considerations	68
2.4.2 Synthesis of compounds.....	69
CHAPTER III SMALL MOLECULE ACTIVATION WITH POCOP IRIDIUM COMPLEXES	122
3.1 Introduction	122
3.2 Results and discussion.....	123
3.2.1 Reaction of (^{p-Me} POCOP ^{iPr})Ir(Bpin) ₂ with CO ₂ and CO	124
3.2.2 Reaction of (^{p-Me} POCOP ^{iPr})Ir(Bpin) ₂ with olefins.....	125
3.2.3 Reaction of (^{p-Me} POCOP ^{iPr})Ir(Bpin) ₂ with an aliphatic alcohol	126
3.2.4 Reaction of (^{p-Me} POCOP ^{iPr})Ir(Bpin) ₂ with an aryl ester	127
3.2.5 Attempt to reaction of (^{p-Me} POCOP ^{iPr})Ir(Bpin) ₂ with a pyridine derivative .	130
3.2.6 Hydrogenolysis of B ₂ pin ₂ with a (^{p-Me} POCOP ^{iPr})Ir(H)(Cl) precatalyst.....	131
3.3 Conclusion.....	132
3.4 Experimental	134
3.4.1 General considerations	134
3.4.2 Synthesis of compounds.....	135
CHAPTER IV NICKEL, PALLADIUM AND IRIDIUM COMPLEXES OF BRIDGING AND MONOMERIC POCS LIGANDS	141
4.1 Introduction	141
4.2 Results and discussion.....	145
4.2.1 Synthesis of POCS ligands.....	145
4.2.2 Synthesis of POCS complexes of nickel and palladium	149
4.2.3 Synthesis of POCS complexes of iridium	151
4.3 Conclusion.....	156
4.4 Experimental	157
4.4.1 General considerations	157
4.4.2 Synthesis of POCS ligands.....	158
4.4.3 X-ray crystallography details of 421 and 424	167

CHAPTER V TRIFLYLOXY-SUBSTITUTED CARBORANES AS USEFUL WEAKLY COORDINATING ANIONS	169
5.1 Introduction	169
5.2 Results and discussion.....	170
5.3 Conclusion.....	184
5.4 Experimental	184
5.4.1 General considerations	184
5.4.2 Synthesis of carborane and palladium compounds	186
5.4.3 Catalytic hydrodefluorination studies	203
5.4.4 X-ray crystallography.....	205
CHAPTER VI CONCLUSION.....	215
REFERENCES	219

LIST OF SCHEMES

	Page
Scheme I-1. C-H bond functionalization (top) and activation pathways (bottom).	2
Scheme I-2. Pyrolysis of ethane, thermal chlorination of methane and Friedel-Crafts alkylation of benzene.	3
Scheme I-3. Hartwig et al. classify transition metal catalyzed C-H functionalization into two categories, directed versus undirected.	4
Scheme I-4. Yu et al. categorize transition metal catalyzed C-H functionalization as first and further functionalization (top).	5
Scheme I-5. Baran et al. categorize C-H functionalization as either guided or innate functionalization.	5
Scheme I-6. Classic examples of intramolecular <i>ortho</i> - C-H activation also known as cyclometalation by Milner et al. and Keim.	7
Scheme I-7. C-H activation of cyclohexane and methane investigated by Bergman et al.	8
Scheme I-8. Catalytic <i>ortho</i> -alkylation of aromatic ketones by Murai and co-workers	9
Scheme I-9. Oxidative acetyoxylation of phenylpyridines by Sanford et al. with proposed catalytic pathway.	11
Scheme I-10. Catalytic formation of organoboronate esters via C-H functionalizations. The net reactions of catalytic borylation of arenes with HBpin or B ₂ pin ₂	12
Scheme I-11. Synthetic methods for the formation of organoboronate esters.	13
Scheme I-12. Formation of organoboronate esters via Ir catalyzed C-H functionalizations. Work of Smith et al. (top) and Hartwig et al. (bottom).	14
Scheme I-13. Catalytic cycle commonly invoked in Ir-catalyzed aromatic borylation and recent analogs (112, 113, 114) to the triboryl intermediate 111.	15
Scheme I-14. <i>meta</i> -selective borylation via ligand secondary interactions devised by Kanai and co-workers.	17
Scheme I-15. <i>para</i> - selective C-H borylation employed by Itami et al.	18

Scheme I-16. Borylation of methane independently reported by Sanford and Mindiola ..	19
Scheme I-17. Transfer and acceptorless dehydrogenation of alkanes using precatalysts 116-H ₂ and 117-H ₂	21
Scheme I-18. Transfer dehydrogenation of COA using precatalyst 118-HCl. Proposed catalytic pathway for the dehydrogenation of COA by 118.	23
Scheme I-19. Transfer dehydrogenation of alkanes and ethers using triptycene backbone Ir pincer complexes.	26
Scheme I-20. Selective catalytic transfer dehydrogenations of heterocycles using (POCSP ^{iPr})Ir by Huang et al.	27
Scheme I-21. Catalytic silylation of alkanes via alkane dehydrogenation and isomerization-hydrosilylation by Huang et al.....	28
Scheme I-22. Alkane metathesis using a tandem alkane dehydrogenation olefin metathesis catalysis by Brookhart, Goldman et al.....	30
Scheme I-23. Catalytic dehydroaromatization of linear alkanes by Ir pincer complexes investigated by Brookhart, Goldman and co-workers. The synthesis of o-xylene and ethylbenzene using propylene is showcased.....	31
Scheme I-24. Catalytic hydrodefluorination of organofluorine compounds with trialkylsilanes using [Ph ₃ C][HCB ₁₁ Cl ₁₁] (top). Silane-fueled proton-catalyzed Friedel-Crafts coupling of fluoroarenes (bottom).	34
Scheme II-1. DHTBA reaction catalyzed by complexes 207, 208 and 209.....	38
Scheme II-2. Synthesis of (POCOP)Ir complexes.	41
Scheme II-3. Synthesis of various (POCOP)Ir compounds.	53
Scheme II-4. Equilibrium between 215-H ₂ and 215-(H) ₂ (solvent)	55
Scheme II-5. Reaction examining possible pathways for ArBpin formation.....	63
Scheme II-6. The net catalytic reaction (top), the proposed catalytic cycle invoking the three-coordinate Ir (I) species 215, and the auxiliary hydride/boryl redistribution equilibria. The <i>t</i> -butyl groups of the ligand backbone have been altered to R _n for clarity.....	64
Scheme III-1. Deoxygenation of CO ₂ to CO with 214-(Bpin) ₂	125
Scheme III-2. 1,2-diboration of ethylene by 214-(Bpin) ₂	126

Scheme III-3. Selective proton transfer to one boryl ligand of 214-(Bpin) ₂ using an aliphatic alcohol.....	127
Scheme III-4. Attempted deoxygenation of methyl benzoate and subsequent cyclometalation by 214.....	128
Scheme III-5. <i>ortho</i> -C-H activation of nitrobenzene and acetophenone by a (PCP)Ir complex studied by Goldman et al.	130
Scheme III-6. Attempted borylation of DMAP resulting in C ₆ D ₅ Bpin and 214-(DMAP).....	131
Scheme III-7. Hydrogenolysis of B ₂ pin ₂ with 214-(H)(Cl) as precatalyst.....	132
Scheme IV-1. The Ozerov group's approach to homobimetallic pincer complexes.....	142
Scheme IV-2. Reduction of the imine arm of 401 by triethylsilane to give 402.....	143
Scheme IV-3. Synthesis of (PCS)Pd by van Koten et al.....	144
Scheme IV-4. Synthetic strategy devised by van Koten et al. for the synthesis of POCS ligands and Pd species.	145
Scheme IV-5. (a) Synthesis of 404 and 405. (b) Synthesis of protected compounds 406 and 407. (c) Synthesis of sodium thiolates 410 and 411. (d) Synthesis of sodium thiolate 413. Compound 407 was synthesized by Wei-Chun Shih of the Ozerov group.....	147
Scheme IV-6. (a) Synthesis of bridging ligands 414 and 415. (b) Attempted synthesis of bridging ligand 416 with observation of P-S bond formation by Wei-Chun Shih. (c) Synthesis of silyl ethers 418 and 419. (d) Synthesis of monomeric ligand 420.....	148
Scheme IV-7. (a) Synthesis of C ₃ linked pincer complexes 421 and 422. (b) Substitution of the chloride ligands of 421 with using AgOTf to give complex 423.....	149
Scheme IV-8. (a) Failed attempt at direct synthesis of 424 by reacting ligand 420 with common Ir starting materials. (b) Synthesis of pyridine adducts 425. (c) Synthesis of 426 and subsequent conversion to 424 with Me ₃ SiCl.	152
Scheme IV-9. Synthesis of bridging (POCS)Ir compounds.....	156
Scheme V-1. Synthesis of Cs[503], Cs[504], Cs[505], Cs[510], Cs[507], Cs[507B] Ph ₃ C[510] and R ₃ Si[510].....	171

Scheme V-2. Side product Cs[506] observed by ^{19}F NMR spectroscopy and MALDI (-) MS during mono-triflyloxylation of Cs[501] in neat HOTf at 65 °C. The compound was not isolated.	172
Scheme V-3. Synthesis of palladium compounds.	181

LIST OF FIGURES

	Page
Figure I-1. Examples of Ir pincer complexes used in catalytic and stoichiometric alkane dehydrogenation studies.	25
Figure I-2. Labelling system for the carba- <i>closo</i> -dodecaborate (–) anion (501) and its chlorinated derivative 502. Dots represent boron atoms.	32
Figure I-3. Examples of reactive cations with carborane anions.	33
Figure II-1. Examples of Ir pincer complexes used in C-H borylation studies.	37
Figure II-2. POCOP (pro)ligands used in this study.	39
Figure II-3. ORTEP ¹⁵⁵ drawings (50% probability ellipsoids) of 215-(H)(Cl). Omitted for clarity: H atoms and methyl groups of isopropyl arms. Selected distance (Å) and angles (°) follow: Ir1-Ir2, 4.040(1); Ir1-Cl1, 2.5169(9); Ir1-Cl2, 2.594(1); Ir1-C1, 2.042(2); P1-Ir1-P2, 158.09(3); C1-Ir1-Cl1, 173.6(1).	42
Figure II-4. ORTEP ¹⁵⁵ drawings (50% probability ellipsoids) of 215-(HBpin) (left) and 214-(Bpin) ₂ (right). Omitted for clarity: H atoms, methyl groups of isopropyl arms. Selected distance (Å) and angles (°) follow: For 215-(HBpin): Ir1-B1, 2.069(4); Ir1-H1, 1.56(3); B1-H1, 1.42(3); P1-Ir1-P2, 159.39(3); B1-Ir1-H1, 43.0(1); C1-Ir1-B1, 149.0(1); C1-Ir1-H1, 168.0(2). For 214-(Bpin) ₂ , the asymmetric unit contains two independent molecules, only values for one fragment are represented here: Ir1-B1, 2.065(4); Ir1-B2, 2.065(4); B1-B2, 2,251(8); P1-Ir1-P2, 156.92(5); C1-Ir1-B1, 146.98(11); B1-Ir1-B2, 66.0(2). All XRD structures were solved by Billy J. McCulloch.	56
Figure II-5. ¹ H NMR (500 MHz, cyclohexane- <i>d</i> ₁₂) spectrum of 215-H ₂ . Upon initial inspection, no hydride signals are observed. Further analysis of the baseline reveals a very broad signal centered at –17.35 ppm. The other hydride resonances were not identified.	57
Figure II-6. Stacked VT ¹ H NMR (500 MHz, toluene- <i>d</i> ₈) spectra of 215-H ₂ from 20 °C (bottom) to –90 °C (top).	58
Figure II-7. ORTEP drawings (50% probability ellipsoids) of 215-H ₂ . Omitted for clarity: H atoms, methyl groups of isopropyl arms. Selected distance (Å) and angles (°) follow: For 215-H ₂ : Ir1-Ir2, 2.6796(7); Ir1-C1, 2.057(3);	

Ir2-C2, 2.044(3); Ir1-C3, 3.939(4); Ir2-C4, 3.619(4) P1-Ir1-P2, 145.01(4); P3-Ir2-P4, 155.47(4). XRD structure solved by Billy J. McCulloch	59
Figure II-8. $^{31}\text{P}\{^1\text{H}\}$ VT NMR (C_6D_6 , 202 MHz) spectra from 20 °C to 80 °C showing the reaction of HBpin and C_6D_6 with 5 mol% 215-(TBE) (Table II-1, Entry 7). As the temperature increased, resonances for compounds 215-(TBE), 215-(Bpin) $_2$ and 215- H_4 increased in intensity.	67
Figure II-9. Stacked ^1H NMR (500 MHz, toluene- d_8) spectra of the hydride region of 215- H_3Bpin from 20 °C (top) to -80 °C (bottom).	82
Figure II-10. $^{31}\text{P}\{^1\text{H}\}$ NMR (202 MHz, toluene- d_8) spectrum of 215- H_3Bpin taken immediately after adding excess H_2 to 215-(HBpin). Sample contains 215- H_4	83
Figure II-11. $^{31}\text{P}\{^1\text{H}\}$ NMR spectrum (202 MHz, C_6D_6) showing a mixture of 215-(HBpin) and 215- H_3Bpin . Spectrum was obtained after freezing a cyclohexane solution of 215- H_3Bpin , removing all solvent in vacuo, subjecting the resultant solids to high vacuum for several hours, then redissolving the solids in C_6D_6	84
Figure II-12. A section of the ^1H NMR (500 MHz, CDCl_3) spectrum showing aromatic resonances (multiplets A, B, C and D) of L-2. The other signals were not identified.	96
Figure II-13. A section of the ^1H NMR (500 MHz, CDCl_3) spectrum showing aliphatic resonances of L-2, seen at 1.37 ppm. The other signals were not identified.	97
Figure II-14. ^{11}B NMR (128 MHz, CDCl_3) spectrum showing L-2 at 30.3 ppm. 214- H_3Bpin is observed at 37.4 ppm.	98
Figure II-15. ^{19}F NMR (470 MHz, CDCl_3) spectrum of L-2 (-103.6 ppm). The minor products were not identified.	99
Figure II-16. Entry 3 - $^{31}\text{P}\{^1\text{H}\}$ NMR (202 MHz, C_6D_6 ,) spectrum taken immediately after mixing HBpin and C_6D_6 with 5 mol% 215-(H)(Cl). Resonances for 215- H_3Bpin and 215- H_2Bpin_2 are observed.	110
Figure II-17. Entry 3 - ^{11}B NMR (128 MHz, C_6D_6 ,) spectrum after heating for 36 h at 100 °C. Resonances of 215- H_3Bpin , $\text{C}_6\text{D}_5\text{Bpin}$, HBpin, and trace HBpin decomposition are observed.	111

Figure II-18. Entry 6 - $^{31}\text{P}\{^1\text{H}\}$ NMR (202 MHz, C_6D_6) spectrum taken immediately after mixing HBpin and C_6D_6 with 5 mol% 215-(H)(Cl) and excess 1-hexene. Resonances for 215- H_3Bpin and 215- H_2Bpin_2 are observed.	112
Figure II-19. Entry 6 - ^1H NMR (400 MHz, C_6D_6). spectrum after reacting HBpin and C_6D_6 with 5 mol% 215-(H)(Cl) and excess 1-hexene at 80 °C for 0.5 h. Resonances for $\text{C}_6\text{D}_5\text{Bpin}$, hexylBpin, and excess 1-hexene are observed.....	113
Figure II-20. Entry 6 - $^{31}\text{P}\{^1\text{H}\}$ NMR (202 MHz, C_6D_6) spectrum taken after reacting HBpin and C_6D_6 with 5 mol% 215-(H)(Cl) and excess 1-hexene at 80 °C for 0.5 h. Resonances for 215-(Bpin) $_2$, 215-(hexene) and 215-(Cl)(Bpin) are observed.	114
Figure II-21. Entry 6 - ^{11}B NMR (128 MHz, C_6D_6) spectrum after reacting HBpin and C_6D_6 with 5 mol% 215-(H)(Cl) and excess 1-hexene at 80 °C for 0.5 h. Resonances for hexylBpin, $\text{C}_6\text{D}_5\text{Bpin}$, ClBpin and 215-(Cl)(Bpin) are observed, as well trace HBpin decomposition products.....	115
Figure II-22. Entry 8 - ^{11}B NMR (128 MHz, C_6D_6) spectrum after reacting HBpin and C_6D_6 with 5 mol% 215-(TBE) and excess 1-hexene at 80 °C for 0.5 h. Resonances for hexylBpin, TBABpin, and $\text{C}_6\text{D}_5\text{Bpin}$ are observed, as well trace HBpin decomposition products.....	116
Figure III-1. Bonding modes of boryl ligands Bpin and Bcat as depicted by Marder et al. ²⁰²	123
Figure IV-1. Creutz-Taube ion (left), Urease homobimetallic active site (middle), cooperating silica bound Nb catalyst (right).....	141
Figure IV-2. (a) ^1H NMR (C_6D_6) spectrum of ligand 414. (b) ^1H NMR (C_6D_6) spectrum of metal complex 421. (c) ^1H NMR (C_6D_6) spectrum of metal complex 422.....	150
Figure IV-3. POV-Ray rendition of the ORTEP drawing ¹⁵⁵ of 421. Hydrogen atoms and distortion about the C_3 bridge has been omitted for clarity. Selected bond distances (Å), angles (°), torsion (°) for 421: Ni1-Cl1, 2.20869(7); C1-N1, 1.883(2); S1-Ni1, 2.1936(7); S1-Ni1-P1, 159.49(3); C2-C7-S1-Ni1, -31.7(2); C6-O1-P1-Ni1, -5.8(1). XRD structure was solved by Billy J. McCulloch.....	151
Figure IV-4. POV-Ray rendition of the ORTEP drawing ¹⁵⁵ of 424. Hydrogen atoms have been omitted for clarity. Selected bond distances (Å), angles (°), torsion (°) for 424: Ir1-Ir2, 3.897(1); Ir1-Cl1, 2.506(1); Ir1-Cl2, 2.615(2); Ir1-C1, 2.0515(5); Ir1-S1, 2.385(2); Ir1-P1, 2.240(2); C1-Ir1-Cl1,	

171.6(2); P1-Ir1-S1, 159.99(5); C6-C7-S1-Ir-1, 29.2(5); C2-O1-P1-Ir1, 0.9(4). XRD structure was solved by Billy J. McCulloch	155
Figure V-1. POV-Ray renditions of the ORTEP drawings ¹⁵⁵ of A. Cs[507], B. Cs[505], C. Cs[511] and D. Ph ₃ C[510] (50% probability ellipsoids) showing selected atom labeling. Omitted for clarity: hydrogen and cesium atoms for all structures, a minor component of cocrystallized Cs[HCB ₁₁ H ₄ Br ₆ OTf] in structure of Cs[507], disorder of one triflyloxy moiety of Cs[511]. All XRD structures were solved by Billy J. McCulloch except C. Cs[511] solved by Bruce Foxman. Anion 511 was synthesized by Weixing Gu.....	174
Figure V-2. Attempted permethylation of Cs[505] with neat MeOTf and excess CaH ₂	175
Figure V-3. Attempted ethylation of Cs[501] in neat HOTf and 1 atm of ethylene at 25 °C for 18h.	176
Figure V-4. POV-Ray renditions of the ORTEP ¹⁵⁵ drawings of E. Et ₃ Si[510] and F. ¹ Pr ₃ Si[510] (50% probability ellipsoids) showing selected atom labeling. Omitted for clarity: hydrogen atoms, the second independent molecule in the asymmetric unit of Et ₃ Si[510], a molecule of fluorobenzene and disorder in the triflyloxy and triisopropylsilyl moieties in ¹ Pr ₃ Si[510]. Crystallographic disorder and the presence of two independent molecules in the asymmetric unit of Et ₃ Si[510] (E) gives rise to multiple metrics that are statistically indistinguishable. All XRD structures were solved by Billy J. McCulloch.....	180
Figure V-5. POV-Ray renditions of the ORTEP drawings ¹⁵⁵ of G. 515, H. 516, I. 513 and J. 517 (50% probability ellipsoids) showing selected atom labeling. Omitted for clarity: hydrogen atoms, isopropyl methyl carbons of 515, isopropyl methyl carbons, a second cation within the asymmetric unit and both anions of 513. All XRD structures were solved by Billy J. McCulloch.	183
Figure V-6. Comparison of ¹ H NMR spectra of various [trityl][WCA] in C ₆ D ₅ Br.....	195

LIST OF TABLES

	Page
Table II-1. C–H borylation experiments using (POCOP)Ir pre-catalysts ^a	44
Table II-2. Effect of varying benzene:1-hexene concentration on PhBpin:hexylBpin ratio ^a	45
Table II-3. Catalytic arene borylation using (POCOP)Ir pre-catalysts ^a	47
Table II-4. C-H borylation experiments using ITHM pre-catalysts ^a	49
Table II-5. Selected NMR data for Bpin-containing Ir pincer complexes	54
Table V-1. Catalytic HDF studies ^a	178
Table V-2. Comparison of ¹ H NMR resonances of various Ph ₃ C[WCA] salts in C ₆ D ₅ Br	195
Table V-3. Comparison of ¹³ C{ ¹ H} NMR resonances of various Ph ₃ C[WCA] salts in C ₆ D ₅ Br	196

CHAPTER I

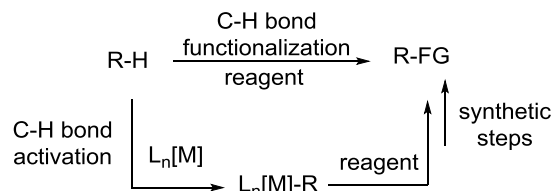
INTRODUCTION AND LITERATURE REVIEW*

1.1 Introduction

A premier focus of organometallic chemistry over the past 50 years has been the use of molecular transition metal catalysts for the functionalization of unactivated C-H bonds.¹ Transition metal catalyzed "C-H bond functionalization" specially refers to cases where a catalyst inserts directly into a C-H bond to affect the transformation resulting in the installation of a new functional group in place of H (Scheme I-1, top).² The insertion step is commonly referred to as "C-H bond activation" although the terms activation and functionalization are occasionally used synonymously. As summarized by Eisenstein, Glorius and coworkers,^{3,4} the C-H bond activation step is categorized into several different types: σ -bond metathesis, oxidative addition, electrophilic activation and Lewis-base assisted metalation or 1,2-addition (Scheme I-1, bottom). The nature of this pathway is highly dependent on many factors including the transition metal catalyst, ligands, solvent, additives and the substrate. This transformation is in contrast to the C-H bond substitutions of classic organic chemistry. Industrially, this organic reactivity is utilized to transform hydrocarbon substrates into value-added products via processes such as ethylene from ethane pyrolysis,⁵ chlorination of methane⁶ and the cumene synthesis via Friedel-Crafts alkylation (Scheme I-2).⁷

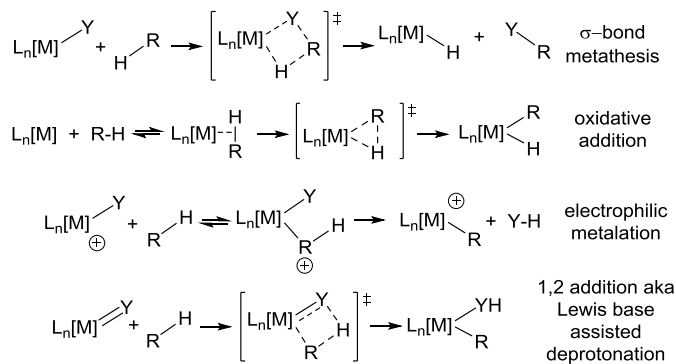
* Reproduced in part from "Triflyoxy-Substituted Carboranes as Useful Weakly Coordinating Anions" by Press, L. P.; McCulloch, B. J.; Gu, W.; Chen, C.; Foxman, B. M.; Ozerov, O. V. *Chem. Commun.*, **2015**, 51, 14043, Copyright [2015] by Royal Society of Chemistry.

Transition Metal Catalyzed C-H Bond Functionalization



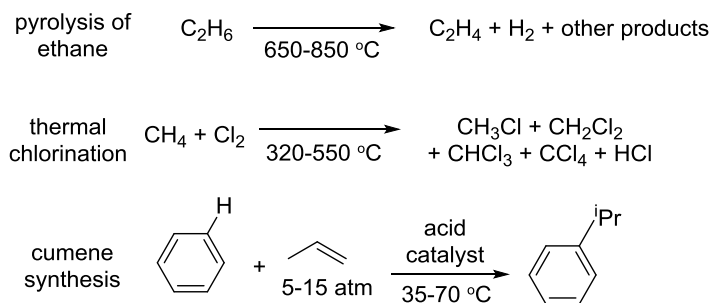
$\text{L}_n[\text{M}]$ = transition metal catalyst FG = functional group

Common C-H Bond Activation Pathways



Scheme I-1. C-H bond functionalization (top) and activation pathways (bottom).

These reactions follow organic reaction pathways such as radical substitution or electrophilic aromatic substitution which tend to be under electronic control and poorly selective. C-H bond functionalization aims to provide useful methodologies for the preparation of organic molecules, particularly under conditions typical of the academic laboratory,³ although industrially applicative processes are naturally of interest.^{1,8}

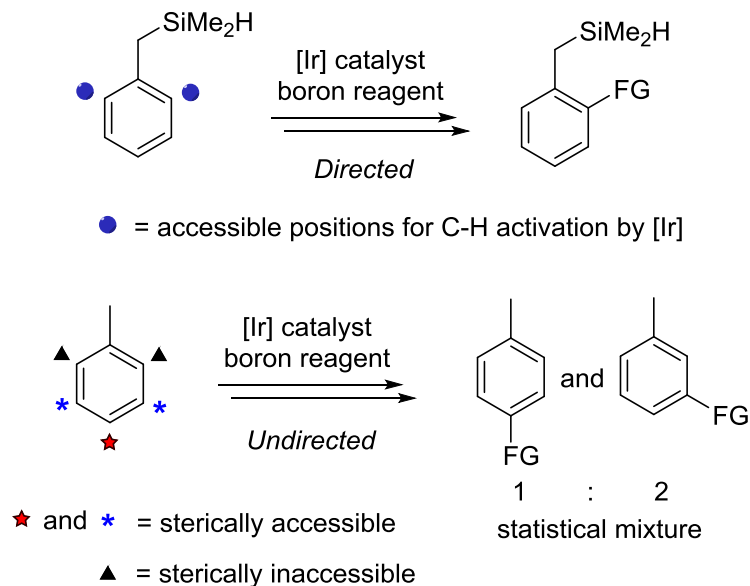


Scheme I-2. Pyrolysis of ethane, thermal chlorination of methane and Friedel-Crafts alkylation of benzene.

1.2 Types of C-H bond functionalization

In general C-H bond functionalizations are categorized based on the nature of preexisting functional groups within the substrate.⁹ In recent reviews, Hartwig et al. have categorized transition metal catalyzed C-H functionalizations as either "directed" or "undirected" functionalization (Scheme I-3).¹⁰ Yu et al. group transition metal catalyzed C-H functionalizations into two distinct subfields called "first functionalization" and "further functionalization" (Scheme I-4).⁹ Baran et al. take a broader approach and have categorized all C-H functionalizations (i.e. organic as well as transition metal-catalyzed transformations) into those that are "guided" versus those that are "innate" (Scheme I-5).¹¹

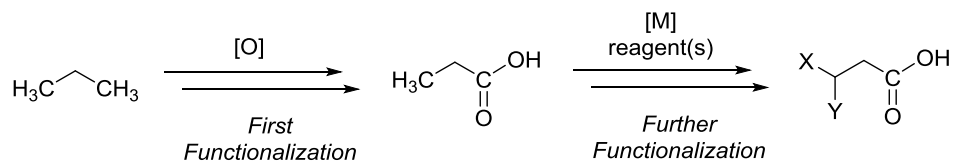
Directed vs. Undirected C-H Functionalization



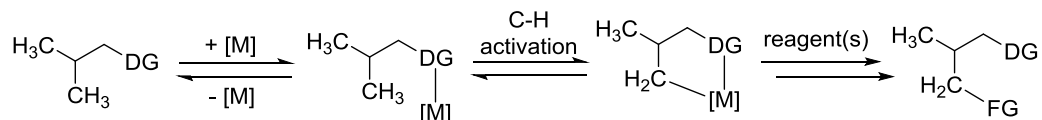
Scheme I-3. Hartwig et al. classify transition metal catalyzed C-H functionalization into two categories, directed versus undirected.

In essence, the labels “directed” and “further functionalization” are similar ways of describing a type of C-H functionalization using substrate(s) that contains a functional group or groups, usually Lewis bases, capable of coordinating to a transition metal center which then affects the transformation via C-H activation. On the other hand, the labels “undirected” and “first functionalization” generally describe C-H functionalizations of alkyl and aryl hydrocarbon substrates or sections of substrates (e.g. *n*-octane, toluene or the

First vs. Further C-H Functionalization

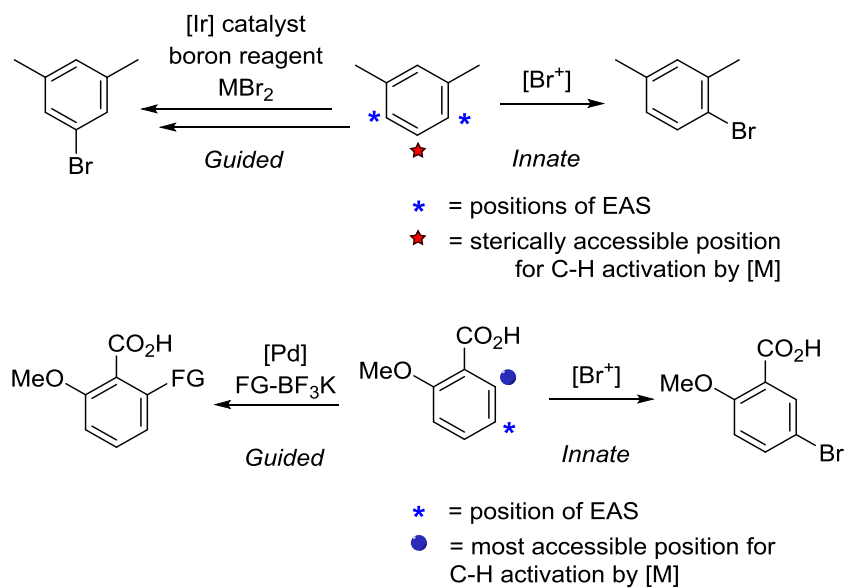


Proximal Directing Group Promoted C-H Activation



Scheme I-4. Yu et al. categorize transition metal catalyzed C-H functionalization as first and further functionalization (top).

Guided vs. Innate C-H Functionalization



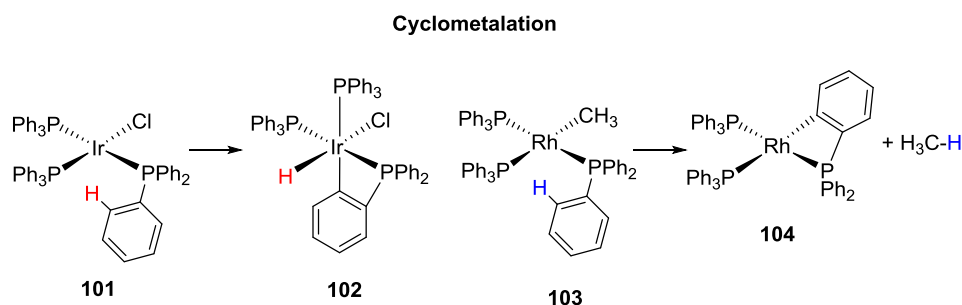
Scheme I-5. Baran et al. categorize C-H functionalization as either guided or innate functionalization.

hydrocarbon section of testosterone) containing no functionality beyond C-H and C-C or aromatic C=C bonds. Organic compounds containing heteroatoms, which by definition contain at least one type of atom other than carbon or hydrogen, often have certain C-H bonds that are more reactive than purely hydrocarbon substrates. Hartwig defines directed functionalization as “those directed by coordination to an existing functional group prior to the cleavage of the C-H bond.”¹⁰ Yu clarifies that “first functionalization” is defined as “the functionalization of substrates that are nonpolar and hydrophobic and thus interact very weakly with polar metal species.”⁹ Therefore, heteroatom containing substrates are generally placed into the “undirected” and “first functionalization” category unless they contain additional functional groups which affect the selectivity of C-H functionalization. For simplicity, we will use the terms “directed” and “undirected” for this discussion. In directed C-H functionalizations, a substrate binds in a particular orientation giving the transition metal complex ample opportunity for C-H bond activation and functionalization by effectively placing the substrate's C-H bonds within the coordination sphere of the metal center. Directed C-H functionalization typically provides excellent selectivity because only specific C-H bonds within a substrate will be metalated via C-H activation. A potential downside to directed C-H functionalizations is that the Lewis base directing functional group(s) must either be removed or tolerated in the final product. Undirected C-H functionalization relies on C-H bond coordination and subsequent activation by a transition metal complex but the C-H bonds of hydrocarbon substrates are weak σ -bases as well as weak π -acids and therefore relatively poor ligands.² Selectivity in these substrates will typically be governed by a combination of

steric and/or electronic factors.¹⁰ This leads to a dilemma where various C-H bonds within hydrocarbon substrates are potential sites for C-H functionalization therefore attempts at undirected functionalization may result in poor selectivity (Scheme I-3). Improving the selectivity of undirected C-H functionalizations is arguably one of the most important topics in synthetic chemistry.

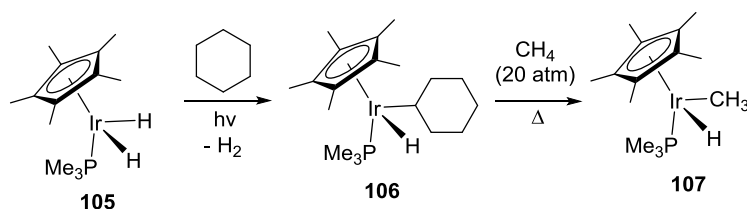
1.3 Early examples of C-H activation and functionalization

Early examples of C-H activation and functionalization include the work of Shilov and Shulpin who demonstrated the Pt catalyzed oxidation of alkanes including methane.¹² Parshall conveniently reviewed intramolecular *ortho*- C-H activations of nitrogen and phosphorous ligands (referred to as cyclometalation) as early as 1970.¹³ Some quintessential examples include cyclometalation in $(PPh_3)_3IrCl$ **101** to give **102** (Scheme I-6, left)¹⁴ and **103** to give **104** (Scheme I-6, right).



Scheme I-6. Classic examples of intramolecular *ortho*- C-H activation also known as cyclometalation by Milner et al. and Keim.

Fujiwara and coworkers investigated catalytic oxidative C-C bond formation.¹⁵⁻¹⁷ In 1979, stoichiometric alkane dehydrogenation using Ir complexes was first reported by Crabtree.¹⁸ This alkane dehydrogenation chemistry was further investigated by Felkin¹⁹⁻²¹ and Crabtree.^{22,23} Bergman²⁴ and Graham²⁵ independently investigated the C-H activation of alkanes by cyclopentadienyl Ir complexes. In those studies Bergman et al. employed compound **105** for the photolytic of cyclohexane to give **106** followed by thermolysis of **106** in the presence of methane (Scheme I-7).



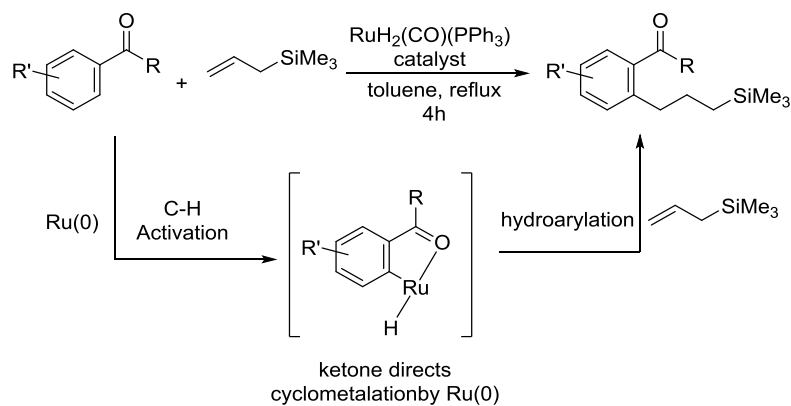
Scheme I-7. C-H activation of cyclohexane and methane investigated by Bergman et al.

In the early 1990s, Goldman demonstrated the high activity of (PMe₃)₂Rh(CO)Cl for catalytic transfer dehydrogenation of alkanes under an H₂ atmosphere.²⁶ Reviews from the 1980s,^{27,23} 1990s^{12,28} and early 2000s^{8,29,30,31} summarized early examples of C-H activation and functionalization. Today C-H functionalization has become one of the most popular topics among synthetic chemists and numerous methodologies have been developed for the transformation of C-H bonds into C-C, C=C, C-Halogen, C-O, C-B and C-Si bonds, among others. Due to the overwhelming number of examples of C-H activation and functionalization some important contributions will unfortunately be

overlooked and a full discussion of all of these transformations is beyond the scope of this introduction. Here we will briefly summarize some common types of C-H functionalizations, as well as discuss some recent advances within these examples relevant to this dissertation.

1.4 Directed C-H functionalizations

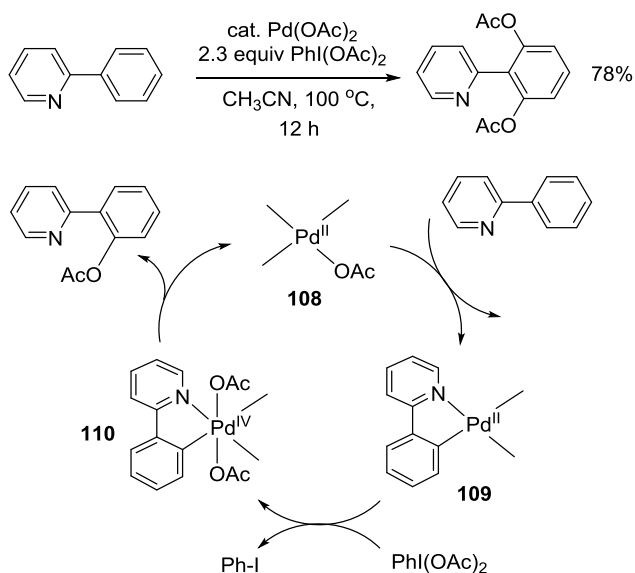
The directed C-H functionalization of arenes is one of the most extensively studied transformations within the topic of C-H functionalization and the astounding number of examples in the literature necessitates brief mention.



Scheme I-8. Catalytic *ortho*-alkylation of aromatic ketones by Murai and co-workers

Murai et al. pioneered one of the first synthetically useful C-H functionalizations with the highly selective Ru catalyzed *ortho*-alkylation of aromatic ketones (Scheme I-8).³² Brookhart and co-workers later demonstrated similar *ortho*-alkylation chemistry with Rh catalysts.³³ Fujiwara et al. used Pd and Pt catalysts for the inter- and intramolecular

hydroarylation of aromatic carboxylates with alkynes.^{34,35} Yu et al. have investigated the concept of weak substrate coordination in Pd catalyzed directed C-H functionalizations.⁹ Sanford and co-workers developed a highly selective Pd catalyzed directed acetyloxylation of C-H bonds.³⁶ They proposed a chelate-directed C-H activation of substrate by **108** to give **109** followed by oxidation to the Pd(IV) intermediate **110** which eliminates the functionalized product and regenerates **108** (Scheme I-9). Sanford et al. have thoroughly investigated the use of strongly coordinating nitrogen containing ligands in Pd catalyzed C-H functionalizations to afford C-O, C-C, C-N and C-halogen bonds.³⁷ Ritter and co-workers identified discrete bimetallic benzo[*h*]quinoline Pd(III) complexes capable of carbon-halogen and carbon-oxygen reductive eliminations and suggested these species as mechanistic alternatives to monometallic Pd(II)-Pd(IV) redox cycles put forth by Sanford et al.³⁸ They later observed Pd(III)-Pd(III) intermediates in catalytic oxidative C-H functionalization studies.³⁹



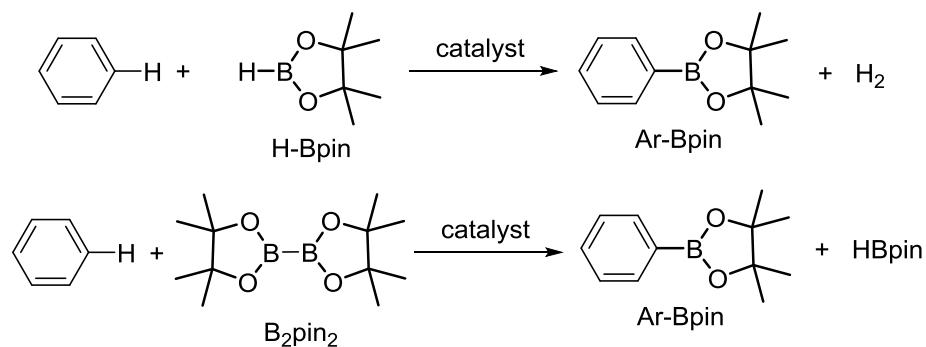
Scheme I-9. Oxidative acetyoxylation of phenylpyridines by Sanford et al. with proposed catalytic pathway.

Daugulis and co-workers have developed Pd catalyzed C-H arylations of directing substrates such as anilides, benzamides, benzoic acids, benzylamines and 2-substituted pyridine derivatives with aryl iodides.⁴⁰ Daugulis et al. have also focused on the C-H arylation of heterocycles using Cu phenanthroline type catalysts.^{40,41} Bergman, Ellman and others have demonstrated the use of Rh catalysts for the olefin-directing hydroarylation of nitrogen heterocycles.⁴² The use of cheaper first row transition metals such as Mn have been utilized in ligand-directed catalytic C-H functionalizations such as hydroarylations, alkenylations, annulations and azidations, among others.^{43,44} White et al. have found Fe porphyrin complexes can catalyze intramolecular allylic C-H aminations.⁴⁵

1.5 Transition metal catalyzed arene C-H bond borylation

1.5.1 Introduction to transition metal catalyzed arene C-H bond borylation

In the last 15-20 years, one type of C-H functionalization known as C-H borylation has grown into a mature synthetic method.^{1,46,47,48,49,50} First noted as an offhand observation in the synthesis of Ir boryl complexes by Marder and coworkers, they observed the formation of organoboronate esters by GC/MS resulting from the reactions of these complexes with hydrocarbon solvents such as toluene.⁵¹ C-H borylation is attractive as it directly converts C-H bonds into organoboronate esters (Scheme I-10), whose use in a large number of synthetic transformations has been well documented.⁵²

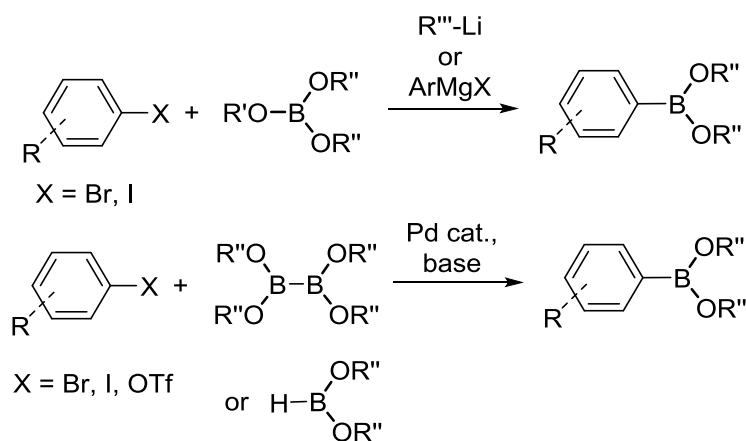


Scheme I-10. Catalytic formation of organoboronate esters via C-H functionalizations.

The net reactions of catalytic borylation of arenes with HBpin or B₂pin₂.

Traditionally, organoboronate esters have been synthesized using the methods of organic chemistry or Pd catalyzed coupling reactions and therefore are reliant on the use of halogenated arenes with strong bases or Grignard reagents (Scheme I-11).⁴⁷

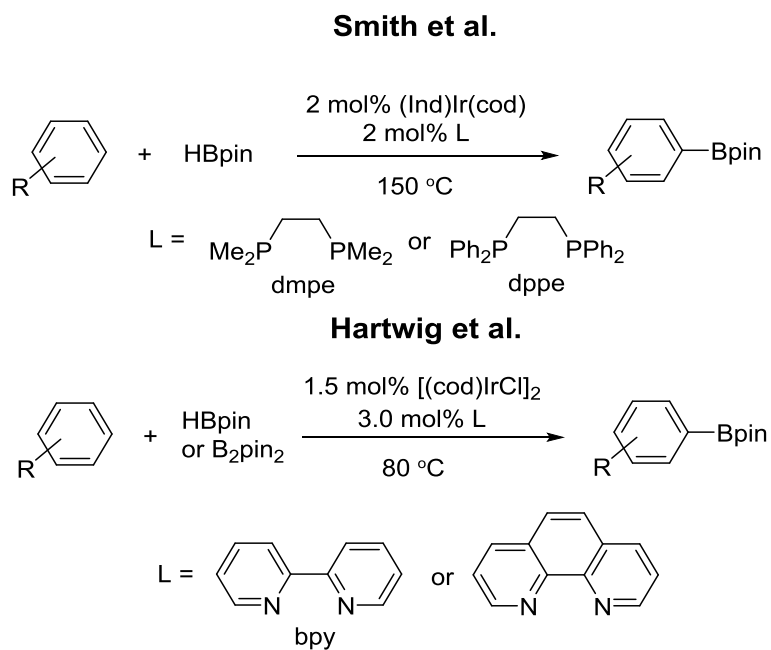
Synthesis of Arylboronates from Aryl Halides



Scheme I-11. Synthetic methods for the formation of organoboronate esters.

The history and scope of C-H borylation has been thoroughly reviewed.^{47,48,49} Early examples of transition metal catalyzed C-H borylation of alkanes utilized Ru,⁵³ Rh,⁵⁴ and Re.⁵⁵ The most impressive reactivity thus far has been achieved with Ir catalysts. Recent successes with Fe/Cu,⁵⁶ Co,^{57,58} Pt,⁵⁹ and even main group⁶⁰ catalysts indicate that catalytic aromatic C-H borylation is not limited to the heavier group 9 metals. Nonetheless, Ir catalysts have proven especially effective in borylation of aromatic C-H bonds where bidentate bis(phosphine),⁵⁰ bipyridine-type or 1,10-

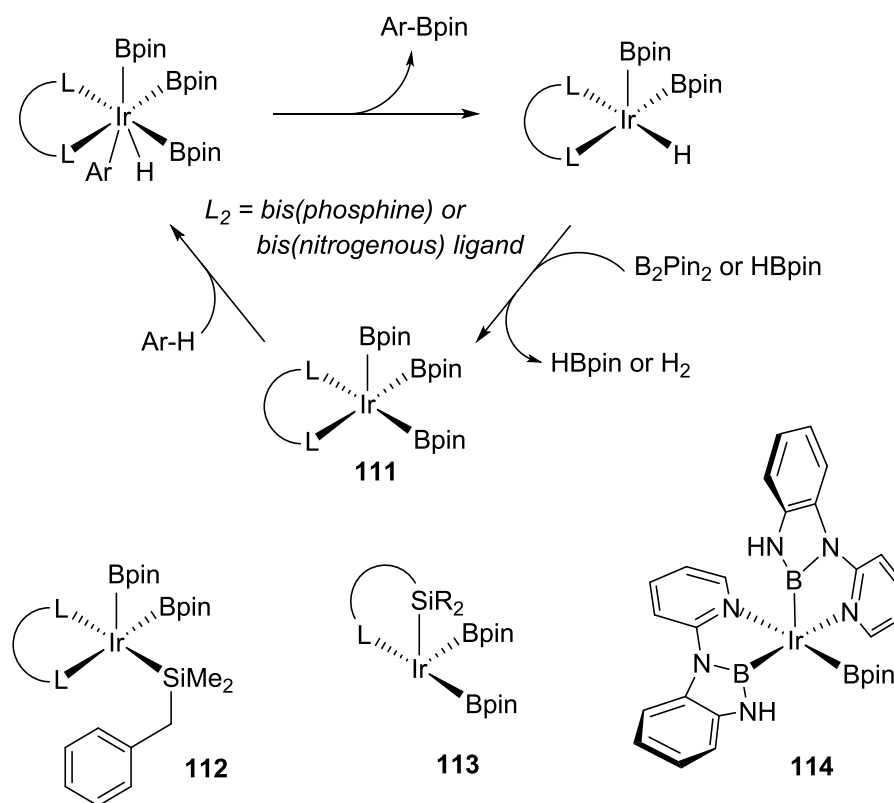
phenanthroline ligands⁶¹ have given rise to remarkable turnover numbers with sterically controlled selectivity (Scheme I-12).



Scheme I-12. Formation of organoboronate esters via Ir catalyzed C-H functionalizations. Work of Smith et al. (top) and Hartwig et al. (bottom).

1.5.2 Mechanism of $L_2Ir(Bpin)_3$ catalyzed C-H borylation

The mechanism of Ir-catalyzed C-H borylation is believed to proceed via a 16-electron triboryl intermediate $L_2Ir(Bpin)_3$ (**111**, Scheme I-13, top), which activates the arene C-H bond via oxidative addition (as shown in Scheme I-13) or the closely related oxidative hydrogen migration pathway^{61,62,63,64}



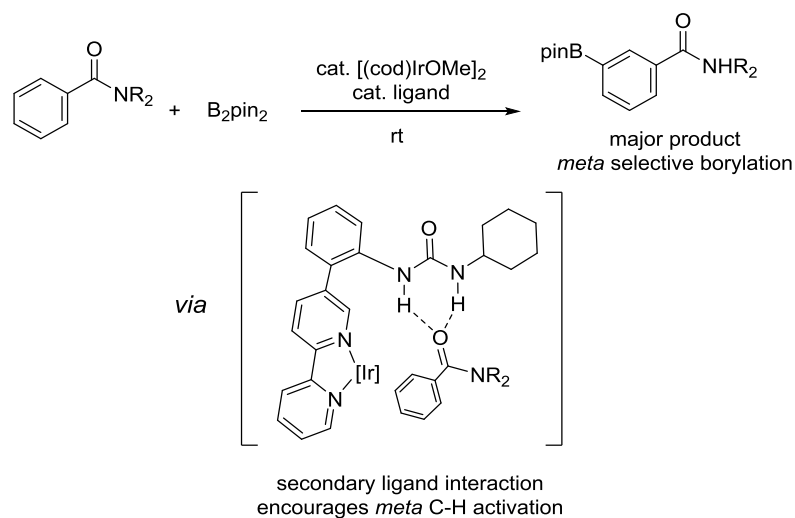
Scheme I-13. Catalytic cycle commonly invoked in Ir-catalyzed aromatic borylation and recent analogs (**112**, **113**, **114**) to the triboryl intermediate **111**.

Some of the most recent advances in Ir-catalyzed C-H borylation rely on access to intermediates that could be viewed as modified $L_2\text{Ir}(\text{Bpin})_3$. Hartwig and co-workers used pendant directing Si-H groups in substrates and proposed the intermediacy of a silyl/diboryl Ir(III) complex (**112**, Scheme I-13, bottom).⁶⁵ Krska, Maleczka, Smith et al. also proposed the intermediacy of a silyl/diboryl Ir(III) complex **113** (Scheme I-13, bottom) in a study demonstrating the efficacy of phosphine/silyl or quinoline/silyl bidentate ligands.⁶⁶ Li et al. demonstrated that a combination of two pyridine/boryl

bidentate ligands on Ir gave rise to a potent catalyst, again with an implied Ir(III) triboryl intermediate **114** (Scheme I-13, bottom).⁶⁷

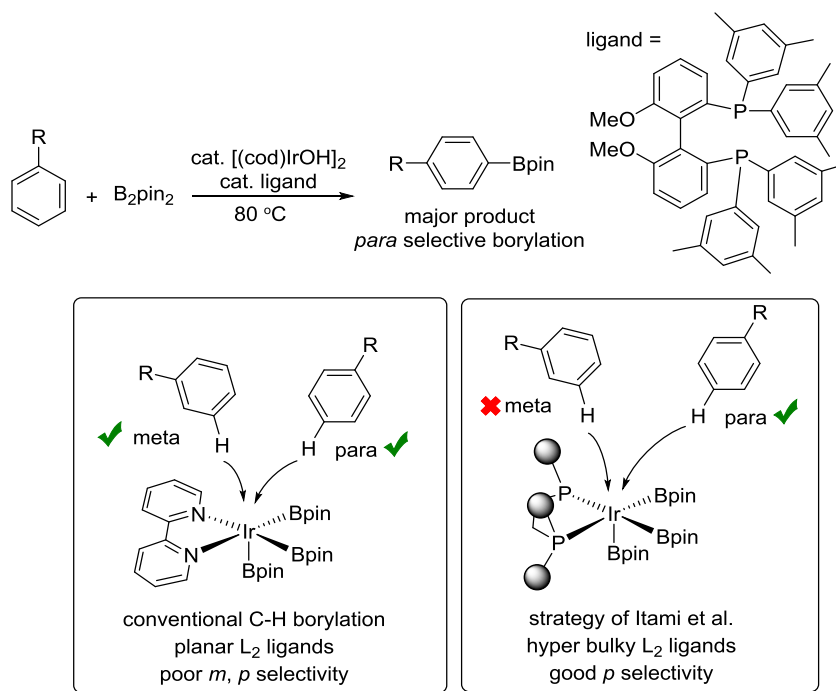
1.5.3 Selectivity in Ir catalyzed arene C-H borylation

Selectivity in the Ir catalyzed C-H borylation of arenes is typically under steric control. C-H borylation of mono-substituted arene substrates (e.g. toluene) often gives near statistical mixtures of 3- and 4-borylated products (Scheme I-3). Exclusive borylation in the 2-position without the use of directing groups such as hydrosilyl,⁶⁵ alkylbenzoates⁶⁸ ^{69,70} alkylamides, methylsulfonate, ethers or chloro is an ongoing challenge. Notably, selective borylation at the 2-position of fluoroarenes has been achieved with Co catalysts.⁵⁷ The borylation of 1,2-di-substituted arenes occurs in the 4-position while 1,3-di-substituted arenes are borylated at the 5-position. Regioselectivity in the borylation of 1,4-di-substituted arenes is dependent on the nature of the substituents on 1- and 4-positions but generally borylation occurs at the less sterically encumbered position.⁷¹ Product yields may also suffer in the borylation of 1,4-di-substituted substrates due to steric hindrance.^{46,71} One recent approach to improve selectivity in Ir catalyzed C-H borylations has been the use of specialized ligands that orient, or only allow access to, specific C-H bonds within a substrate towards the Ir metal center. Kanai and co-workers developed modified bipyridine ligands containing pendant urea groups (Scheme I-14).⁷²



Scheme I-14. *meta*-selective borylation via ligand secondary interactions devised by Kanai and co-workers.

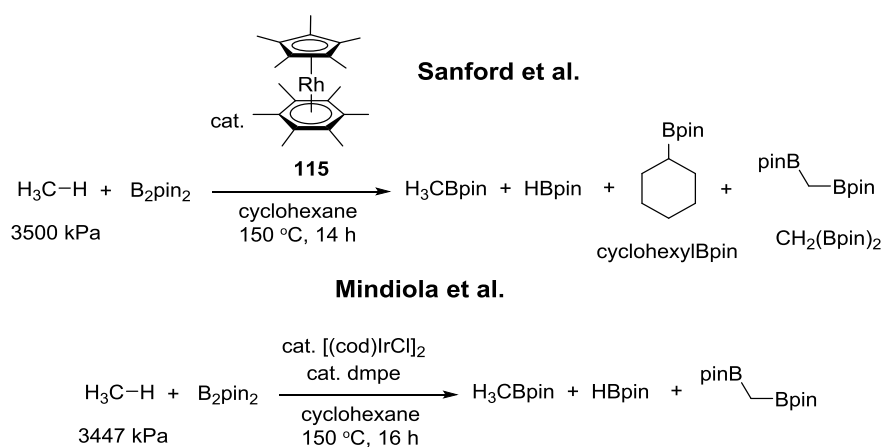
They found these modified ligands, when used with $[(\text{cod})\text{IrOMe}]_2$ gave *meta*-selective C-H borylation of mono- and 1,2-di-substituted arenes. Kanai et al. postulated this improved selectivity was the result of hydrogen-bonding secondary interactions between the ligand and substrate where the ligand's pendant urea tended to orient the substrate's 3-position (*meta*-) C-H bonds toward the Ir metal center. Using bulky bi-phenyl bis(phosphine) ligands, Itami and co-workers were able to selectively borylate mono-substituted arenes in the 4- position (Scheme I-15).⁷³



Scheme I-15. *para*-selective C-H borylation employed by Itami et al.

A topic that has frequented the literature for some time is the mild transition metal catalyzed functionalization of methane.²³ Methane is an extremely abundant hydrocarbon typically used as fuel in various capacities.⁷⁴ Selective functionalization of methane has been long standing challenge in organometallic chemistry and the topic has been discussed in various reviews.^{12,27,75} In 2016, the groups of Sanford and Mendiola simultaneously published reports for the borylation of methane and ethane.^{76,77} The Sanford group achieved up to 68 TON for the borylation of methane (3500 kPa) with B₂pin₂ to CH₃Bpin (51% yield) at 150 °C using 0.75 mol% (Cp*)Rh(C₆Me₆) (**115**) as catalyst and cyclohexane as solvent (Scheme I-16, top). The cyclohexane solvent was also borylated in the process and optimized conditions generated a

CH₃Bpin:cyclohexylBpin ratio as high as 59:1 with yields of CH₃Bpin up to 99%. They also observed diborylation of methane to give CH₂(Bpin)₂. The Mindiola group investigated Smith and Hartwig type Ir catalysts for the borylation of methane (Scheme I-16, bottom). They observed up to 104 TON for the borylation of methane (3447 kPa) with B₂pin₂ to give CH₃Bpin (52% yield) at 150 °C using [(cod)IrCl]₂/2 dmpe as catalyst and cyclohexane as solvent. They also observed diborylation of methane under certain conditions.

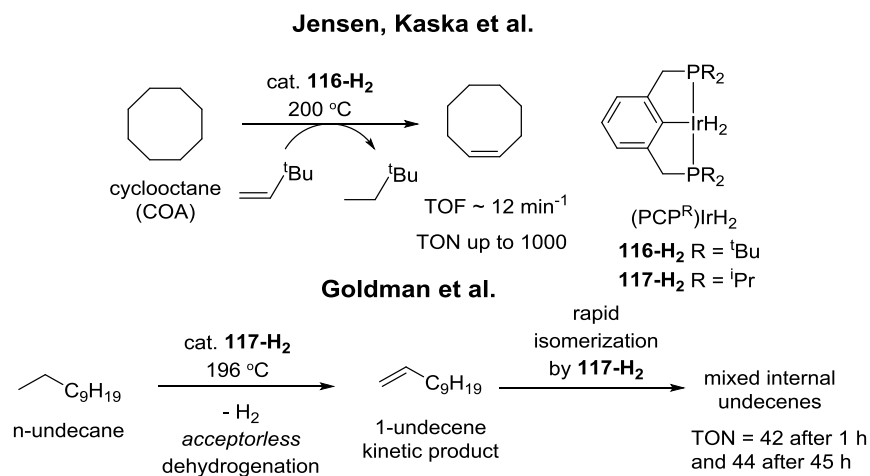


Scheme I-16. Borylation of methane independently reported by Sanford and Mindiola.

1.6 Homogeneous transition metal-catalyzed alkane dehydrogenation

1.6.1 Alkane dehydrogenation background

Olefins, particularly linear α -olefins, are extremely valuable commodity chemicals used in the production of detergents, polyethylene copolymers and synthetic lubricants.⁷⁸ Several processes exist for the industrial production of linear α -olefins including homogeneous Ni catalyzed ethylene oligomerization⁷⁸ (e.g. the Shell higher olefin process) and heterogeneous catalytic dehydrogenation of higher alkanes using Pt/Sn on alumina.⁷⁹ An alternative synthesis of linear α -olefins is the use of homogeneous molecular transition metal catalyst that dehydrogenate alkanes to alkenes.⁸⁰ Stoichiometric alkane dehydrogenation using cationic Ir complexes and *tert*-butylethylene as H₂ acceptor was first reported by Crabtree et al.¹⁸ As previously noted this dehydrogenation chemistry was further investigated by Felkin, Crabtree et al.⁸¹ In the early 1990s, Goldman demonstrated the high activity of (PMe₃)₂Rh(CO)Cl for catalytic transfer dehydrogenation of alkanes under an H₂ atmosphere.²⁶ Turn over numbers (TON) up to 950 were observed after 15 minutes in the dehydrogenation of cyclooctane (COA) to cyclooctene (COE) using norbornene as H₂-acceptor at 100 °C under 1000 psi of H₂.²⁶

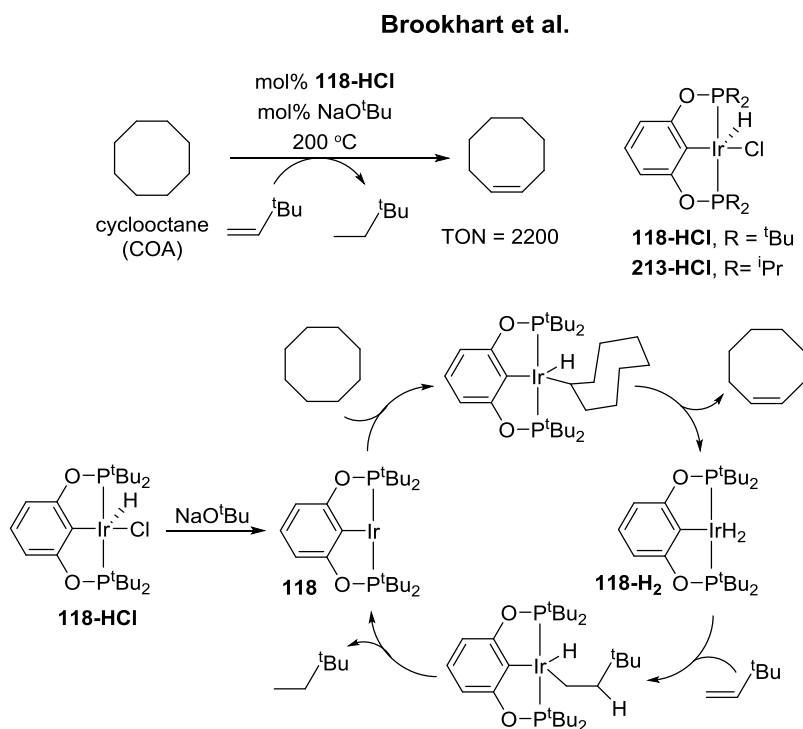


Scheme I-17. Transfer and acceptorless dehydrogenation of alkanes using precatalysts **116-H₂** and **117-H₂**.

1.6.2 Ir pincer complexes for alkane dehydrogenation

In the late 1990s, Jensen, Kaska, Goldman et al. reported (PCP^{tBu})IrH₂ pincer complex **116-H₂** for the catalytic transfer dehydrogenation⁸² and acceptorless dehydrogenation⁸³ of alkanes including COA (Scheme I-17, top).⁸⁴ Turnover frequencies of up to 12 turnovers per minute and 1000 turnovers in total were observed at 200 °C in transfer dehydrogenation experiments. The rate of acceptorless dehydrogenation of COA under similar conditions was considerably slower at only 20 turnovers per hour with a maximum of 36 turnovers (achieved only after removing H₂ using freeze-pump thaw cycles). Total turnover numbers in transfer dehydrogenation experiments were found to be limited not by catalyst decomposition but by product inhibition. The authors also noted that the reactions were inhibited by the presence of N₂. Liu and Goldman demonstrated the first high turnover dehydrogenation of linear alkanes using the less

sterically encumbered (PCP^{iPr})IrH₂ **117-H₂** (Scheme I-17, bottom).⁸⁵ Neat *n*-undecane was dehydrogenated to a mixture of internal undecenes giving 42 turnovers after 1 h at 196 °C without the use of an H₂ acceptor. Continuous heating at 196 °C (45 h in total) gave only 2 additional turnovers (44 turnovers in total) indicating the reaction had been severely retarded by either catalyst decomposition or product inhibition with further experiments proving the latter. When an H₂ acceptor such as *tert*-butylethylene (TBE) was used, **117-H₂** selectively dehydrogenated *n*-undecane to 1-undecene but the α-olefin product was found to be rapidly isomerized to internal undecenes by **117-H₂**. Several follow up studies investigated modifications to the PCP ligands including the use of *para*- functionalized PCP ligands,⁸⁶ synthesis of an anthrphos PCP-type Ir complex,^{87,88} phosphines substituted with extremely bulky adamantyl groups,⁸⁹ among many other modifications.⁸⁰ One notable development in Ir catalyzed alkane dehydrogenation chemistry was the use of resorcinol based POCOP ligands by the groups of Brookhart and Jensen (Scheme I-18, top right).^{90,91} Utilization of precatalyst **118-HCl** (dehydrochlorinated with 1 equiv. of NaO^tBu) gave up to 2200 TON in the transfer dehydrogenation of COA (Scheme I-18, top). The proposed catalytic cycle (Scheme I-17, bottom) invokes a transient three-coordinate 14-electron species **118** that reactions with the C-H bonds of COA via oxidative addition. β-hydride elimination generates **118-H₂** which hydrogenates *tert*-butylethylene to regenerate the 14-electron fragment **118**; compounds of **213** would follow a similar scheme.



Scheme I-18. Transfer dehydrogenation of COA using precatalyst **118-HCl**. Proposed catalytic pathway for the dehydrogenation of COA by **118**.

Interestingly, DFT calculations indicate the metal center of **118**, a three-coordinate 14-electron species, is notably less sterically encumbered in comparison to the metal center about its (PCP^{tBu})Ir analog **116** despite their apparent similarity.⁸⁶ Calculations also indicate **118** is slightly more electron rich at the metal center compared to **116** as a result of π -donation into the arene ring from the oxygen atoms of the (POCOP^{tBu}) ligand.⁸⁶ In terms of the first step in the mechanism of alkane dehydrogenation by either PCP or POCOP type Ir complexes, access to a transient three-coordinate 14-electron species either by reductive elimination of free H₂, by the

hydrogenation of sacrificial olefin or dehydrochlorination of the Ir hydrochloride complex is apparently required for catalysis. Overall, complexes **116** and **118** have been observed to proceed through slightly different mechanisms as a result of the geometric and electronic differences between the two catalysts.⁸⁰ These differences also result in (POCOP^{tBu})Ir being a better precatalyst for the transfer dehydrogenation of COA than (PCP^{tBu})Ir, yet is worse for the transfer dehydrogenation of linear alkanes. This phenomena is presumably due to strong olefin binding to the metal center of (POCOP^{tBu})Ir.⁸⁰

1.6.3 Recent advances in alkane dehydrogenation catalyzed by Ir pincer complexes

Since the original studies by Jensen, Kaska, Goldman and Brookhart a number of different Ir pincer complexes have been developed for use as alkane dehydrogenation catalyst and the topic has been reviewed (Figure I-1).^{80,92}

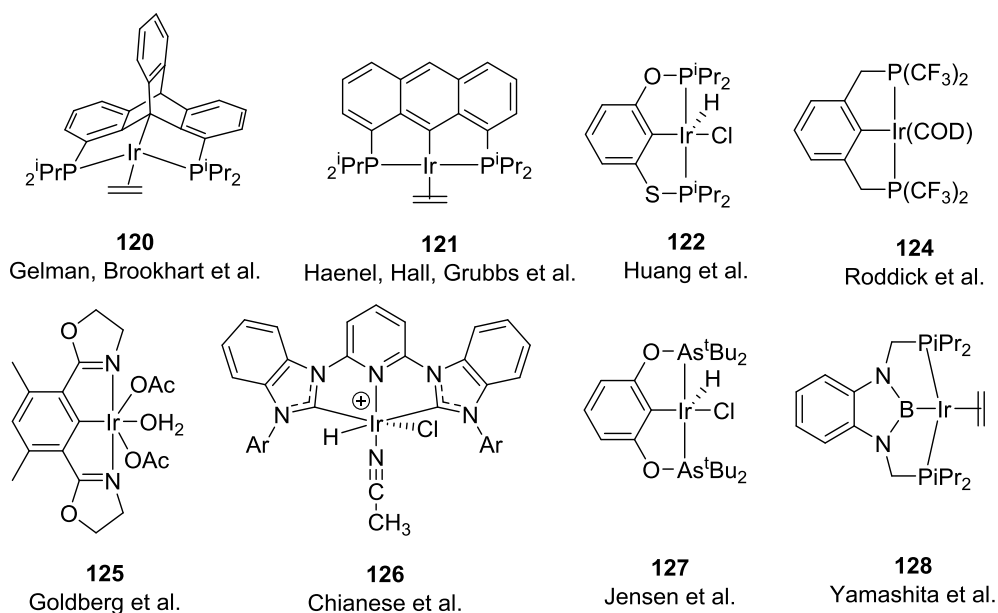
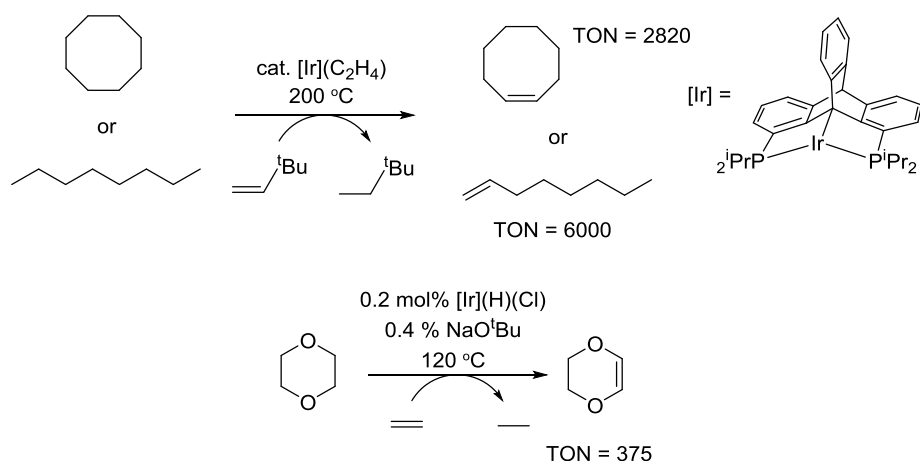


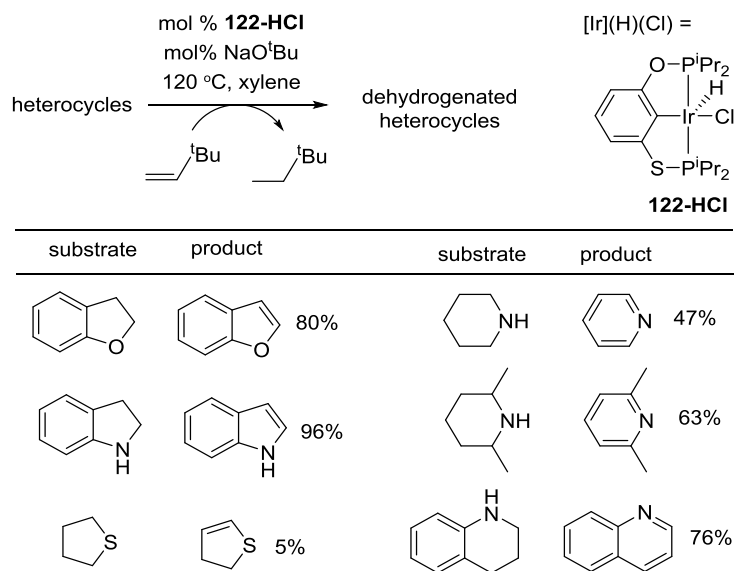
Figure I-1. Examples of Ir pincer complexes used in catalytic and stoichiometric alkane dehydrogenation studies.

Initially developed by Gelmen et al.,⁹³ Brookhart and co-workers utilized triptycene the PCP type Ir complex **120** (Scheme I-1) for alkane transfer dehydrogenation and found high activity (up to 6000 TON) at 200 °C with substrates such as COA and *n*-octane.⁹⁴



Scheme I-19. Transfer dehydrogenation of alkanes and ethers using triptycene backbone Ir pincer complexes.

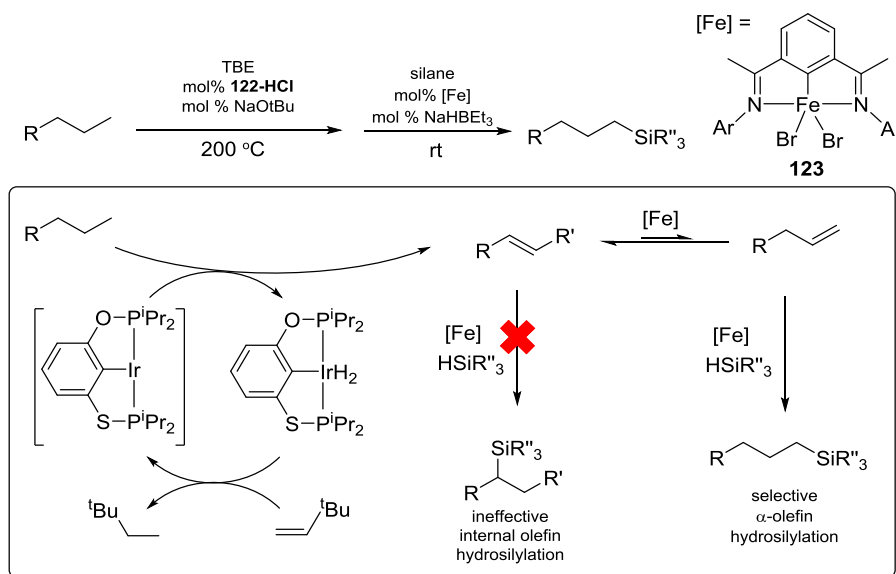
Early work by Jensen and Kaska found **116-H₂** dehydrogenated tetrahydrofuran to furan with up to 57 TON.⁹⁵ Complex **120** as well as **117** and **121** were found to give high yields for the transfer dehydrogenation of cyclic and acyclic ethers using ethylene as H₂ acceptor (Scheme I-19, bottom).⁹⁶ In that study, the triptycene Ir complexes were also modified to allow support of the triptycene Ir complexes on alumina for heterogeneous catalysis studies.⁹⁴



Scheme I-20. Selective catalytic transfer dehydrogenations of heterocycles using (POCSP^{iPr})Ir by Huang et al.

Zhuang and co-workers synthesized and tested complex **122-HCl** (Figure I-1) for the transfer dehydrogenation of cyclic and linear alkanes then independently compared the results with those of **116** and **118**.⁹⁷ They found **122** showed considerable activity in the transfer dehydrogenation of n-octane at 200 °C with up to 500 TON observed after 1 h. Under identical conditions **116** gave 135 TON while **118** gave 135 TON. In the same study, **122** was also found to effectively catalyze the transfer dehydrogenation of a broad range of N and O containing heterocycles with catalyst loadings as low as 0.1 mol% and excellent yields of dehydrogenated heterocycles (Scheme I-20). In a follow up study, Huang et al. developed a method for the catalytic conversion of alkanes to linear

alkylsilanes using a tandem dehydrogenation-isomerization-hydrosilylation scheme (Scheme I-21).⁹⁸



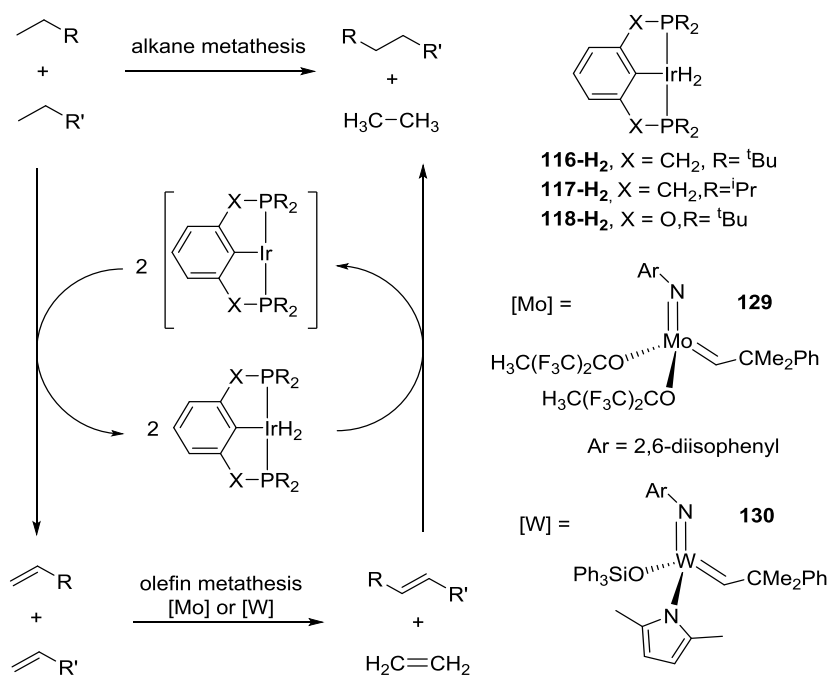
Scheme I-21. Catalytic silylation of alkanes via alkane dehydrogenation and isomerization-hydrosilylation by Huang et al.

Compound **122-HCl** was utilized as the transfer alkane dehydrogenation precatalyst in tandem with Chirik's anti-Markovnikov olefin hydrosilylation precatalysts such as **123** (Scheme 1-21).⁹⁹ The system was not limited to silanes as they also synthesized terminal alkylboronate esters in moderate to excellent yields. Goldman and co-workers studied the effect of immobilization of (PCP)Ir type complexes in the catalytic dehydrogenation of n-alkanes to linear alpha-olefins.¹⁰⁰ Roddick and co-workers developed PCP ligands with trifluoromethyl substituted phosphines and

synthesized their Ir complexes including (PCP^{CF₃})Ir(COD) (**124**, Figure I-1).¹⁰¹ The complex was found to catalyze the acceptorless dehydrogenation of COA with TON up to 3020 after 64 h at 200 °C.⁹² Goldman, Goldberg et al. found the bis(oxazoliny) complex (NCN)Ir(OAc)₂(H₂O) (**125**, Figure I-1) originally developed by Nishiyama et al.¹⁰² gave stoichiometric quantities of dehydrogenation products when heated to 200 °C for 72 h in the presence of *n*-octane.¹⁰³ This transformation is notable in that it occurred in the presence of N₂, excess olefin (1-hexene, 10 equiv.) as well as H₂O (120 equiv.) which are all compounds known to be inhibitors of alkane dehydrogenation.⁸⁰ Yamashita and Tanaoue synthesized complex an (PBP)Ir complex (**128**, Figure I-1) and investigated the compounds capability as a transfer dehydrogenation catalyst.¹⁰⁴ Up to 43 TON were observed in the dehydrogenation of COA at 220 °C using TBE as H₂ acceptor with added lithium tetramethylpiperidide.

1.6.4 Synthesis of alkanes and aromatics using Ir pincer catalysts

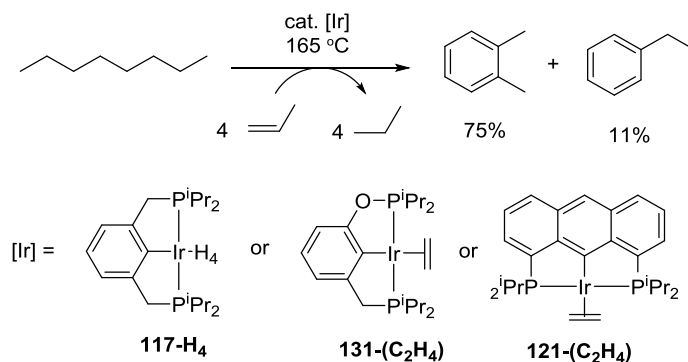
Brookhart, Goldman et al. investigated catalytic alkane metathesis via a tandem alkane-dehydrogenation-olefin-metathesis scheme (Scheme I-22).¹⁰⁵ Various PCP and POCOP type Ir complexes were utilized as alkane dehydrogenation catalysts in conjunction with olefin metathesis catalysts, such as Shrock's Mo-F12 (**129**, Scheme I-22).^{105,106} The studies found *n*-hexane (135 equiv.) was converted into a mixture of C₂ to C₁₅ linear alkanes after 24 h at 125 °C. Later efforts utilized the more thermally stable W complex **130** (Scheme I-22) developed by Shrock and co-workers which resulted in an order of magnitude increase in overall catalytic activity compared to previous studies that used Mo.¹⁰⁷



Scheme I-22. Alkane metathesis using a tandem alkane dehydrogenation olefin metathesis catalysis by Brookhart, Goldman et al.

In 2011 Brookhart et al. reported the catalytic dehydroaromatization of linear alkanes using various Ir pincer complexes with less sterically encumbering isopropyl substituents.¹⁰⁸ Dehydroaromatization of *n*-octane at 165 °C with Ir pincers precatalysts **117-H₄**, **121-(C₂H₄)** and **131-(C₂H₄)** gave up to an 86% overall yield of alkybenzenes (*o*-xylene and ethylbenzene) utilizing low cost H₂ acceptors such a propylene (Scheme 1-23). Longer chained linear alkanes such as *n*-decane and *n*-dodecane gave more complex mixtures comprised of various alkybenzenes. The aromatic products were proposed to form by a multi-step process invoking transfer dehydrogenation of linear

alkanes to linear trienes followed by classic electrocyclizations to give mixed cyclic dienes that were further dehydrogenation to mixtures of alkylaromatics.



Scheme I-23. Catalytic dehydroaromatization of linear alkanes by Ir pincer complexes investigated by Brookhart, Goldman and co-workers. The synthesis of o-xylene and ethylbenzene using propylene is showcased.

1.7 Introduction to carboranes

A mechanistic step common to most of the previously described examples of transition metal catalyzed C-H functionalization is the C-H activation (Scheme I-1) of a hydrocarbon substrate by a neutral coordinatively unsaturated metal center. In general, the binding of substrate to an open coordination site(s) is a critical step in the mechanism of most homogeneously catalyzed reactions.^{109,110} One way to achieve coordinative unsaturation in otherwise saturated transition metal complexes is by abstraction of anionic X-type ligand(s) (i.e. halide, pseudo-halide, hydride, alkyl ligand) with salts containing weakly coordinating anions (WCAs).¹¹¹⁻¹¹³ WCAs are exceptionally poor

nucleophiles and are a requisite synthetic complement to the study of highly reactive cations in condensed phases.^{111,112,114-117} Among the most desirable properties in a WCA are low basicity, resistance to decomposition, resistance to oxidation, and solubility in weakly coordinating solvents. Derivatives of monocarba-closo-dodecaborate $[\text{HCB}_{11}\text{H}_{11}]^-$ (**501**) (or carborane anion for brevity, Figure I-2)^{111,115} possess a very attractive combination of these properties that has permitted examination of a number of remarkable cations (Figure I-3).¹¹⁸⁻¹²³ This includes some of the strongest known Bronsted-acids which have been studied by Reed et al.^{122,124,125} Najafian et al have described **501** as having 3-D aromaticity¹²⁶ which contributes to the anions remarkable thermodynamic stability. Other popular WCAs include fluorinated tetraarylborates and fluorinated tetraalkoxyaluminates¹¹⁷

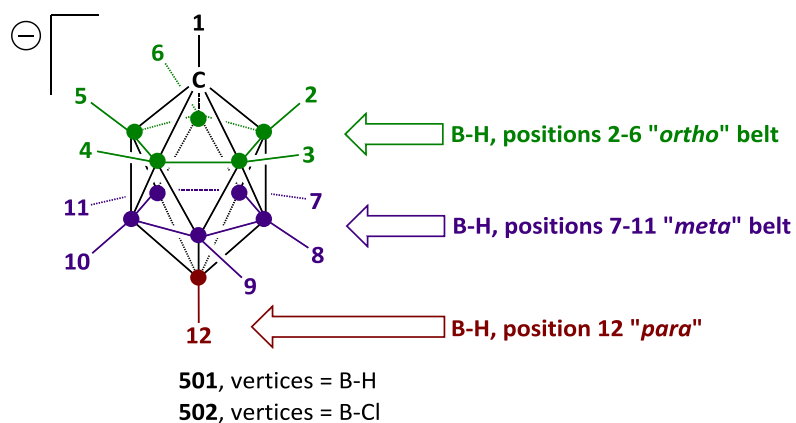


Figure I-2. Labelling system for the carba-*closo*-dodecaborate ($-$) anion (**501**) and its chlorinated derivative **502**. Dots represent boron atoms.

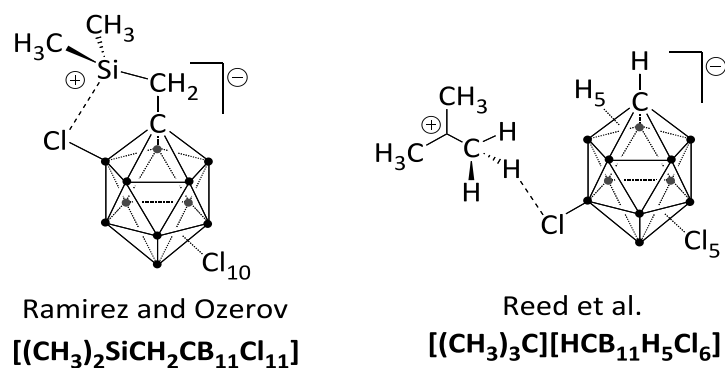
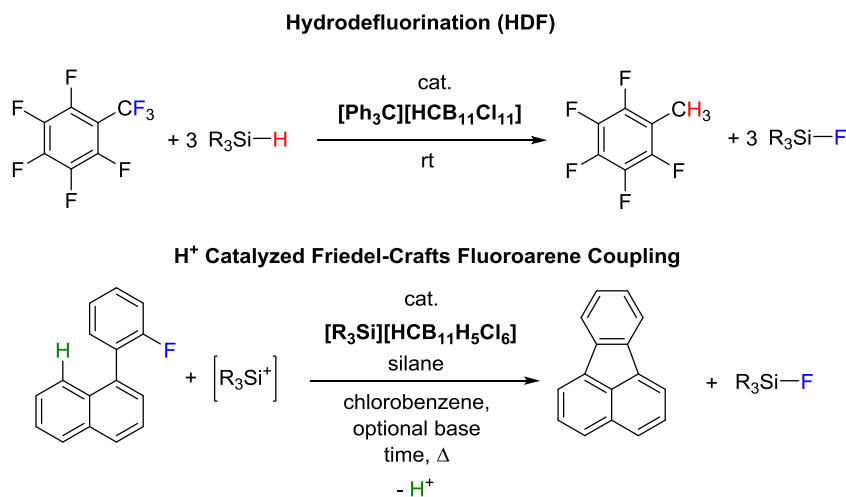


Figure I-3. Examples of reactive cations with carborane anions.

which are synthetically more easily accessible and very weakly basic, but are less robust than halogenated carborane anions. Carborane anions tend to be much more prone to forming crystalline solids, which is crucial for X-ray diffraction studies. Ozerov and co-workers utilized halogenated derivatives of **501**, including, **502** (Figure I-2), in the hydrodefluorination of organofluorine compounds with alkyl silanes (Scheme I-24).^{127,128} Siegel et al. investigated halogenated carborane anions in the silane-fueled proton-catalyzed Friedel-Crafts coupling of fluoroarenes (Scheme I-24, bottom).¹²⁹



Scheme I-24. Catalytic hydrodefluorination of organofluorine compounds with trialkylsilanes using $[\text{Ph}_3\text{C}][\text{HCB}_{11}\text{Cl}_{11}]$ (top). Silane-fueled proton-catalyzed Friedel-Crafts coupling of fluoroarenes (bottom).

1.7.1 Carborane functionalization

The C-H position of **501** and its halogenated derivatives can be readily functionalized.^{111,130,131} For example, the C-H vertex of **502** can be deprotonated with alkoxide bases allowing straightforward C-alkylation.¹³¹ In more recent examples, Lavallo and co-workers have developed carboranyl phosphine^{132,133,134} and carboranyl N-heterocyclic carbene¹³⁵ ligands bearing **501** and its derivatives. The B-H positions of **501** are also readily functionalized. The B-H bonds of **501** are hydridic and the 12-position (Figure I-2) is the most reactive towards electrophiles followed by positions 7-11 (Figure I-2) with positions 2-6 (Figure I-2) being the least nucleophilic.¹¹¹ An astounding number of derivatives of **501** are found throughout the literature but the two most common types of B-H substitution are halogenation and alkylation.¹¹¹ Michl and

co-workers have extensively investigated the alkylation¹³⁶⁻¹⁴¹ of **501** including the use of microwave-assisted alkylations¹⁴¹ to give methyl and ethyl substituted derivatives of **501**. The Ozerov group has developed methods for the chlorination and bromination of **501** using readily available halogenating reagents such as SO_2Cl_2 , SbCl_5 and Br_2 .¹⁴²

CHAPTER II
HIGH-TURNOVER AROMATIC C-H BORYLATION CATALYZED BY
POCOP-TYPE PINCER COMPLEXES OF IRIDIUM[†]

2.1 Introduction

The use of pincer complexes for catalytic C-H functionalization has been realized for over 20 years yet the use of pincer complexes in C-H borylation is still an emerging area of interest. With the lessons of C-H borylation discussed throughout Chapter 1 in mind, the notion of borylation catalysis with Ir supported by a tridentate, monoanionic pincer ligand appeared plausible. Some efforts in pincer-ligated Ir-catalyzed arene borylation have been reported. Shimada et al.¹⁴³ determined that (PSiP)Ir precatalyst **201** gave 5-80 turnovers in the borylation of benzene with B₂pin₂ after 1 d at 120 °C (Figure II-1). Driess and Hartwig tested iridium complexes **202**, **203**, and **204** (Figure II-1) supported by the sterically bulky (POCOP^{tBu}), (SiCSi) and (GeCGe) ligands, respectively, finding that they gave low TON (<20) under similar conditions.¹⁴⁴

[†] Reproduced in part from “High-Turnover Aromatic C-H Borylation Catalyzed by POCOP-type Pincer Complexes of Iridium” by Press, L. P.; Kosanovich, A. J.; McCulloch, B. J.; Ozerov, O. V. *J. Am. Chem. Soc.* **2016**, ASAP. Copyright [2016] by The American Chemical Society. All X-ray structures were solved by Billy McCulloch.

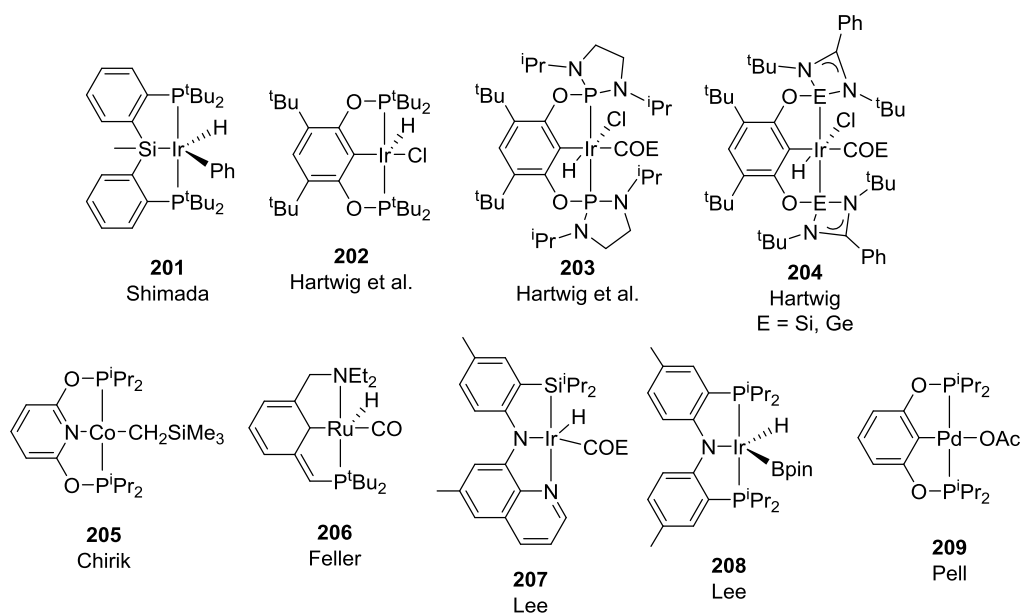
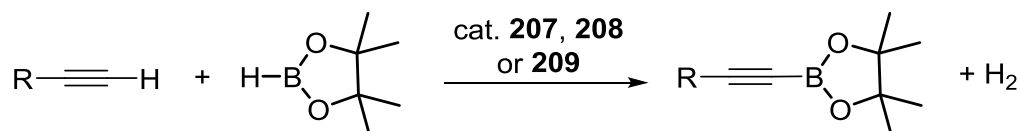


Figure II-1. Examples of Ir pincer complexes used in C-H borylation studies.

Importantly, they noted a modest increase in the yield of C-H borylated product upon addition of cyclooctene (COE) as a sacrificial hydrogen acceptor.¹⁴⁴ It was remarked that the sterically imposing pincers used in their study may have been detrimental to catalysis. Chirik's group has successfully used cobalt pincer complexes such as **205** (Figure II-1) in the catalytic borylation of arenes and heteroarenes,^{57,145} but those examples utilize neutral, tridentate pincers and must function via a different mechanism. Feller and Milstein reported the (PCN)Ru complex **206** slowly catalyzed the borylation of benzene with B₂pin₂ after 72 h at 90 °C giving 37 TON (Figure II-1).¹⁴⁶ The Ozerov group developed the catalytic dehydrogenative borylation of terminal alkynes (DHBTA, Scheme I-1) by pincer complexes (SiNN)Ir **207**, (PNP)Ir **208** and (POCOP)Pd **209** (Figure II-1), among others.¹⁴⁷⁻¹⁴⁹ DHBTA appears to be orthogonal to C-H

borylation of aromatic C-H bonds in that our Ir DHBTA catalysts based on amido-containing pincers showed no propensity towards the borylation of arenes, while the bipyridine-based Ir catalysts for aromatic C-H borylation were incapable of DHBTA.¹⁴⁷



Scheme II-1. DHTBA reaction catalyzed by complexes 207, 208 and 209.

However, in the course of exploring the potential of pincer-based Ir complexes for borylation, we came across a catalytic system for the C-H borylation of arenes whose activity and longevity rivals that of the state-of-the-art Ir catalysts supported by neutral bidentate ligands. The key to our findings lies in the use of smaller POCOP-type pincers vs the study of Driess and Hartwig, as well as in the use of smaller olefins as hydrogen acceptors. In contrast to the systems summarized in Scheme I-12 and Scheme I-13, the evidence in our case points to C-H activation not at an Ir(III) boryl intermediate, but rather at an Ir(I) center, in a step analogous to the C-H activation step in the studies of catalytic alkane dehydrogenation and many other reactions by POCOP and PCP-type pincer complexes of iridium (Scheme I-18).⁸⁰

2.2 Results and discussion

2.2.1 Synthesis of (POCOP)Ir(H)(Cl) and (POCOP)Ir(olefin) precatalysts

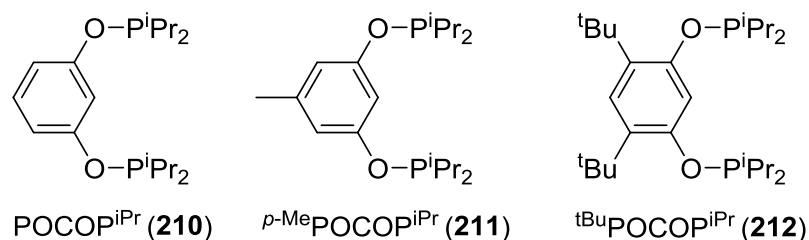
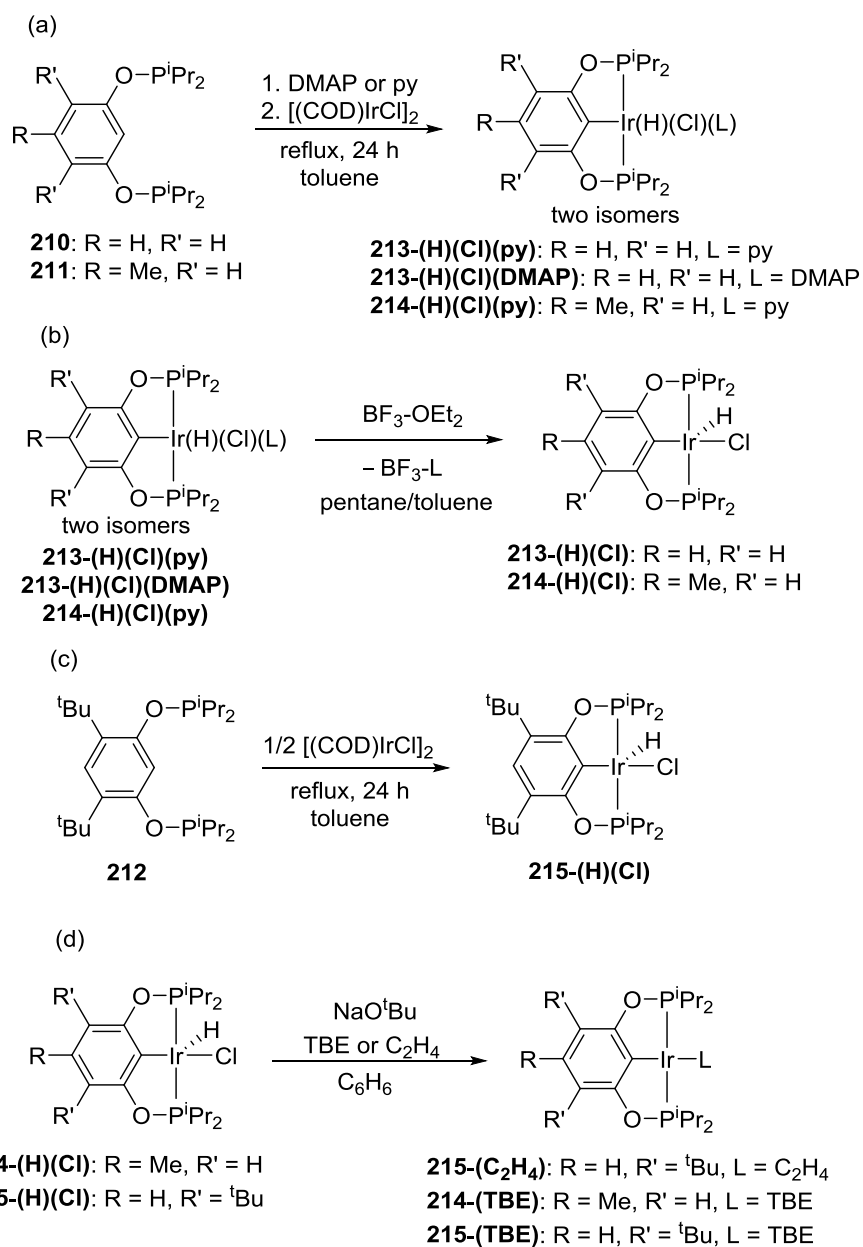


Figure II-2. POCOP (pro)ligands used in this study.

Introduction of monoanionic L₂X type pincer ligands into the coordination sphere of Ir is commonly accomplished by metalation of the proligand with [(COD)IrCl]₂ or [(COE)₂IrCl]₂, whereby oxidative addition of the central element-hydrogen bond leads to compounds of the general formula: (pincer)Ir(H)(Cl). For POCOPⁱPr (**210**, Figure II-2), the corresponding synthesis has been described by Morales-Morales,⁹¹ but in our hands, reaction of ligand **210** with [(COD)IrCl]₂ or [(COE)₂IrCl]₂ in toluene at reflux for 24 h led only to complex mixtures. Instead, we were able to access pure hydrido-chloride complexes **213-(H)(Cl)** and **214-(H)(Cl)** via a procedure analogous to the one utilized in the synthesis of (POCOPⁱPr)Rh compounds.^{150,151} Reacting [(COD)IrCl]₂ with pyridine or DMAP, followed by the addition of **210** and *p*-MePOCOPⁱPr (**211**, Figure II-2), gave adducts **213-(H)(Cl)(DMAP)** and **214-(H)(Cl)(py)** (Scheme II-2a). The pyridine ligand was then abstracted from **213-**

(H)(Cl)(DMAP) (two isomers) or **214-(H)(Cl)(py)** (two isomers) with $\text{BF}_3 \cdot \text{Et}_2\text{O}$ to give moderate yields of pure **213-(H)(Cl)** and **214-(H)(Cl)** (Scheme II-2b). A recent report by Waterman and co-workers showed that a direct reaction of **210** with $[(\text{COE})_2\text{IrCl}]_2$ at 120 °C for 24 h in toluene under an atmosphere of H_2 gave **213-(H)(Cl)** in excellent yields.^{152,153} The more strictly rigid $^{\text{tBu}}\text{POCOP}^{\text{iPr}}$ (**212**, Figure II-2), carrying two *tert*-butyl substituents on its central aromatic ring, did not require the pyridine addition/abstraction protocol, and pure **215-(H)(Cl)** was isolated from direct metalation in excellent yield (Scheme II-2c). Dehydrochlorination of **214-(H)(Cl)** or **215-(H)(Cl)** with NaO^{tBu} in the presence of ethylene or 3,3-dimethyl-1-butene (*tert*-butylethylene or TBE) provided the corresponding olefin adducts **215-(C₂H₄)**, **214-(TBE)** and **215-(TBE)** (Scheme II-2d).

Complexes **213-(H)(Cl)**, **214-(H)(Cl)** and **215-(H)(Cl)** display a triplet hydride resonance at ca. -37 ppm in their ^1H NMR spectra. This is somewhat downfield from the hydride signals for the analogous complex **202** (ca. -42 ppm, Figure II-1).¹⁴⁴ The structures of **213-(H)(Cl)** (reported by Waterman et al.)^{152,153} and **215-(H)(Cl)** (this work, Figure II-3, *vide infra*) in the solid state present as chloride-bridged dimers, in contrast to the monomeric solid-state structures determined for the $(\text{POCOP}^{\text{tBu}})\text{Ir}(\text{H})(\text{Cl})$ analogs.^{144,154} In solution **213-(H)(Cl)**, **214-(H)(Cl)** and **215-(H)(Cl)** likely exist in rapid equilibrium between dimeric and monomeric forms, resulting in the observation of an ^1H NMR chemical shift that is a weighted average of the two.



Scheme II-2. Synthesis of (POCOP)Ir complexes.

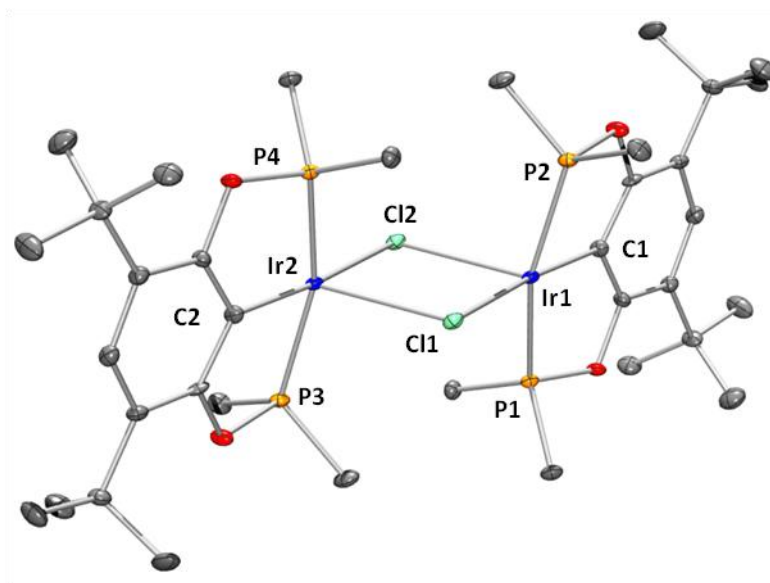


Figure II-3. ORTEP¹⁵⁵ drawings (50% probability ellipsoids) of **215-(H)(Cl)**. Omitted for clarity: H atoms and methyl groups of isopropyl arms. Selected distance (Å) and angles (°) follow: Ir1-Ir2, 4.040(1); Ir1-Cl1, 2.5169(9); Ir1-Cl2, 2.594(1); Ir1-C1, 2.042(2); P1-Ir1-P2, 158.09(3); C1-Ir1-Cl1, 173.6(1).

2.2.2 Catalytic arene borylation studies with (POCOP)Ir pre-catalysts

Initial experiments using 5 mol% **213-(H)(Cl)**, **214-(H)(Cl)**, **215-(H)(Cl)** or **215-(TBE)** as pre-catalysts for the borylation of C₆D₆ with HBpin or B₂pin₂ at temperatures up to 100 °C for 72 h resulted in only stoichiometric formation (1 turnover) of C₆D₅Bpin (**A**) (Table II-1, entries 1–3, 7, 11). Repeating the HBpin experiments using 1-hexene as a hydrogen acceptor (Table II-1, entries 4-6, 8) yielded 75-88% of C₆D₅Bpin and 11-24% of hexylBpin (Table II-1, entry 5) after 30 min at 80 °C. The use of TBE as H₂ acceptor (Table II-1, entry 10) diminished the rate of C₆D₆ borylation relative to the rates

with ethylene (Table II-1, entry 13) or 1-hexene (Table II-1, entry 6). The reaction of C_6D_6 and HBpin with 5 mol% of **215-(H)(Cl)** and ethylene at 80 °C (Table II-1, entry 13) was complete within minutes of heating, while an analogous reaction using 1-hexene took 0.5 h to reach completion (Table II-1, entry 6). We surmised the order of increased rate of C_6D_5Bpin formation (ethylene > 1-hexene > TBE) could be explained by the smaller ethylene ligand having an increased rate of coordination and subsequent olefin insertion into the Ir-H or Ir-B bonds. Ethylene has previously been demonstrated to be a capable hydrogen acceptor in other dehydrogenative transformations catalyzed by POCOP-iridium systems.^{96,156} Remarkably, we found that borylation of C_6D_6 with ethylene as the hydrogen acceptor could use as little as 0.1 or even just 0.004 mol% precatalyst **215-(H)(Cl)** (Table II-1, entries 14 and 15), resulting in 83% yield of C_6D_5Bpin after 14 h at 80 °C. This translates to a turnover number (TON) of over 20,000 and turnover frequency (TOF) of 1480 h^{-1} . An attempt at borylation with B_2pin_2 was unaffected by addition of 1-hexene (Table II-1, entry 12); only 1 equivalent of C_6D_5Bpin was produced. Performing the reaction with HBpin under argon flow in an open vessel (to potentially allow evolution of H_2 byproduct) also resulted in only one equiv. of C_6D_5Bpin (Table II-1, entry 9).

In catalytic reactions utilizing precatalyst **215-(H)(Cl)**, the fate of the Ir complex after all HBpin had been consumed was either the respective olefin complex (POCOP)Ir(olefin) or the chloro boryl complex (POCOP)Ir(Cl)(Bpin) [**215-(Bpin)(Cl)**]. For example, utilizing **215-(H)(Cl)** with ethylene (Table II-1, entry 13), **215-(Bpin)(Cl)** and **215-(C₂H₄)** were observed as the main products among several other compounds by

^1H and $^{31}\text{P}\{^1\text{H}\}$ NMR spectroscopy. The catalytic reaction utilizing **215-(H)(Cl)** with 1-hexene (Table II-1, entry 6) contained **215-(Bpin)(Cl)** as well as **215-(hexene)** after catalysis, while experiments using **215-(TBE)** with 1-hexene (Table II-1, entry 8) gave almost exclusively **215-(hexene)** as the final organometallic product.

Table II-1. C–H borylation experiments using (POCOP)Ir pre-catalysts^a

Entry	pre-cat	mol %	boryl reagent	H ₂ acceptor	temp (°C)	time (h)	TON	TOF (h ⁻¹)	Yield(%) C ₆ D ₅ Bpin	Yield(%) alkylBpin
1	213-(H)(Cl)	5.0	HBpin	none	100	36	1	<1	6	---
2	214-(H)(Cl)	5.0	HBpin	none	100	36	1	<1	4	---
3	215-(H)(Cl)	5.0	HBpin	none	100	36	1	<1	6	---
4	213-(H)(Cl)	5.0	HBpin	1-hexene	80	0.5	16	32	77	22
5	214-(H)(Cl)	5.0	HBpin	1-hexene	80	0.5	17	34	85	14
6	215-(H)(Cl)	5.0	HBpin	1-hexene	80	0.5	15	30	75	24
7	215-(TBE)	5.0	HBpin	none	80	1	1	<1	6	---
8	215-(TBE)	5.0	HBpin	1-hexene	80	0.5	18	36	88	11
9	215-(TBE)	5.0	HBpin	none	80	0.5	1	<1	5	---
10	215-(TBE)	5.0	HBpin	TBE	80	1	13	13	66	33
11	215-(TBE)	5.0	B ₂ pin ₂	none	100	72	1	<1	5	---
12	215-(TBE)	5.0	B ₂ pin ₂	1-hexene	100	72	1	<1	5	<1
13	215-(H)(Cl)	5.0	HBpin	ethylene	80	< 0.2	16	80	80	19
14	215-(H)(Cl)	0.1	HBpin	ethylene	80	0.5	760	1520	76	24
15	215-(H)(Cl)	0.004	HBpin	ethylene	80	14	20750	1480	83	17

^a. All entries used a 1:25 HBpin (0.28 mmol):C₆D₆ (7 mmol) ratio and a 1:3 HBpin (0.28 mmol):olefin (0.84 mmol) ratio. Entries 1-12 used cyclohexane internal standard (0.19 mmol). Entries 13-15 used mesitylene internal standard (0.072 mmol). Yields of C₆D₅Bpin and RBpin are spectroscopic yields. In entries where the sum of C₆D₅Bpin and RBpin yield are <100% the remaining percent was unadulterated HBpin.

We performed a series of benzene borylation experiments using 0.1 mol% **214-(H)(Cl)** as precatalyst and varied the concentrations of benzene and 1-hexene relative to the constant (0.4 M) concentration of HBpin (Table II-2). It was clear that the degree of consumption of HBpin increased with increased benzene concentration, but there was no consistent trend with respect to the effect of 1-hexene concentration.

Table II-2. Effect of varying benzene:1-hexene concentration on PhBpin:hexylBpin ratio^a

(POCOP)Ir pre-catalyst
214-(H)(Cl)
n-heptane, 80 °C

Entry	C ₆ H ₆ (M)	1-hexene (M)	PhBpin (%) ^b	hexylBpin (%) ^b
1	0.4	0	0	0
2	0.4	0.4	4	23
3	0.4	0.9	4	26
4	0.4	1.3	3	29
5	2.2	0.4	21	16
6	2.2	0.9	34	33
7	2.2	1.3	46	47
8	4.4	0.4	53	16
9	4.4	0.9	65	35
10	4.4	1.3	69	31
11	11	0.4	78	22
12 ^c	11	0.9	82	18
13 ^c	11	1.3	80	20

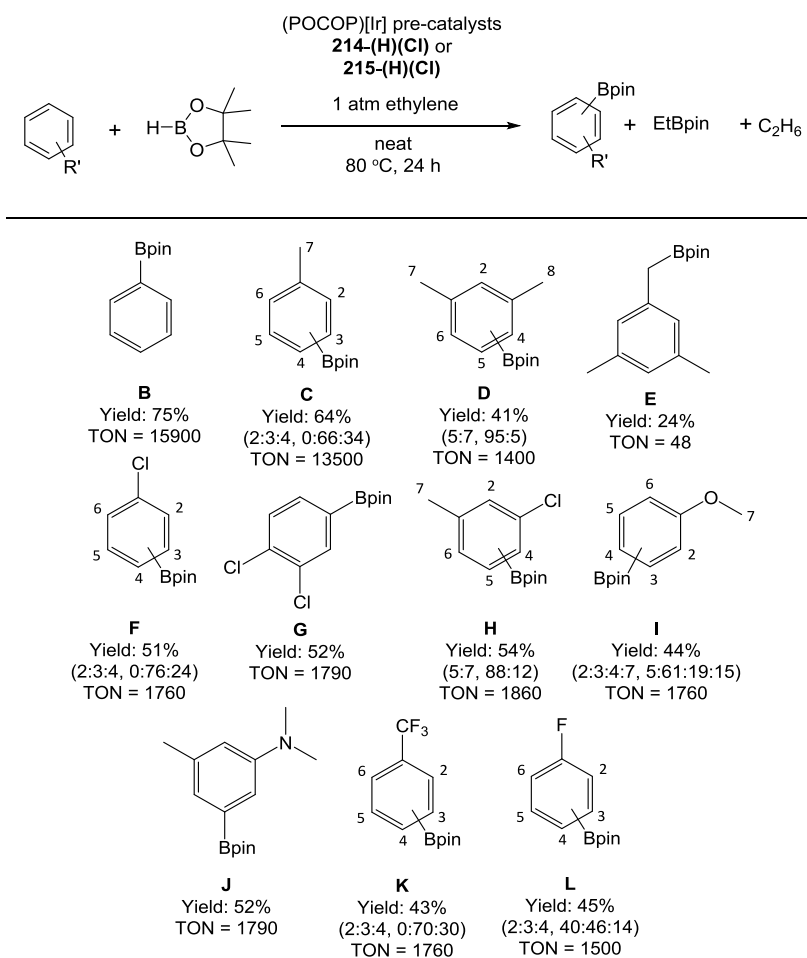
a. Each entry contains HBpin (0.4 M) as the limiting reagent. **214-(H)(Cl)** (0.60 μmol) was added as a stock solution in benzene. *n*-heptane was added as required to normalize each entry to a total volume of 1.6 mL. All entries were heated to 80 °C and monitored by ¹¹B NMR after 18 h and 36 h. b. In entries where the sum of PhBpin and hexylBpin conversion values was < 100%, the remaining % was unadulterated HBpin. c. All HBpin was consumed after 18 h

2.2.3 Preparative scale catalytic arene borylation using (POCOP)Ir precatalysts

In a series of 0.20 to 0.35 gram scale reactions, the high activity of the (POCOP)Ir system was demonstrated in experiments utilizing 0.005 mol% of **215-**

(H)(Cl) in the reaction of HBpin with benzene and ethylene (3:1 to HBpin) (**Table II-3**, entry **B**). C₆H₅Bpin (**B**) was isolated in a 75% yield which translates to TON = 15,900 with a TOF = 700 h⁻¹. Expanding the substrate scope to various substituted arenes (**Table II-3**) including toluene, *m*-xylene, mesitylene, chlorobenzene, *o*-dichlorobenzene, *m*-chlorotoluene, anisole, N,N-dimethyl-*m*-toluidine, and benzotrifluoride, we found high turnovers with moderate yields of ArBpin after 24 h at 80 °C using pre-catalysts **214-(H)(Cl)** and **215-(H)(Cl)**. The selectivity of the borylated products was decidedly under steric control which is typical of most iridium-catalyzed C-H borylations.⁴⁹ Mono-substituted arenes gave nearly statistical mixtures of *ortho*- and *para*-borylated products while 1,2-disubstituted or 1,3-disubstituted arenes were borylated exclusively in the 4 or 5 position, respectively. An exception was fluorobenzene which was borylated at the *ortho*, *meta* and *para* positions in a 40:46:14 ratio (**Table II-3**, Entry **L**). In addition, we observed up to 15% sp³ C-H borylation in *m*-xylene, *m*-chlorotoluene, and anisole. Metal catalyzed borylation of benzylic CH bonds has been demonstrated with various systems including Rh,¹⁵⁷ Pd,¹⁵⁸ Ir^{159,160} and more recently Co.¹⁴⁵ When mesitylene was used, we observed exclusive borylation at the sp³ C-H bond that proceeded much more slowly than the borylation of aromatic C-H bonds in other substrates.

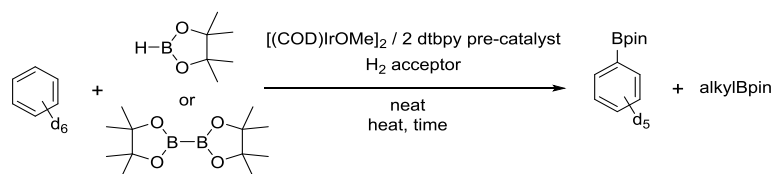
Table II-3. Catalytic arene borylation using (POCOP)Ir pre-catalysts^a



a. Entry **B** and **C** utilized 0.005 mol% of **215-(H)(Cl)**. Entries **D-L** utilized 0.03 mol% of **214-(H)(Cl)** except entry **E** which used 0.5 mol% of **214-(H)(Cl)**. All reactions were run in neat arene for 24 h at 80 °C with 1 atm of ethylene (4 mmol total) added to the reactor headspace. Isolated yields (%) of ArBpin are calculated based on HBpin. Catalyst loading is expressed by [(mol of pre-catalyst/mol of HBpin) × 100]. TONs were calculated by [(mol of HBpin added) × (isolated yield of ArBpin)/(mol of pre-catalyst)].

2.2.4 Comparison with the ITHM arene borylation system

We investigated one variation of the ITHM (Ishiyama, Takagi, Hartwig, and Miyaura)⁴⁶ arene borylation catalyst system¹⁶¹ (i.e. [(COD)IrOMe]₂ with 4,4'-di-*tert*-butyl-2,2'-bipyridine or dtbpy) and the effects of adding excess olefin (Table II-4). Reacting HBpin or B₂pin₂ with neat C₆D₆ utilizing [(COD)IrOMe]₂/2 dtbpy as pre-catalyst gave high yields of C₆D₅Bpin (Table II-4, entries 1 and 3) while an identical reaction setup in parallel where 1-hexene was added resulted in a large amount of olefin hydroboration product (Table II-4, entries 2 and 4). Repeating the high TON experiments reported in the literature,⁶² we found [(COD)IrCl]₂/2 dtbpy precatalyst with B₂pin₂ in benzene indeed gave a high TON (7000) after 24 h at 100 °C (Table II-4, entry 5). However, catalysis was totally inhibited by addition of ethylene (Table II-4, entry 6). We also found that [(COD)IrOMe]₂ in the absence of added ligand catalyzed the reaction of HBpin with neat C₆D₆ giving C₆D₅Bpin in 17% yield (Table II-4, entry 7) after 18 h at 80 °C, but addition of 1-hexene resulted predominantly in hydroboration (91% yield of hexylBpin, Table II-4, entry 8). All in all, it appears that the ITHM catalyst system is inhibited by the addition of small sacrificial olefins.

Table II-4. C-H borylation experiments using ITHM pre-catalysts^a

Entry	pre-cat	mol %	boryl reagent	H ₂ acceptor	temp (°C)	time (h)	TON	Yield (%)	
								C ₆ D ₅ Bpin	alkylBpin
1	[(cod)IrOMe] ₂ /2 dtbpy	2.5/5.0	HBpin	none	80	1.5	72	---	
2	[(cod)IrOMe] ₂ /2dtbpy	2.5/5.0	HBpin	1-hexene	80	0.5	21	74	
3	[(cod)IrOMe] ₂ /2 dtbpy	2.5/5.0	B ₂ pin ₂	none	80	1	87	---	
4	[(cod)IrOMe] ₂ /2 dtbpy	2.5/5.0	B ₂ pin ₂	1-hexene	80	0.5	57	37	
5	[(cod)IrCl] ₂ /2 dtbpy	0.0015/0.003	B ₂ pin ₂	none	100	24	7000	21	---
6	[(cod)IrCl] ₂ /2 dtbpy	0.0015/0.003	B ₂ pin ₂	ethylene	100	24	<1	<1	2
7	[(cod)IrOMe] ₂	2.5	HBpin	none	80	18	17	---	
8	[(cod)IrOMe] ₂	2.5	HBpin	1-hexene	80	0.5	<1	91	

a. Entries with HBpin used a 1:25 HBpin (0.28 mmol):C₆D₆ (7 mmol) ratio. Entries 3 and 4 used a 1:25 B₂pin₂(0.28 mmol):C₆D₆ (7 mmol) ratio. Entries with added olefin used a 1:3 HBpin (0.28 mmol):olefin (0.84 mmol) ratio. Entries 1-8 used cyclohexane internal standard (0.19 mmol). Yields of C₆D₅Bpin and RBpin are spectroscopic yields. In entries where the sum of C₆D₅Bpin and RBpin yield are <100% the remaining percent was unadulterated HBpin and/or B₂pin₂.

2.2.5 Synthesis of relevant (POCOP)Ir compounds

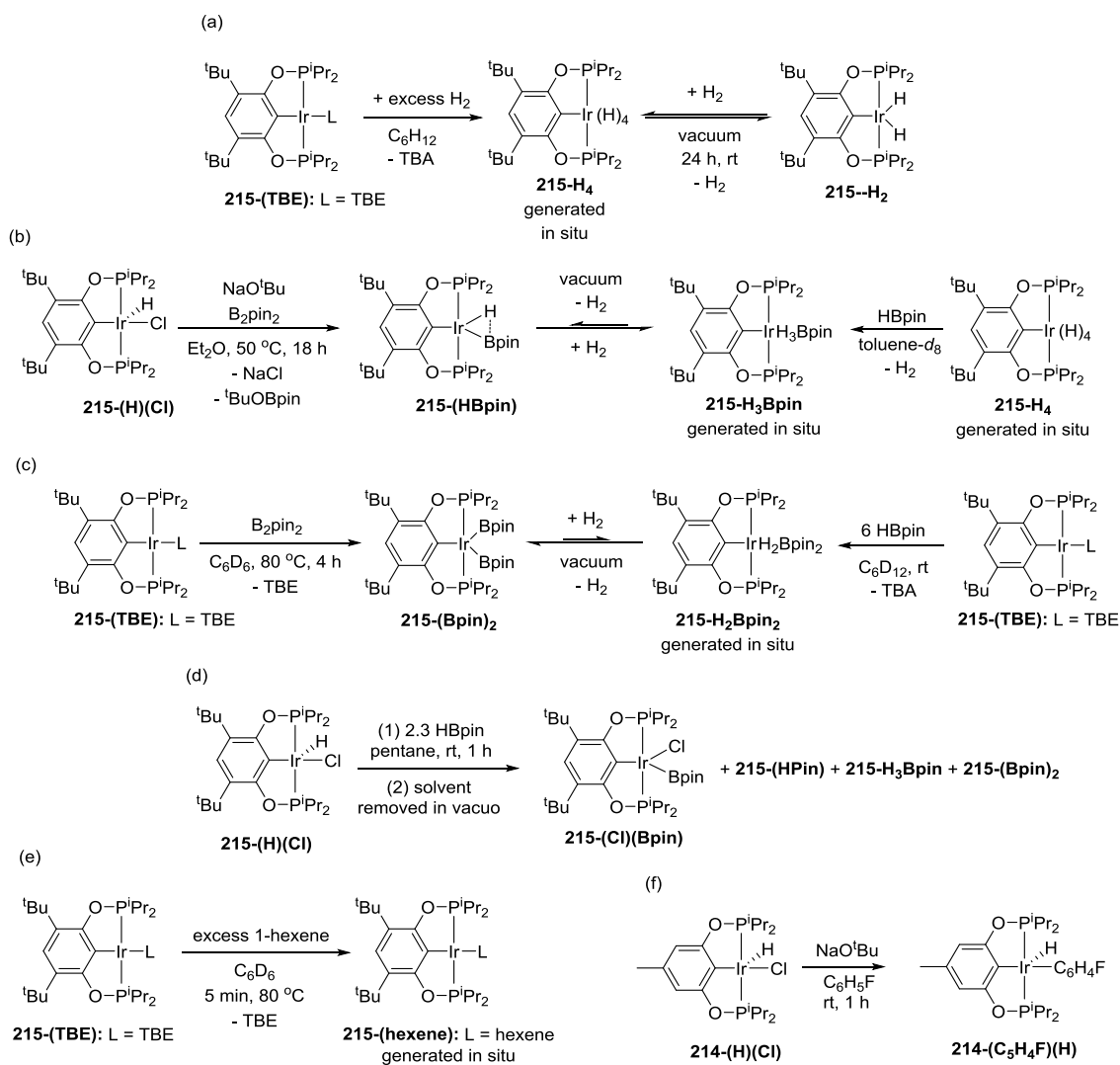
We sought to prepare Ir complexes that may be plausibly relevant to borylation, and also to examine the reactions of pre-catalysts **215-(H)(Cl)** and **215-(TBE)** with HBpin. Considering the similar activity engendered by the three POCOP-type ligands discussed, we selected Ir complexes of ligand **212** and **211** for these studies out of synthetic convenience.

Treatment of the TBE complex **215-(TBE)** with excess H₂ generated the polyhydride compound **215-H₄** *in situ* (Scheme II-3a). Similar to (POCOP^{tBu})Ir(H)₄ (**118-H₄**),¹⁶² attempts to isolate **215-H₄** by removal of solvent in vacuo (24 h of dynamic vacuum at ambient temperature) resulted in loss of H₂ to give **215-H₂** (Scheme II-3a). The HBpin complex **215-(HBpin)** was synthesized and isolated by treatment of **212-(H)(Cl)** with B₂pin₂ and NaO^tBu in diethyl ether at 50 °C for 18 h (Scheme II-3b). Complex **215-H₃Bpin** exists in equilibrium with **215-(HBpin)** and H₂, and was observed as the dominant product *in situ* upon exposure of **215-(HBpin)** to an H₂ atmosphere, or by adding HBpin to **215-H₄** (Scheme II-3b). Facile loss of H₂ precluded isolation of **215-H₃Bpin** in a pure form. The diboryl complex **215-(Bpin)₂** was independently prepared and isolated via thermolysis of **215-(TBE)** with B₂pin₂ in benzene (Scheme II-3c). Compounds **215-H₃Bpin** and/or **215-(Bpin)₂** were occasionally observed as impurities in varying amounts (up to 20%) during the synthesis of **215-(HBpin)**. Reacting **215-(TBE)** with excess HBpin (20 equiv) in C₆D₆, then heating to reflux under argon flow for 0.5 h gave a mixture of **215-(Bpin)₂** and a second C_{2v} symmetric compound, tentatively assigned as **215-H₂Bpin₂**. Similar to compound **215-H₃Bpin**, loss of H₂ precluded the isolation of **215-H₂Bpin₂**. When **215-(TBE)** was reacted with HBpin (6 equiv) in cyclohexane-*d*₁₂ at ambient temperature, **215-H₂Bpin₂** was observed as the major product *in situ* (Scheme II-3c). Subjecting the resultant mixture to high vacuum gave a mixture comprised of mostly **215-(Bpin)₂**. We attempted to prepare pure **215-H₃Bpin** by treating **215-(H)(Cl)** with 2.3 equiv of HBpin in pentane at ambient temperature. We anticipated the reaction would generate **215-H₃Bpin** and ClBpin,

whereupon the volatile ClBpin could be easily removed *in vacuo*. Unexpectedly, the reaction resulted in a mixture of four compounds including **215-(HBpin)** (9%), **215-H₃Bpin** (5%), **215-(Bpin)₂** (33%), and **215-(Cl)(Bpin)** (52%) (Scheme II-3d). Using column chromatography, compound **215-(Cl)(Bpin)** was isolated out of this mixture in 42% yield. The TBE ligand of **215-(TBE)** was readily displaced, as heating a C₆D₆ solution of **215-(TBE)** containing excess 1-hexene at 80 °C gave **215-(hexene)** within minutes (Scheme II-3e).

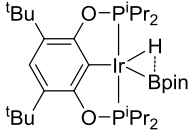
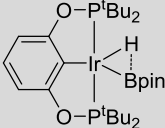
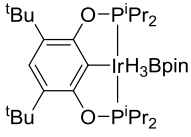
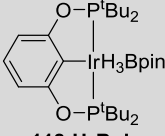
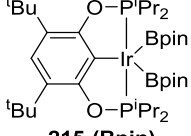
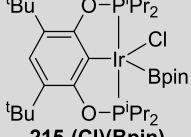
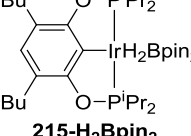
We investigated various routes to synthesize pure hydrido/phenyl complexes of (POCOP)Ir, but were only able to obtain complex mixtures. This includes: (a) reaction of **3c** with 1 equiv of PhLi (as a solution in di-*n*-butyl ether) in C₆D₆ at ambient temperature. (b) dehydrochlorination of **3c** with NaO^tBu in C₆D₆. (c) Thermolysis of **215-(TBE)** in C₆D₆ at 90 °C for up to 24 h. Dehydrochlorination of **215-(H)(Cl)** with NaO^tBu in neat C₆H₆ prepared free of ethers and halocarbons did give one major product in the ³¹P{¹H} NMR spectrum ($\delta = 177.5$ ppm) as well as a broad hydride signal (ca. –42 ppm, C₆H₆) in the ¹H NMR spectrum. Brown solids were obtained by filtering the solution through Celite followed by lyophilization. NMR analysis at ambient temperature in cyclohexane-*d*₁₂ revealed no hydride resonances in the ¹H NMR spectrum, while the ³¹P{¹H} NMR spectrum contained multiple products. These results are consistent with the behavior of POCOP and PCP-supported hydrido-aryl complexes reported in the literature as Goldman et al. found (PCP^{tBu})Ir(Ph)(H) [**116-(Ph)(H)**] displayed only PCP ligand resonances at room temperature, and low temperature VT NMR studies were required to observe the hydride resonance.¹⁶³ Brookhart et al.¹⁶²

reported difficulty observing the hydride resonances for the isomers of (POCOP^{tBu})Ir(tolyl)(H) [**118-(tolyl)(H)**] at temperatures above 10 °C. Previous work in the Ozerov group found that (PNP)Rh(C₆H₄F)(H) existed as multiple isomers in solution, with broad hydride resonances that were unobservable without the assistance of low temperature NMR studies.¹⁶⁴ Fluorobenzene is expected to give a more favorable C-H oxidative compared to benzene.¹⁶⁵ Indeed, use of fluorobenzene gave more promising results as dehydrochlorination of **215-(H)(Cl)** with NaO^tBu in neat C₆H₅F gave **215-(C₆H₄F)(H)** as the major product, though several other compounds were observed. Alternatively, we found that dehydrochlorination of **214-(H)(Cl)** with NaO^tBu in neat fluorobenzene gave (^{p-Me}POCOP^{iPr})Ir(C₆H₄F)(H) [**214-(C₆H₄F)(H)**] in excellent yield and purity (Scheme II-3f). The broad hydride signal of **214-(C₆H₄F)(H)** observed at room temperature (−42.5 ppm, cyclohexane-*d*₁₂) is comparable to the hydride resonance observed for **118-(tolyl)(H)**.¹⁶² The chemical shift is indicative of a five-coordinate, square pyramidal complex with the hydride trans to an empty site while the broad nature of the hydride resonance likely indicates some fluxional process including the possibility that **214-(C₆H₄F)(H)** may exist as multiple isomers of (^{p-Me}POCOP^{iPr})Ir(C₆H₄F)(H) in solution.



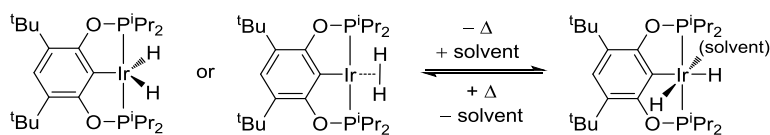
Scheme II-3. Synthesis of various (POCOP)Ir compounds.

Table II-5. Selected NMR data for Bpin-containing Ir pincer complexes

compound	^1H NMR hydride δ	^{11}B NMR δ	solvent
 215-(HBpin)	-10.64, br s	27.6	toluene- d_8
 118-(HBpin)	-13.15, br s	29.0	THF- d_8
 215-H₃Bpin	-8.10, 1H br s -10.09, 2H br s	37.0	toluene- d_8
 118-H₃Bpin	-8.00, 1H br s -10.00, 2H br s	37.0	THF- d_8
 215-(Bpin)₂	n/a	33.6	C ₆ D ₆
 215-(Cl)(Bpin)	n/a	12.0	C ₆ D ₆
 215-H₂Bpin₂	-8.30, 2H, t	unknown	C ₆ D ₆

2.2.6 XRD and NMR characterization of Ir hydrido-boryl complexes

The metrics in the X-ray structure of **215-(HBpin)** (Figure II-4, left) as well as the ^1H and ^{11}B NMR data (Table II-5) indicate the compound is a B–H σ -complex, comparable to **118-(HBpin)** reported by Heinekey and co-workers.¹⁶⁶ In that study, Heinekey and co-workers also characterized **118-H₃Bpin**. They report ^1H and ^{11}B NMR data similar to what we observe for **215-H₃Bpin** (Table II-5). An XRD study of **214-(Bpin)₂** (Figure II-4, right) supports its assignment as an Ir(III) diboryl complex, as the B1–B2 distance in **214-(Bpin)₂** (2.251(8) Å) is ca. 1/3 longer than the B–B bond distance in free B₂pin₂ (1.7040(9) Å).¹⁶⁷ The hydride resonance of **215-H₂** in cyclohexane-*d*₁₂ was broad at ambient temperature. Further inspection of the baseline of the ^1H NMR spectrum of **215-H₂** revealed a broad resonance with a chemical shift ($\delta = -17.35$ ppm, Figure II-5) that is comparable to (POCOP^{tBu})IrH₂ (**118-H₂**, $\delta = -16.99$ ppm, toluene-*d*₈, 23 °C) reported by Brookhart.¹⁶⁸



Scheme II-4. Equilibrium between **215-H₂** and **215-(H)₂(solvent)**.

A VT ^1H NMR (Figure II-6) study of **215-H₂** in toluene-*d*₈ revealed that **215-H₂** behaves in a similar fashion to **118-H₂** where **215-H₂** is in equilibrium with a six-coordinate solvent adduct **215-(H)₂(solvent)** (Scheme II-4) that is favored at lower

temperatures. This phenomena is evident with the observation of an upfield hydride resonance corresponding to a hydride ligand trans to a bound solvent molecule ($\delta = -31.69$ ppm, -90 °C, top of Figure II-6) and a downfield resonance corresponding to a second hydride ligand trans to the aryl carbon of the POCOP^{iPr} ligand ($\delta = -2.46$ ppm, -90 °C, top of Figure II-6). XRD analysis of crystals of **215-H₂** grown at room temperature from a benzene solution layered with pentane gave a dimeric form of **215-H₂** (Figure II-7).

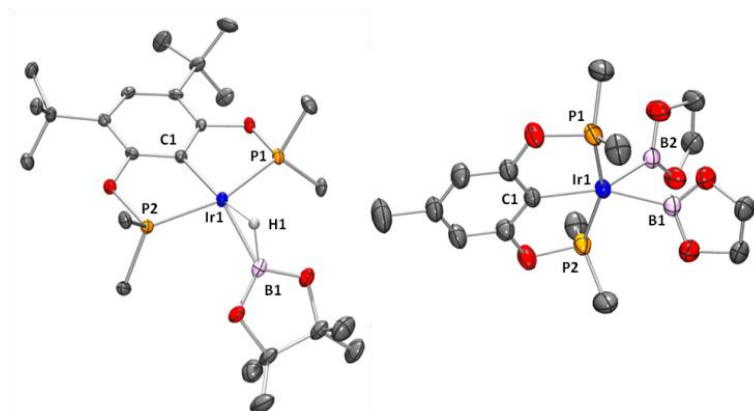


Figure II-4. ORTEP¹⁵⁵ drawings (50% probability ellipsoids) of **215-(HBpin)** (left) and **214-(Bpin)₂** (right). Omitted for clarity: H atoms, methyl groups of isopropyl arms. Selected distance (Å) and angles (°) follow: For **215-(HBpin)**: Ir1-B1, 2.069(4); Ir1-H1, 1.56(3); B1-H1, 1.42(3); P1-Ir1-P2, 159.39(3); B1-Ir1-H1, 43.0(1); C1-Ir1-B1, 149.0(1); C1-Ir1-H1, 168.0(2). For **214-(Bpin)₂**, the asymmetric unit contains two independent molecules, only values for one fragment are represented here: Ir1-B1, 2.065(4); Ir1-B2, 2.065(4); B1-B2, 2,251(8); P1-Ir1-P2, 156.92(5); C1-Ir1-B1, 146.98(11); B1-Ir-B2, 66.0(2). All XRD structures were solved by Billy J. McCulloch.

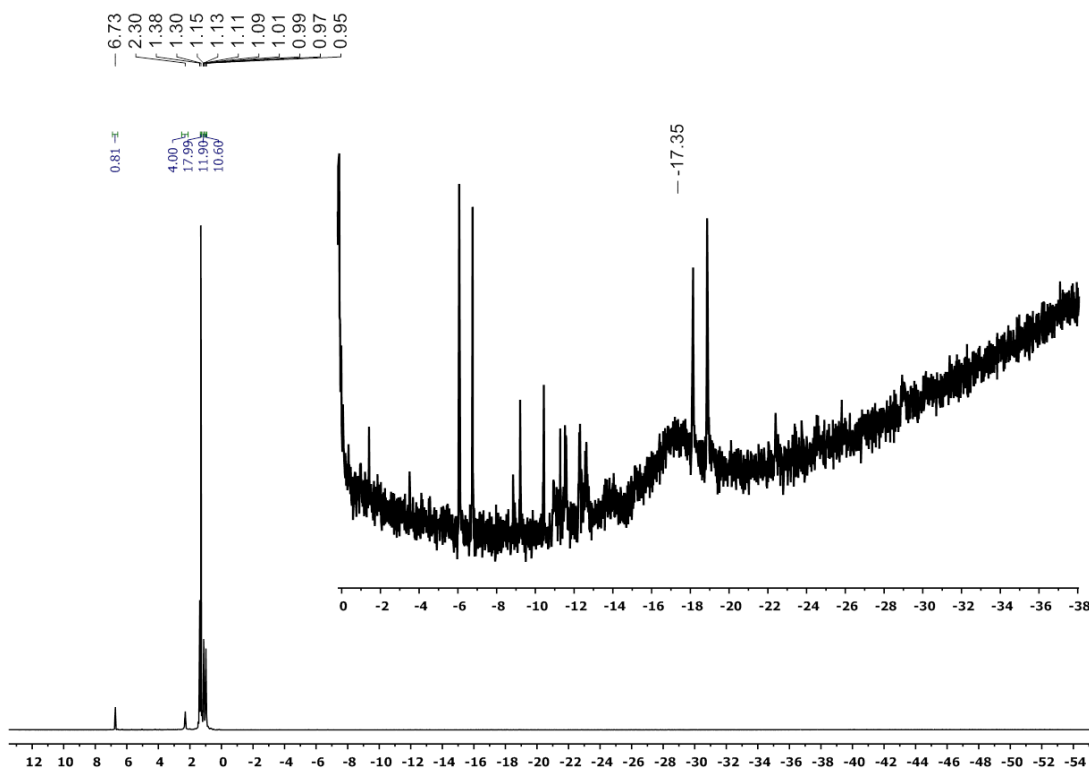


Figure II-5. ^1H NMR (500 MHz, cyclohexane- d_{12}) spectrum of **215-H₂**. Upon initial inspection, no hydride signals are observed. Further analysis of the baseline reveals a very broad signal centered at -17.35 ppm. The other hydride resonances were not identified.

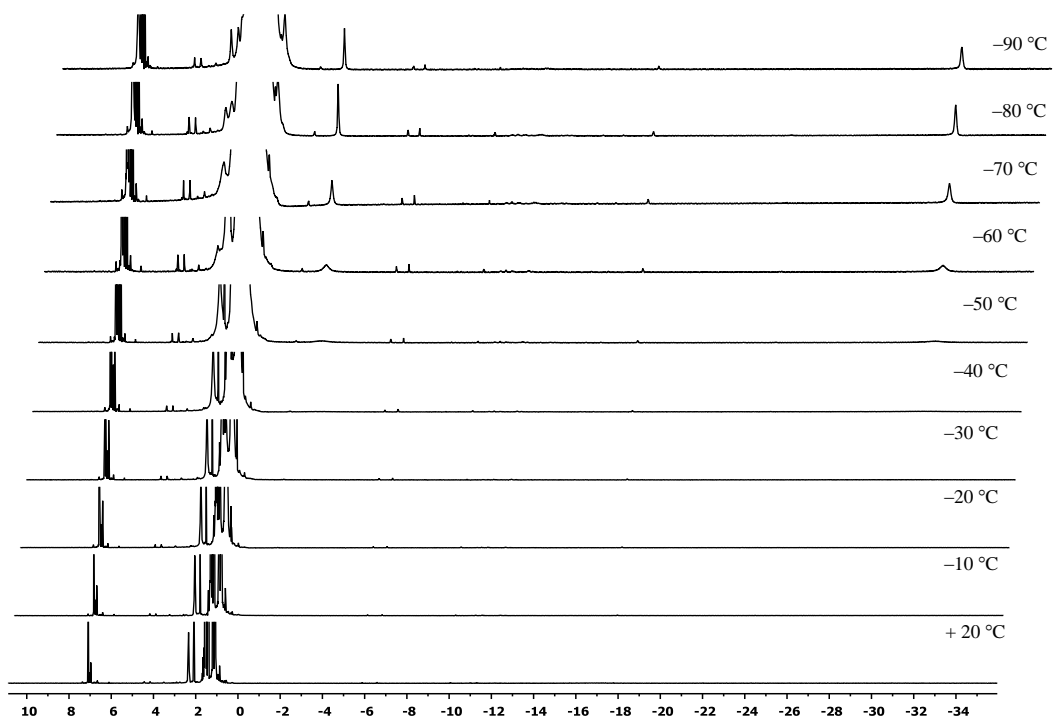


Figure II-6. Stacked VT ^1H NMR (500 MHz, $\text{toluene-}d_8$) spectra of **215-H₂** from $20\text{ }^\circ\text{C}$ (bottom) to $-90\text{ }^\circ\text{C}$ (top).

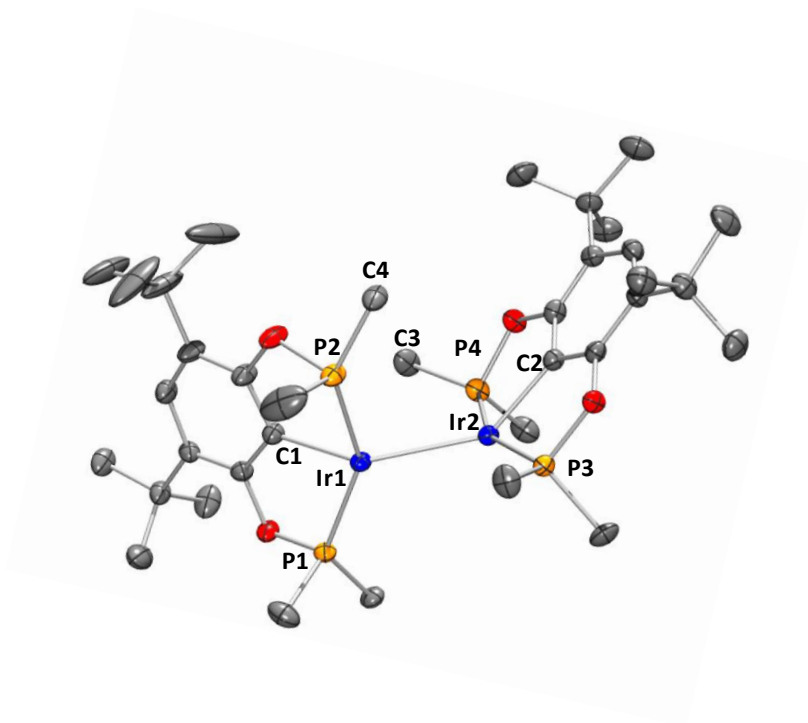


Figure II-7. ORTEP drawings (50% probability ellipsoids) of **215-H₂**. Omitted for clarity: H atoms, methyl groups of isopropyl arms. Selected distance (Å) and angles (°) follow: For **215-H₂**: Ir1-Ir2, 2.6796(7); Ir1-C1, 2.057(3); Ir2-C2, 2.044(3); Ir1-C3, 3.939(4); Ir2-C4, 3.619(4) P1-Ir1-P2, 145.01(4); P3-Ir2-P4, 155.47(4). XRD structure solved by Billy J. McCulloch.

2.2.7 C-H borylation mechanistic analysis

We were interested in exploring the nature of the C-H (or C-D) activation step that leads to the formation of the C-B bond in the arylboronate product, and in the nature of the step(s) that are involved in the hydrogenation of the olefin. The design of our pincer-based catalysts was inspired by the ITHM/Smith-Maleczka catalysts.^{46,47,50} By analogy,^{61,61-63} we initially anticipated that C-H bond activation of the arene should be

taking place at an unsaturated Ir(III) center carrying an Ir-Bpin functionality. The three compounds fitting this bill that are plausibly accessible in the catalytic mixture are **215-(HBpin)**, **215-(Bpin)₂**, and **215-(Cl)(Bpin)**. The ground state of **215-(HBpin)** is an Ir(I) σ -B-H complex, but the Ir(III) boryl/hydride form may be thermally accessible. Compound **215-(Cl)(Bpin)** could only be involved if **215-(H)(Cl)** is used as a pre-catalyst; if **215-(TBE)** is used as a pre-catalyst, there is no chlorine in the system. From the fact that **215-(Cl)(Bpin)** and **215-(TBE)** both work comparably as precursors, the necessity of **215-(Cl)(Bpin)** as an intermediate in catalysis can be ruled out. Indeed, thermolysis of **215-(Cl)(Bpin)** in C₆D₆ at 80 °C for 30 min generated no C₆D₅Bpin while heating **215-(Cl)(Bpin)** for up to 24 h at 80 °C gave a small quantity of Bpin decomposition products (ca. 21.5 ppm) in the ¹¹B NMR spectra, but C₆D₅Bpin was still not observed.

Compounds **215-(HBpin)** and **214-(Bpin)₂/215-(Bpin)₂** are stable (excluding H/D exchange observed between **215-(HBpin)** and solvent) in C₆D₆ or toluene-*d*₈ at ambient temperature for at least 48 h within NMR detection limits. Heating a C₆D₆ solution of **215-(HBpin)** at 80 °C for 30 min revealed only 15% of C₆D₅Bpin in the ¹H NMR spectrum (Scheme II-5a). At the same time, we observed rapid disappearance of the hydride signal for **215-(HBpin)** during the thermolysis experiment, while all other resonances of **215-(HBpin)** remained unchanged in the ¹H NMR spectrum (Scheme II-5a), indicating rapid H/D exchange with benzene solvent. Compound **215-(HBpin)** was distinguishable in the corresponding ³¹P{¹H} NMR spectrum from its deuterated isotopologue, **215-(DBpin)**. As the resonance for **215-(HBpin)** (190.7 ppm, C₆D₆)

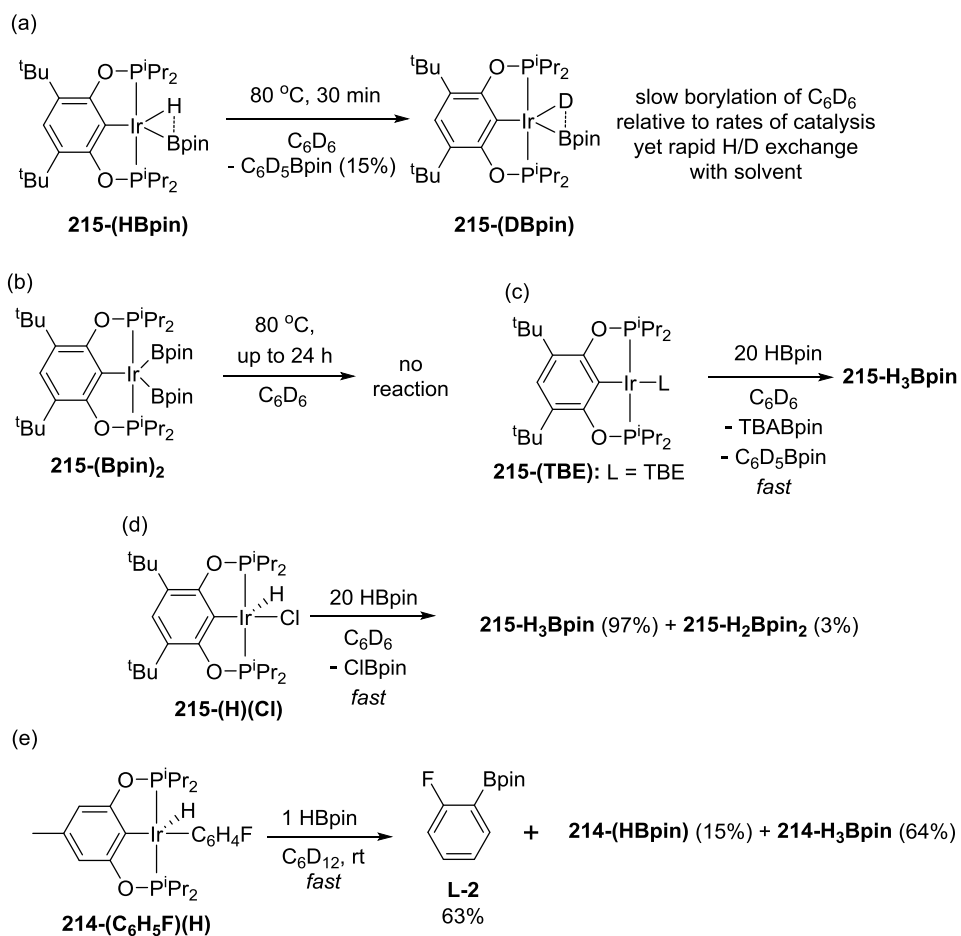
rapidly disappeared, a resonance for **215-DBpin** (190.6 ppm, C₆D₆) concurrently increased in intensity. Although C₆D₅Bpin can be produced from the reaction of **215-(HBpin)** with C₆D₆, the rate of stoichiometric borylation is too slow to correspond to the relevant C-H activation step in catalytic borylation. Compound **215-(Bpin)₂** was stable in C₆D₆ at 80 °C for up to 24 h and no C₆D₅Bpin was observed (Scheme II-5b). We also prepared **214-(Bpin)₂** via analogous reaction of **214-(TBE)** with B₂pin₂ and it displayed similar stability in C₆D₆ at room temperature and 80 °C over 24 h. These experiments show that reactions of benzene with **215-(HBpin)**, **215-(Bpin)₂** or **215-(Cl)(Bpin)** cannot be part of the catalytic cycle producing PhBpin.

With these results in mind, we considered alternative species that may be responsible for the C-H activation step in borylation catalysis. One natural candidate is the three-coordinate, 14-electron species (POCOP)Ir (**215**) (Scheme II-6), whose propensity for oxidative addition of various C-H bonds is well documented.⁸⁰ This is not an observable species, but can be accessed by reductive elimination from five-coordinate Ir(III) complexes, or by dissociation of a neutral ligand from four-coordinate Ir(I) complexes such as **215-(C₂H₄)** or **215-(TBE)**.

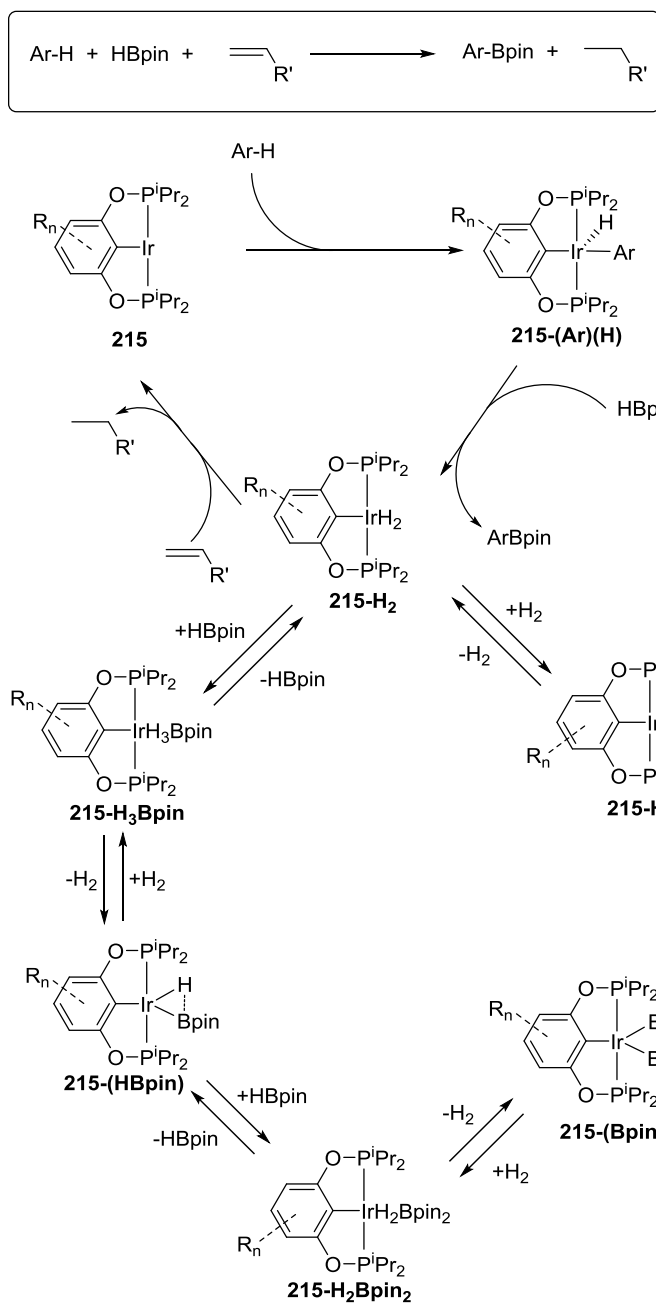
When **215-(TBE)** was treated with HBpin (20 equiv) in C₆D₆ at ambient temperature, we immediately observed only **215-H₃Bpin** in the ³¹P{¹H} NMR spectrum, while the ¹H and ¹¹B NMR spectra contained resonances for **215-H₃Bpin**, 1 equiv of TBABpin, 1 equiv of C₆D₅Bpin and the remaining HBpin (Scheme II-5c). While this reaction does produce C₆D₅Bpin, it cannot be responsible for all of the C₆D₅Bpin produced in catalysis because only a minor fraction of the hydroboration product

(e.g., TBABpin) is produced in a catalytic reaction. In other words, access to intermediate **215** in catalysis cannot rely on olefin hydroboration because hydroboration products are not generated in amounts equal to the arene borylation products. Reacting the other precatalyst, **215-(H)(Cl)**, with HBpin (20 equiv) in C₆D₆ at ambient temperature immediately generated complexes **215-H₃Bpin** and **215-H₂Bpin₂** in a 97:3 ratio (Scheme II-5d), but C₆D₅Bpin was not observed. Removal of the two Bpin groups from **215-(Bpin)₂** via diboration of an olefin is apparently inaccessible as no diboration products were observed in catalytic experiments reacting B₂pin₂ with C₆D₆, utilizing precatalyst **215-(TBE)** and 1-hexene (Table II-1, entry 12).

On the other hand, when compound **214-(C₆H₄F)(H)** was allowed to react with 1 equiv of HBpin in thawing C₆D₁₂, the *ortho*-borlyated product 2-Bpin-C₆H₄F (**L-2**) was obtained (Scheme II-5e). Our values for **L-2** match ¹H and ¹⁹F NMR data collected in CDCl₃ found within in the literature and no other isomers were observed.¹⁶⁹ The ¹⁹F NMR spectrum of this mixture contained resonances for **L-2** and free fluorobenzene, while careful monitoring of the organometallic products revealed mainly **214-H₃Bpin** (64%) and **214-(HBpin)** (15%) with various other known and unknown compounds present. The spectroscopic yield of **L-2** was found to be 63%. An analogous experiment reacting **214-(C₆H₄F)(H)** with 1 equiv of HBpin using C₆H₅F as solvent (in order to ensure the solubility of **214-(C₆H₄F)(H)**) gave comparable results in terms of **L-2** yield (67%), as well as the organometallic products observed: **214-(HBpin)** (8%), **214-H₃Bpin** (54%), **214-H₂** (3%) and **214-(C₆H₄F)(H)** (30%).



Scheme II-5. Reaction examining possible pathways for ArBpin formation.



Scheme II-6. The net catalytic reaction (top), the proposed catalytic cycle invoking the three-coordinate Ir (I) species **215**, and the auxiliary hydride/boryl redistribution equilibria. The *t*-butyl groups of the ligand backbone have been altered to R_n for clarity.

The rapid formation of the arylboronate in the reaction of **215-(Ar)(H)** with HBpin is consistent with it being part of a catalytic cycle that involves **215** (Scheme II-6). Generation of (POCOP)Ir (**215**) permits oxidative addition of Ar-H to Ir to produce **215-(Ar)(H)**, which then reacts with HBpin to generate the Ar-Bpin product. It is important to note that **215-(Ar)(H)** cannot be producing ArBpin by reductively eliminating an Ar-H molecule and adding HBpin to the resultant (POCOP)Ir to give **215-(HBpin)**, because **215-(HBpin)** does not react with free Ar-H fast enough. It is possible that the reactions of **4** with Ar-H also proceed via **215**, by elimination of HBpin, which would nonetheless be a slow process. The net catalytic reaction (Scheme II-6) does not produce free H₂ and so the equilibria between **215-(HBpin)** – **215-(Bpin)₂**, **215-H₂**, **215-H₄**, **215-H₂Bpin₂**, H₂ and HBpin (Scheme II-6) are important as a way to access **215-H₂** by the redistribution of H and Bpin groups.

In the catalytic experiments reacting HBpin with C₆D₆, compound **215-H₃Bpin** is the initial resting state of the system at room temperature. As mentioned, reacting **215-(TBE)** with HBpin (20 equiv) in C₆D₆ gives **215-H₃Bpin** at ambient temperature. After heating the solution to 80 °C for 1 h (Table II-1, Entry 7) we observed compound **215-H₃Bpin** and compound **215-H₂Bpin₂** in an 86:14 ratio with trace quantities of compounds **215-(HBpin)**, **215-(Bpin)₂** and **215-H₄** (Figure II-8, bottom). While heating the solution, we observed a color change from colorless to yellow with a transition back to colorless upon cooling. A variable temperature ³¹P{¹H} NMR study (Figure II-8) of the sample found that upon heating the solution from ambient temperature to 80 °C, the mixture of compounds **215-H₃Bpin** and **215-H₂Bpin₂** were found to be in equilibrium

with compounds **215-(HBpin)**, **215-(Bpin)₂** and **215-H₄**. This observation is in agreement with our previous experiments that established relationships between **215-H₃Bpin**, **215-(HBpin)** and H₂; **215-H₂Bpin₂**, **215-(Bpin)₂** and H₂; **215-H₄**, **215-H₂** and H₂. Notably, the complex **215-(Ar)(H)** which we would anticipate at ca. 178 ppm in the ³¹P{¹H} NMR spectrum is not observed. Compound **215-H₂** is also not observed, but the presence of **215-H₄** implies accessibility of **215-H₂** at 80 °C. Sacrificial olefin therefore removes H₂ from **215-H₂** to provide the resultant 14 e⁻ (^tBuPOCOPⁱPr)Ir fragment **215** the opportunity to react with arene.

2.3 Conclusion

This work demonstrates that high activity and high turnover number in aromatic C-H borylation is possible with POCOP-type pincer-based Ir catalysts. The use of hydrogen acceptors and their involvement in hydroboration as a minor side reaction places some limits on the applicability of this system. But, it is important to note that the presented system uses the simplest, cheapest olefins as hydrogen acceptors, whose cost is a small fraction of the borylating agent (HBpin) and is considerably lower than that of many simple arene substrates. (POCOP)Ir catalysts were found to be compatible with arene substrates containing C-O, C-N, and C-Hal bonds, and in general, display similar, sterically governed regioselectivity as that of the non-pincer Ir catalysts reported in the literature. An array of Ir complexes relevant to catalysis was independently synthesized, characterized, and their role in catalysis examined.

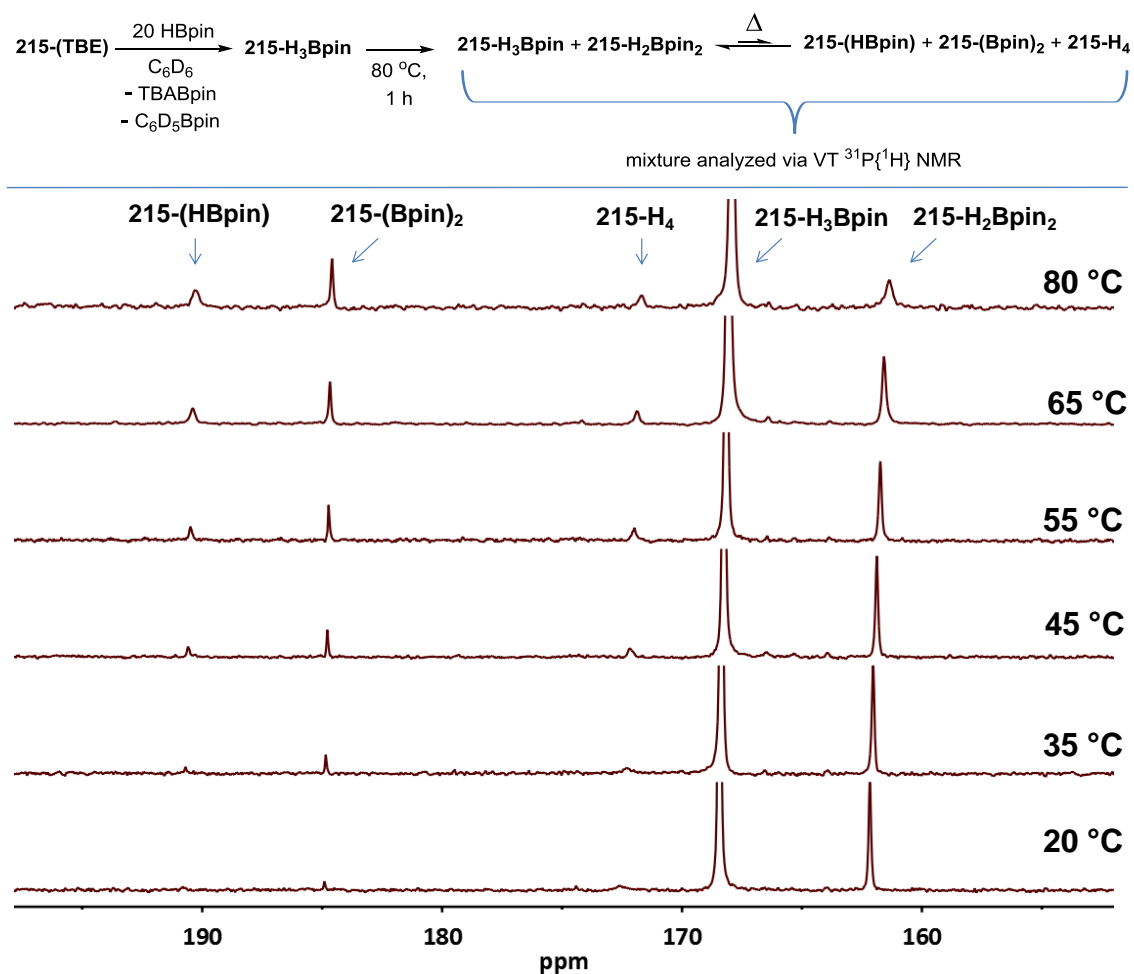


Figure II-8. $^{31}\text{P}\{^1\text{H}\}$ VT NMR (C_6D_6 , 202 MHz) spectra from 20 °C to 80 °C showing the reaction of HBpin and C_6D_6 with 5 mol% **215-(TBE)** (Table II-1, Entry 7). As the temperature increased, resonances for compounds **215-(TBE)**, **215-(Bpin)₂** and **215-H₄** increased in intensity.

Analysis of plausible mechanistic pathways led to the rather unexpected conclusion that, in contrast to Ir catalysts supported by neutral bidentate ligands, the C-H activation step in the borylation catalysis described here appears to take place not at an Ir(III) boryl center, but at an Ir(I) center devoid of boryl ligands. This is connected to the perceived role of olefin. Olefin hydrogenation is part of the net stoichiometry of the catalytic reaction, but the role olefin hydrogenation is not merely to consume H₂ equivalents released in C-H borylation, but rather to provide access to a specific reactive species instrumental to the C-H activation step – the 14-electron (POCOP)Ir. It may be speculatively proffered here that analogous pathways may need to be considered in the analysis of other Ir-based borylation catalysts.

2.4 Experimental

2.4.1 General considerations

Unless specified otherwise, all manipulations were performed under an argon atmosphere using standard Schlenk or glovebox techniques. Pentane, diethyl ether, tetrahydrofuran, mesitylene and benzene were dried over sodium–benzophenone ketyl, distilled or vacuum transferred and stored over molecular sieves in an Ar-filled glovebox. Pyridine was dried over CaH₂ then vacuum transferred and stored over molecular sieves in an Ar-filled glovebox. 4,6-di-*tert*-butylresorcinol was purified by recrystallization from THF/pentane at –30 °C prior to use. [(COD)IrCl]₂ was synthesized according to published procedures.¹⁷⁰ [(COD)Ir(OMe)]₂ was synthesized according to published procedures.¹⁷¹ All other chemicals were used as received from commercial vendors. All NMR spectra were recorded on a Varian Inova 300 spectrometer (¹H NMR

299.951 MHz, $^{31}\text{P}\{^1\text{H}\}$ NMR 121.425 MHz, $^{13}\text{C}\{^1\text{H}\}$ NMR 75.413 MHz), Varian Mercury 300 spectrometer ($^{13}\text{C}\{^1\text{H}\}$ NMR 75.426 MHz), Varian Inova 400 spectrometer (^1H NMR, 399.755 MHz; $^{13}\text{C}\{^1\text{H}\}$ NMR, 100.518 MHz; ^{11}B NMR 128 MHz, $^{31}\text{P}\{^1\text{H}\}$ NMR 181.822 MHz), or a Varian Inova NMR 500 (^1H NMR, 499.425 MHz/ 499.683 MHz; $^{13}\text{C}\{^1\text{H}\}$ NMR, 75.424 MHz/ 125.580 MHz; $^{31}\text{P}\{^1\text{H}\}$ NMR, 202.171 MHz; ^{19}F NMR, 469.854 MHz) spectrometer. All spectra were recorded at ambient temperature unless otherwise noted. Chemical shifts are reported in δ /ppm. For ^1H and $^{13}\text{C}\{^1\text{H}\}$ NMR spectra, the residual solvent peak was used as an internal reference.¹⁷² ^1H NMR spectra recorded in cyclohexane- d_{12} were referenced by setting the residual solvent peak to 1.39 ppm. ^{11}B NMR spectra were referenced externally using neat BF_3OEt_2 at $\delta = 0$ ppm, $^{31}\text{P}\{^1\text{H}\}$ NMR spectra were referenced externally using 85% H_3PO_4 at $\delta = 0$ ppm, and ^{19}F NMR spectra were referenced externally using 1.0 M $\text{CF}_3\text{CO}_2\text{H}$ in CDCl_3 at $\delta = -78.5$ ppm.

2.4.2 Synthesis of compounds

(POCOP^{iPr})-H ligand (210) – Ligand **210** was prepared according to modified literature procedures.¹⁷³ In a Schlenk flask equipped with a magnetic stir bar, resorcinol (1.08 g, 9.81 mmol) was dissolved in 20 mL of THF. NEt_3 (4.42 mL, 31.7 mmol) was added, followed by ClP^iPr_2 (3.06 g, 19.2 mmol) and a white precipitate immediately formed. The reaction was stirred at room temperature for 12 h in a glovebox. The solution was then filtered through Celite over a coarse frit, and the solvent was removed in vacuo to provide **210** as a clear oil. The product was determined to be >95% pure by NMR spectroscopy, and was used as prepared. Yield: 3.10 g (92%). ^1H NMR (500 MHz,

C_6D_6): δ 7.37 (m, 1H, Ar-*H*), 7.01 (t, 1H, Ar-*H*), 6.92 (m, 2H, Ar-*H*), 1.75 (m, 4H, PCH(CH₃)₂), 1.10 (m, 12H, PCH(CH₃)₂), 0.96 (dd, $J_{H-H} = 15.9$ Hz, $J_{P-H} = 7.5$ Hz, 12H, PCH(CH₃)₂). $^{31}P\{^1H\}$ NMR (202 MHz, C_6D_6): δ 147.3. $^{13}C\{^1H\}$ NMR (126 MHz, C_6D_6): δ 161.0 (d, $J_{P-C} = 9.0$ Hz, Ar), 130.1 (s, Ar), 112.3 (d, $J_{P-C} = 11.1$ Hz, Ar), 109.5 (t, $J_{P-C} = 11.3$ Hz, Ar), 28.6 (d, $J_{P-C} = 18.3$ Hz, PCH(CH₃)₂), 17.9 (d, $J_{P-C} = 20.5$ Hz, PCH(CH₃)₂), 17.2 (d, $J_{P-C} = 8.7$ Hz, PCH(CH₃)₂).

(*p*-MePOCOP^{iPr})-H ligand (211) – Ligand **211** was prepared according to modified literature procedures.¹⁷⁴ In a Schlenk flask equipped with a magnetic stir bar, 5-methylresorcinol (2.30 g, 18.5 mmol) was dissolved in 30 mL of THF. NEt₃ (5.40 mL, 38.7 mmol) was added followed by ClP^{iPr}Pr₂ (6.04 mL, 38.0 mmol) and immediately a white precipitate formed. The reaction was stirred at room temperature for 12 h in a glovebox. The solution was then filtered through Celite over a coarse frit, and the solvent was removed in vacuo to provide **211** as a clear oil. The product was used determined to be >95% pure by NMR spectroscopy, and was used as prepared. Yield: 6.40 g (97%). 1H NMR (500 MHz, C_6D_6): δ 7.27 (s, 1H, Ar-*H*), 6.83 (s, 2H, Ar-*H*), 2.07 (s, 3H, Ar-CH₃), 1.75 (m, 4H, PCH(CH₃)₂), 1.14 (m, 12H, PCH(CH₃)₂), 0.98 (dd, $J_{H-H} = 15.9$ Hz, $J_{P-H} = 7.5$ Hz, 12H, PCH(CH₃)₂). $^{31}P\{^1H\}$ NMR (202 MHz, C_6D_6): δ 146.3. $^{13}C\{^1H\}$ NMR (126 MHz, C_6D_6): δ 160.9 (d, $J_{P-C} = 9.3$ Hz, Ar), 140.3 (s, Ar), 113.1 (d, $J_{P-C} = 10.3$ Hz, Ar), 106.6 (t, $J_{P-C} = 11.5$ Hz, Ar), 28.6 (d, $J_{P-C} = 18.4$ Hz, PCH(CH₃)₂), 21.6 (s, Ar-CH₃), 17.9 (d, $J_{P-C} = 20.7$ Hz, PCH(CH₃)₂), 17.2 (d, $J_{P-C} = 8.8$ Hz, PCH(CH₃)₂).

(^tBuPOCOPⁱPr)-H ligand (212) – Ligand **212** was prepared according to modified literature procedures.¹⁷⁵ In a 50 mL Kimax vial equipped with a magnetic stir bar, 4,6-di-*tert*-butylresorcinol (1.07 g, 4.81 mmol) was dissolved in 40 mL of toluene. NEt₃ (2.00 mL, 14.3 mmol) was added followed by ClPⁱPr₂ (1.51 mL, 9.49 mmol). The vial was sealed, brought out of the glovebox, and the reaction was stirred at 110 °C for 24 h. The resultant mixture was filtered through Celite and the solvent was removed in vacuo, providing a yellow oil that solidified over time. The crude solid was determined to be 90% pure **212** by NMR spectroscopy. Recrystallization from pentane at –30 °C provided the product as large white crystals. Yield: 1.00 g (46%). ¹H NMR (500 MHz, toluene-*d*₈): δ 8.39 (m, 1H, Ar-*H*), 7.38 (s, 1H, Ar-*H*), 1.82 (m, 4H, PCH(CH₃)₂), 1.49 (s, 18H, Ar-C(CH₃)₃), 1.13 (dd, *J*_{H-H} = 10.9 Hz, *J*_{P-H} = 7.0 Hz, 12H, PCH(CH₃)₂), 1.01 (dd, *J*_{H-H} = 15.0 Hz, *J*_{P-H} = 7.2 Hz, 12H, PCH(CH₃)₂). ³¹P{¹H} NMR (202 MHz, toluene-*d*₈): δ 138.4. ³¹P{¹H} NMR (202 MHz, C₆D₆): δ 138.8. ¹³C{¹H} NMR (126 MHz, C₆D₆): δ 156.3 (m, Ar), 129.8 (s, Ar), 125.6 (s, Ar), 106.7 (t, *J*_{P-C} = 30.5 Hz, Ar-H), 34.9 (s, Ar-C(CH₃)₃), 30.8 (s, Ar-C(CH₃)₃), 28.3 (d, *J*_{P-C} = 19.2 Hz, PCH(CH₃)₂), 17.9 (m, PCH(CH₃)₂).

213-(H)(Cl)(DMAP) – Note: Order of addition is important and should be followed as written in order to avoid formation of unidentified side products. [(COD)IrCl]₂ (752 mg, 1.12 mmol) and 40 mL of toluene were added to a 100 mL Hi-Vac valve round-bottom flask equipped with a magnetic stir bar. DMAP (299 mg, 2.45 mmol) was added, giving a yellow solution. Subsequent addition of ligand **210** (770 mg, 2.25 mmol) in toluene gave a yellow–orange solution. The flask was then sealed and

brought out of the glovebox. The reaction was heated at 110 °C for 24 h to form a light yellow solution. All solvent was removed in vacuo, and the resultant white solid was dissolved in CH₂Cl₂, filtered through Celite, layered with pentane, and placed in a –30 °C glovebox freezer overnight providing a white precipitate. After decanting the supernatant the white precipitate was repeatedly washed with pentane and dried in vacuo. ¹H NMR spectroscopy revealed the product contained a small amount of free DMAP (ca. 4%). The product was determined to be a mixture of two isomers via ¹H and ³¹P{¹H} NMR spectroscopy, and was used without further separation. Yield: 1.32 g (85%). **Isomer A** (65%): ¹H NMR (500 MHz, C₆D₆): δ 9.97 (br d, *J*_{H-H} = 6.2 Hz, 1H, (CH₃)₂N-C₅H₄N), 7.38 (br d, *J*_{H-H} = 6.8 Hz, 1H, (CH₃)₂N-C₅H₄N), 6.91 (t, *J*_{H-H} = 7.7 Hz, 1H, Ar-*H*), 6.83 (d, *J*_{H-H} = 7.7 Hz, 2H, Ar-*H*), 5.92 (br s, 1H, (CH₃)₂N-C₅H₄N), 5.28 (br s, 1H, (CH₃)₂N-C₅H₄N), 2.40 (m, 2H, PCH(CH₃)₂), 2.11 (m, 2H, PCH(CH₃)₂), 1.97 (s, 6H, (CH₃)₂N-C₅H₄N), 1.44 (dvt, *J*_{H-H} = 7.5 Hz, *J*_{P-H} = 7.5 Hz, 6H, PCH(CH₃)₂), 1.23 (dvt, *J*_{H-H} = 7.5 Hz, *J*_{P-H} = 7.5 Hz, 6H, PCH(CH₃)₂), 1.19–1.14 (m, 12H, PCH(CH₃)₂), –20.43 (t, *J*_{P-H} = 16.0 Hz, 1H, Ir-*H*). ³¹P{¹H} NMR (202 MHz, C₆D₆): δ 149.4. **Isomer B** (35%): ¹H NMR (500 MHz, C₆D₆): δ 9.23 (br d, *J*_{H-H} = 5.5 Hz, 2H, (CH₃)₂N-C₅H₄N), 5.73 (d, *J*_{H-H} = 5.9 Hz, 2H, (CH₃)₂N-C₅H₄N), 3.74 (m, 2H, PCH(CH₃)₂), 2.02 (s, 6H, (CH₃)₂N-C₅H₄N), 1.31–1.27 (m, 6H, PCH(CH₃)₂), 0.89–0.84 (m, 6H, PCH(CH₃)₂), –20.82 (t, *J*_{P-H} = 15.1 Hz, 1H, Ir-*H*). The resonances corresponding to the aromatic backbone, the second set of isopropyl methines and two sets of isopropyl methyl protons could not be identified due to overlap with isomer A. ³¹P{¹H} NMR (202 MHz, C₆D₆):

δ 147.7. Anal. Calcd. for **213-(H)(Cl)(DMAP)**: C, 43.53 ; H, 6.13. Found: C, 43.49 ; H, 6.02.

213-(H)(Cl)(py) – Note: Order of addition is important and should be followed as written in order to avoid formation of unidentified side products. [(COD)IrCl]₂ (391 mg, 0.582 mmol) and 15 mL of toluene were added to a 50 mL Hi-Vac valve round-bottom flask equipped with a magnetic stir bar. Pyridine (135 μ L, 1.68 mmol) was added, giving a yellow solution. Subsequent addition of ligand **210** (399 mg, 1.17 mmol) in toluene produced a yellow–orange solution. The flask was then sealed and brought out of the glovebox. The reaction was heated at 110 °C for 24 h to form a light yellow solution. All solvent was removed in vacuo and the resultant white solid was dissolved in CH₂Cl₂, filtered through Celite, layered with pentane, and placed in a –30 °C glovebox freezer overnight providing a white precipitate. After decanting the supernatant, the precipitate was washed with pentane and dried in vacuo to provide **213-(H)(Cl)(py)** as a white, crystalline solid of analytical purity. The product was determined to be an 87:13 mixture of two isomers via ¹H and ³¹P{¹H} NMR spectroscopy. Yield: 616 mg (81%). **Isomer A** (87%): ¹H NMR (500 MHz, C₆D₆): δ 10.44 (br s, 1H, Py-*H*), 7.80 (br s, 1H, Py-*H*), 6.88 (t, $J_{\text{H-H}} = 7.5$ Hz, 1H, Ar-*H*), 6.78 (d, $J_{\text{H-H}} = 7.5$ Hz, 2H, Ar-*H*), 6.64 (t, $J_{\text{H-H}} = 7.5$ Hz, 1H, Py-*H*), 6.53 (br s, 1H, Py-*H*), 5.96 (br s, 1H, Py-*H*), 2.34 (m, 2H, PCH(CH₃)₂), 1.91 (m, 2H, PCHC(CH₃)₂), 1.39 (dvt, $J_{\text{H-H}} = 9$ Hz, $J_{\text{P-H}} = 8$ Hz, 6H, PCH(CH₃)₂), 1.18 (dvt, $J_{\text{H-H}} = 7.5$ Hz, $J_{\text{P-H}} = 7.5$ Hz, 6H, PCH(CH₃)₂), 1.06 (dvt, $J_{\text{H-H}} = 7.5$ Hz, $J_{\text{P-H}} = 6.5$ Hz, 6H, PCH(CH₃)₂), 0.96 (dvt, $J_{\text{H-H}} = 8$ Hz, $J_{\text{P-H}} = 8$ Hz, 6H, PCH(CH₃)₂), –20.88 (t, $J_{\text{P-H}} = 16$ Hz, 1H, Ir-*H*). ³¹P{¹H} NMR

(202 MHz, C₆D₆): δ 148.8 (87%). **Isomer B** (13%): ¹H NMR (500 MHz, C₆D₆): 9.63 (br s, 1H, Py-*H*), 6.73 (t, $J_{\text{H-H}} = 7.5$ Hz, 1H, Ar-*H*), 6.32 (t, $J_{\text{H-H}} = 7.5$ Hz, 1H, Py-*H*), -20.75 (t, $J_{\text{P-H}} = 15$ Hz, 1H, Ir-*H*). ³¹P{¹H} NMR (202 MHz, C₆D₆): δ 147.0. Anal. Calcd. for **213-(H)(Cl)(py)**: C, 42.55 ; H, 5.75. Found: C, 42.69 ; H, 5.67.

214-(H)(Cl)(py) – Note: Order of addition is important and should be followed as written in order to avoid unidentified side products. [(COD)IrCl]₂ (285 mg, 0.424 mmol) and 15 mL of toluene were added to a 50 mL Hi-Vac valve round-bottom flask equipped with a magnetic stir bar. Pyridine (71 μ L, 0.881 mmol) was added, giving a yellow solution. Subsequent addition of ligand **211** (303 mg, 0.850 mmol) in toluene produced a yellow orange solution. The flask was sealed and brought out of the glovebox. The reaction was heated at 110 °C for 24 h, forming a light yellow solution. Allowing the flask to cool to room temperature caused a white solid to precipitate out of solution. All solvent was removed in vacuo and the flask was brought into a glovebox. The resultant white solid was dissolved in CH₂Cl₂, filtered through a plug of Celite, layered with pentane, and placed in a -30 °C freezer overnight resulting in precipitation of a white, crystalline solid. After decanting the supernatant, the precipitate was washed with pentane and dried in vacuo to yield **214-(H)(Cl)(py)** in analytically pure form. The product was determined to be an 86:14 mixture of two isomers via ¹H and ³¹P{¹H} NMR spectroscopy. Yield: 461 mg (74%). **Isomer A** (86%): ¹H NMR (500 MHz, C₆D₆): δ 10.1 (br s, 1H, Py-*H*), 7.85 (br s, 1H, Py-*H*), 6.64 (d, $J_{\text{H-H}} = 0.5$ Hz, 2H, Ar-*H*), 6.63 signal partially obscured (tt, $J_{\text{H-H}} = 7.5$ Hz, $J_{\text{H-H}} = 1.5$ Hz, 1H, Py-*H*), 6.53 (br t, $J_{\text{H-H}} = 6.0$ Hz, 1H, Py-*H*), 5.98 (br t, $J_{\text{H-H}} = 6.0$ Hz, 1H, Py-*H*), 2.35 (m, 2H, PCH(CH₃)₂), 2.23

(t, $J_{\text{H-H}} = 0.5$ Hz, 3H, Ar- CH_3), 1.41 (dvt, $J_{\text{H-H}} = 11$ Hz, $J_{\text{P-H}} = 7.0$ Hz, 6H, $\text{PCH}(\text{CH}_3)_2$), 1.19 (dvt, $J_{\text{H-H}} = 8$ Hz, $J_{\text{P-H}} = 7.0$ Hz, 6H, $\text{PCH}(\text{CH}_3)_2$), 1.08 (dvt, $J_{\text{H-H}} = 7.0$ Hz, $J_{\text{P-H}} = 7.0$ Hz, 6H, $\text{PCH}(\text{CH}_3)_2$), 0.98 (dvt, $J_{\text{H-H}} = 8.5$ Hz, $J_{\text{P-H}} = 7.5$ Hz, 6H, $\text{PCH}(\text{CH}_3)_2$), -20.99 (t, $J_{\text{P-H}} = 16.0$ Hz, 1H, Ir- H). $^{31}\text{P}\{^1\text{H}\}$ NMR (202 MHz, C_6D_6): δ 149.4. **Isomer B** (14%): ^1H NMR (500 MHz, C_6D_6): δ 9.66 (br d, $J_{\text{H-H}} = 4$ Hz, 1H, 2',6'-Py- H), 6.70 (tt, $J_{\text{H-H}} = 7.5$ Hz, $J_{\text{H-H}} = 1.5$ Hz, 1H, Py- H), 6.61 (d, $J_{\text{H-H}} = 0.5$ Hz, 2H, Ar- H), 6.31 (m, 2H, 3', Py- H), 3.69 (m, 2H, $\text{PCH}(\text{CH}_3)_2$), 2.29 (m, 2H, $\text{PCH}(\text{CH}_3)_2$), 2.24 (t, $J_{\text{H-H}} = 0.5$ Hz, 3H, Ar- CH_3), 1.23 (dvt, $J_{\text{H-H}} = 6.5$ Hz, $J_{\text{P-H}} = 7.0$ Hz, 6H, $\text{PCH}(\text{CH}_3)_2$), 1.10 (dvt, $J_{\text{H-H}} = 10$ Hz, $J_{\text{P-H}} = 7.5$ Hz, 6H, $\text{PCH}(\text{CH}_3)_2$), 0.70 (dvt, $J_{\text{H-H}} = 10$ Hz, $J_{\text{P-H}} = 7.0$ Hz, 6H, $\text{PCH}(\text{CH}_3)_2$), -20.91 (t, $J_{\text{P-H}} = 15.0$ Hz, 1H, Ir- H). The fourth expected dvt resonance corresponding to the isopropyl methyl was not observed and presumably overlaps with signals of isomer A. $^{31}\text{P}\{^1\text{H}\}$ NMR (202 MHz, C_6D_6): δ 147.5. Anal. Calcd. for **214-(H)(Cl)(py)**: C, 43.47 ; H, 5.93. Found: C, 43.53 ; H, 6.04.

213-(H)(Cl) – Compound **213-(H)(Cl)(DMAP)** (404 mg, 0.584 mmol) and 20 mL of toluene were added to a 50 mL Hi-Vac valve round-bottom flask equipped with a magnetic stir bar. To this suspension $\text{BF}_3 \cdot \text{OEt}_2$ (250 μL , 2.03 mmol) was added, causing the mixture to become red in color. The flask was brought out of the glovebox and heated at 110 $^\circ\text{C}$ for 1 h, resulting in a dark red solution with formation of some insoluble precipitate. The flask was then placed in a -30 $^\circ\text{C}$ glovebox freezer overnight. The contents were filtered cold through a plug of Celite, and the Celite was subsequently washed with cold pentane to ensure full product transfer. Removal of solvent in vacuo resulted in formation of a tan, yellow solid. The composition of the resultant solids was

determined by ^1H NMR spectroscopy to be 95% **213-(H)(Cl)** and 5% $\text{BF}_3\cdot\text{DMAP}$. The isolated mixture was then filtered through a short plug of silica gel using a 5:1 pentane:toluene solvent mixture (60 mL). All solvent was removed in vacuo providing **213-(H)(Cl)** as an analytically pure, tan solid. Yield: 158 mg (48%). ^1H NMR (500 MHz, C_6D_6): δ 6.80 (t, $J_{\text{H-H}} = 8.0$ Hz, 1H, Ar-H), 6.70 (d, $J_{\text{H-H}} = 8.0$ Hz, 2H, Ar-H), 2.63 (m, 2H, $\text{PCH}(\text{CH}_3)_2$), 2.25 (m, 2H, $\text{PCH}(\text{CH}_3)_2$), 1.23 (dvt, $J_{\text{H-H}} = 8.5$ Hz, $J_{\text{P-H}} = 8.0$ Hz, 6H, $\text{PCH}(\text{CH}_3)_2$), 1.07 (m, 12H, $\text{PCH}(\text{CH}_3)_2$), 0.99 (dvt, $J_{\text{H-H}} = 7.5$ Hz, $J_{\text{P-H}} = 7.5$ Hz, 6H, $\text{PCH}(\text{CH}_3)_2$), -37.0 (t, $J_{\text{P-H}} = 12$ Hz, 1H, Ir-H). $^{31}\text{P}\{^1\text{H}\}$ NMR (202 MHz, C_6D_6): δ 173.4. $^{13}\text{C}\{^1\text{H}\}$ NMR (126 MHz, C_6D_6): δ 166.2 (t, $J_{\text{P-C}} = 6.4$ Hz, Ar), 125.7 (s, Ar), 114.3 (br s, Ar), 105.6 (t, $J_{\text{P-C}} = 5.4$ Hz, Ar), 31.4 (t, $J_{\text{P-C}} = 14.7$ Hz, $\text{PCH}(\text{CH}_3)_2$), 29.3 (t, $J_{\text{P-C}} = 16.3$ Hz, $\text{PCH}(\text{CH}_3)_2$), 17.4 (s, $\text{PCH}(\text{CH}_3)_2$), 16.9 (s, $\text{PCH}(\text{CH}_3)_2$), 16.7 (s, $\text{PCH}(\text{CH}_3)_2$). Anal. Calcd. for **213-(H)(Cl)**: C, 37.93 ; H, 5.66. Found: C, 38.14 ; H, 5.39.

214-(H)(Cl)– Compound **214-(H)(Cl)(py)** (250 mg, 0.377 mmol) and 10 mL of a 5:1 pentane:toluene were added to a 50 mL Hi-Vac valve round-bottom flask equipped with a magnetic stir bar. To that suspension $\text{BF}_3\cdot\text{OEt}_2$ (300 μL , 2.43 mmol) was added, causing an immediate color change to dark red. The flask was brought out of the glovebox and heated at 70 $^\circ\text{C}$ for 24 h. The resulting dark red solution was cooled to room temperature and brought back into the glovebox. 10 mL of pentane was added and the mixture was stirred overnight at room temperature. The dark red solution was then filtered through Celite over a fine frit. Removal of the solvent in vacuo resulted in formation of a red residue. The residue was washed with toluene and pentane, and

subsequently dried in vacuo to ensure removal of all $\text{BF}_3 \cdot \text{OEt}_2$. The residue was dissolved in a 5:1 pentane:toluene solvent mixture and filtered through a thin plug of silica (approximately 2–3 mm deep) over a fine frit before all solvent was once again removed in vacuo, providing a red residue. This residue was dissolved into a minimum of toluene, layered with pentane, and placed in a $-30\text{ }^\circ\text{C}$ freezer overnight, resulting in precipitation of orange solids. After decanting the supernatant, the precipitate was washed with cold pentane, dried in vacuo, and collected as orange-yellow, crystalline solid. Yield: 160 mg (73%). ^1H NMR (500 MHz, C_6D_6): δ 6.55 (s, 2H, Ar-H), 2.64 (m, 2H, PCH(CH_3)₂), 2.27 (m, 2H, PCH(CH_3)₂), 2.12 (s, 3H, Ar- CH_3), 1.25 (dvt, $J_{\text{H-H}} = 8.5$ Hz, $J_{\text{P-H}} = 8.0$ Hz, 6H, PCH(CH_3)₂), 1.11 (dvt, $J_{\text{H-H}} = 6.5$ Hz, $J_{\text{P-H}} = 7.5$ Hz, 6H, PCH(CH_3)₂), 1.09 (dvt, $J_{\text{H-H}} = 8.5$ Hz, $J_{\text{P-H}} = 7.0$ Hz, 6H, PCH(CH_3)₂), 1.01 (dvt, $J_{\text{H-H}} = 7$ Hz, $J_{\text{P-H}} = 8$ Hz, 6H, PCH(CH_3)₂), -37.1 (t, $J_{\text{P-H}} = 12$ Hz, 1H, Ir-H). $^{31}\text{P}\{^1\text{H}\}$ NMR (202 MHz, C_6D_6): δ 173.8. $^{13}\text{C}\{^1\text{H}\}$ NMR (126 MHz, C_6D_6): 166.1 (t, $J_{\text{P-C}} = 6.3$ Hz, Ar), 150.4 (s, Ar), 135.8 (s, Ar), 106.6 (t, $J_{\text{P-C}} = 7.1$ Hz, Ar), 31.5 (t, $J_{\text{P-C}} = 14.7$ Hz, PCH(CH_3)₂), 29.3 (t, $J_{\text{P-C}} = 16.5$ Hz, PCH(CH_3)₂), 21.6 (Ar- CH_3), 17.4 (s, PCH(CH_3)₂), 16.9 (m, PCH(CH_3)₂), 16.7 (s, PCH(CH_3)₂). Anal. Calcd. for **214-(H)(Cl)**: C, 39.07 ; H, 5.87. Found: C, 39.09 ; H, 6.02.

Reaction of 213-(H)(Cl) and 214-(H)(Cl) with pyridine – Compound **213-(H)(Cl)** (14 mg, 0.025 mmol) or **214-(H)(Cl)** (15 mg, 0.026 mmol) were each added to a separate J. Young NMR tube and dissolved in C_6D_6 . Pyridine (0.028 mmol, 50 μL of a 0.55 M C_6D_6 stock solution) was added to each J. Young NMR tube and the samples were mixed. Immediately, in both reactions, a color change occurred from red to clear

yellow. Analysis via ^1H and $^{31}\text{P}\{^1\text{H}\}$ NMR spectroscopy showed quantitative formation of **213-(H)(Cl)(py)** or **214-(H)(Cl)(py)**, each as a mixture of two isomers in a ratio similar to that observed in the syntheses from **210** or **211** with $[(\text{COD})\text{IrCl}]_2$.

215-(H)(Cl) – $[(\text{COD})\text{IrCl}]_2$ (177 mg, 0.264 mmol) and 15 mL of toluene were added to a 50 mL Hi-Vac valve round-bottom flask equipped with a magnetic stir bar. Ligand **212** (242 mg, 0.532 mmol) was added as a solution in toluene and the reaction was heated for 24 h at 110 °C, giving a dark red-brown solution. The reaction flask was brought into a glovebox, filtered through Celite, and solvent was removed in vacuo. The resulting tan yellow solid was dissolved in a minimum of pentane and placed into a –30 °C freezer overnight, causing a tan colored precipitate to form. After decanting the supernatant, all solvent was removed in vacuo, and the product was collected as a tan-yellow solid. Single crystals suitable for X-ray analysis were obtained by slow evaporation of pentane at room temperature. Yield: 291 mg (80%). ^1H NMR (500 MHz, toluene- d_8): δ 7.08 (s, 1H, Ar-*H*), 2.66 (m, 2H, PCH(CH₃)₂), 2.27 (m, 2H, PCH(CH₃)₂), 1.48 (s, 18H, Ar-C(CH₃)₃), 1.25 (dvt, $J_{\text{H-H}} = 8.6$ Hz, $J_{\text{P-H}} = 8.4$ Hz, 6H, PCH(CH₃)₂), 1.08 (m, 18H, PCH(CH₃)₂), –36.6 (t, $J_{\text{P-H}} = 13.6$ Hz, 1H, Ir-*H*). $^{31}\text{P}\{^1\text{H}\}$ NMR (202 MHz, toluene- d_8): δ 173.2. $^{13}\text{C}\{^1\text{H}\}$ NMR (126 MHz, toluene- d_8): δ 161.5 (t, $J_{\text{P-C}} = 5.9$ Hz, Ar), 126.7 (t, $J_{\text{P-C}} = 4.7$ Hz, Ar), 120.7 (s, Ar), 115.9 (s, Ar), 34.6 (s, Ar-C(CH₃)₃), 31.4 (t, $J_{\text{P-C}} = 14.9$ Hz, PCH(CH₃)₂), 30.3 (s, Ar-C(CH₃)₃), 29.4 (t, $J_{\text{P-C}} = 16.9$ Hz, PCH(CH₃)₂), 17.6 (s, PCH(CH₃)₂), 16.9 (s, PCH(CH₃)₂), 16.8 (s, PCH(CH₃)₂). ^1H NMR (500 MHz, C₆D₆): 7.15 (s, 1H, Ar-*H*), 2.69 (m, 2H, PCH(CH₃)₂), 2.30 (m, 2H, PCH(CH₃)₂), 1.50 (s, 18H, Ar-C(CH₃)₃), 1.27 (dvt, $J_{\text{H-H}} = 7$ Hz, $J_{\text{P-H}} = 8$ Hz, 6H,

PCH(CH₃)₂), 1.10 (m, 12H, PCH(CH₃)₂), 1.03 (dvt, $J_{\text{H-H}} = 8$ Hz, $J_{\text{P-H}} = 7.3$ Hz, 6H, PCH(CH₃)₂), -36.6 (t, $J_{\text{P-H}} = 13.5$ Hz, 1H, Ir-H). ³¹P {¹H} (202 MHz, C₆D₆): δ 173.5.

Anal. Calcd. for **215-(H)(Cl)**: C, 47.65 ; H, 7.58. Found: C, 48.05 ; H, 7.54.

215-(HBpin) – Compound **215-(H)(Cl)** (79 mg, 0.12 mmol), B₂pin₂ (31 mg, 0.12 mmol) and diethyl ether were added to a J. Young NMR tube. The components were mixed well, NaO^tBu (12 mg, 0.13 mmol) was added, and the reaction was placed into a 50 °C oil bath for 18 h with periodic mixing. Analysis via ³¹P{¹H} NMR spectroscopy revealed **215-(HBpin)** as the major product. Up to 10% of unidentified minor products were observed in the ³¹P{¹H} NMR spectrum at 175.0 ppm and 172.6 ppm. The mixture was filtered through Celite, and all solvent was removed in vacuo, providing an orange residue. The residue was dissolved in a minimal amount of pentane, filtered, and placed in a -30 °C glovebox freezer, giving orange crystals. Analysis by ¹¹B NMR spectroscopy revealed some ROBpin side product (21.4 ppm in toluene-*d*₈, ~10%) co-crystallized with **215-(HBpin)**, while a minor amount of **215-(Bpin)₂** and an unidentified compound (174.6 ppm in toluene-*d*₈) was observed in the ³¹P{¹H} NMR spectrum. Though difficulties in separation precluded collection of suitable elemental analysis data, X-ray quality crystals of **215-(HBpin)** were able to be obtained by slow evaporation of pentane at room temperature. Yield: 55 mg (61%). ¹H NMR (500 MHz, -60 °C, toluene-*d*₈): δ 7.33 (s, 1H, Ar-H), 3.02 (br m, 2H, PCH(CH₃)₂), 2.21 (br s, 2H, PCH(CH₃)₂), 1.64 (s, 18H, Ar-C(CH₃)₃), 1.38 (br dvt, $J_{\text{H-H}} = 7.7$ Hz, $J_{\text{P-H}} = 7.6$ Hz, 6H, PCH(CH₃)₂), 1.26-1.15 (m, 18H, PCH(CH₃)₂), 1.13 (s, 12H, Bpin CH₃), -10.31 (br s, 1H, Ir-H). ¹H NMR (500 MHz, toluene-*d*₈): δ 7.33 (s, 1H, Ar-H), 3.07-2.17 (br m,

integrates to only 2H, PCH(CH₃)₂), 1.56 (s, 18H, Ar-C(CH₃)₃), 1.32-1.13 (br m, 24H, PCH(CH₃)₂), 1.11 (s, 12H, Bpin CH₃), -10.6 (br s, 1H, Ir-H). ¹¹B NMR (128 MHz, toluene-*d*₈): δ 27.6 (br s). ¹³C{¹H} NMR (126 MHz, toluene-*d*₈): δ 165.2 (t, *J*_{P-C} = 7.3 Hz, Ar), 153.0 (t, *J*_{P-C} = 6.4 Hz, Ar), 126.3 (s, Ar), 125.2 (t, overlaps with toluene-*d*₈ signal, *J*_{P-C} = 5.0 Hz, Ar), 82.1 (s, Bpin tertiary carbon), 34.9 (s, Ar-C(CH₃)₃), 30.5 (s, Ar-C(CH₃)₃), 30.0 (t, *J*_{P-C} = 15.7 Hz, PCH(CH₃)₂), 25.0 (s, Bpin CH₃), 18.5 (br s, PCH(CH₃)₂). ³¹P{¹H} NMR (202 MHz, toluene-*d*₈): δ 190.5. ³¹P{¹H} NMR (202 MHz, Et₂O): δ 190.9.

Thermolysis of 215-(HBpin) in C₆D₆ – A J. Young NMR tube was charged with **215-(HBpin)** (20 mg, 0.026 mmol) and C₆D₆ (700 μL). The sample was determined to contain some **215-H₃Bpin**. The sample was placed into an 80 °C oil bath for 30 min, then 1,4-dioxane (5.0 μL, 0.058 mmol) was added via C₆D₆ stock solution and the reaction was monitored by NMR spectroscopy. A 15% spectroscopic yield of C₆D₅Bpin was observed and the hydride resonances corresponding to **215-(HBpin)** and **215-H₃Bpin** were no longer observed, however, signals corresponding to both **215-(HBpin)** and **215-H₃Bpin** were observed by ³¹P{¹H} NMR indicating rapid H/D exchange with the solvent.

Formation of 215-H₃Bpin in situ – A J. Young tube was charged with **215-(HBpin)** (21 mg, 0.027 mmol) and toluene-*d*₈. The solution was then frozen, degassed, and refilled with 1 atm of H₂, resulting in an immediate color change from red-orange to colorless-pink (Figure S2). Analysis by ³¹P{¹H} NMR spectroscopy revealed predominant formation of **215-H₃Bpin** (96%) as well as a minor quantity of **215-H₄**

(4%). Attempts to isolate **215-H₃Bpin** by removing all solvent in vacuo and subjecting the resultant solids to dynamic high vacuum for several hours resulted in mixtures of **215-H₃Bpin** (81%) and **215-(HBpin)** (19%) (Figure S3). Adding excess H₂ to the reaction mixture regenerated **215-H₃Bpin**. This is similar to the behavior of (POCOP^{tBu})IrH₃Bpin reported by Heinekey et. al.¹⁶⁶ where (POCOP^{tBu})Ir(HBpin) **118-(HBpin)** can be generated by reacting (POCOP^{tBu})IrH₂ **118-H₂** with HBpin, then placing the resulting solids under dynamic high vacuum. ¹H NMR (−80 °C, toluene-*d*₈): δ 7.24 (s, 1H, Ar-*H*), 2.73 (br m, 2H, PCH(CH₃)₂), 1.85 (br s, 2H, PCH(CH₃)₂), 1.60 (s, 18H, Ar-C(CH₃)₃), 1.47 (br dvt, *J*_{H-H} = 7.7 Hz, *J*_{P-H} = 7.6 Hz, 6H, PCH(CH₃)₂), 1.22-1.15 (m, 12H, PCH(CH₃)₂), 1.13 (br s, 6H, Bpin CH₃), 1.10 (br s, 6H, Bpin CH₃), 0.93 (m, 6H, PCH(CH₃)₂), −7.96 (br m, 1H, Ir-*H*), −9.81 (br s, 1H, Ir-*H*), −9.97 (td, *J*_{H-H} = 6.8 Hz, *J*_{P-H} = 16 Hz, 1H, Ir-*H*). ¹¹B NMR (128 MHz, toluene-*d*₈): δ 37.0 (br s). ³¹P{¹H} NMR (202 MHz, toluene-*d*₈): δ 168.2. ¹³C{¹H} NMR (126 MHz, toluene-*d*₈): δ 159.2 (t, *J*_{P-C} = 5.7 Hz, Ar), 125.8 (t, *J*_{P-C} = 4.6 Hz, Ar), 124.0 (t, *J*_{P-C} = 5.0 Hz, Ar), 120.3 (s, Ar), 83.2 (s, Bpin tertiary carbon), 34.6 (s, Ar-C(CH₃)₃), 30.5 (s, Ar-C(CH₃)₃), 28.6 (br s, PCH(CH₃)₂), 24.8 (s, Bpin CH₃), 18.6 (br s, PCH(CH₃)₂), 17.0 (br s, PCH(CH₃)₂), 15.4 (br s, PCH(CH₃)₂).

Alternative synthesis of 215-H₃Bpin *in situ* – A J. Young NMR tube was charged with **215-(TBE)** (40 mg, 0.055 mmol), toluene-*d*₈, and cyclohexane (5.0 μL, 0.046 mmol). The J. Young tube was then frozen, degassed, refilled with 1.5 atm of H₂, and the solution was allowed then swirled. This process was repeated twice, and after 10 minutes a color change was observed from dark red to light yellow. ¹H and ³¹P{¹H}

NMR spectroscopy revealed quantitative formation of **215-H₄** and TBA. The NMR tube was brought back into the glovebox and HBpin (9.0 μ L, 0.062 mmol) was added. Within the time of mixing, ¹H, ¹¹B, and ³¹P{¹H} NMR spectroscopy revealed quantitative formation of **215-H₃Bpin**, which was studied by low temperature VT NMR spectroscopy down to -80 °C (Figure S1). At room temperature the three hydride ligands of **215-H₃Bpin** appear as two broad singlets; $\delta = -8.10$ ppm and -10.09 ppm in a 1:2 ratio, respectively. At -20 °C the broad resonance at -10.09 ppm began to diverge into two broad signals, with complete divergence observed at -50 °C (See Figure S1 below).

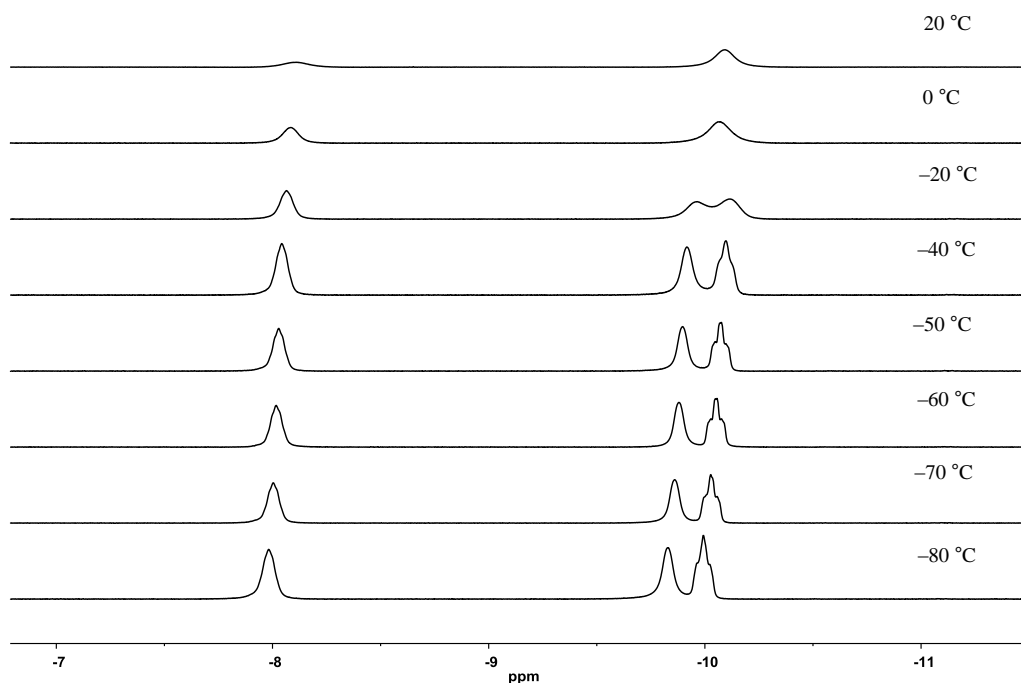


Figure II-9. Stacked ¹H NMR (500 MHz, toluene-*d*₈) spectra of the hydride region of **215-H₃Bpin** from 20 °C (top) to -80 °C (bottom).

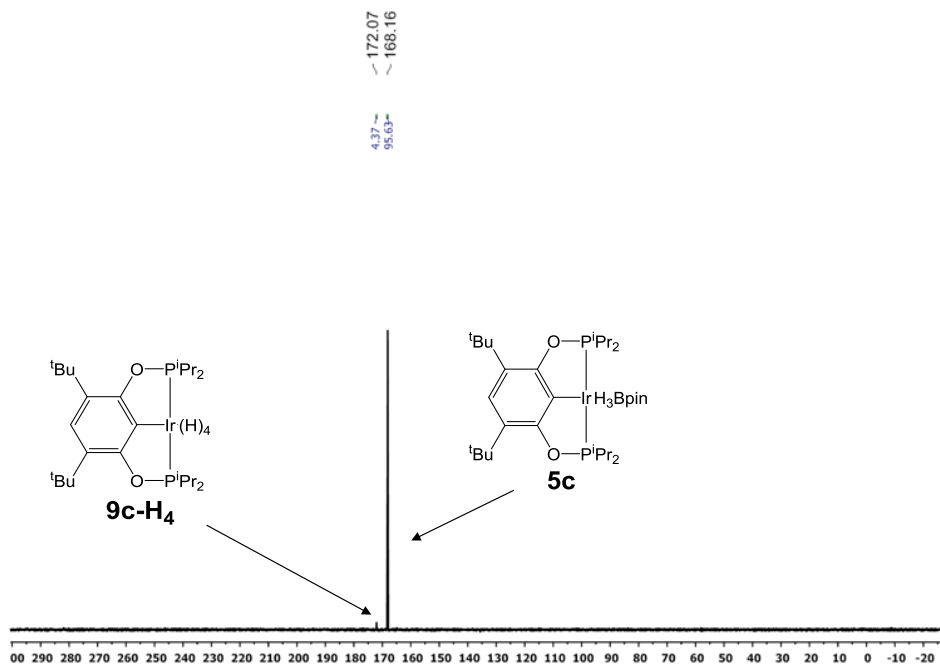


Figure II-10. $^{31}\text{P}\{^1\text{H}\}$ NMR (202 MHz, toluene- d_8) spectrum of **215-H₃Bpin** taken immediately after adding excess H_2 to **215-(HBpin)**. Sample contains **215-H₄**.

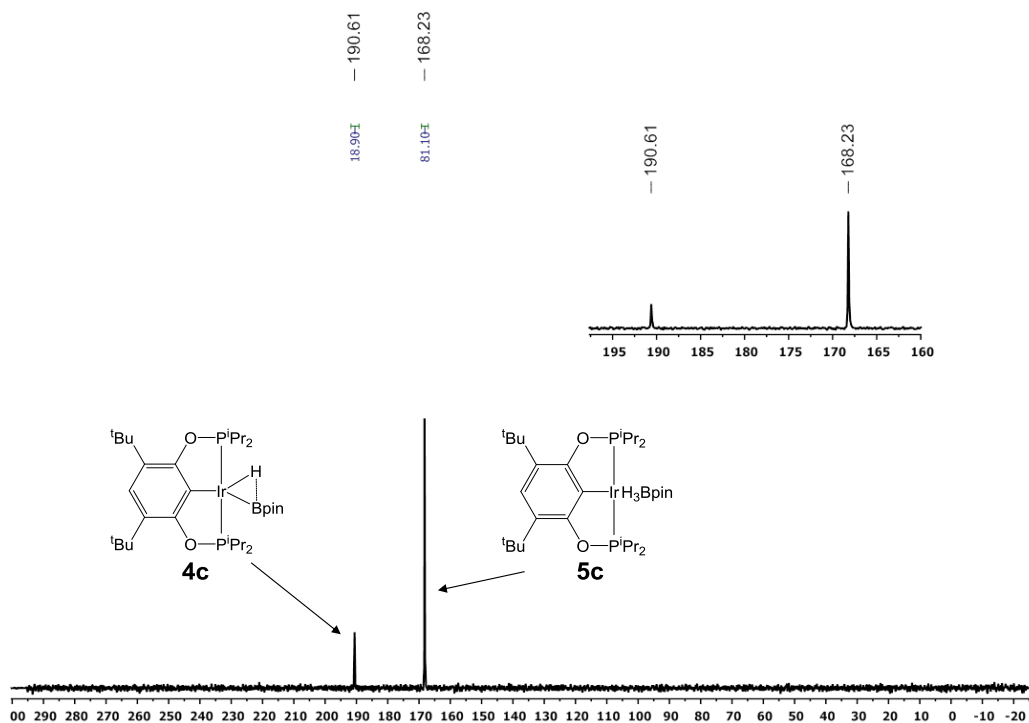


Figure II-11. $^{31}\text{P}\{^1\text{H}\}$ NMR spectrum (202 MHz, C_6D_6) showing a mixture of **215-HBpin** (**4c**) and **215-H₃Bpin** (**5c**). Spectrum was obtained after freezing a cyclohexane solution of **215-H₃Bpin**, removing all solvent in vacuo, subjecting the resultant solids to high vacuum for several hours, then re-dissolving the solids in C_6D_6 .

214-(Bpin)₂ – Compound **214-(TBE)** (366 mg, 0.580 mmol) and 10 mL of benzene were added to a 50 mL Hi-Vac valve round-bottom flask equipped with a magnetic stir bar. B_2pin_2 (148 mg, 0.583 mmol) was added and the reaction was heated for 12 h in a 70 °C oil bath giving a light red solution. The resultant solution was filtered through Celite, and solvent was removed in vacuo giving an orange residue. The residue was dissolved in minimal toluene, layered with pentane and placed in a –30 °C freezer

overnight resulting in precipitation of solids. Decanting the supernatant and drying in vacuo provided **214-(Bpin)₂** as a crystalline, orange-red solid. A single crystal suitable for X-ray analysis was obtained from pentane at $-30\text{ }^{\circ}\text{C}$. Yield: 342 mg (74%). ^1H NMR (500 MHz, C_6D_6): δ 6.77 (s, 2H, Ar-*H*), 2.92 (m, 4H, PCH(CH₃)₂), 2.15 (s, 3H, Ar-CH₃), 1.37 (m, 24H, PCH(CH₃)₂), 1.16 (s, 24H, Bpin CH₃). ^{11}B (128 MHz, C_6D_6): 33.5. $^{13}\text{C}\{^1\text{H}\}$ NMR (126 MHz, C_6D_6): δ 170.3 (t, $J_{\text{P-C}} = 6.9$ Hz, Ar), 154.2 (t, $J_{\text{P-C}} = 7.1$ Hz, Ar), 144.2 (s, Ar), 104.3 (m, Ar), 81.9 (s, Bpin tertiary carbon), 30.7 (t, $J_{\text{P-C}} = 15.3$ Hz, PCH(CH₃)₂), 25.7 (s, Bpin CH₃), 22.2 (Ar-CH₃), 18 (s, PCH(CH₃)₂), 16.6 (s, PCH(CH₃)₂). $^{31}\text{P}\{^1\text{H}\}$ NMR (202 MHz, C_6D_6): δ 185.9. Anal. Calcd. for **214-(Bpin)₂**: C, 46.45 ; H, 7.17. Found: C, 46.38 ; H, 7.21.

215-(Bpin)₂ – A J. Young NMR tube was charged with **215-(TBE)** (33 mg, 0.045 mmol), B_2pin_2 (12 mg, 0.047 mmol), mesitylene (10 μL , 0.096 mmol) and C_6D_6 . The tube was placed in an $80\text{ }^{\circ}\text{C}$ oil bath overnight. ^1H and $^{31}\text{P}\{^1\text{H}\}$ NMR spectroscopy revealed quantitative formation of **215-(Bpin)₂**. All solvent was removed in vacuo and the resulting orange solid was dissolved in a minimum of pentane and placed in a $-30\text{ }^{\circ}\text{C}$ freezer overnight, resulting in precipitation of solids. Decanting the supernatant and drying the solids in vacuo provided **215-(Bpin)₂** as orange-red crystals. Yield: 36 mg (88%). ^1H NMR (500 MHz, C_6D_6): δ 7.45 (s, 1H, Ar-*H*), 2.93 (m, 4H, PCH(CH₃)₂), 1.59 (s, 18H, Ar-C(CH₃)₃), 1.41-1.32 (m, 24H, PCH(CH₃)₃), 1.18 (s, 24H, Bpin CH₃). ^{11}B (128 MHz, C_6D_6): δ 33.6. $^{13}\text{C}\{^1\text{H}\}$ NMR (126 MHz, C_6D_6): δ 165.2 (t, $J_{\text{P-C}} = 6$ Hz, Ar), 161.6 (t, $J_{\text{P-C}} = 7$ Hz, Ar), 128.6 (s, Ar), 124.9 (t, $J_{\text{P-C}} = 5$ Hz, Ar), 81.9 (s, Bpin tertiary carbon), 35.0 (s, Ar-C(CH₃)₃), 30.9 (t, $J_{\text{P-C}} = 15.7$ Hz, PCH(CH₃)₃), 30.6 (s, Ar-C(CH₃)₃),

25.8 (s, Bpin CH₃), 17.9 (t, $J_{P-C} = 2.1$ Hz, PCH(CH₃)₃), 16.9 (s, PCH(CH₃)₃). ³¹P{¹H} NMR (202 MHz, C₆D₆): δ 184.8. Anal. Calcd. for **215-(Bpin)₂**: C, 50.73 ; H, 7.95. Found: C, 51.12; H, 8.21.

Thermolysis of 215-(Bpin)₂ in C₆D₆ – A J. Young NMR tube was charged with **215-(Bpin)₂** (31 mg, 0.034 mmol) and C₆D₆. The reaction was placed into an 80 °C oil bath and monitored periodically by NMR spectroscopy for up to 24 h, C₆D₅Bpin was not observed during that time nor were any new organometallic or organic products; only **215-(Bpin)₂** was observed.

215-(C₂H₄) – Compound **215-(H)(Cl)** (210 mg, 0.318 mmol) and 10 mL of benzene were added to a 100 mL Hi-Vac valve round-bottom flask equipped with a magnetic stir bar. NaO^tBu was added (34 mg, 0.35 mmol) and the flask was brought out of the glovebox, degassed, and charged with 1 atm of ethylene (C₂H₄). The reaction was stirred for 12 h at RT, giving a dark red solution. The solution was filtered through Celite, and solvent was removed in vacuo, resulting in formation of brown solids. The solids were dissolved in hexamethyldisiloxane and pentane, giving a red solution, then placed in a –30 °C freezer overnight. The supernatant was decanted, and the precipitate dried under reduced pressure to provide **215-(C₂H₄)** as a brown powder. Yield: 149 mg (72%). ¹H NMR (500 MHz, C₆D₆): δ 7.28 (s, 1H, Ar-*H*), 2.62 (t, $J_{P-H} =$ Hz, 4H, Ir(C₂H₄), 2.28 (m, 4H, PCH(CH₃)₂), 1.60 (s, 18H, Ar-C(CH₃)₃), 1.10 (dvt, $J_{H-H} = 6.9$ Hz, $J_{P-H} = 6.7$ Hz, 12H, PCH(CH₃)₂), 1.02 (dvt, $J_{H-H} = 8.7$ Hz, $J_{P-H} = 7.4$ Hz, 12H, PCH(CH₃)₂). ³¹P{¹H} NMR (202 MHz, C₆D₆): δ 181.7. ¹³C{¹H} NMR (126 MHz, C₆D₆): δ 161.4 (t, $J_{P-C} = 9.4$ Hz, Ar), 145.0 (t, $J_{P-C} = 9.8$ Hz, Ar), 125.48 (t, $J_{P-C} = 5.6$ Hz, Ar), 120.2 (s,

Ar), 34.9 (s, C₂H₄), 34.0 (s, Ar-C(CH₃)), 31.0 (t, $J_{P-C} = 13.1$ Hz, PCH(CH₃)₂), 30.7 (s, Ar-C(CH₃)), 17.9 (t, $J_{P-C} = 2.5$ Hz, PCH(CH₃)₂), 17.45 (s, PCH(CH₃)₂). Anal. Calcd. for **215-(C₂H₄)**: C, 49.91 ; H, 7.63. Found: C, 52.95 ; H, 7.36.

214-(TBE) – Compound **214-(H)(Cl)** (308 mg, 0.53 mmol) and 10 mL were added to a 50 mL Hi-Vac valve round-bottom flask equipped with a magnetic stir bar. Via syringe, *tert*-butylethylene (410 μ L, 3.2 mmol) was added, followed by NaO^tBu (56 mg, 0.58 mmol). The reaction was stirred for 12 h at RT, producing a dark red solution. The solution was filtered through Celite and solvent was removed in vacuo, giving the product as a red solid. The product may be recrystallized from pentane at -30 °C or used without further purification. Yield: 226 mg (66%). ¹H NMR (500 MHz, C₆D₆): δ 6.75 (s, 2H, Ar-H), 4.21 (m, 1H, TBE), 3.66 (m, 1H, TBE), 2.94 (d, $J_{H-H} = 8$ Hz, 1H, TBE), 2.57 (m, 2H, PCH(CH₃)₂), 2.33 (m, 2H, PCH(CH₃)₂), 2.16 (s, 3H, Ar-CH₃), 1.26-1.19 (m, 12H, PCH(CH₃)₂), 1.14 (s, 9H, TBE -C(CH₃)₃), 1.08-0.98 (m, 12H, PCH(CH₃)₂). ³¹P{¹H} NMR (202 MHz, C₆D₆): δ 173.4 (br s). ¹³C{¹H} NMR (126 MHz, C₆D₆): δ 167.9 (t, $J_{P-C} = 8.3$ Hz, Ar), 141.3 (t, $J_{P-C} = 8.5$ Hz, Ar), 138 (s, Ar), 104.7 (t, $J_{P-C} = 6.1$ Hz, Ar), 67.8 (TBE), 37.9 (TBE), 34.2 (TBE C(CH₃)₃), 31.1 (t, $J_{P-C} = 14.2$ Hz, PCH(CH₃)₂), 30.9 (TBE C(CH₃)₃), 21.9 (Ar-CH₃), 18.4 (s, PCH(CH₃)₂), 17.4 (s, PCH(CH₃)₂), 17.2 (s, PCH(CH₃)₂). Anal. Calcd. for **214-(TBE)**: C, 47.53 ; H, 7.18. Found: C, 47.75; H, 7.40.

215-(TBE) – Compound **215-(H)(Cl)** (357 mg, 0.523 mmol) and 10 mL of benzene were added to a 50 mL Schlenk flask equipped with a magnetic stir bar. *tert*-butylethylene (2.5 mL, 18 mmol) was added, followed by NaO^tBu (60 mg, 0.624 mmol).

The reaction was stirred for 6 h at RT, giving a dark red solution. All solvent was removed in vacuo providing a red residue. The residue was dissolved in pentane and filtered through Celite. Removal of volatiles gave **215-(TBE)** as a red solid in $\geq 96\%$ purity, found suitable for further use. The side products were not identified and no hydride signals were observed. Recrystallization of the product from a pentane/*tert*-butylethylene solvent mixture at $-30\text{ }^{\circ}\text{C}$ did give a TBE solvate of **215-(TBE)** labeled **215-(TBE) • TBE** but the compound was not used for further chemistry. Yield of **215-(TBE)**: 231 mg (60%). ^1H NMR (500 MHz, C_6D_6): δ 7.33 (s, 1H, Ar-*H*), 4.21 (m, 1H, Ir(TBE)), 3.65 (m, 1H, Ir(TBE)), 2.91 (d, $J_{\text{H-H}} = 10\text{ Hz}$, 1H, Ir(TBE)), 2.57 (m, 2H, PCH(CH_3)₃), 2.31 (m, 2H, PCH(CH_3)₃), 1.59 (s, 18H, Ar-C(CH_3)₃), 1.27-1.23 (br m, 6H, PCH(CH_3)₃), 1.22-1.18 (m, 6H, PCH(CH_3)₃), 1.15 (s, 9H, Ir(TBE)), 1.10-0.97 (br m, 12H, PCH(CH_3)₃). $^{31}\text{P}\{^1\text{H}\}$ NMR (202 MHz, C_6D_6): δ 172.3 (br s). $^{13}\text{C}\{^1\text{H}\}$ NMR (126 MHz, C_6D_6): δ 163.2 (t, $J_{\text{P-C}} = 8\text{ Hz}$, Ar), 148.2 (t, $J_{\text{P-C}} = 8\text{ Hz}$, Ar), 124.7 (m, Ar), 122.7 (s, Ar), 67.2 (s, Ir(TBE)), 37.6 (s, Ir(TBE)), 34.9 (s, Ar-C(CH_3)), 34.2 (s, Ir(TBE)), 31.1 (m, PCH(CH_3)₂), 30.9 (s, Ir(TBE)), 30.7 (s, Ar-C(CH_3)), 18.6 (br m, PCH(CH_3)₂), 17.4 (br m, PCH(CH_3)₂). Anal. Calcd. for **215-(TBE)**: C, 52.65 ; H, 8.15. Found: C, 52.62; H, 7.94. Anal. Calcd. for **215-(TBE) • TBE**: C, 56.06 ; H, 8.79. Found: C, 55.87; H, 8.63.

Thermolysis of 214-(TBE) in C_6D_6 - A J. Young NMR tube was charged with **214-(TBE)** (22mg, 0.034 mmol) and C_6D_6 . Via syringe, cyclohexane (5 μL) was added as internal standard. The reaction was placed into a $90\text{ }^{\circ}\text{C}$ oil bath and after 18 h numerous unidentified products (> 10) were observed by $^{31}\text{P}\{^1\text{H}\}$ NMR spectroscopy.

Only 2,2-dimethylbutane (TBA) was identifiable in the ^1H NMR spectrum, and the cyclohexane internal standard appeared to have been consumed.

Reaction of 215-(TBE) with 2 equiv of HBpin in C_6D_6 - attempting to make pure 215-(HBpin) – A J. Young NMR tube was loaded with **215-(TBE)** (20 mg, 0.027 mmol), C_6D_6 (700 μL), cyclohexane (10 μL), and HBpin (8.0 μL , 0.055 mmol). The resulting light red solution was immediately analyzed via ^1H , ^{11}B and $^{31}\text{P}\{^1\text{H}\}$ NMR spectroscopy. The ^{11}B NMR spectrum showed the formation of **215- H_3Bpin** (16%), TBABpin (39%), PhBpin (39%), and a HBpin decomposition product (6%). The $^{31}\text{P}\{^1\text{H}\}$ NMR spectrum showed **215- H_3Bpin** (79%), **215-(TBE)** (13%), **215-(HBpin)** (2%) and a singlet at 190.74 ppm (6%) tentatively assigned as **215-(DBpin)**.

Reaction of 215-(TBE) with 2 equiv of HBpin in cyclohexane- d_{12} - attempting to make pure 215-(HBpin) – A J. Young NMR tube was loaded with **215-(TBE)** (20 mg, 0.027 mmol), cyclohexane- d_{12} (700 μL) and HBpin (8.0 μL , 0.055 mmol). The resulting reddish yellow solution was immediately analyzed via ^1H , ^{11}B and $^{31}\text{P}\{^1\text{H}\}$ NMR spectroscopy. The $^{31}\text{P}\{^1\text{H}\}$ NMR spectrum contained **215- H_3Bpin** (31%), **215-(Bpin) $_2$** (24%), **215-(HBpin)** (40%) and **215- H_2Bpin_2** (4%). The ^{11}B NMR spectrum showed a large, broad singlet at ~ 34.4 ppm which is the expected chemical shift of TBABpin. This signal obscured the ^{11}B NMR signals of **215- H_3Bpin** and **215-(Bpin) $_2$** . The ^{11}B NMR signal of **215-(HBpin)**, expected at ~ 25 -30 ppm could not be confirmed. Significant quantities of HBpin decomposition product (15%) were observed.

Synthesis of 215- H_2 – Compound **215-(TBE)** (102 mg, 0.140 mmol) and 3 mL of cyclohexane were added to a 50 mL Hi-Vac valve round-bottom flask equipped with

a magnetic stir bar. The flask was brought out of the glovebox, degassed, and refilled with 1 atm of H₂. The reaction was stirred for 4 h at RT, forming a light yellow solution. The solvent was frozen and removed in vacuo, yielding brown solids which were left under high vacuum for 24 h, and were determined to be >95% pure **215-H₂** by ¹H and ³¹P{¹H} NMR spectroscopy. An unidentified product (4%) was observed by ³¹P{¹H} NMR spectroscopy at 178.6 ppm. The hydride resonance of **215-H₂** in cyclohexane-*d*₁₂ was broad at ambient temperature. Further inspection of the baseline revealed a broad resonance with a chemical shift ($\delta = -17.35$ ppm) that is comparable to (POCOP^{tBu})IrH₂ ($\delta = -16.99$ ppm, toluene-*d*₈, 23 °C) reported by Brookhart.¹⁶⁸ A VT ¹H and ³¹P{¹H} NMR study of **215-H₂** in toluene-*d*₈ revealed that at lower temperature **215-H₂** behaves in a similar fashion to (POCOP^{tBu})IrH₂. Yield: 76 mg (84%). ¹H NMR (500 MHz, cyclohexane-*d*₁₂): δ 6.73 (s, 1H, Ar-*H*), 2.30 (br, 4H, PCH(CH₃)₂), 1.30 (s, 18H, Ar-C(CH₃)₃), 1.14-1.10 (m, 12H, PCH(CH₃)₂), 1.00-0.96 (m, 12H, PCH(CH₃)₂), -17.17 (br, 2H). ³¹P{¹H} NMR (202 MHz, cyclohexane-*d*₁₂): δ 179.2. ¹³C{¹H} NMR (126 MHz, cyclohexane-*d*₁₂): δ 158.8 (t, *J*_{P-C} = 6.6 Hz, Ar), 125.8 (t, *J*_{P-C} = 3.9 Hz, Ar), 119.4 (s, Ar), 106.0 (s, Ar), 35.0 (s, Ar-C(CH₃)), 33.9 (t, *J*_{P-C} = 16.5 Hz, PCH(CH₃)₂), 30.8 (s, Ar-C(CH₃)), 19.3 (s, PCH(CH₃)₂), 19.0 (s, PCH(CH₃)₂).

Formation of 215-H₄ *in situ* – A J. Young NMR tube was charged with **215-(TBE)** (17 mg, 0.021 mmol) and C₆D₆ (700 μ L). The solution was frozen, degassed, and refilled with 2 atm of H₂. A color change immediately occurred from dark red as the solution turned nearly colorless and >95% pure **215-H₄** was observed to have formed by ¹H and ³¹P{¹H} NMR spectroscopy. 2,2-dimethylbutane was observed in the ¹H NMR

spectrum. ^1H NMR (500 MHz, C_6D_6): δ 7.17 (s, 1H, Ar-*H*), 1.78 (m, 4H, $\text{PCH}(\text{CH}_3)_2$), 1.52 (s, 18H, Ar- $\text{C}(\text{CH}_3)_3$), 1.08 (dvt, $J_{\text{H-H}} = 8$ Hz, $J_{\text{P-H}} = 7$ Hz, 12H, $\text{PCH}(\text{CH}_3)_2$), 0.97 (dvt, $J_{\text{H-H}} = 11$ Hz, $J_{\text{P-H}} = 7$ Hz, 12H, $\text{PCH}(\text{CH}_3)_2$), -8.81 (t, $J_{\text{P-H}} = 10.3$ Hz, 4H, Ir- H_4). $^{31}\text{P}\{^1\text{H}\}$ NMR (202 MHz, C_6D_6): δ 172.3. $^{13}\text{C}\{^1\text{H}\}$ NMR (126 MHz, C_6D_6): δ 158.5 (t, $J_{\text{P-C}} = 5.5$ Hz, Ar), 126.4 (t, $J_{\text{P-C}} = 4.6$ Hz, Ar), 121.7 (t, $J_{\text{P-C}} = 5$ Hz, Ar), 120.7 (s, Ar), 34.6 (s, Ar- $\text{C}(\text{CH}_3)$), 30.9 (t, $J_{\text{P-C}} = 18.1$ Hz, $\text{PCH}(\text{CH}_3)_2$), 30.6 (s, Ar- $\text{C}(\text{CH}_3)$), 18.4 (t, $J_{\text{P-C}} = 3.7$ Hz, $\text{PCH}(\text{CH}_3)_2$), 17.9 (s, $\text{PCH}(\text{CH}_3)_2$).

(215-(Cl)(Bpin)) - In a 50 mL Schlenk flask equipped with a magnetic stir bar was dissolved **215-(H)(Cl)** (193 mg, 0.283 mmol) in 15 mL of pentane, giving a red solution. HBpin (95.0 μL , 0.655 mmol) was added, and the solution immediately went colorless with formation of a white precipitate. The reaction was stirred for 1 h at RT, giving a yellow solution. Volatiles were removed in vacuo to afford yellow solids. These solids were washed with pentane and dried in vacuo ($\times 5$). ^1H and $^{31}\text{P}\{^1\text{H}\}$ NMR spectroscopy revealed the yellow solids to be a composed of several products including **215-(HBpin)** (9%), **215-(Bpin) $_2$** (33%), **215-H $_3$ Bpin** (5%) and an unidentified product (54%), observed as a singlet at 165.5 ppm via $^{31}\text{P}\{^1\text{H}\}$ NMR, tentatively assigned as **215-(Cl)(Bpin)**. The yellow solids were dissolved in pentane and filtered through a plug of silica, yielding a colorless filtrate. The silica was washed with pentane, then THF, eluting a bright yellow solution. All solvent was removed in vacuo, giving pure **215-(Cl)(Bpin)** as a bright yellow solid. Yield: 95 mg (42%). ^1H NMR (500 MHz, C_6D_6): δ 7.13 (s, 1H, Ar-*H*), 3.30 (m, 2H, $\text{PCH}(\text{CH}_3)_2$), 2.84 (m, 2H, $\text{PCH}(\text{CH}_3)_2$), 1.64-1.59 (m, 6H, $\text{PCH}(\text{CH}_3)_2$), 1.54 (s, 18H, Ar- $\text{C}(\text{CH}_3)_3$), 1.42-1.35 (m, 12H, $\text{PCH}(\text{CH}_3)_2$), 1.14-1.10

(m, 6H, PCH(CH₃)₂), 0.74 (s, 12H, Bpin CH₃). ¹¹B (128 MHz, C₆D₆): δ 12.0 (br s). ³¹P{¹H} NMR (202 MHz, C₆D₆): δ 165.5 (s). ¹³C{¹H} NMR (126 MHz, C₆D₆): δ 161.7 (t, J_{P-C} = 6 Hz, Ar), 126.6 (t, J_{P-C} = 5 Hz, Ar), 124.4 (m, Ar), 120.3 (s), 83.3 (s, Bpin tertiary carbon), 34.7 (s, Ar-C(CH₃)₃), 32.9 (t, J_{P-C} = 14 Hz, PCH(CH₃)₂), 31.5 (t, J_{P-C} = 16 Hz, PCH(CH₃)₂), 30.4 (s, Ar-C(CH₃)₃), 19.4 (s, PCH(CH₃)₂), 17.7 (t, J_{P-C} = 5 Hz, PCH(CH₃)₂), 16.3 (s, PCH(CH₃)₂), 16.2 (t, J_{P-C} = 4 Hz, PCH(CH₃)₂). Anal. Calcd. for **215-(Cl)(Bpin)**: C, 47.55 ; H, 7.36. Found: C, 47.52; H, 7.23.

Thermolysis of 215-(Cl)(Bpin) in C₆D₆ – A J. Young NMR tube was charged with **215-(Cl)(Bpin)** (17 mg, 0.021 mmol) and C₆D₆. The reaction was placed into an 80 °C oil bath and monitored periodically by NMR spectroscopy for up to 24 h. C₆D₅Bpin was not observed during that time, nor was there any evidence of new organometallic or organic products; only **215-(Cl)(Bpin)** was observed.

Reaction of 215-(Cl)(Bpin) with with 1 atm H₂ – A J. Young NMR tube was loaded with **215-(Cl)(Bpin)** (18 mg, 0.022 mmol) and C₆D₆ (700 μL). The tube was frozen, degassed, and refilled with 1 atm of H₂. No reaction was observed by ¹H, ¹¹B or ³¹P{¹H} NMR spectroscopy after 24 h at RT.

Synthesis of 215-H₂Bpin₂ in situ - A J. Young NMR tube was charged with **215-(TBE)** (33 mg, 0.045 mmol) and cyclohexane-*d*₁₂ (700 μL). HBpin (40 μL, 0.27 mmol) was added. The color changed from dark red to yellow within time of mixing. The sample was then analyzed via ¹H, ¹¹B and ³¹P{¹H} NMR spectroscopy. The ¹H NMR spectrum contained a C_{2v} symmetric product with a hydride resonance at -8.69 ppm (t, J = 13 Hz, 2H). The ¹¹B NMR spectrum contained only TBABpin and excess

HBpin, indicating that the ^{11}B NMR resonance for **215-H₂Bpin₂** is either broad, or obscured by the resonance of TBABpin or HBpin. The $^{31}\text{P}\{^1\text{H}\}$ spectrum contained resonances for **215-(Bpin)₂** (184.6 ppm, 11%), **215-H₃Bpin** (167.5 ppm, 31%), and **215-H₂Bpin₂** (161.8 ppm, 58%). Subjecting the volatiles to vacuum gave yellow solids mostly comprised of **215-(Bpin)₂**. Compound **215-H₂Bpin₂** was also observed as the major product during, under the reaction conditions listed in (Table II-1, Entry 9). ^1H NMR (400 MHz, C₆D₆): δ 7.18 (s, 1H, Ar-H), 2.66 (m, 4H, PCH(CH₃)₂), 1.55 (s, 18H, Ar-C(CH₃)₃), 1.14 (s, 24H, Bpin CH₃), the resonances for the isopropyl methyl protons were not observed presumably due to overlap with other signals, -8.30 (t, $J_{\text{P-H}} = 14.8$ Hz, 2H, Ir-H). $^{31}\text{P}\{^1\text{H}\}$ NMR (182 MHz, C₆D₆): δ 162.2.

Synthesis of 215-(hexene) *in situ* - A J. Young NMR tube was charged with **215-(TBE)** (12 mg, 0.016 mmol), C₆D₆ (700 μL) and 1-hexene (50 μL , 0.88 mmol). The NMR tube was placed in an 80 °C oil bath for 10 minutes, then analyzed by ^1H and $^{31}\text{P}\{^1\text{H}\}$ NMR spectroscopy. The broad signal corresponding to **215-(TBE)** in the $^{31}\text{P}\{^1\text{H}\}$ NMR spectrum disappeared and a new product tentatively assigned as **215-(hexene)** was observed at 177.4 ppm. Free TBE was observed in the ^1H NMR spectrum.

Synthesis of 214-(C₆H₅F)(H) - A vial was loaded with **214-(H)(Cl)** (115 mg, 0.197 mmol), NaO^tBu (21 mg, 0.22 mmol) and 3 mL of fluorobenzene. The reaction was stirred at RT for 3 h, filtered through Celite, and all solvent was removed in vacuo to provide **214-(C₆H₅F)(H)** as a brick red solid. Isolated samples of **214-(C₆H₅F)(H)** contained small amounts of residual fluorobenzene. Yield: 119 mg (94%). ^1H NMR (500 MHz, cyclohexane-*d*₁₂): δ 6.45 (s, 2H, Ar-H), 2.52 (br, 4H, PCH(CH₃)₂), 2.22 (s, 3H,

Ar-CH₃), 1.13 (m, 12H, PCH(CH₃)₂), 0.96 (m, *J* = 16.7, 8.0 Hz, 12H, PCH(CH₃)₂), –43.51 (br, 1H, Ir-*H*). ¹⁹F (470 MHz, cyclohexane-*d*₁₂): δ –90.87 (br). ³¹P{¹H} NMR (202 MHz, cyclohexane-*d*₁₂): δ 177.8.

Reaction of 214-(C₆H₅F)(H) with HBpin at room temperature in an inert solvent (cyclohexane-*d*₁₂) – A J. Young tube was loaded with **214-(C₆H₅F)(H)** (44 mg, 0.068 mmol) and cyclohexane-*d*₁₂ (700 μL). A small amount of solid persisted at the bottom of the NMR tube. The solvent was frozen and HBpin (10 μL, 0.069 mmol) was added. The sample was allowed to thaw, mixed for a few seconds (at which point the color instantly changed from red to yellow) then analyzed within 2 minutes by NMR spectroscopy. By ¹H NMR, the downfield hydride resonance of **214-(C₆H₅F)(H)** disappeared with multiple unidentified hydride resonances observed between –6 and –20 ppm. Resonances corresponding to free fluorobenzene were also observed. The ¹¹B spectrum contained **214-H₃Bpin** (40%) and a product at 30.4 ppm (60%) (Figure II-14) which was later identified as the ortho- borylated fluorobenzene product herein referred to as **L-2**. Trace quantities (<1%) of HBpin decomposition were observed (21.4 ppm). The ¹⁹F NMR spectrum contained resonances for **L-2** (45%, –101.6 ppm), free fluorobenzene (52%, –113.4 ppm) and an unknown compound (3%, –88.3 ppm). The ³¹P{¹H} spectrum revealed numerous products including **214-(HBpin)** (190.7 ppm, 15%), **214-H₃Bpin** (167.4 ppm, 64%), and **214-H₂** (179.2 ppm, 3%). Trace quantities of **214-(Bpin)₂** were observed, but the remaining products were not identified. The sample was brought into a glovebox and all solvent was removed in vacuo giving a red residue. This residue was dissolved in CDCl₃, and C₆F₆ (10 μL, 0.087 mmol) was added as an

internal standard for NMR analysis. The borylated arene product, **L-2**, was unambiguously assigned via literature comparison (Figure II-12).¹⁶⁹ Two, near overlapping, unidentified singlets, both appearing at roughly 1.35 ppm, are similar in chemical shift to the *meta*- and *para*- isomers reported in the literature (Figure II-13),¹⁷⁶ but arene resonances corresponding to those isomers were not observed nor were definitive signals for the *meta*- and *para*- isomers observed in the ¹⁹F spectrum (Figure II-15). The spectroscopic yield of **L-2**, determined by ¹⁹F NMR, was 63%.

Reaction of 214-(C₆H₅F)(H) with HBpin at room temperature in neat fluorobenzene – A J. Young tube was charged with **214-(C₆H₅F)(H)** (44 mg, 0.068 mmol) and fluorobenzene (700 μL) giving a dark red solution. HBpin (10 μL, 0.069 mmol) was added and the sample was immediately analyzed by NMR spectroscopy. The ¹¹B NMR spectrum contained resonances for **214-(HBpin)** (~9%), **L-2** (69%), and **214-H₃Bpin** (22%). The ¹⁹F NMR spectrum contained resonances for **214-(C₆H₅F)(H)** (33%) and **L-2** (67%). The ³¹P{¹H} NMR spectrum contained resonances for **214-(HBpin)** (8%), **214-H₂** (3%), **214-(C₆H₅F)(H)** (30%), **214-H₃Bpin** (54%) and an unidentified compound at 167.0 ppm (6%).

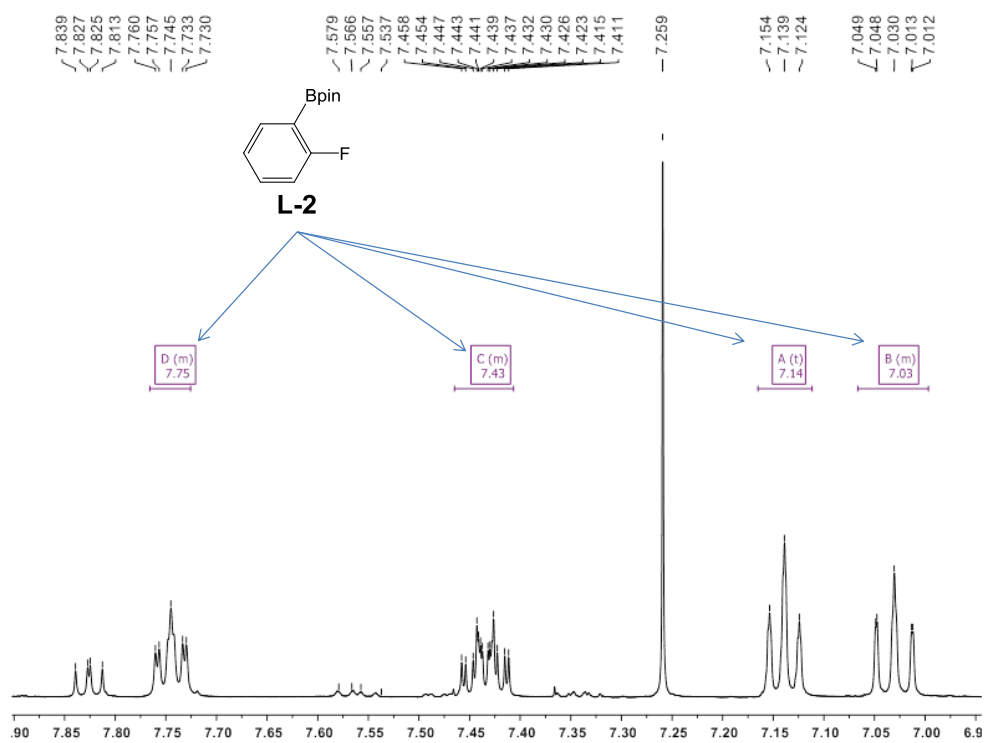


Figure II-12. A section of the ^1H NMR (500 MHz, CDCl_3) spectrum showing aromatic resonances (multiplets A, B, C and D) of **L-2**. The other signals were not identified.

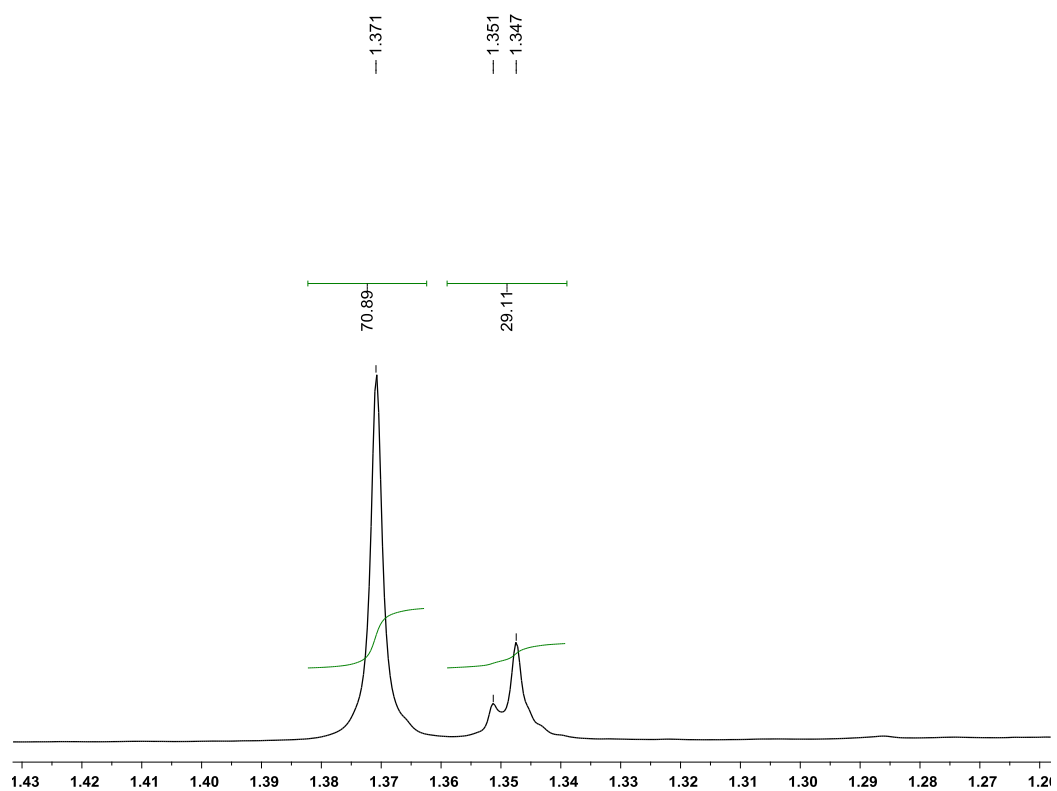


Figure II-13. A section of the ^1H NMR (500 MHz, CDCl_3) spectrum showing aliphatic resonances of **L-2**, seen at 1.37 ppm. The other signals were not identified.

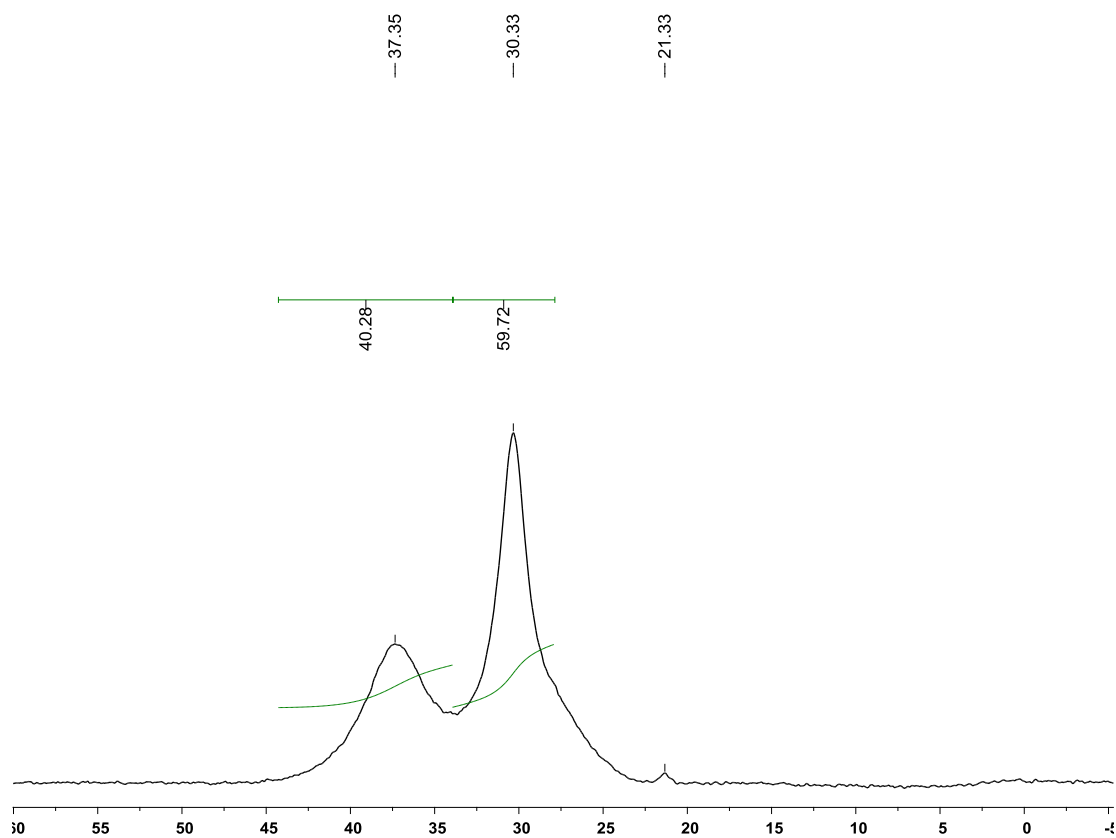


Figure II-14. ^{11}B NMR (128 MHz, CDCl_3) spectrum showing **L-2** at 30.3 ppm. **214-H₃Bpin** is observed at 37.4 ppm.

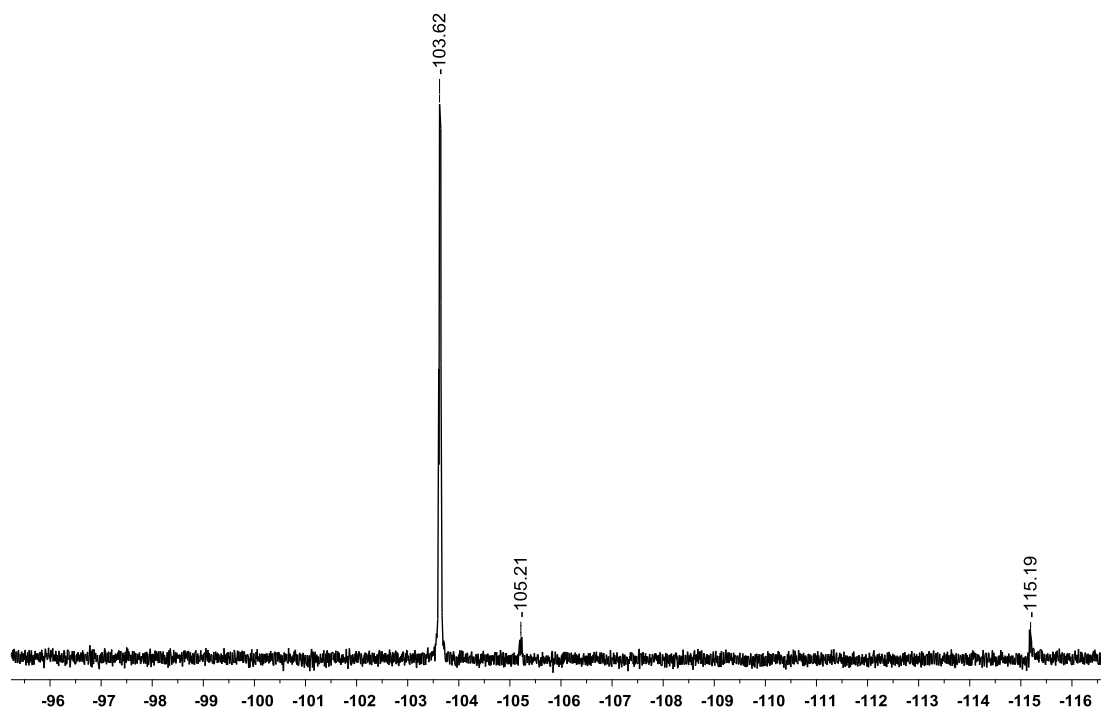


Figure II-15. ^{19}F NMR (470 MHz, CDCl_3) spectrum of **L-2** (-103.6 ppm). The minor products were not identified.

General procedure for J. Young NMR tube catalytic C-H borylation reactions from Table II-1 – In a glovebox, a J. Young tube was loaded with pre-catalyst (added either as a solid or by stock solution), HBpin or B_2pin_2 (as noted), cyclohexane or mesitylene as an internal standard, and C_6D_6 . Stock solutions of **213-(H)(Cl)**, **214-(H)(Cl)**, **215-(H)(Cl)** and **215-(TBE)** were prepared by weighing the respective compound into a glass vial and dissolving in a known amount of benzene or C_6D_6 . A representative example of a 0.021 M stock solution preparation for compound

215-(H)(Cl): Compound **215-(H)(Cl)** (14 mg, 0.021 mmol) was added to a glass vial and dissolved in 1.0 mL of benzene. This solution was diluted by a factor of ten (0.0021 M) and the resulting solution was diluted by a factor of ten (0.00021 M). Addition of ethylene was performed by charging a container of known volume with 1 atm of ethylene, then subsequently condensing the reagent into a degassed J. Young tube, using liquid nitrogen. 1-hexene and TBE were added via syringe during the initial loading of all reaction components into the NMR tube. The J. Young NMR tube was then placed into an oil bath at the indicated temperature for the time reported, and monitored by ^1H , ^{11}B , and $^{31}\text{P}\{^1\text{H}\}$ NMR spectroscopy. Turnover numbers (TONs) and *in situ* yields (% $\text{C}_6\text{D}_5\text{Bpin}$) were determined by comparing integration of the cyclohexane or mesitylene internal standard to the Bpin methyl signals of $\text{C}_6\text{D}_5\text{Bpin}$ ($\delta = 1.11$ ppm in C_6D_6). Detailed descriptions of each entry are provided below.

Entries 1-15 refer to Table II-1 - Entry 1 – Reaction of HBpin with neat C₆D₆ and 5 mol% of 213-(H)(Cl) - A J. Young tube was loaded with **213-(H)(Cl)** (8.0 mg, 0.014 mmol). HBpin (40 μL, 0.28 mmol) was added followed by cyclohexane (20 μL, 0.19 mmol) as an internal standard, and 700 μL of C₆D₆. The colorless solution was immediately analyzed by ¹H, ¹¹B, and ³¹P{¹H} NMR spectroscopy, then again after the NMR tube was placed into a 100 °C oil for 1 h and 36 h. Prior to heating, the ³¹P{¹H} NMR spectrum contained: **213-H₃Bpin** (97%), **213-H₂Bpin₂** (3%). After 1 h at 100 °C, the ³¹P{¹H} NMR spectrum contained: **213-H₃Bpin** (57%), **213-H₂Bpin₂** (43%). ¹¹B NMR spectrum contained: **213-H₃Bpin** (4%), HBpin (96%), and HBpin decomposition products (<1%). No C₆D₅Bpin was observed. After 36 h at 100 °C, the ³¹P{¹H} NMR spectrum contained: **213-H₃Bpin** (87%), **213-H₂Bpin₂** (13%). ¹¹B NMR spectrum contained: **213-H₃Bpin** (3%), C₆D₅Bpin (3%), HBpin (93%), and HBpin decomposition products (<1%). A 6% yield of C₆D₅Bpin was determined by ¹H NMR spectroscopy.

Entry 2 – Reaction of HBpin with neat C₆D₆ and 5 mol% of 214-(H)(Cl) - A J. Young tube was loaded with **214-(H)(Cl)** (8.0 mg, 0.014 mmol). HBpin (40 μL, 0.28 mmol) was added followed by cyclohexane (20 μL, 0.19 mmol) as an internal standard, and 700 μL of C₆D₆. The colorless solution was immediately analyzed by ¹H, ¹¹B, and ³¹P{¹H} NMR spectroscopy, then again after the NMR tube was placed into an 100 °C oil bath for 1 h and 36 h. Prior to heating, the ³¹P{¹H} NMR spectrum contained: **214-H₃Bpin** (96%) and **214-H₂Bpin₂** (4%). After 1 h at 100 °C, the ³¹P{¹H} NMR spectrum contained: **214-H₃Bpin** (52%) and **214-H₂Bpin₂** (48%). The ¹¹B NMR spectrum contained **214-H₃Bpin**, HBpin, and HBpin decomposition products (<1%). No

C₆D₅Bpin was observed. After 36 h at 100 °C, the ³¹P{¹H} NMR spectrum contained **214-H₃Bpin** (86%) and **214-H₂Bpin₂** (14%). The ¹¹B NMR spectrum contained: **214-H₃Bpin** (2%), C₆D₅Bpin (2%), HBpin (95%), and HBpin decomposition products (1%). A 4% yield of C₆D₅Bpin was observed via ¹H NMR spectroscopy.

Entry 3 – Reaction of HBpin with neat C₆D₆ and 5 mol% of 215-(H)(Cl) - A J. Young tube was loaded with **215-(H)(Cl)** (9.4 mg, 0.014 mmol) . HBpin (40 μL, 0.28 mmol) was added followed by cyclohexane (20 μL, 0.19 mmol) as an internal standard and 700 μL of C₆D₆. The colorless solution was immediately analyzed by ¹H, ¹¹B, and ³¹P{¹H} NMR spectroscopy, then again after the NMR tube was placed into an 100 °C oil bath for 1 h and 36 h. Prior to heating, the ³¹P{¹H} NMR spectrum contained: **215-H₃Bpin** (97%) and **215-H₂Bpin₂** (3%) (Figure II-16). After 1 h at 100 °C, the ³¹P{¹H} NMR spectrum contained: **215-H₃Bpin** (65%) and **215-H₂Bpin₂** (35%). The ¹¹B NMR spectrum contained: **215-H₃Bpin**, HBpin and HBpin decomposition products (<1%). No C₆D₅Bpin was observed. After 36 h at 100 °C, the ³¹P{¹H} NMR spectrum contained: **215-H₃Bpin** (86%) and **215-H₂Bpin₂** (14%). The ¹¹B NMR spectrum contained: **215-H₃Bpin** (1%), C₆D₅Bpin (4%), HBpin (94%), and HBpin decomposition products (1%) (Figure II-17). A 6% yield of C₆D₅Bpin was observed via ¹H NMR spectroscopy.

Entry 4 – Reaction of HBpin with neat C₆D₆, excess 1-hexene and 5 mol% of 213-(H)(Cl) - A J. Young tube was loaded with **213-(H)(Cl)** (8.0 mg, 0.014 mmol). HBpin (40 μL, 0.28 mmol) was added followed by 1-hexene (105 μL, 0.840 mmol), cyclohexane (20 μL, 0.185 mmol) as an internal standard, and 700 μL of C₆D₆. The colorless solution was immediately analyzed by ¹H, ¹¹B, and ³¹P{¹H} NMR

spectroscopy, then again after the NMR tube was placed into an 80 °C oil bath for 0.5 h. Prior to heating, the $^{31}\text{P}\{^1\text{H}\}$ NMR spectrum contained: **213-H₃Bpin** (81%) and **213-H₂Bpin₂** (18%). The ^{11}B NMR spectrum contained: **213-H₃Bpin** (3%), hexylBpin (5%), C₆D₅Bpin (5%), HBpin (87%), and HBpin decomposition products (<1%). After 0.5 h at 80 °C, the $^{31}\text{P}\{^1\text{H}\}$ NMR spectrum contained: **213-(hexene)** (22%) and **213-H₂Bpin₂** (78%). The ^{11}B NMR spectrum contained: hexylBpin (17%), C₆D₅Bpin (69%), ClBpin (5%), and **213-(Cl)(Bpin)** (9%). A 77% yield of C₆D₅Bpin was determined by ^1H NMR spectroscopy.

Entry 5 – Reaction of HBpin with neat C₆D₆, excess 1-hexene, and 5 mol% of 214-(H)(Cl) - A J. Young tube was loaded with **214-(H)(Cl)** (8.0 mg, 0.014 mmol) of **214-(H)(Cl)**. HBpin (40 μL, 0.28 mmol) was added, followed by 1-hexene (105 μL, 0.840 mmol), cyclohexane (20 μL, 0.185 mmol) as an internal standard, and 700 μL of C₆D₆. The colorless solution was immediately analyzed by ^1H , ^{11}B , and $^{31}\text{P}\{^1\text{H}\}$ NMR spectroscopy, then again after the NMR tube was placed into an 80 °C oil bath for 0.5 h. Prior to heating, the $^{31}\text{P}\{^1\text{H}\}$ NMR spectrum contained: **214-H₃Bpin** (85%) and **214-H₂Bpin₂** (15%). The ^{11}B NMR spectrum contained: **214-H₃Bpin** (4%), hexylBpin (3%), C₆D₅Bpin (8%), HBpin (85%) and HBpin decomposition products (<1%). After 0.5 h at 80 °C, the $^{31}\text{P}\{^1\text{H}\}$ NMR spectrum contained: **214-(hexene)** (14%), **214-(Bpin)₂** (11%), and **214-H₂Bpin₂** (75%). ^{11}B NMR spectroscopy revealed hexylBpin (9%), C₆D₅Bpin (83%), ClBpin (6%), and **214-(Cl)(Bpin)** (2%). An 85% yield of C₆D₅Bpin was determined by ^1H NMR spectroscopy.

Entry 6 – Reaction of HBpin with neat C₆D₆, excess 1-hexene, and 5 mol% of 215-(H)(Cl) - A J. Young tube was loaded with **215-(H)(Cl)** (9.4 mg, 0.014 mmol). HBpin (40 μL, 0.28 mmol) was added followed by 1-hexene (105 μL, 0.84 mmol), cyclohexane (20 μL, 0.19 mmol) as an internal standard, and 700 μL of C₆D₆. The colorless solution was immediately analyzed by ¹H, ¹¹B, and ³¹P{¹H} NMR spectroscopy, then again after the NMR tube was placed into an 80 °C oil bath for 0.5 h. Prior to heating, the ³¹P{¹H} NMR spectrum contained: **215-H₃Bpin** (91%) and **215-H₂Bpin₂** (9%) (Figure II-18). The ¹¹B NMR spectrum contained: **215-H₃Bpin** (2%), hexylBpin (2%), C₆D₅Bpin (6%), HBpin (89%) and HBpin decomposition products (<1%). After 0.5 h at 80 °C, the ³¹P{¹H} NMR spectrum contained: **215-(hexene)** (15%), an unidentified singlet (2%) at 176.3 ppm, **215-(Bpin)₂** (2%), and **215-(Cl)(Bpin)** (81%) (Figure II-20). The ¹¹B NMR spectrum contained: hexylBpin (23%), C₆D₅Bpin (73%), ClBpin (2%), and **215-(Cl)(Bpin)** (1%) (Figure II-21). A 75% yield of C₆D₅Bpin was determined by ¹H NMR spectroscopy (Figure II-19).

Entry 7 - Reaction of HBpin with neat C₆D₆ and 5 mol% of 215-(TBE) - A J. Young tube was loaded with **215-(TBE)** (10 mg, 0.014 mmol). HBpin (40 μL, 0.28 mmol) was added, followed by cyclohexane (20 μL, 0.19 mmol) as an internal standard, and 700 μL of C₆D₆. In the time of mixing, the dark red solution became a dull, light yellow, then nearly colorless, and was immediately analyzed by ¹H, ¹¹B, and ³¹P{¹H} NMR spectroscopy. The NMR tube was placed into an 80 °C oil bath and monitored by ¹H, ¹¹B, and ³¹P{¹H} NMR spectroscopy after 1 h, followed by variable temperature ¹¹B and ³¹P{¹H} NMR spectroscopy from RT to +80 °C. Heating caused the colorless

solution to turn yellow and, upon cooling, back to colorless. Prior to heating, the $^{31}\text{P}\{^1\text{H}\}$ NMR spectrum contained only **215-H₃Bpin**. The ^{11}B NMR spectrum contained: **215-H₃Bpin** (4%), TBABpin (6%), C₆D₅Bpin (6%), HBpin (84%), and HBpin decomposition products (1%). After 1 h at 80 °C, the $^{31}\text{P}\{^1\text{H}\}$ NMR spectrum contained: **215-H₃Bpin** (86%) and **215-H₂Bpin₂** (14%). The ^{11}B NMR spectrum contained: **215-H₃Bpin** (4%), TBABpin (6%), C₆D₅Bpin (6%), HBpin (84%), and HBpin decomposition products (1%). Variable temperature $^{31}\text{P}\{^1\text{H}\}$ NMR spectroscopy from RT to +80 °C showed the gradual formation of **215-(HBpin)** (4%), **215-(Bpin)₂** (4%), and **215** (2%) in conjunction with **215-H₃Bpin** (84%) and **215-H₂Bpin₂** (6%). The formation of compounds **215-(HBpin)** and **215-(Bpin)₂** explains the dramatic color change from colorless to bright yellow that occurred upon heating; **215-(HBpin)** and **215-(Bpin)₂** are bright yellow compounds as solids and in solution.

Entry 8 – Reaction of HBpin with neat C₆D₆, excess 1-hexene, and 5 mol% of 215-(TBE) - A J. Young tube was loaded with **215-(TBE)** (10 mg, 0.014 mmol). HBpin (40 μL, 0.28 mmol) was added, followed by 1-hexene (105 μL, 0.840 mmol), cyclohexane (20 μL, 0.185 mmol) as an internal standard, and 700 μL of C₆D₆. Upon mixing, the dark red solution changed to light yellow, then to near colorless, and was immediately analyzed by ^1H , ^{11}B , and $^{31}\text{P}\{^1\text{H}\}$ NMR spectroscopy, then again after the NMR tube was placed into an 80 °C oil bath for 0.5 h. Prior to heating, the $^{31}\text{P}\{^1\text{H}\}$ NMR spectrum contained: **215-H₃Bpin** (88%) and **215-H₂Bpin₂** (12%). The ^{11}B NMR spectrum contained: **215-H₃Bpin** (3%), hexylBpin/TBABpin (7%), C₆D₅Bpin (10%), HBpin (79%), and HBpin decomposition products (<1%). After 0.5 h at 80 °C, the

$^{31}\text{P}\{^1\text{H}\}$ NMR spectrum contained: **215-(hexene)** (69%), an unidentified singlet (6%) at 175.9 ppm, **215-(Bpin)₂** (12%), **215-(HBpin)** (<1%), and an unidentified product at 182.8 ppm. The ^{11}B NMR spectrum contained: hexylBpin (17%), $\text{C}_6\text{D}_5\text{Bpin}$ (82%), and HBpin decomposition products (<1%) (Figure II-22). An 88% yield of $\text{C}_6\text{D}_5\text{Bpin}$ was determined by ^1H NMR spectroscopy.

Entry 9 - Reaction of HBpin with neat C_6D_6 and 5 mol% of 215-(TBE) in an open reaction vessel - A 100 mL Hi-Vac valve round-bottom flask was loaded with **215-(TBE)** (10 mg, 0.014 mmol), HBpin (40 μL , 0.28 mmol), and 1 mL of C_6D_6 . The flask was sealed, brought out of the glovebox, attached to a Schlenk line, and placed into a 100 $^\circ\text{C}$ oil bath. The flask was opened to argon flow and the flask neck was cooled to prevent solvent loss. The reaction was vigorously stirred for 30 min, brought back into the glovebox, and the bright yellow solution was transferred to a J. Young NMR tube. Cyclohexane (20 μL , 0.185 mmol) was added as an internal standard, and the sample was analyzed via ^1H , ^{11}B , and $^{31}\text{P}\{^1\text{H}\}$ NMR spectroscopy. The ^{11}B NMR spectrum contained: TBABpin (5%), $\text{C}_6\text{D}_5\text{Bpin}$ (5%), HBpin (85%), and HBpin decomposition products (4%). The $^{31}\text{P}\{^1\text{H}\}$ NMR spectrum contained: **215-(Bpin)₂** (62%) and **215-H₂Bpin₂** (38%). A 5% yield of $\text{C}_6\text{D}_5\text{Bpin}$ was determined by ^1H NMR spectroscopy.

Entry 10 – Reaction of HBpin with neat C_6D_6 , excess TBE, and 5 mol% of 215-(TBE) - A J. Young tube was loaded with **215-(TBE)** (10 mg, 0.014 mmol). HBpin (40 μL , 0.28 mmol) was added, followed by TBE (110 μL , 0.850 mmol), cyclohexane (20 μL , 0.185 mmol) as an internal standard, and 700 μL of C_6D_6 . Upon mixing, the dark red solution changed to light yellow, and was immediately analyzed by ^1H , ^{11}B , and

$^{31}\text{P}\{^1\text{H}\}$ NMR spectroscopy, then again after the NMR tube was placed into an 80 °C oil bath for 0.5 h and 1 h. Prior to heating, the $^{31}\text{P}\{^1\text{H}\}$ NMR spectrum contained: **215-H₃Bpin** (49%), **215-(Bpin)₂** (7%), and **215-H₂Bpin₂** (44%). The ^{11}B NMR spectrum contained: TBABpin (27%), HBpin (73%), C₆D₅Bpin (<1%), and HBpin decomposition products (<1%). After 0.5 h at 80 °C, the ^{11}B NMR spectrum contained: TBABpin (35%), C₆D₅Bpin (20%), H(D)Bpin (44%), and HBpin decomposition (<1%). After 1 h at 80 °C, the ^{11}B NMR spectrum contained: TBABpin (38%), C₆D₅Bpin (60%), and HBpin decomposition (2%). The $^{31}\text{P}\{^1\text{H}\}$ NMR spectrum contained: **215-(HBpin)** (24%), **215-H₃Bpin** (58%), and **215-(Bpin)₂** (18%). A 66% yield of C₆D₅Bpin was determined by ^1H NMR spectroscopy.

Entry 11 – Reaction of B₂pin₂ with neat C₆D₆ and 5 mol% of 215-(TBE) - A J. Young tube was loaded with **215-(TBE)** (10 mg, 0.014 mmol). B₂pin₂ (71 mg, 0.28 mmol) was added, followed by cyclohexane (20 μL, 0.19 mmol) as an internal standard, and 700 μL of C₆D₆. The dark red solution was immediately analyzed by ^1H , ^{11}B , and $^{31}\text{P}\{^1\text{H}\}$ NMR spectroscopy, then again after the NMR tube was placed into a 100 °C oil bath for 0.5 h, 2 h, and 72 h. After 2 h, the reaction color changed from dark red to yellow and the $^{31}\text{P}\{^1\text{H}\}$ NMR spectrum contained only **215-(Bpin)₂**, while the ^1H NMR spectrum showed no C₆D₅Bpin formation. After 72 h at 100 °C, the $^{31}\text{P}\{^1\text{H}\}$ NMR spectrum contained **215-(Bpin)₂** (81%) with an unidentified product at 185.4 ppm (19%, doublet, $J = 69$ Hz). A 5% yield of C₆D₅Bpin was determined by ^1H NMR spectroscopy.

Entry 12 – Reaction of B₂pin₂ with neat C₆D₆, excess 1-hexene, and 5 mol% of 215-(TBE) - A J. Young tube was loaded with **215-(TBE)** (10 mg, 0.014 mmol).

B₂pin₂ (71 mg, 0.28 mmol) was added, followed by 1-hexene (105 μL, 0.84 mmol), cyclohexane (20 μL, 0.19 mmol) as an internal standard, and 700 μL of C₆D₆. The dark red solution was immediately analyzed by ¹H, ¹¹B, and ³¹P{¹H} NMR spectroscopy, then again after the NMR tube was placed into a 100 °C oil bath for 0.5 h, 2 h, and 72 h. After 2 h, the reaction color changed from dark red to red-yellow and the ³¹P{¹H} NMR spectrum contained **215-(Bpin)₂** (78%) and **215-(hexene)** (22%), while the ¹H NMR spectrum showed no C₆D₅Bpin formation. After 72 h at 100 °C, the ³¹P{¹H} NMR spectrum contained **215-(Bpin)₂** (79%) with an unidentified product at 185.4 ppm (21%, doublet, *J* = 69 Hz). A 5% yield of C₆D₅Bpin was determined by ¹H NMR spectroscopy.

Entry 13 – Reaction of HBpin with neat C₆D₆, excess ethylene, and 5 mol% of 215-(H)(Cl) - A J. Young tube was loaded with **215-(H)(Cl)** (9.4 mg, 0.014 mmol). HBpin (40 μL, 0.28 mmol) was added, followed by 700 μL of benzene, resulting in a colorless solution. The solution was frozen then degassed, and ethylene (0.6 mmol) was condensed into the NMR tube. The NMR was placed into an 80 °C oil bath, and after <10 minutes, became yellow. ¹¹B NMR spectroscopy revealed: EtBpin (16%), C₆D₅Bpin (80%), ClBpin (3%), and HBpin decomposition products (2%).

Entry 14 – Reaction of HBpin with neat C₆D₆, excess ethylene, and 0.1 mol% of 215-(H)(Cl) – A J. Young tube was charged with a 2.1 mM C₆D₆ solution of **215-(H)(Cl)** (125 μL, 0.25 μmol). HBpin (40 μL, 0.28 mmol) was added, followed by mesitylene (10 μL, 0.072 mmol) as an internal standard, and 600 μL of C₆D₆. The solution was frozen then degassed, and ethylene (0.6 mmol) was condensed into the NMR tube. The solution was immediately analyzed by ¹H NMR spectroscopy, then

again after the NMR tube was placed into an 80 °C oil bath for 0.5 h. After 0.5 h at 80 °C, a 76% yield of C₆D₅Bpin was determined by ¹H NMR spectroscopy.

Entry 15 – Reaction of HBpin with neat C₆D₆, excess ethylene, and 0.004 mol% of 215-(H)(Cl) - A J. Young tube was charged with a 0.21 mM C₆D₆ solution of **215-(H)(Cl)** (50 μL, 0.01 μmol). HBpin (40 μL, 0.28 mmol) was added, followed by mesitylene (10 μL, 0.072 mmol) as an internal standard, and 600 μL of C₆D₆. The solution was frozen then degassed, and ethylene (0.6 mmol) was condensed into the NMR tube. The solution was immediately analyzed by ¹H NMR spectroscopy, then again after the NMR tube was placed into an 80 °C oil bath for 14 h. After 14 h at 80 °C, an 83% yield of C₆D₅Bpin was determined by ¹H NMR spectroscopy.

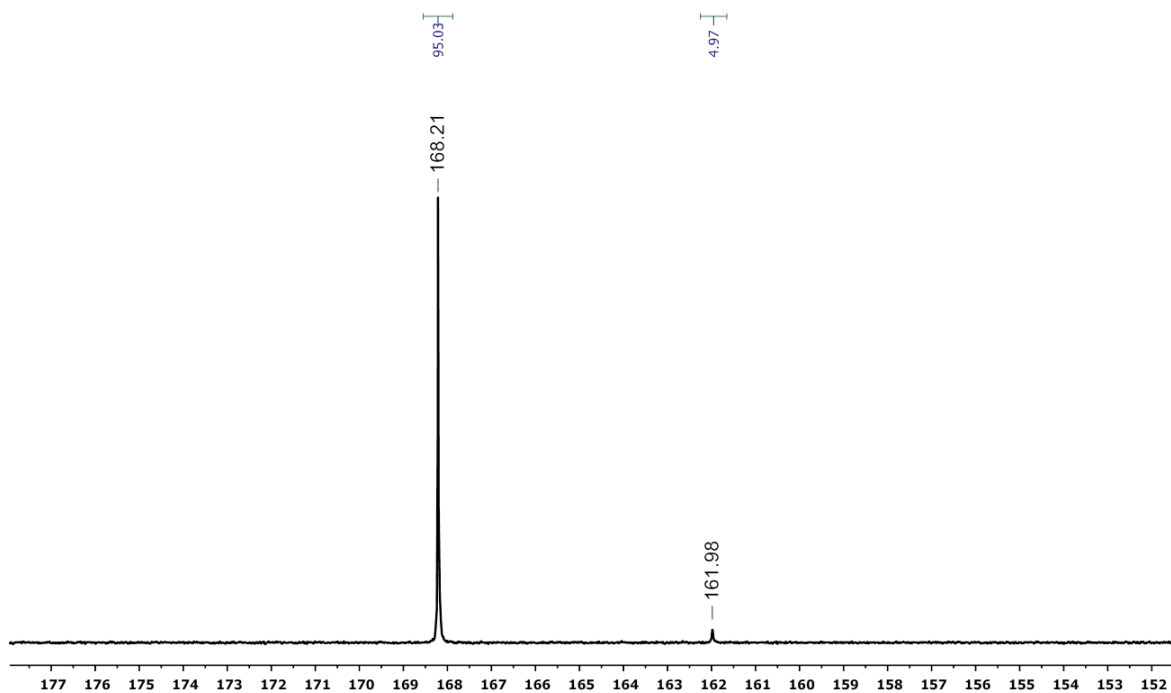


Figure II-16. Entry 3 – $^{31}\text{P}\{^1\text{H}\}$ NMR (202 MHz, C_6D_6) spectrum taken immediately after mixing HBpin and C_6D_6 with 5 mol% **215-(H)(Cl)**. Resonances for **215- H_3Bpin** and **215- H_2Bpin_2** are observed.

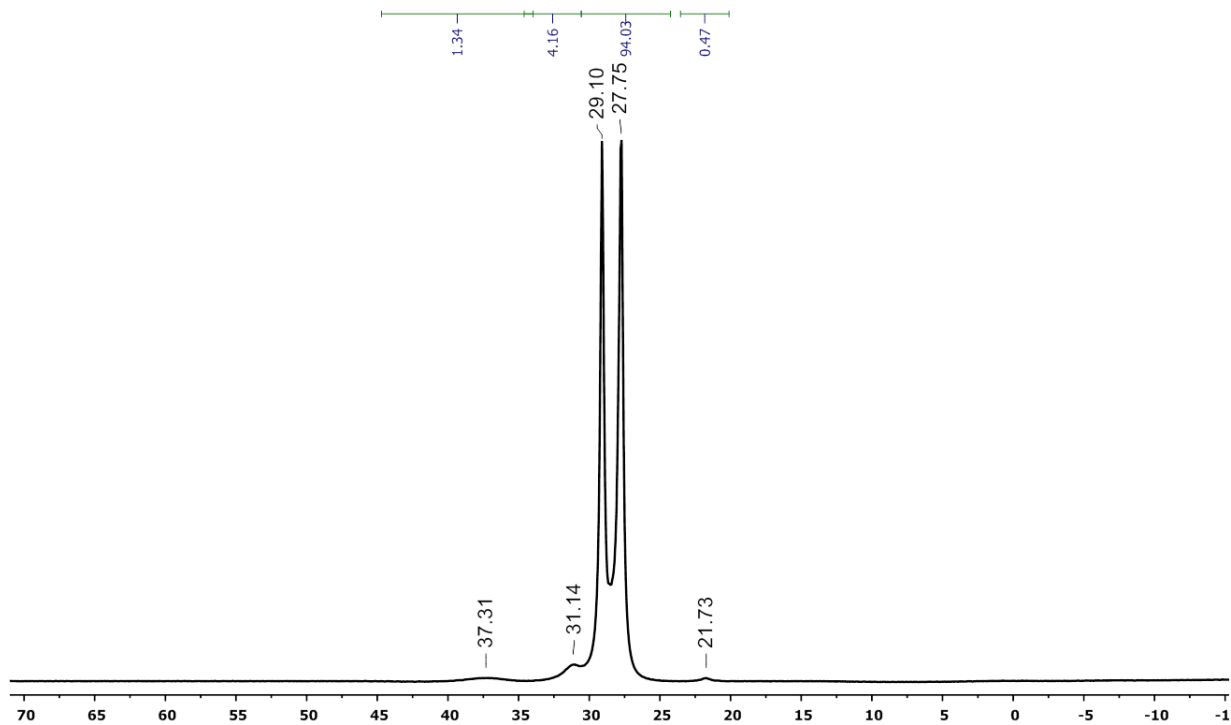


Figure II-17. Entry 3 ^{11}B NMR (128 MHz, C_6D_6) spectrum after heating for 36 h at 100 °C. Resonances of **215- H_3Bpin** , $\text{C}_6\text{D}_5\text{Bpin}$, HBpin , and trace HBpin decomposition are observed.

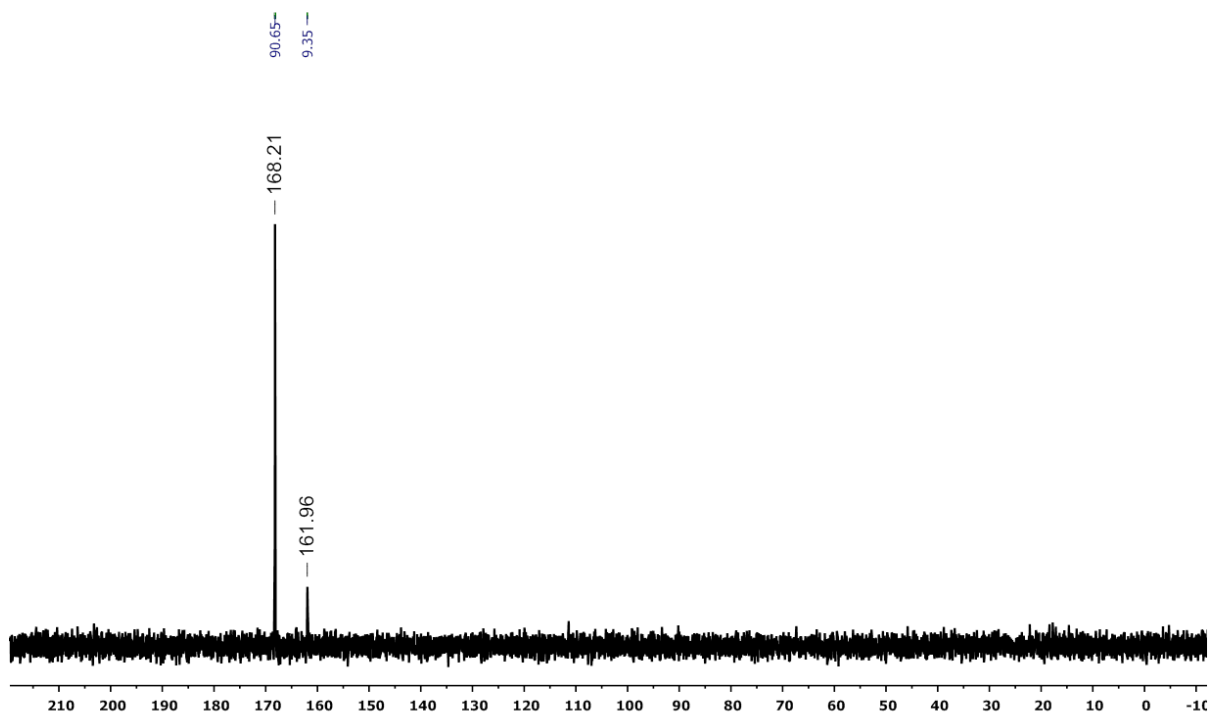


Figure II-18. Entry 6 - $^{31}\text{P}\{^1\text{H}\}$ NMR (202 MHz, C_6D_6) spectrum taken immediately after mixing HBpin and C_6D_6 with 5 mol% **215-(H)(Cl)** and excess 1-hexene. Resonances for **215- H_3Bpin** and **215- H_2Bpin_2** are observed.

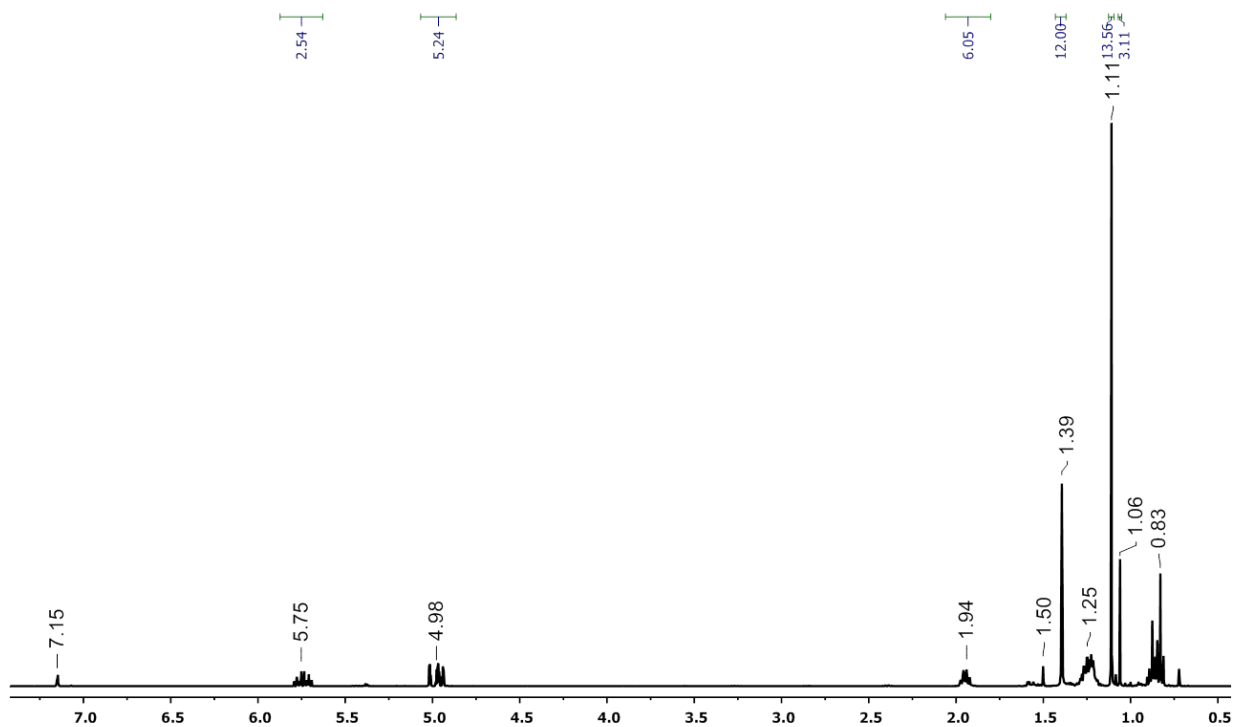


Figure II-19. Entry 6 – ¹H NMR (400 MHz, C₆D₆) spectrum after reacting HBpin and C₆D₆ with 5 mol% **215-(H)(Cl)** and excess 1-hexene at 80 °C for 0.5 h. Resonances for C₆D₅Bpin, hexylBpin, and excess 1-hexene are observed.

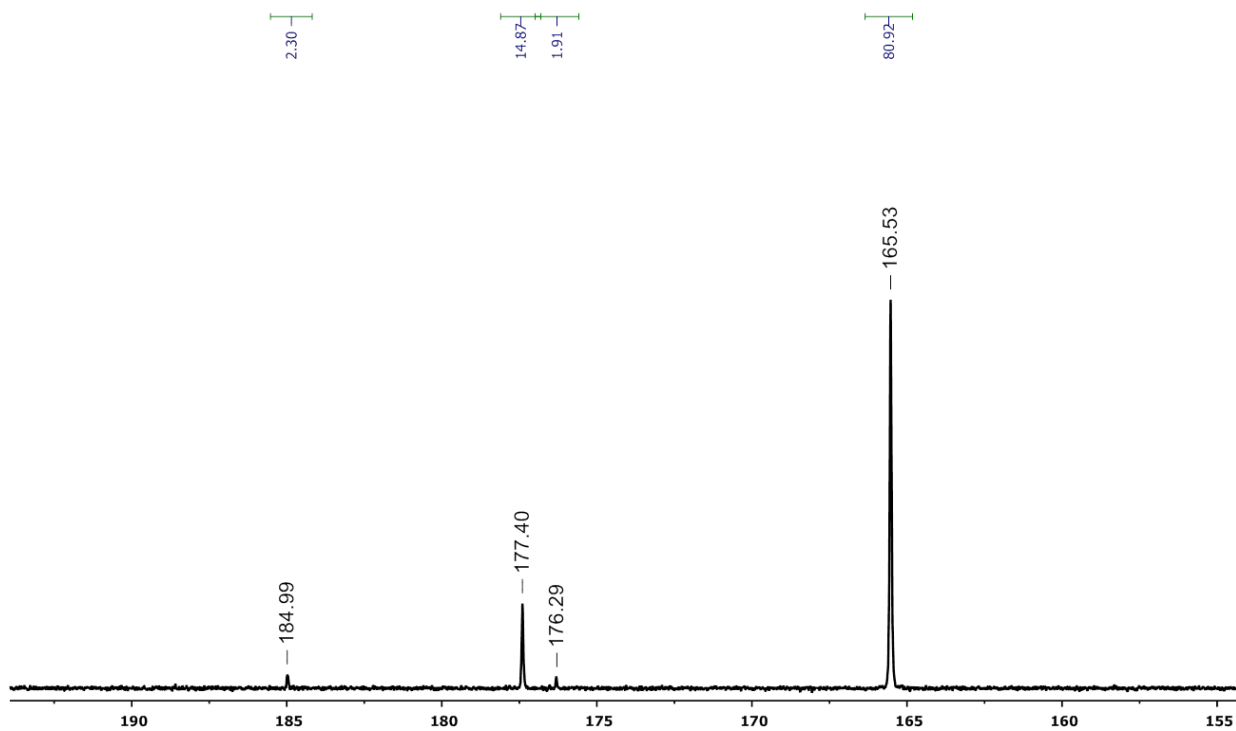


Figure II-20. Entry 6 – $^{31}\text{P}\{^1\text{H}\}$ NMR (202 MHz, C_6D_6) spectrum taken after reacting HBpin and C_6D_6 with 5 mol% **215-(H)(Cl)** and excess 1-hexene at 80 °C for 0.5 h. Resonances for **215-(Bpin)₂**, **215-(hexene)** and **215-(Cl)(Bpin)** are observed.

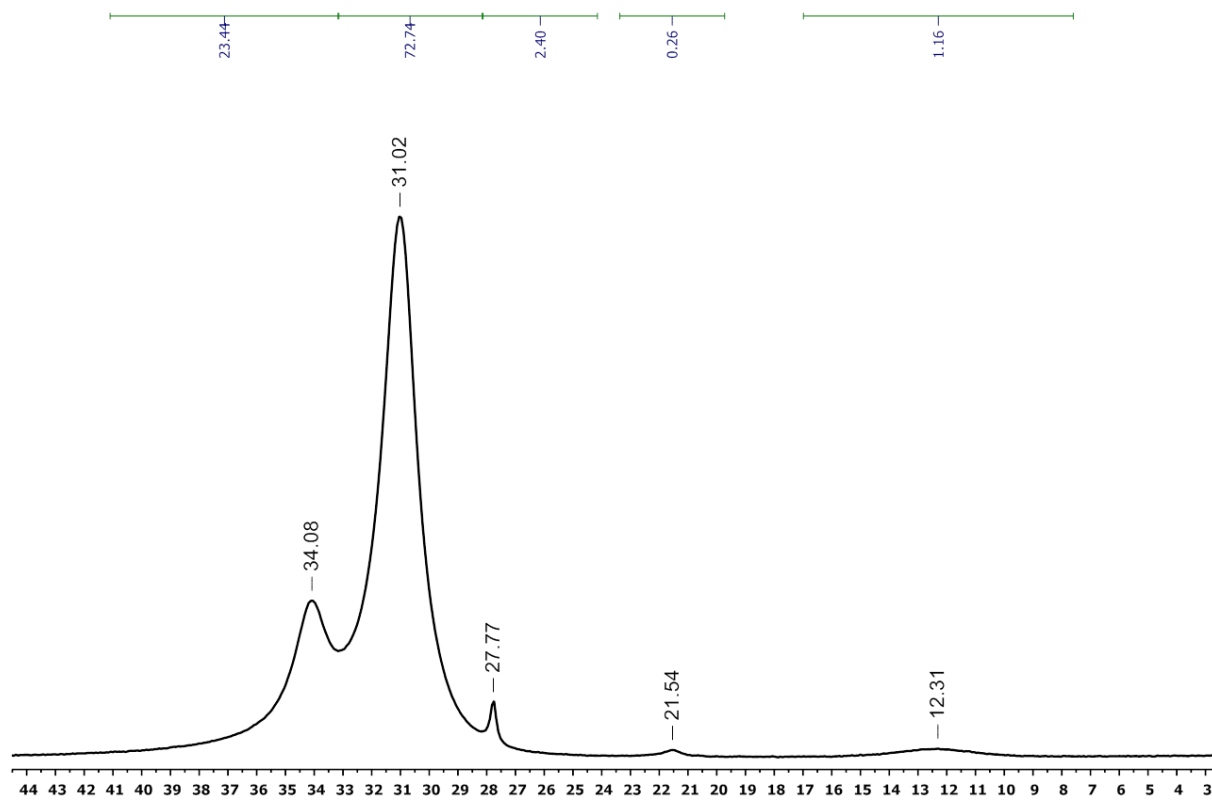


Figure II-21. Entry 6 – ^{11}B NMR (128 MHz, C_6D_6) spectrum after reacting HBpin and C_6D_6 with 5 mol% **215-(H)(Cl)** and excess 1-hexene at 80 °C for 0.5 h. Resonances for hexylBpin, $\text{C}_6\text{D}_5\text{Bpin}$, ClBpin and **215-(Cl)(Bpin)** are observed, as well trace HBpin decomposition products.

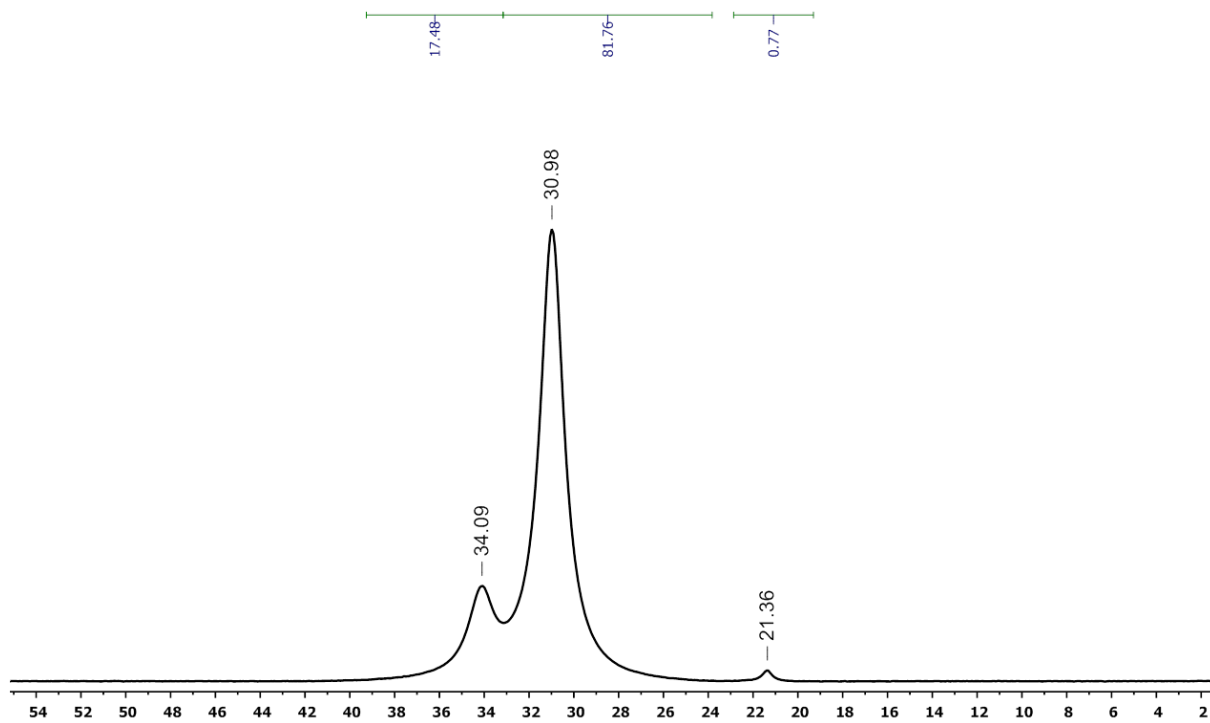


Figure II-22. Entry 8 – ^{11}B NMR (128 MHz, C_6D_6) spectrum after reacting HBpin and C_6D_6 with 5 mol% **215-(TBE)** and excess 1-hexene at 80 °C for 0.5 h. Resonances for hexylBpin, TBABpin, and $\text{C}_6\text{D}_5\text{Bpin}$ are observed, as well trace HBpin decomposition products.

Entries 1-8 refer to Table II-4 - Entry 1 - Reaction of HBpin with neat C₆D₆, 2.5 mol% [(COD)Ir(OMe)]₂, and 5 mol% dtbpy - A J. Young tube was loaded with a 0.035 M C₆D₆ stock solution of [(COD)Ir(OMe)]₂ (200 μL, 0.007 mmol) and a 0.14 M C₆D₆ stock solution of dtbpy (100 μL, 0.014 mmol). 400 μL of C₆D₆ was added, and the contents of the NMR tube were mixed. HBpin (40 μL, 0.28 mmol) was added, followed by cyclohexane (20 μL, 0.19 mmol) as an internal standard. The NMR tube was placed in an 80 °C oil bath and monitored via ¹H and ¹¹B NMR spectroscopy. After 1.5 h: C₆D₅Bpin yield was 72 %.

Entry 2 - Reaction of HBpin with neat C₆D₆, 2.5 mol% [(COD)Ir(OMe)]₂, and 5 mol% dtbpy with excess 1-hexene - A J. Young tube was loaded with a 0.035 M C₆D₆ stock solution of [(COD)Ir(OMe)]₂ (200 μL, 0.007 mmol) and a 0.14 M C₆D₆ stock solution of dtbpy (100 μL, 0.014 mmol). 300 μL of C₆D₆ was added, and the contents of the NMR tube were mixed. HBpin (40 μL, 0.28 mmol), 1-hexene (105 μL, 0.84 mmol), and cyclohexane (20 μL, 0.19 mmol) as an internal standard were added. The NMR tube was placed in an 80 °C oil bath and monitored via ¹H and ¹¹B NMR spectroscopy. After 0.5 h, C₆D₅Bpin yield was 21% and hexylBpin yield was 74%.

Entry 3 - Reaction of B₂pin₂ with neat C₆D₆, 2.5 mol% [(COD)Ir(OMe)]₂, and 5 mol% dtbpy - A J. Young tube was loaded with a 0.035 M C₆D₆ stock solution of [(COD)Ir(OMe)]₂ (200 μL, 0.007 mmol) and a 0.14 M C₆D₆ stock solution of dtbpy (100 μL, 0.014 mmol). 200 μL of C₆D₆ was added, and the contents of the NMR tube were mixed. A 1.4 M C₆D₆ stock solution of B₂pin₂ (200 μL, 0.28 mmol) and cyclohexane (20 μL, 0.185 mmol) as an internal standard were added. The NMR tube was placed in an 80

°C oil bath and monitored via ^1H and ^{11}B NMR spectroscopy. After 0.5 h, $\text{C}_6\text{D}_5\text{Bpin}$ yield was 87%.

Entry 4 - Reaction of B_2pin_2 with neat C_6D_6 , 2.5 mol% $[(\text{COD})\text{Ir}(\text{OMe})_2]$, and 5 mol% dtbpy with excess 1-hexene - A J. Young tube was loaded with a 0.035 M C_6D_6 stock solution of $[(\text{COD})\text{Ir}(\text{OMe})_2]$ (200 μL , 0.007 mmol) and a 0.14 M C_6D_6 stock solution of dtbpy (100 μL , 0.014 mmol). 100 μL of C_6D_6 was added, and the contents of the NMR tube were mixed. A 1.4 M C_6D_6 stock solution of B_2pin_2 (200 μL , 0.28 mmol), 1-hexene (105 μL 0.84 mmol), and cyclohexane (20 μL , 0.19 mmol) as an internal standard were added. The NMR tube was placed in an 80 °C oil bath and monitored via ^1H and ^{11}B NMR spectroscopy. After 0.5 h, $\text{C}_6\text{D}_5\text{Bpin}$ yield was 57% and hexylBpin yield was 37%.

Entry 5 – Repeat of the maximum turnover experiment⁶² by Hartwig et al - Reaction of B_2pin_2 with neat C_6D_6 , 0.0015 mol% $[(\text{COD})\text{IrCl}_2]$, and 0.003 mol% dtbpy - A J. Young tube was loaded with B_2pin_2 (500 mg, 1.97 mmol), cyclohexane (50 μL , 0.462 mmol), and 750 μL of C_6D_6 . Then $[(\text{COD})\text{IrCl}_2]$ (0.03 μmol) and dtbpy (0.07 μmol) were added via stock solutions. The J. Young tube was mixed and placed into a 100 °C oil bath for 24 h. ^1H NMR spectroscopy revealed a 21% yield of $\text{C}_6\text{D}_5\text{Bpin}$.

Entry 6 – Repeat of the maximum turnover experiment by Hartwig et al - Reaction of B_2pin_2 with neat C_6D_6 , 0.0015 mol% $[(\text{COD})\text{IrCl}_2]$, and 0.003 mol% dtbpy with 1 atm of ethylene added to NMR tube headspace - A J. Young tube was loaded with B_2pin_2 (500 mg, 1.97 mmol), cyclohexane (50 μL , 0.462 mmol), and 750 μL of C_6D_6 . Then $[(\text{COD})\text{IrCl}_2]$ (0.03 μmol) and dtbpy (0.07 μmol) were added via stock

solutions. The J. Young tube was mixed, degassed, charged with 1 atm of ethylene, and then placed into a 100 °C oil bath for 24 h. ¹H NMR spectroscopy revealed EtBpin (2%) and trace quantities of C₆D₅Bpin (<1%).

Entry 7 - Reaction of HBpin with neat C₆D₆, 2.5 mol% [(COD)Ir(OMe)]₂ - A J. Young tube was loaded with a 0.035 M C₆D₆ stock solution of [(COD)Ir(OMe)]₂ (200 μL, 0.007 mmol) and 500 μL of neat C₆D₆. After mixing, HBpin (40 μL, 0.28 mmol) was added, followed by cyclohexane (20 μL, 0.19 mmol) as an internal standard. The NMR tube was placed in an 80 °C oil bath and monitored via ¹H and ¹¹B NMR spectroscopy. After 0.5 h, trace PhBpin was observed. After 18 h, the C₆D₅Bpin yield was 14%.

Entry 8 - Reaction of HBpin with neat C₆D₆, 2.5 mol% [(COD)Ir(OMe)]₂ with excess 1-hexene - A J. Young tube was loaded with a 0.035 M C₆D₆ stock solution of [(COD)Ir(OMe)]₂ (200 μL, 0.007 mmol) and 400 μL of neat C₆D₆. After mixing, HBpin (40 μL, 0.28 mmol), 1-hexene (105 μL, 0.84 mmol), and cyclohexane (20 μL, 0.19 mmol) as an internal standard were added. The NMR tube was placed in an 80 °C oil bath and monitored via ¹H and ¹¹B NMR spectroscopy. After 0.5 h, the C₆D₅Bpin yield was <1% while the hexylBpin yield was 91%.

General procedure for Table II-2. Effect of HBpin:benzene:1-hexene ratio concentration on PhBpin:hexylBpin ratio – In a glovebox, a series of J. Young NMR tubes were each loaded with a 0.01M benzene stock solution of **214-(H)(Cl)** (60 μL, 0.60 μmol) and HBpin (98 μL, 0.676 mmol). Benzene and 1-hexene were added in the quantities indicated in the tables below, relative to HBpin (mole:mole). A known amount

of heptane was added, as required, to normalize the total solvent volume of each experiment ($V_{\text{TOT}} = 1.6 \text{ mL}$). The J. Young NMR tubes were then placed into an $80 \text{ }^{\circ}\text{C}$ oil bath and monitored by ^{11}B NMR spectroscopy after 18 h and 36 h. In all entries, trace (<1%) quantities of unknown HBpin decomposition products were observed by ^{11}B NMR spectroscopy. In entries where the sum of PhBpin and hexylBpin conversion values was less than 100%, the remaining % was unadulterated HBpin as seen in the ^{11}B NMR spectra below.

General procedures for Table II-3, entries 1-11 - A 100 mL Hi-Vac valve round-bottom flask was charged with 100 μL of a 0.08 M benzene stock solution of **214-(H)(Cl)** and solvent was removed in vacuo. For entry **4**, **214-(H)(Cl)** (8.0 mg, 0.014 mmol) was added as a solid. Via syringe, arene substrate and HBpin were added, and the flask was sealed and brought out of the glovebox. The flask was mixed, frozen, and degassed. The resultant solution was allowed to thaw to room temperature and the flask headspace was charged with 1 atm of ethylene. The flask was then placed into an $80 \text{ }^{\circ}\text{C}$ oil bath for 24 h before being brought into a glovebox. For entries **3-11**, 300 μL of cyclohexane was added as an internal standard, and an aliquot of the reaction solution was dissolved in C_6D_6 and analyzed via ^1H and ^{11}B NMR spectroscopy. Work-up was as follows: all solvents and EtBpin were removed in vacuo. The ArBpin products were dissolved in pentane, then run through a plug of silica, affording the ArBpin products in high purity (>95% by ^1H and ^{11}B NMR). Catalyst loadings were calculated by dividing moles of iridium compound added by moles of HBpin added, times 100. Isolated yields of ArBpin were calculated based on HBpin. Isolated yields were consistent with

spectroscopic yields determined before work-up via ^1H NMR evidence. TONs were calculated by multiplying the moles of HBpin added and the isolated yield of ArBpin (expressed as a fraction), then dividing by the moles of iridium compound added. TOFs were calculated by dividing TON by 24 h.

CHAPTER III

SMALL MOLECULE ACTIVATION WITH POCOP IRIIDIUM COMPLEXES

3.1 Introduction

The activation of small molecules is at the heart of many critical transformations in nature and synthetic chemistry including nitrogen fixation,^{177,178} gas-to-liquid processes¹⁷⁹ and hydroformylation,¹⁸⁰ among many others. The transformation of CO₂ to useful chemicals or fuels has been a topic of considerable interest and has been reviewed elsewhere.¹⁸¹ In terms of homogeneous catalysis, the reduction of CO₂ with boranes or silanes has been demonstrated with organometallic^{182,183,184,185} and main group catalysts.^{186,187} Tanaka and Nozaki found (PNP)Ir was an excellent CO₂ hydrogenation catalyst with TOF up to 150,000 h⁻¹ and over 3 x 10⁶ TON.¹⁸⁸ Brookhart and coworkers have also shown the cleavage of C-O bonds of alkyl ethers and the C-X bonds of alkyl halides using a (POCOP)Ir complex and silane.^{113,189} Brookhart et al. demonstrated the reduction of a CO ligand of a (POCOP)Ir complex using silanes.¹⁹⁰ Brookhart and coworkers showed amides were selectively reduced to amines.^{191,192} Brookhart et al. also showed the redistribution of trialkyl silanes by (POCOP)Ir complexes.¹⁹³ Cationic (POCOP)Ir complexes were found to be competent catalysts for the hydrosilylation of carbonyl containing substrates.¹⁹⁴ Goldman et al. showed (POCCH₂P)Ir complexes catalyzed the hydroaryloxylation of olefins.¹⁹⁵ Work by the Goldberg group showed partial deoxygenation of alcohols using (POCOP)Ir complexes.^{196,197} Iridium complexes ligated with the POCOP ligand are ubiquitous in the literature although typically the bulkier tetra(*tert*-butyl) substituted phosphinite ligand is used in these transformations.

Less work has been shown with isopropyl, ethyl or methyl substituted POCOP ligands mainly due to the synthetic challenges associated with smaller ligands.^{198,199,200} Brookhart and coworkers demonstrated selective catalytic hydrogenation with molecular single crystals of a (POCOP)Ir complex with bulky electron withdrawing (trifluoromethyl)phenyl substituents²⁰¹ but phenyl substituted POCOP ligands on iridium are by and large rare throughout the literature. Here we demonstrate the reactivity of (POCOP)Ir boryl complexes with small molecules such as CO₂, CO, ethylene and alcohols.

3.2 Results and discussion

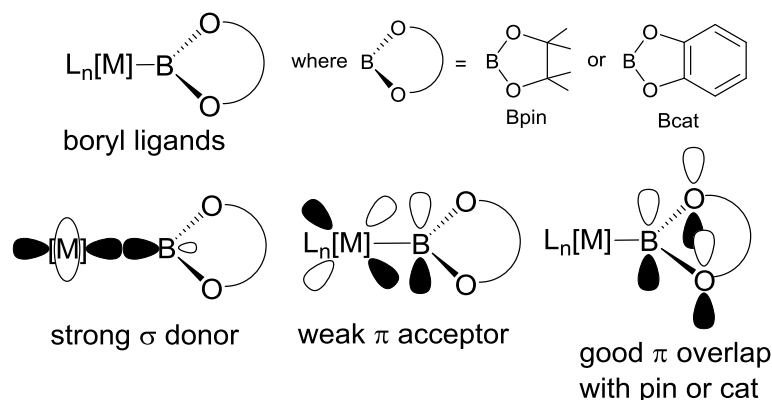


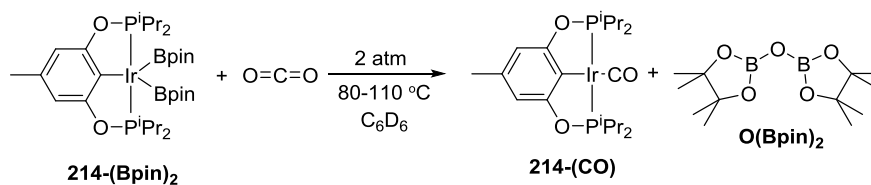
Figure III-1. Bonding modes of boryl ligands Bpin and Bcat as depicted by Marder et al.²⁰²

Two of the most common boryl ligands, Bpin and Bcat (pin= pinacolate, cat = catecholate), are strong σ -donors, weak π -acceptors and on late transition metals (Figure

I-1), typically exhibit nucleophilic behavior.²⁰² Metal-catalyzed hydroboration has been utilized since the 1980s and is a well-known method for the preparation of organoboron reagents.²⁰³ Transition metal-boryl complexes and σ -borane complexes have been hypothesized, and in many cases shown to be directly involved in these transformations.²⁰⁴ The structure and bonding of these ligands with group 9 metals has been particularly well studied but the investigation of late metal-boryl pincer complexes in remains as an area of interest.

3.2.1 Reaction of (*p*-MePOCOP^{iPr})Ir(Bpin)₂ with CO₂ and CO

The diboryl Ir pincer complex **214-(Bpin)₂** was found to deoxygenate CO₂ to CO. Reacting **214-(Bpin)₂** with CO₂ (1 atm) in C₆D₆ at 80 °C gave quantitative yields of **214-(CO)** and O(Bpin)₂ after 24 h (Scheme III-1). Reaction of **214-(Bpin)₂** with CO₂ (2 atm) in C₆D₆ at 110 °C for 16 h gave a 70% yield of O(Bpin)₂ and a 30% yield of C₆D₅Bpin while **214-(CO)** was observed as the major organometallic product. Previous studies found compound **214-(Bpin)₂** did not react with C₆D₆ at 80 °C after 24 h (Scheme II-5) but higher temperatures were not investigated. Nonetheless, the observation of C₆D₅Bpin indicates the borylation of benzene competes with the deoxygenation of CO₂ at higher temperature schemes. One plausible pathway to generate C₆D₅Bpin is the reductive elimination of B₂pin₂ from **214-(Bpin)₂** to give the three-coordinate fragment, **214**, which then reacts with C₆D₆ by oxidative addition and the resulting **214-(D)(Ph)** reacts with B₂pin₂.

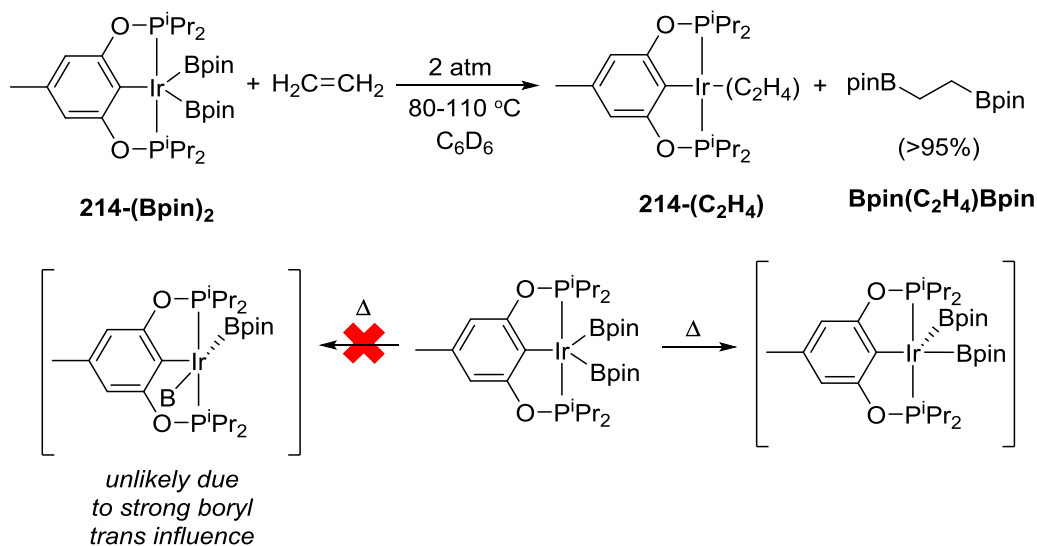


Scheme III-1. Deoxygenation of CO₂ to CO with **214-(Bpin)₂**.

Adding CO (2 atm) to **214-(Bpin)₂** resulted in the extrusion of B₂pin₂ and formation of **214-Ir(CO)₂**. Compound **214-Ir(CO)₂** was independently synthesized and characterization in situ by adding CO (2 atm) to **214-Ir(TBE)** while removal of volatiles gave pure **214-(CO)**. Brookhart et al. previously observed a dicarbonyl Ir complex in situ after adding excess CO to compound **120** (Chapter 1, Figure I-1).⁹⁴ The compound was identified by NMR spectroscopy but could not be isolated due to loss of one CO ligand. This reactivity is identical to the reactivity we have observed between **214-(CO)₂** and **214-(CO)**. Compounds **213-(CO)** and **215-(CO)** were synthesized in a similar manner. Compound **214-(CO)** was also synthesized by dehydrochlorination of **214-(H)(Cl)** with NaO^tBu in the presence of TBE followed by the addition of CO.

3.2.2 Reaction of (*p*-MePOCOPⁱPr)Ir(Bpin)₂ with olefins

Insertion of coordinated olefin or alkyne ligands into metal-boryl bonds has been proposed as a key step in metal catalyzed 1,2-diborylation chemistries.^{205,206} We observed Bpin(C₂H₄)Bpin in a >95% yield in situ when **214-(Bpin)₂** was reacted with ethylene (2 atm) in C₆D₆ at 110 °C for 30 h (Scheme III-2, top). The major organometallic product was **214-(C₂H₄)**. In order for the insertion to occur, ethylene must first coordinate to the 16-electron Ir(III) complex.



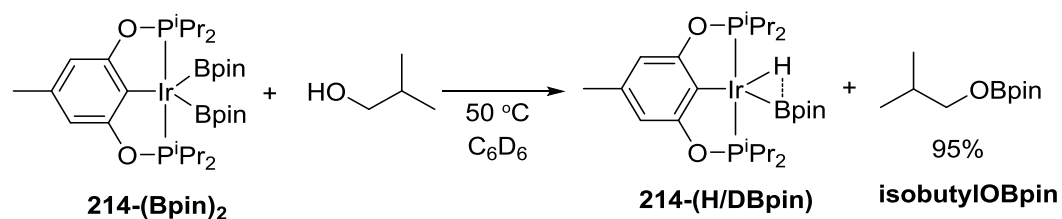
Scheme III-2. 1,2-diboration of ethylene by **214-(Bpin)₂**.

The Y-shaped **214-(Bpin)₂** complex likely distorts to a C_s symmetric square pyramidal geometry (Scheme III-2, bottom right), with one Bpin ligand trans to an empty site and the second trans to the aryl carbon of the POCOP ligand. The alternative, where both boryls become trans to one another and retained C_{2v} symmetry seems less likely due to the strong σ -donating nature of boryl ligands (Scheme III-2, bottom left).

3.2.3 Reaction of (*p*-Me POCOP^{iPr})Ir(Bpin)₂ with an aliphatic alcohol

We investigated the reactivity of **214-(Bpin)₂** with a protic reagent as a means to synthesize **214-(HBpin)** and to study the nature of the Ir-boryl ligands. Reaction of **214-(Bpin)₂** with one equiv of isobutanol in C_6D_6 at 50 °C for 24 h gave a 94% yield of **214-(H/DBpin)** and isobutylOBpin in an 95% yield (**Scheme III-3**). This demonstrates one of the two boryl ligands of **214-(Bpin)₂** can be selectively protonated to as a means to generate **214-(HBpin)**. It is interesting to note that the **214-(HBpin)** product did not also

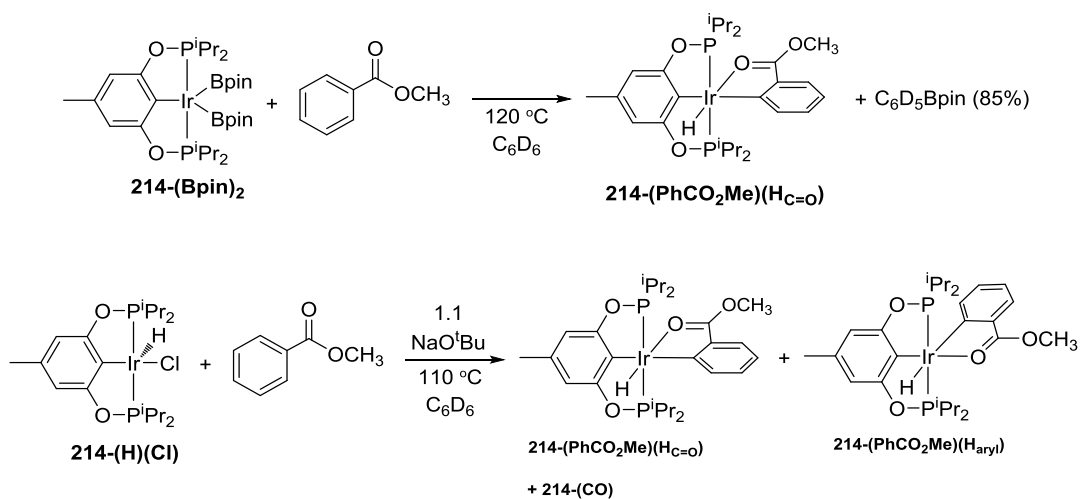
react with isobutanol to form **214-H₂** as one might expect because of the reduced steric profile of **214-(HBpin)** relative to **214-(Bpin)₂**.



Scheme III-3. Selective proton transfer to one boryl ligand of **214-(Bpin)₂** using an aliphatic alcohol.

3.2.4 Reaction of (*p*-Me POCOP^{iPr})Ir(Bpin)₂ with an aryl ester

We attempted to deoxygenate methyl benzoate with **214-(Bpin)₂** under thermal conditions. After 6 h at 120 °C, thermolysis of **214-(Bpin)₂** in C₆D₆ with one equiv of methyl benzoate present unexpectedly resulted in the exclusive borylation of C₆D₅Bpin in an 85% yield (Scheme III-4, top).

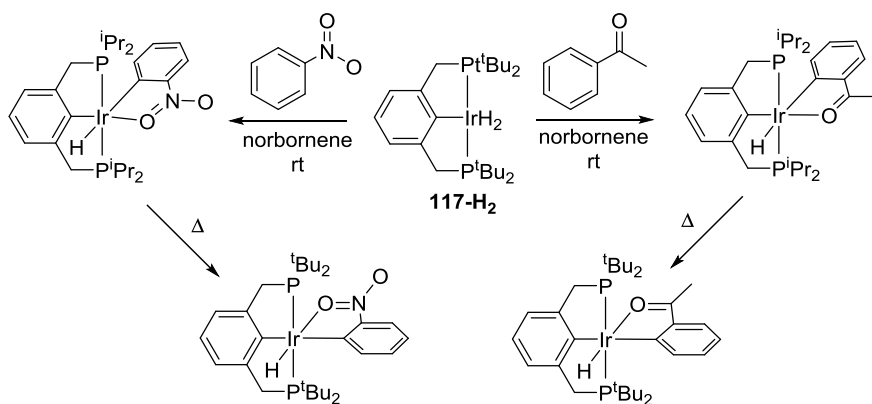


Scheme III-4. Attempted deoxygenation of methyl benzoate and subsequent cyclometalation by **214**.

One organometallic product was observed as a broad resonance in $^{31}\text{P}\{^1\text{H}\}$ NMR spectrum ($\delta = 157.5$ ppm, C_6D_6) but due to considerable H/D exchange with the C_6D_6 solvent the identity of this product was not immediately evident in the corresponding ^1H NMR spectrum. The $^{13}\text{C}\{^1\text{H}\}$ NMR spectrum did not contain downfield resonances consistent with the formation of either a metal carbene or a metal carbonyl complex. The ^1H NMR spectrum contained a single hydride resonance ($\delta = -26.36$ ppm, t, $J = 16.7$ Hz, C_6D_6) that is consistent with a hydride ligand trans to the oxygen of a C=O group.²⁰⁷ The product was tentatively assigned as **214-(PhCO₂Me)(HC=O)** (Scheme III-4, top). Indeed, dehydrochlorination of **214-(H)(Cl)** with NaO^tBu in C_6D_6 in the presence of an excess of methyl benzoate followed by heating to $110\text{ }^\circ\text{C}$ for 1 h gave three products including **214-Ir(CO)** (21%) and the

compound assigned as **214-(PhCO₂Me)(H_{C=O})** (23%). The third compound exhibited a downfield hydride resonance ($\delta = -9.98$ ppm, t, $J = 16.6$ Hz, C₆D₆) typical of a hydride ligand trans to an aryl carbon²⁰⁷ and the compound was tentatively assigned as **214-(PhCO₂Me)(H_{aryl})** (56%, Scheme III-4, bottom).

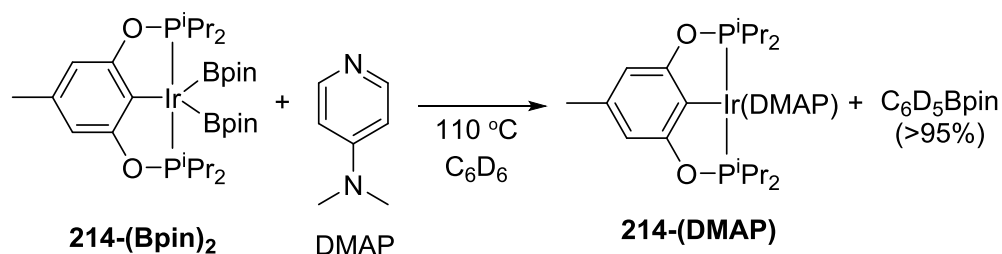
The subsequent cyclometalation of methyl benzoate by the (POCOP)Ir fragment is in-line with the reactivity of other group 9 pincer systems towards directing substrates. For example, Goldman et al. found in the presence of norbornene, (PCP)IrH₂ (**117-H₂**, Scheme III-5) cyclometalated nitrobenzene exclusively giving an *ortho*-C-H activation product with aryl trans to hydride (Scheme III-5).²⁰¹ Upon heating the aryl trans to hydride isomer converted to an carbonyl trans to hydride species (Scheme III-5). Under similar conditions, the *ortho*-C-H activation of acetophenone was also observed, giving (PCP)Ir(PhCO₂Me)(H_{trans to aryl}) which converted to the more thermodynamically favored (PCP)Ir(PhCO₂Me)(H_{trans to C=O}) after heating to 135 °C (Scheme III-5).²⁰⁸ Ozerov et al. found the reaction of (PNP)IrH₂ with norbornene and chlorobenzene gave C-H activation products that could be converted to *ortho*-C-H activation product after heating to 70 °C.²⁰⁹ The Ozerov group also extensively studied the reaction of (PNP)Rh complexes with aryl halides and aryl esters where *ortho*-C-H activation products were observed.^{164,210} C-O bond cleavage by the (PNP)Rh fragment was also observed in reactions with aryl esters under thermolytic conditions¹⁶⁴ giving precedent to formation of **214-(CO)** that we observe during the dehydrochlorination of **214-(H)(Cl)** in the presence of methyl benzoate (Scheme III-4).



Scheme III-5. *ortho*-C-H activation of nitrobenzene and acetophenone by a (PCP)Ir complex studied by Goldman et al.

3.2.5 Attempt to reaction of (*p*-Me POCOP^{iPr})Ir(Bpin)₂ with a pyridine derivative

The C-H borylation of pyridine and its derivatives is of considerable interest to synthetic chemists, particularly those within the pharmaceutical industry.²¹¹ We proceed to attempt the stoichiometric borylation 4-dimethylaminopyridine (DMAP) using **214-(Bpin)₂**. Thermolysis of **214-(Bpin)₂** in the presence of one equiv of DMAP in C₆D₆ at 110 °C for 2 h gave no reaction while after 18 h the borylation of the C₆D₆ solvent to give C₆D₅Bpin was observed in a >95% yield (Scheme III-6).

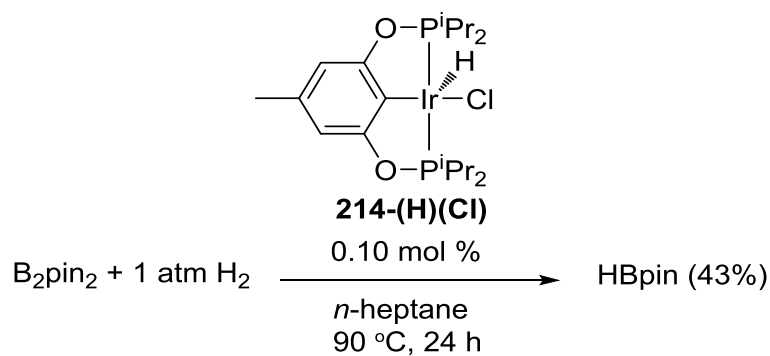


Scheme III-6. Attempted borylation of DMAP resulting in C₆D₅Bpin and **214-(DMAP)**.

The main organometallic product observed was **214-(DMAP)** (68%, (Scheme III-6) which was independently synthesized in quantitative yield by reacting **214-(TBE)** with one equiv of DMAP in C₆D₆ at 60 °C for 2 min. The other two products observed in the ³¹P{¹H} NMR spectrum, one resonating at 169.2 ppm (4%) and the second at 161.1 ppm (28%), were not identified. Multiple hydride signals were evidently belonging to various minor impurities were observed in the ¹H NMR spectrum.

3.2.6 Hydrogenolysis of B₂pin₂ with a (*p*-Me POCOP^{*i*Pr})Ir(H)(Cl) precatalyst

The catalytic hydrogenolysis of B₂pin₂ to form HBpin or DBpin is synthetically attractive because B₂pin₂ is a relatively air stable solid while HBpin is a volatile liquid which readily decomposes upon exposure to moisture and therefore must be stored under an inert atmosphere.²¹²



Scheme III-7. Hydrogenolysis of B_2pin_2 with **214-(H)(Cl)** as precatalyst.

We observed that the exposure of **214-(Bpin)₂** to an excess of H_2 (2 atm) gives **214-(HBpin)**, **214-H₂Bpin₂** and **214-H₃Bpin** after 15 mins at ambient temperature and after 30 mins **214-H₃Bpin** is the major product with free HBpin observed by ^1H and ^{11}B NMR. Using 0.10 mol% of **214-(H)(Cl)** as precatalyst, B_2pin_2 was reacted with H_2 (1 atm) in *n*-heptane at 90 °C for 24 h to give a 43% yield of HBpin (Scheme III-7). This translates to 430 TON which is highly competitive with other catalysts reported in the literature for the catalytic hydrogenolysis of B_2pin_2 . For example, the hydrogenolysis of B_2pin_2 with H_2 to HBpin using 0.18 mol% Pd/C reportedly²¹² gave 503 TON at ambient temperature after 20 h while dtbpy/ $[(\text{cod})\text{IrOMe}]_2$ catalyzed the hydrogenolysis of B_2pin_2 with D_2 to form DBpin, giving 155 TON after 24 h at ambient temperature.²¹³

3.3 Conclusion

The reactivity of (POCOP)Ir complexes for the activation of small molecules has been investigated. The Ir(III) diboryl complex **214-(Bpin)₂** was found to undergo several transformations including the deoxygenation of CO_2 to CO, the stoichiometric 1,2-

diboration of ethylene, and selective protonation of one boryl ligand of **214-(Bpin)₂** with an aliphatic alcohol. Attempts to deoxygenate methyl benzoate resulted in clean borylation of the C₆D₆ solvent and formation of **214-(PhCO₂Me)(H_{C=O})**. Similarly, attempts to borylate DMAP resulted in smooth borylation of C₆D₆ solvent and formation of mostly **214-(DMAP)**. The use of **214-Ir(H)(Cl)** in the catalytic hydrogenolysis of B₂pin₂ was demonstrated and its catalytic activity is on par with the state of the art catalysts reported in the literature. The facile reaction of both **214-Ir(Bpin)₂** and **214-(HBpin)** with H₂, among several other pertinent reactions, likely plays a role in this catalytic transformation.

3.4 Experimental

3.4.1 General considerations

Unless specified otherwise, all manipulations were performed under an argon atmosphere using standard Schlenk or glovebox techniques. Pentane, diethyl ether, tetrahydrofuran, mesitylene and benzene were dried over sodium–benzophenone ketyl, distilled or vacuum transferred and stored over molecular sieves in an Ar–filled glovebox. All other chemicals were used as received from commercial vendors. All NMR spectra were recorded on a Varian Inova 300 spectrometer (^1H NMR 299.951 MHz, $^{31}\text{P}\{^1\text{H}\}$ NMR 121.425 MHz, $^{13}\text{C}\{^1\text{H}\}$ NMR 75.413 MHz), Varian Mercury 300 spectrometer ($^{13}\text{C}\{^1\text{H}\}$ NMR 75.426 MHz), Varian Inova 400 spectrometer (^1H NMR, 399.755 MHz; $^{13}\text{C}\{^1\text{H}\}$ NMR, 100.518 MHz; ^{11}B NMR 128 MHz, $^{31}\text{P}\{^1\text{H}\}$ NMR 181.822 MHz), or a Varian Inova NMR 500 (^1H NMR, 499.425 MHz/ 499.683 MHz; $^{13}\text{C}\{^1\text{H}\}$ NMR, 75.424 MHz/ 125.580 MHz; $^{31}\text{P}\{^1\text{H}\}$ NMR, 202.171 MHz; ^{19}F NMR, 469.854 MHz) spectrometer. All spectra were recorded at ambient temperature unless otherwise noted. Chemical shifts are reported in δ /ppm. For ^1H and $^{13}\text{C}\{^1\text{H}\}$ NMR spectra, the residual solvent peak was used as an internal reference.¹⁷² ^{11}B NMR spectra were referenced externally using neat BF_3OEt_2 at $\delta = 0$ ppm, $^{31}\text{P}\{^1\text{H}\}$ NMR spectra were referenced externally using 85% H_3PO_4 at $\delta = 0$ ppm, and ^{19}F NMR spectra were referenced externally using 1.0 M $\text{CF}_3\text{CO}_2\text{H}$ in CDCl_3 at $\delta = -78.5$ ppm. FT-IR spectra were collected using a Bruker ALPHA-P FT-IR Spectrometer with a diamond ATR head.

3.4.2 Synthesis of compounds

Reaction of 214-(Bpin)₂ with excess CO₂ at 80 °C – Compound **214-(Bpin)₂** (22 mg, 0.027 mmol) was added to a J. Young NMR tube and dissolved in C₆D₆. After an initial degassing via freeze–pump–thaw, the headspace of the NMR tube was charged with CO₂ (1 atm) resulting in no reaction after 20 minutes at room temperature. Heating at 80 °C for 24 h resulted in quantitative formation of **214-Ir(CO)** and O(Bpin)₂ as seen by ¹H, ¹¹B and ³¹P{¹H} NMR spectroscopic analysis. Removal of volatiles followed by dissolution of the resulting residue in CDCl₃ and comparing to literature values confirmed the identity of O(Bpin)₂. ²¹⁴O(Bpin)₂ ¹H NMR (RT, C₆D₆): δ 1.01 (s, 24H, pin CH₃). ¹¹B NMR (RT, C₆D₆): δ 21.5 (br s). ¹³C{¹H} NMR (RT, C₆D₆): δ 82.9, 24.7.

Reaction of 214-(Bpin)₂ with excess CO₂ at 110 °C – Compound **214-(Bpin)₂** (31 mg, 0.037 mmol) was added to a J. Young NMR tube and dissolved in C₆D₆. After an initial degassing via freeze–pump–thaw, the headspace of the NMR tube was charged with CO₂ (2 atm) and the reaction was placed in a 110 °C oil bath for up to 16 h. After that time, O(Bpin)₂ was observed in a 70% yield and C₆D₅Bpin was observed in a 30% yield.

General procedure for synthesis of 213-(CO), 214-Ir(CO), and 215-(CO) – 213-(H)(Cl) (150 mg, 0.26 mmol), **214-(H)(Cl)** (65 mg, 0.11 mmol), or **215-(H)(Cl)** (109 mg, 0.16 mmol) were added to a 50 mL Teflon screw cap round bottom flask and dissolved in benzene. To this TBE (100 μL, 0.78 mmol) was added via syringe followed by NaO^tBu (34.0 mg, 0.35 mmol for **213-(H)(Cl)**), (11.8 mg, 0.12 mmol for **214-(H)(Cl)**), (16.9 mg, 0.18 mmol for **215-(H)(Cl)**). The reaction was stirred for 4 hours

and then, after an initial degassing via freeze–pump–thaw, the headspace of the flask was charged with 1 atm of carbon monoxide. This resulted in an immediate color change from a dark red to orange-yellow solution. The reaction was stirred an additional 2 hours, transferred into a glovebox, filtered through a thin pad of silica over Celite, and solvent removed in vacuo giving a orange-yellow solids. Yield (**213-(CO)**): 81 mg (55%), Yield (**214-(CO)**): 56 mg (88%), Yield (**215-(CO)**): 71 mg (66%).

Synthesis of 213-(CO) – Compound **213-(CO)** was recently reported by Heinekey et al.²⁰⁰ ¹H NMR (RT, C₆D₆): δ 6.90 (t, *J*_{H-H} = 10 Hz, 1H, Ar-*H*), 6.85 (d, *J*_{H-H} = 10 Hz, 1H, Ar-*H*), 2.13 (m, 4H, CH(CH₃)₂), 1.10 (m, 24H, CH(CH₃)₂). ³¹P{¹H} (RT, C₆D₆): δ 190.5. ¹³C{¹H} (RT, C₆D₆): δ 198.6 (t, *J*_{P-C} = 5.0 Hz, Ir-CO), 169.4 (t, *J*_{P-C} = 9.0 Hz, Ar), 148.8 (t, *J*_{P-C} = 9.0 Hz, Ar), 129.9 (s, Ar), 104.4 (t, *J*_{P-C} = 7.0 Hz, Ar), 31.7 (t, *J*_{P-C} = 16.1 Hz, PCH(CH₃)₂), 18.5 (t, *J*_{P-C} = 3.0 Hz, PCH(CH₃)₂), 17.6 (s, PCH(CH₃)₂). IR ν(CO) = 1937 cm⁻¹. Anal. Calcd. for **213-(CO)**: C, 40.63 ; H, 5.56. Found: C, 40.54 ; H, 5.61.

Synthesis of 214-(CO)- ¹H NMR (RT, C₆D₆): δ 6.69 (s, 2H, Ar-*H*), 2.14 (m, 4H, CH(CH₃)₂), 2.12 (s, 3H), 1.12 (m, 24H, CH(CH₃)₂). ³¹P{¹H} (RT, C₆D₆): δ 190.2. ¹³C{¹H} (RT, C₆D₆): δ 198.6 (t, *J*_{P-C} = 4.5 Hz, Ir-CO), 169.4 (t, *J*_{P-C} = 8.5 Hz, Ar), 145.8 (t, *J*_{P-C} = 9.1 Hz, Ar), 140.3 (s, Ar), 105.4 (t, *J*_{P-C} = 6.1 Hz, Ar), 31.7 (t, *J*_{P-C} = 16.3 Hz, PCH(CH₃)₂), 21.9 (s, Ar-CH₃), 18.5 (t, *J*_{P-C} = 3.4 Hz, PCH(CH₃)₂), 17.6 (s, PCH(CH₃)₂). IR ν(CO) = 1936 cm⁻¹. Anal. Calcd. for **214-(CO)**: C, 41.73 ; H, 5.78 . Found: C, 41.75 ; H, 5.86.

Synthesis of 215-Ir(CO) – ^1H NMR (RT, C_6D_6): δ 7.25 (s, Ar-H), 2.15 (m, 4H, $\text{CH}(\text{CH}_3)_2$), 1.53 (s, 18H, Ar-C(CH_3) $_3$), 1.13 (m, 24H, $\text{CH}(\text{CH}_3)_2$). $^{31}\text{P}\{^1\text{H}\}$ (RT, C_6D_6): δ 189.0. $^{13}\text{C}\{^1\text{H}\}$ (RT, C_6D_6): δ 198.3 (t, $J_{\text{P-C}} = 4.0$ Hz, Ir-CO), 164.7 (t, $J_{\text{P-C}} = 7.0$ Hz, Ar), 152.7 (t, $J_{\text{P-C}} = 7.0$ Hz, Ar), 126.0 (t, $J_{\text{P-C}} = 4.0$ Hz, Ar), 124.5 (s, Ar), 34.9 (s, Ar-C(CH_3) $_3$), 31.7 (t, $J_{\text{P-C}} = 13.1$ Hz, PCH(CH_3) $_2$), 30.5 (s, Ar-C(CH_3) $_3$), 18.5 (t, $J_{\text{P-C}} = 3.0$ Hz, PCH(CH_3) $_2$), 17.8 (s, PCH(CH_3) $_2$). IR $\nu(\text{CO}) = 1939$ cm^{-1} . Anal. Calcd. for **215-(CO)**: C, 48.13 ; H, 7.03. Found: C, 48.18; H, 6.95.

Synthesis of 214-(CO) $_2$ in situ - A J. Young NMR tube was charged with **214-(TBE)** (23 mg, 0.036 mmol) and C_6D_6 . The solution was frozen then the headspace was evacuated and charged with CO (2 atm). The solution changed color from dark red to yellow. The reaction was analyzed by NMR spectroscopy and found to be >95% pure **214-(CO) $_2$** . Free TBE was observed in the ^1H NMR spectrum. ^1H NMR (RT, C_6D_6): δ 6.58 (s, 2H- Ar-H), 2.17 (s, 3H, Ar- CH_3), 2.16-2.08 (m, 4H, PCH(CH_3) $_2$), 1.10-1.02 (m, 24H, PCH(CH_3) $_2$). $^{31}\text{P}\{^1\text{H}\}$ (RT, C_6D_6): δ 171.8.

Reaction of 214-(Bpin) $_2$ with excess CO – Compound **214-(Bpin) $_2$** (21 mg, 0.027 mmol) was added to a J. Young NMR tube and dissolved in C_6D_6 . After an initial degassing via freeze-pump-thaw, the headspace of the NMR tube was charged with 1 atm of carbon monoxide resulting in an instant color change from bright yellow to colorless-yellow. Analysis via $^{31}\text{P}\{^1\text{H}\}$ NMR spectroscopy revealed quantitative conversion to **214-(CO) $_2$** . ^1H NMR revealed a sharp singlet at 1.01 ppm representing 24 protons indicating free B_2pin_2 . A sharp singlet at 31 ppm via ^{11}B NMR also indicated

free B₂pin₂. Removal of solvent *in vacuo* followed by dissolving the resulting yellow solids in C₆D₆ found pure **214-(CO)** and free B₂pin₂.

Reaction of 214-(Bpin)₂ with excess ethylene – Compound **214-(Bpin)₂** (33 mg, 0.041 mmol) was added to a J. Young NMR tube and dissolved in C₆D₆. After an initial degassing via freeze–pump–thaw, the headspace of the NMR tube was charged with ethylene (2 atm) resulting in no reaction after 20 minutes at room temperature. After 3 h at 110 °C the reaction changed from yellow to light red and **214-(C₂H₄)** (32%) was observed in ³¹P{¹H} NMR spectrum. After 30 h at 110 °C BpinCH₂CH₂Bpin was observed in a 93% yield and **214-(C₂H₄)** (94%) was the main organometallic product. Removal of volatiles followed by dissolution of the resulting residue in CDCl₃ and comparing to literature values confirmed the identity of BpinCH₂CH₂Bpin.²¹⁵ BpinCH₂CH₂Bpin: ¹H NMR (RT, C₆D₆): δ 1.21 (br s, 4H), 1.09 (s, 24H). ¹¹B NMR (RT, C₆D₆): 34.2. ¹³C{¹H} NMR (RT, C₆D₆): δ 82.8, 25.0, 5.2 (br s, (Bpin)CH₂CH₂(Bpin)).

Reaction of 214-(Bpin)₂ with isobutanol – A J. Young NMR tube was loaded with 32 mg (0.040 mmol) of **214-(Bpin)₂**, 10 μL of cyclohexane and 700 μL of C₆D₆. Via syringe, 60 μL of a 0.7 M isobutanol in C₆D₆ stock solution was added. The reaction was monitored by ¹H and ³¹P{¹H} NMR spectroscopy after after 4, 12 and 24 h at 50 °C. After 24 h, a 94% yield of **214-Ir(Hpin)** (comprised of 80% **[Ir](HBpin)**/14%**[Ir](DBpin)** due to solvent H/D exchange) was observed and isobutylOBpin was observed in a 95% yield. The ¹H and ¹¹B NMR features of isobutylOBpin matched those reported in the literature.²¹⁶ **isobutylOBpin** ¹H NMR (RT, C₆D₆): δ 3.74 (d, *J* = 6.5 Hz, 2H, CH(CH₃)₂CH₂OBpin), 1.84-1.73 (m, *J* = 6.5 Hz,

$\text{CH}(\text{CH}_3)_2\text{CH}_2\text{OBpin}$), 1.05 (s, $\text{CH}(\text{CH}_3)_2\text{CH}_2\text{OBpin}$'s CH_3), 0.84 (d, $J = 6.5$ Hz, 2H, $\text{CH}(\text{CH}_3)_2\text{CH}_2\text{OBpin}$). ^{11}B NMR (RT, C_6D_6): 25.5.

Reaction of 214-(Bpin)₂ with methyl benzoate - A J. Young NMR tube was charged with **214-(Bpin)₂** (38 mg, 0.047 mmol), methyl benzoate (6.5 μL , 0.052 mmol) and C_6D_6 . No reaction was observed at ambient temperature or at 95 °C for 12 h. The reaction was placed into a 120 °C oil bath for 6 h after which $\text{C}_6\text{D}_5\text{Bpin}$ was observed in an 85% yield. The remaining boron containing products were not identified but based on their ^{11}B NMR chemical shift of ca. 22.4-21.5 ppm they are likely a mixture of ROBpin esters. All **214-(Bpin)₂** had been consumed and **214-(PhCO₂Me)(H_{C=O})** was observed as the sole organometallic product.

Dehydrochlorination of 214-(H)(Cl) in the presence of methyl benzoate - A J. Young NMR tube was charged with **214-(H)(Cl)** (35mg, 0.060 mmol), methyl benzoate (36 mg, 0.26 mmol), NaO^tBu (8.0 mg, 0.083 mmol) and C_6D_6 . Numerous products were observe minutes after mixing but after 1 h at 110 °C this mixture converged to **214-(PhCO₂Me)(H_{C=O})** (24%), **214-(PhCO₂Me)(H_{aryl})** (54%) and **214-(CO)** (22%).

Reaction of 214-(Bpin)₂ with 4-dimethylaminopyridine - A J. Young NMR tube was loaded with **214-(Bpin)₂** (33 mg, 0.041 mmol), DMAP (8.0 mg, 0.065 mmol) and C_6D_6 . No reaction was observed at ambient temperature or after 2 h at 110 °C. After 18 h at 110 °C, $\text{C}_6\text{D}_5\text{Bpin}$ was observed in a >95% yield with three organometallic products of which only **214-(DMAP)** (68%) was identified. Numerous unidentified hydride signals resulting from minor were observed in the ^1H NMR spectrum.

Synthesis of 214-(DMAP) - A J. Young NMR tube was loaded with **214-(TBE)** (28 mg, 0.044 mmol), DMAP (7.0 mg, 0.057 mmol) and C₆D₆. The reaction was placed into a 60 °C oil bath for 2 min. Compound **214-(DMAP)** was observed as the sole product in the ³¹P{¹H} NMR spectrum as a singlet at 173.7 ppm and free TBE was observed in the ¹H NMR spectrum.

Hydrogenolysis of B₂pin₂ with H₂ and 0.1 mol% 214-(H)(Cl) - A 100 mL Hi-Vac valve round-bottom flask was loaded with 95 μL a 0.01 M benzene stock solution of **214-(H)(Cl)** and all solvent was removed in vacuo. 265 mg (1.04 mmol) of B₂pin₂ and 3 mL of heptane were added. The flask was sealed, brought out of the glovebox, degassed via freeze-pump thaw and filled with 1 atm of H₂ then placed into a 90 °C oil bath for 24 h. Note: After 12 h some white material precipitated, presumably unreacted B₂pin₂, along the walls of the flask and the flask was swirled to re-dissolve it. The flask was brought back into a glovebox, 300 μL (2.77 mmol) of cyclohexane was added and the flask contents were mixed. An aliquot of the solution was transferred to a J. Young NMR tube and analyzed via ¹H and ¹¹B NMR spectroscopy. The yield of HBpin was determined to be 43% by ¹H NMR spectroscopy with minimal formation (~ 2%) of HBpin decomposition products.

CHAPTER IV

NICKEL, PALLADIUM AND IRIIDIUM COMPLEXES OF BRIDGING AND MONOMERIC POCS LIGANDS

4.1 Introduction

The study of hetero- and homo-binuclear metal complexes has been an area of intense study over the last 70 years. Taube *et al.* studied intramolecular electron transfer within hetero- and homo-binuclear metal complexes, referred to as Creutz-Taube ions (Figure IV-1),²¹⁷ which played a key role in his reception of the 1983 the Nobel Prize in Chemistry.²¹⁸ Many metalloproteins found in nature contain homo- and hetero-binuclear metal centers responsible for critical transformations including urea hydrolysis (Figure IV-1),²¹⁹ oxygen reduction and lignin degradation.²²⁰ Cooperative effects between neighboring metal centers have been proposed in various heterogeneous processes including the Fischer-Tropsch process²²¹ and molecular catalysts immobilized on solid supports (Figure IV-1).²²² Mankad has reviewed selectivity effects in bimetallic catalysis.²²³

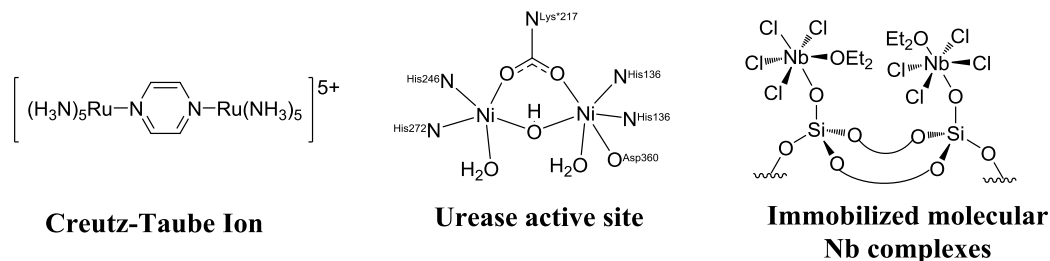
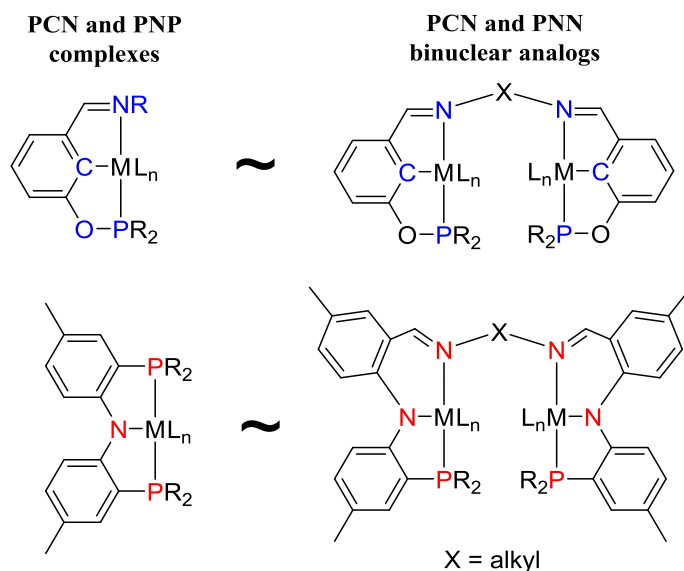


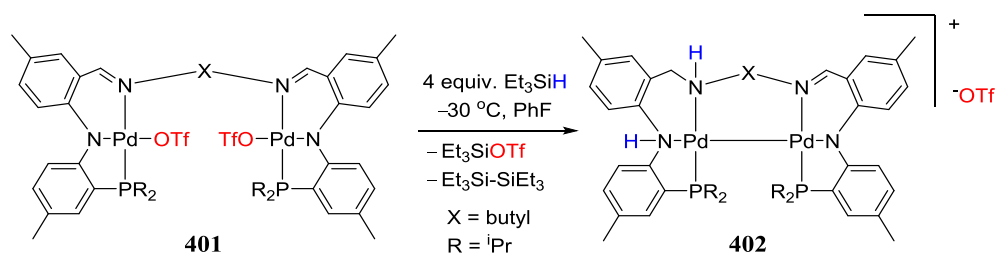
Figure IV-1. Creutz-Taube ion (left), Urease homobimetallic active site (middle), cooperating silica bound Nb catalyst (right).



Scheme IV-1. The Ozerov group’s approach to homobimetallic pincer complexes.

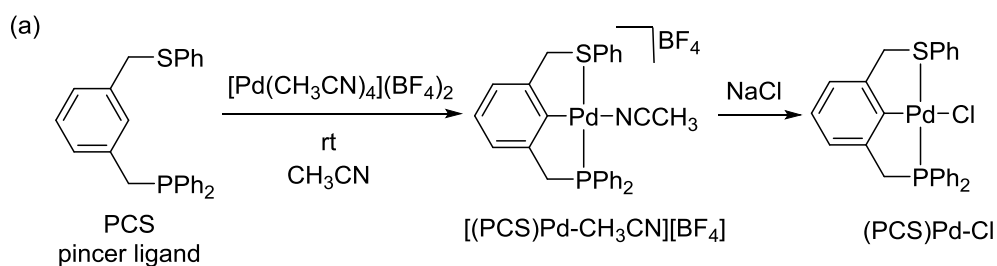
The use of tridentate “pincer” ligands has become ubiquitous in transition-metal chemistry, especially transition-metal catalysis. Pincer ligands are highly modular (both sterically and electronically) and they tend to form well-defined complexes with transition metals.²²⁴ Merging the theme of pincer ligands with the theme of bridging binuclear complexes creates a whole range of possibilities in the field of pincer complexes. The Ozerov group became interested in the study of cooperating metal centers supported by bridged, binuclear ligands with PCN and PNP type pincer frameworks (Scheme IV-1).²²⁵ The modular design was intended to facilitate a cooperative effect between two metal centers and a molecule of substrate. In 2011, the Ozerov group reported the synthesis and characterization of several PCN and PNN binucleating pincer ligands and their Pd complexes. Monomeric PCN and PNP

complexes of Pd are well known in the literature²²⁴ and their innate framework was chosen on the grounds of synthetic convenience and similarity with pincer complexes previously developed in the Ozerov group. The reactivity, as well as the electronic communication, between metal centers was found to be dependent on the linker length of the bridge. In at least two cases, the imine side arms of the PNN complexes were found to be susceptible to hydrogenation.²²⁵ In one example, 4 equiv. of triethylsilane reacted with **401** at $-30\text{ }^{\circ}\text{C}$ in fluorobenzene to form a new complex **402** containing a reduced imine arm as well as a Pd-Pd bond (Scheme IV-2). Presumably other reducing agents such as H_2 and boranes (R_2BH) would reduce the imine arm(s) in a similar fashion. Transition-metal catalyzed C-H borylation produces H_2 as a byproduct and transition-metal catalyzed hydrogenolysis of C-O bonds typically requires high pressures and temperatures.¹⁹⁷ Bridging binuclear pincer complexes bearing PNN and PCN ligands, such as those described in Scheme IV-1, would likely be deactivated under such catalytic conditions and the subject requires further study.



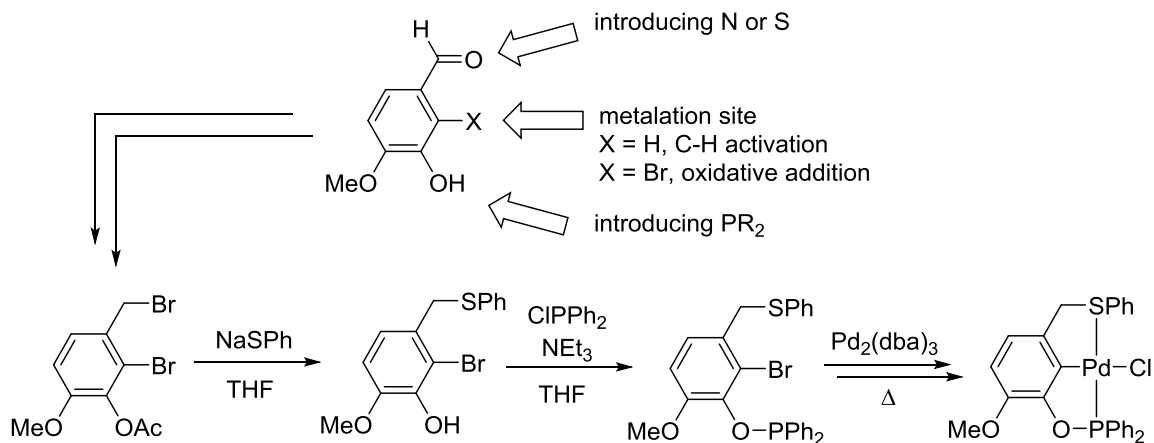
Scheme IV-2. Reduction of the imine arm of **401** by triethylsilane to give **402**.

The reactivity of the imine arm(s) within PNN complexes inspired a thioether tethered POCS binuclear ligand design, described herein. The availability of various dithiols and chlorodialkylphosphines allows bridging POCS type ligands the same modular design as the PCN and PNN systems. Monomeric PCS complexes of Pd such as (PCS)Pd-Cl (Scheme IV-3) were first described in the literature by van Koten et al. where they found use as homoallylation catalysts.²²⁶ van Koten et al. later devised a synthetic strategy for the synthesis of PCN type ligands from isovanillin (Scheme IV-4).²²⁷ In that same study, they also devised a synthesis of POCS ligands using isovanillin bromide (Scheme IV-4).



Scheme IV-3. Synthesis of (PCS)Pd by van Koten et al.

Van Koten et al. PCS ligand synthetic strategy



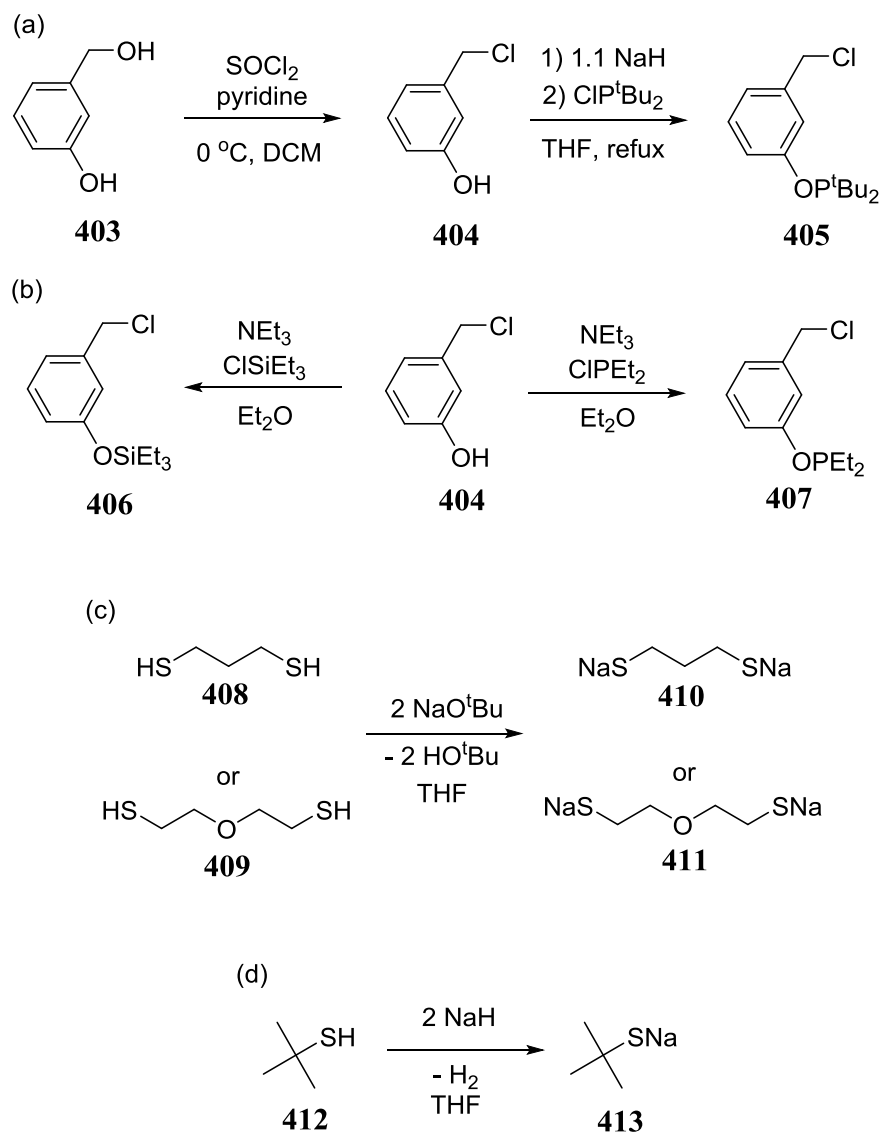
Scheme IV-4. Synthetic strategy devised by van Koten et al. for the synthesis of POCS ligands and Pd species.

4.2 Results and discussion

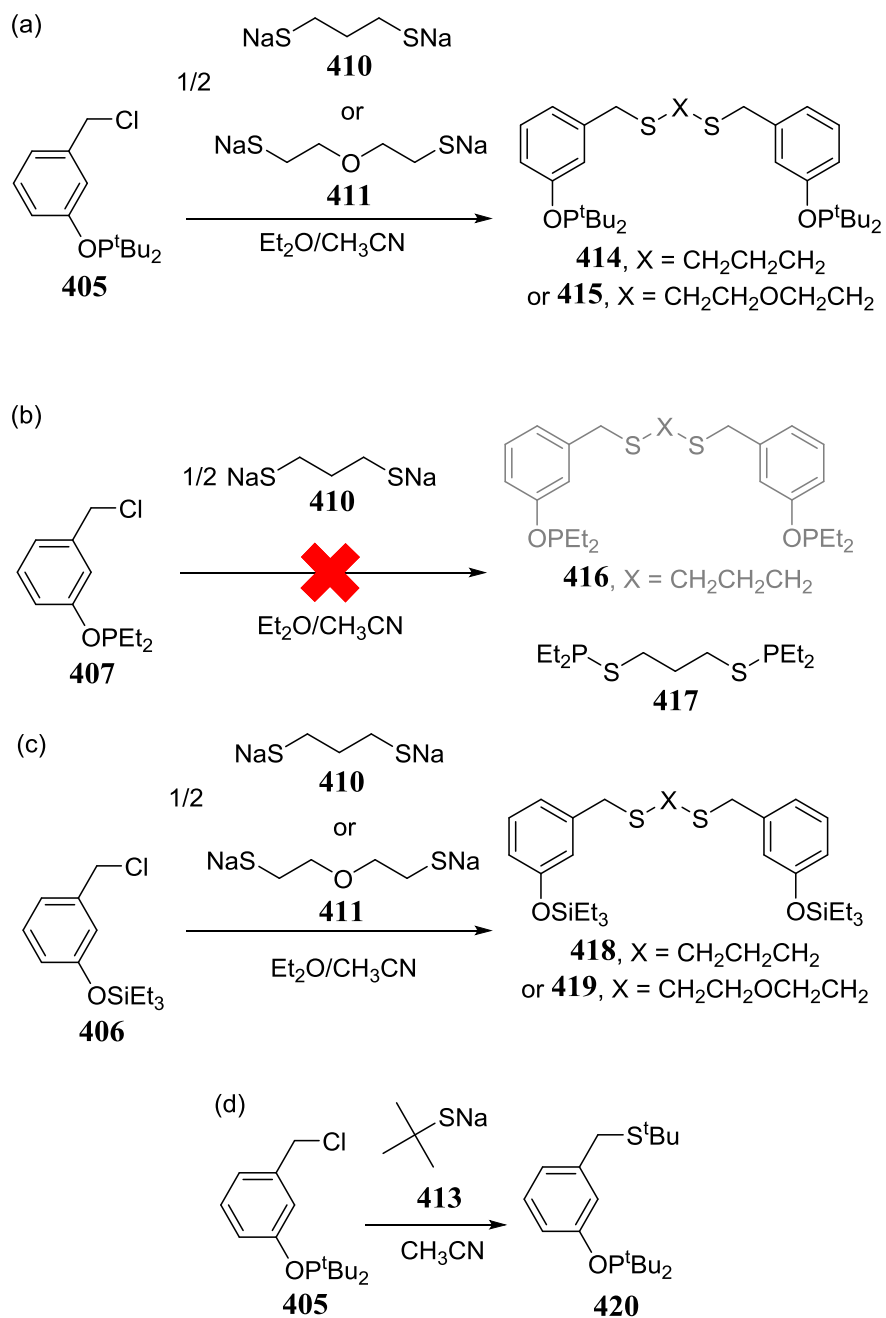
4.2.1 Synthesis of POCS ligands

Following modified literature procedures,²²⁸ 3-hydroxybenzyl alcohol (**403**) was chlorinated with SOCl₂ in the presence of a base to afford 3-hydroxybenzyl chloride (**404**) in excellent yield and purity (Scheme IV-5). Compound **404** tended to slowly polymerize over time and as a result the compound was best used immediately after preparation. The compound 3-(di-*tert*-butylphosphino)benzyl chloride (**405**) was prepared by deprotonation of **404** *in situ* with NaH in THF followed by addition of chlorodi-*tert*-butylphosphine (Scheme IV-5). The compound 3-(diethylphosphino)benzyl chloride (**407**) was prepared by reacting **404** with triethylamine and chlorodiethylphosphine (Scheme IV-5). Compound **407** was

synthesized by Wei-Chun Shih of the Ozerov group. The compounds 1,3-propanedithiol (**408**) and 2-mercaptoethyl ether (**409**) were deprotonated with NaO^tBu in THF to give the corresponding dithiolate sodium salts (Scheme IV-5). Sodium *tert*-butylthiolate (**413**) was prepared by deprotonation of *tert*-butylthiol (**412**) with NaH in THF (Scheme IV-5). Reacting of 2 equiv. of **405** with 1 equiv. of **410** or **411** gave ligands **414** and **415** in good yields (Scheme IV-6). Obtaining ligand **415** in high purity (>95%) proved to be a challenge and efforts to separate the ligand from impurities were not successful. As a result, no further chemistry was performed with ligand **415**. When **407** was reacted with **410** the product of P-S bond formation was observed (by Wei-Chun Shih of the Ozerov group) instead of the desired ligand **416** (Scheme IV-6). The formation of P-S bonds over C-S bonds can be explained by the small steric profile of the phosphinite ethyl arms (compared to P^tBu₂) and the good nucleophilicity of the thiolate anion. As a means to circumventing the undesired P-S bond formation, the trimethylsilyl protected compound **406** was synthesized from **404**, trimethylsilyl chloride and triethylamine (Scheme IV-6). The silyl protected benzyl chloride could then be reacted with **410** or **411** to give **418** and **419** respectively (Scheme IV-6). Monomeric ligand **420** was prepared in quantitative yield by reacting **413** with **405** (Scheme IV-6). Ligands **414** and **415** are both C_{2v} symmetric by ¹H NMR spectroscopy while monomeric ligand **420** is C_s symmetric. The ³¹P{¹H} NMR resonances of the **405** (δ = 153.6 ppm, C₆D₆) precursor and subsequent ligands (**414** δ = 153.1 ppm, **415** δ = 153.6 ppm, **420** δ = 152.7 ppm, all in C₆D₆) are typical of other di-*tert*-butyl phosphinite ligands such as POCOP^{tBu} (δ = 153.0 ppm, C₆D₆).



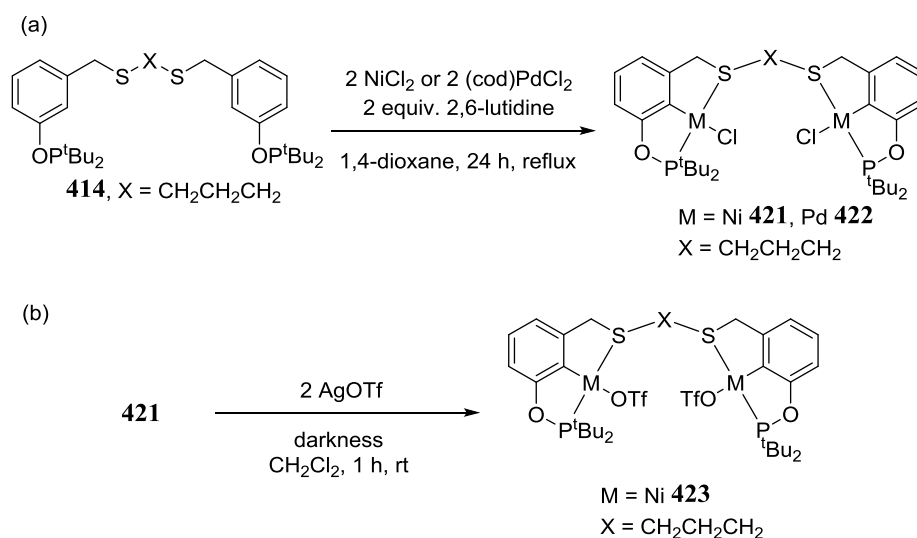
Scheme IV-5. (a) Synthesis of **404** and **405**. (b) Synthesis of protected compounds **406** and **407**. (c) Synthesis of sodium thiolates **410** and **411**. (d) Synthesis of sodium thiolate **413**. Compound **407** was synthesized by Wei-Chun Shih of the Ozerov group.



Scheme IV-6. (a) Synthesis of bridging ligands **414** and **415**. (b) Attempted synthesis of bridging ligand **416** with observation of P-S bond formation by Wei-Chun Shih. (c) Synthesis of silyl ethers **418** and **419**. (d) Synthesis of monomeric ligand **420**.

4.2.2 Synthesis of POCS complexes of nickel and palladium

Ligand **414** readily reacted with 2 equiv. of anhydrous NiCl_2 and 2 equiv. of 2, 6-lutidine in refluxing 1,4-dioxane after 24 h giving an 85% isolated yield of the C_3 linked Ni complex **421** (Scheme IV-7). The analogous Pd complex was synthesized in a similar fashion as **421** using $(\text{cod})\text{PdCl}_2$ giving **422** in an 82% isolated yield (Scheme IV-7).



Scheme IV-7. (a) Synthesis of C_3 linked pincer complexes **421** and **422**. (b) Substitution of the chloride ligands of **421** with using AgOTf to give complex **423**.

Both metalations were sensitive to the amount of 2,6-lutidine added and adding more than 2 equiv. contributed to the formation of unidentified side products. Similar to the ligand, both compounds are C_{2v} symmetric in their respective ^1H NMR spectra (Figure IV-2) with a notable downfield shift of the resonance corresponding to the CH_2

protons of the thioether sidearm upon coordination to nickel and palladium (**414** $\delta = 3.38$ ppm, **421** $\delta = 3.66$ ppm, **422** $\delta = 3.84$ ppm, all in C_6D_6). A modest broadening of the C_3 bridge CH_2 protons resonances as well as a downfield shift, relative to the free ligand, is also observed in both complexes. The $^{31}P\{^1H\}$ NMR resonances (**421** $\delta = 198.2$ ppm, **422** $\delta = 202.0$ ppm, C_6D_6) were comparable to $(POCOP^{tBu})Ni(Cl)$ ($\delta = 187.2$ ppm, $CDCl_3$)²²⁹ and $(POCOP^{tBu})Pd(Cl)$ ($\delta = 192.1$ ppm, $CDCl_3$).²³⁰ Interestingly, an XRD study of **421** indicated the sulfur side arm moieties are not in the plane of the pincer motif with a torsion angle about the C2-C7-S1-Ni1 atoms of $-31.7(2)^\circ$ (Figure IV-3).

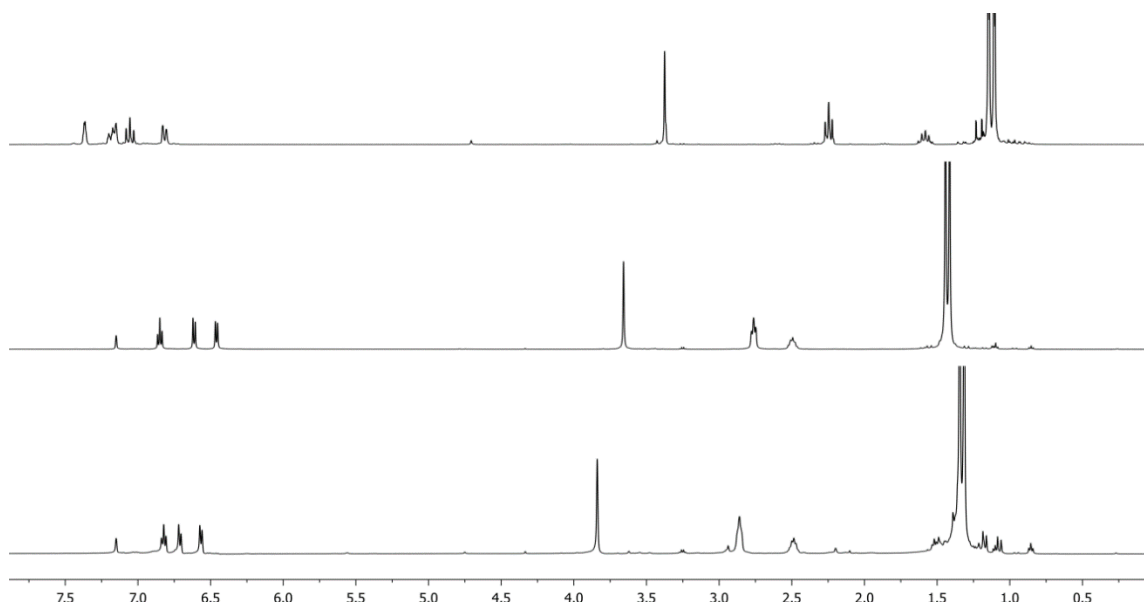


Figure IV-2. (a) 1H NMR (C_6D_6) spectrum of ligand **414**. (b) 1H NMR (C_6D_6) spectrum of metal complex **421**. (c) 1H NMR (C_6D_6) spectrum of metal complex **422**.

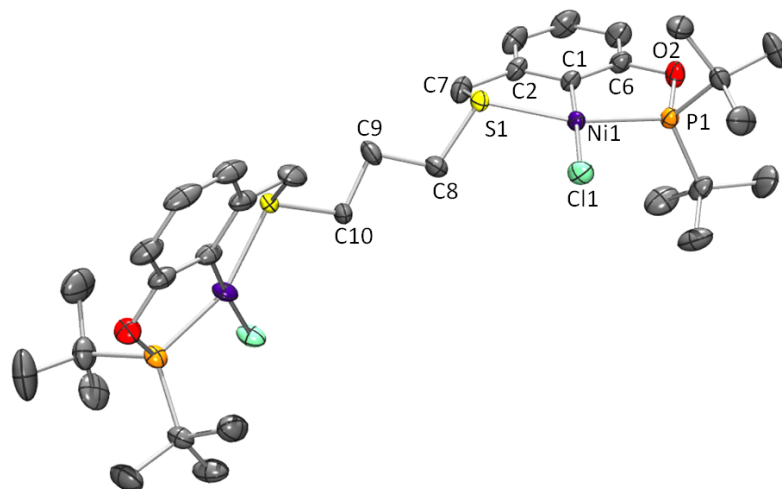
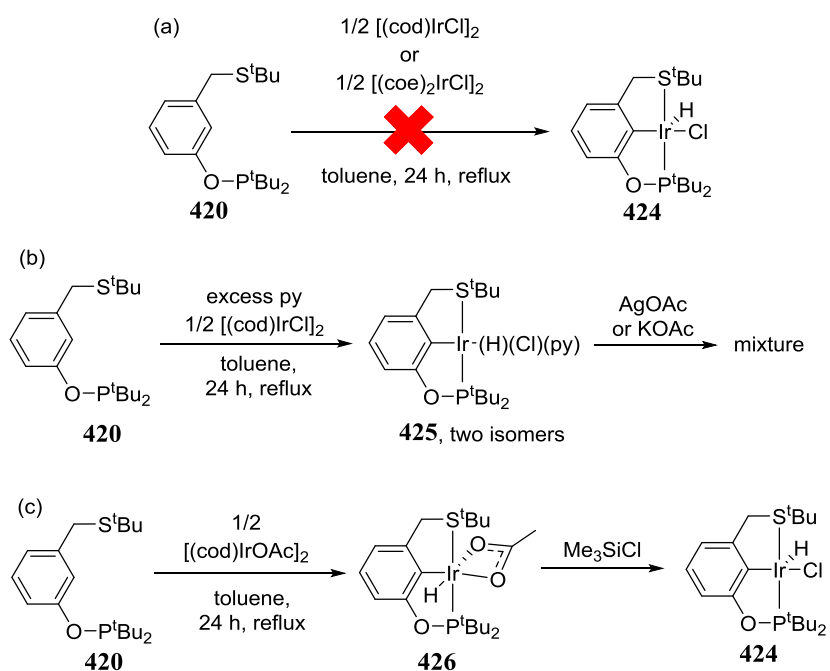


Figure IV-3. POV-Ray rendition of the ORTEP drawing¹⁵⁵ of **421**. Hydrogen atoms and distortion about the C₃ bridge has been omitted for clarity. Selected bond distances (Å), angles (°), torsion (°) for **421**: Ni1-Cl1, 2.20869(7); C1-N1, 1.883(2); S1-Ni1, 2.1936(7); S1-Ni1-P1, 159.49(3); C2-C7-S1-Ni1, -31.7(2); C6-O1-P1-Ni1, -5.8(1). XRD structure was solved by Billy J. McCulloch.

4.2.3 Synthesis of POCS complexes of iridium

Due to synthetic challenges we anticipated with iridium complexes of ligand **414**, our initial efforts were confined to the monomeric ligand **420**. Direct reaction of ligand **420** with [(cod)IrCl]₂ or [(coe)₂IrCl]₂ did not give the target complex, **424** (Scheme IV-8a) and numerous unidentified products, in both cases, were observed by NMR spectroscopy. Utilizing the tactic employed for the synthesis of (POCOP^{iPr})Rh and Ir compounds where [(cod)MCl]₂ or [(coe)₂MCl]₂ (where M = Rh or Ir) and POCOP^{iPr} ligand are reacted in the presence of excess DMAP or pyridine to generate

(POCOP^{iPr})M(H)(Cl)(py), we were able to synthesize **425** (two isomers, Scheme IV-8b). Two hydride resonances are observed in close proximity (two doublets, $\delta \approx -22.0$ ppm, $J_{\text{P-H}} \approx 23$ Hz, C₆D₆) which have chemical shifts comparable to **213-(H)(Cl)(py)** (two observed isomers, $\delta \approx -21.0$ ppm, C₆D₆, Scheme II-2 of Chapter 2) and (PCP)Ir(H)(Cl)(py) complexes²³¹ indicating Ir-H ligands trans to a chloride



Scheme IV-8. (a) Failed attempt at direct synthesis of **424** by reacting ligand **420** with common Ir starting materials. (b) Synthesis of pyridine adducts **425**. (c) Synthesis of **426** and subsequent conversion to **424** with Me₃SiCl.

or pyridine ligands. The $^{31}\text{P}\{^1\text{H}\}$ NMR spectrum of **425** contains two singlets in close proximity ($\delta \approx 150.0$ ppm, C_6D_6) which are of comparable chemical shift to **213-(H)(Cl)(py)** (two observed isomers, $\delta \approx 148$ ppm, C_6D_6). Attempts to abstract the pyridine ligand of **425** with $\text{BF}_3 \cdot \text{OEt}_2$ gave a mixture of unidentified compounds and further efforts with $\text{BF}_3 \cdot \text{OEt}_2$ were abandoned. **425** by reacted with excess AgOAc or KOAc to give mixtures partially comprised of **426** (Scheme IV-8b). Indeed, the direction reaction of $[(\text{cod})\text{IrOAc}]_2$ with ligand **420** gave the hydrido-acetate compound **426** (Scheme IV-8c). The ^1H NMR spectrum of compound **426** shows a single C_s symmetric compound with two distinct and well resolved resonances corresponding to the CH_2 protons of the methylene arm. The ^1H NMR spectrum also contains two sharp doublets ($\delta = 1.38$ ppm, $J_{\text{P-H}} = 11.6$ Hz and 1.33 ppm, $J_{\text{P-H}} = 11.2$ Hz, C_6D_6) corresponding to the *tert*-butyl groups of P and a sharp singlet ($\delta = 1.12$ ppm) corresponding to the *tert*-butyl group of S. The hydride resonance of **426** is a sharp and well resolved (doublet, $\delta = -28.84$ ppm, $J_{\text{P-H}} = 19.6$ Hz, C_6D_6). This data indicates a rigid preferred orientation of the $\text{CH}_2\text{S}^t\text{Bu}$ arm and that **426** is one isomer. Reacting **426** with Me_3SiCl gave **424** (Scheme IV-8c) in 90% purity. The ^1H NMR resonances of **424** are broad including two very broad and overlapping hydride resonances centered about ca. -27.00 ppm (C_6D_6). Comparing the chemical shift of the hydride resonances of **424** to Brookhart's monomeric square pyramidal ($\text{POCOP}^{t\text{Bu}}\text{Ir}(\text{H})(\text{Cl})$) (**118-(H)(Cl)**, Scheme I-18) (t, $\delta = -41.39$ ppm, CD_2Cl_2)⁹⁰ indicates the hydride ligands are likely not trans to an empty site. Two doublets, one broad and one sharp, are seen in the ^1H NMR spectrum (br d, $\delta = 1.64$ $J_{\text{P-H}} = 12.3$ Hz, and d, $\delta = 1.52$ $J_{\text{P-H}} = 14.0$ Hz) corresponding to

the *tert*-butyl groups of P and a broad singlet ($\delta = 1.11$ ppm) corresponding to the *tert*-butyl group of S. Two near overlapping singlets are observed in the $^{31}\text{P}\{^1\text{H}\}$ NMR spectrum of **424** ($\delta = 156.15$ and 155.86 ppm, C_6D_6). This data suggests **424** is likely comprised of two isomers (of closely related connectivity) with ^1H NMR resonances having near identical chemical shift. An XRD study of **424** revealed a dimeric structure (Figure IV-4) with slightly staggered bridging chloride ligands and a C1-Ir1-Cl2 angle of $94.3(2)^\circ$. In comparison, the analogous C-Ir-Cl angle of **215-(H)(Cl)** (Chapter 2, Figure II-3) is considerably more obtuse at $110.8(1)^\circ$. If **424** (or isomers thereof) is also dimeric in solution this difference in angle could explain the downfield hydride chemical shift of **424** because the hydride ligand is more effectively trans to a chloride ligand in **424** than in **215-(H)(Cl)**. The existence of two isomers could be the result of a kinetic and thermodynamic orientation of the $\text{CH}_2\text{S}^t\text{Bu}$ and further studies are required.

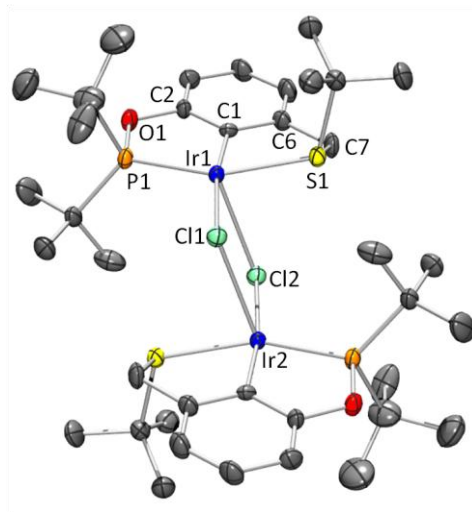
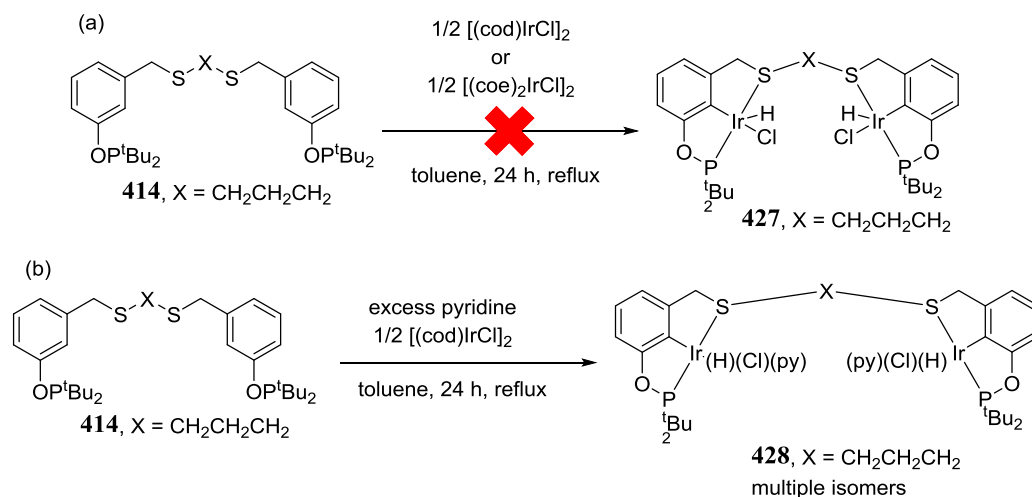


Figure IV-4. POV-Ray rendition of the ORTEP drawing¹⁵⁵ of **424**. Hydrogen atoms have been omitted for clarity. Selected bond distances (Å), angles (°), torsion (°) for **424**: Ir1-Ir2, 3.897(1); Ir1-Cl1, 2.506(1); Ir1-Cl2, 2.615(2); Ir1-C1, 2.0515(5); Ir1-S1, 2.385(2); Ir1-P1, 2.240(2); C1-Ir1-Cl1, 171.6(2); P1-Ir1-S1, 159.99(5); C6-C7-S1-Ir-1, 29.2(5); C2-O1-P1-Ir1, 0.9(4). XRD structure was solved by Billy J. McCulloch.

Similar to the monomeric POCS ligand, reacting ligand **414** with $[(\text{COD})\text{IrCl}]_2$ or $[(\text{COE})_2\text{IrCl}]_2$ did not give the target complex **427** (Scheme IV-9a). Reacting ligand **414** with $[(\text{COD})\text{IrCl}]_2$ in the presence of excess pyridine we were able to synthesize $(^t\text{BuPOCS}^{\text{C}3})[\text{Ir}(\text{H})(\text{Cl})(\text{py})]_2$ **428** (Scheme IV-9a). The isolated material was comprised of multiple isomers which inhibited full characterization by ^1H NMR spectroscopy. Multiple hydride resonances (doublets, $\delta \approx -22.5$ ppm, $J_{\text{P-H}} = 24$ Hz, 1:1 C_6D_6 :py, Scheme IV-9b), with chemical shifts similar to the hydride resonances of **425**, are observed in close proximity and no other hydride



Scheme IV-9. Synthesis of bridging (POCS)Ir compounds.

signals are observed. The $^{31}\text{P}\{^1\text{H}\}$ NMR spectrum of **428** contains multiple singlets in close proximity ($\delta \approx 150.4$ ppm, 1:1 C₆D₆:py) which are also of comparable chemical shift to **425**.

4.3 Conclusion

The synthesis and characterization of POCS compounds of Ni, Pd and Ir has been described. The POCS ligands are readily synthesized on multi-gram scales from common starting materials. The precursor compound **404** (Scheme IV-5) is an extremely useful starting material that can provide access to a variety of monomeric and bridging POCS ligands. POCS complexes of Ni and Pd are readily prepared under mild conditions and halide ligand substitution (chloride to triflate) was demonstrated for Ni. A C₃ bridging (POCS)Ni compound **421** was characterized by an XRD study. Mononuclear POCS complexes of Ir were prepared and characterized. A mononuclear

(POCS)Ir dimer **424** was characterized by an XRD study. Direct reaction of bridging POCS ligand with common Ir starting materials to form 5-coordinate unsaturated Ir metal centers was not successful although a 6-coordinate pyridine adduct (multiple isomers) was synthesized and characterized.

4.4 Experimental

4.4.1 General considerations

Unless specified otherwise, all manipulations were performed under an argon atmosphere using standard Schlenk or glovebox techniques. Pentane, diethyl ether, tetrahydrofuran, mesitylene and benzene were dried over sodium–benzophenone ketyl, distilled or vacuum transferred and stored over molecular sieves in an Ar-filled glovebox. All other chemicals were used as received from commercial vendors. All NMR spectra were recorded on a Varian Inova 300 spectrometer (^1H NMR 299.951 MHz, $^{31}\text{P}\{^1\text{H}\}$ NMR 121.425 MHz, $^{13}\text{C}\{^1\text{H}\}$ NMR 75.413 MHz), Varian Mercury 300 spectrometer ($^{13}\text{C}\{^1\text{H}\}$ NMR 75.426 MHz), Varian Inova 400 spectrometer (^1H NMR, 399.755 MHz; $^{13}\text{C}\{^1\text{H}\}$ NMR, 100.518 MHz; ^{11}B NMR 128 MHz, $^{31}\text{P}\{^1\text{H}\}$ NMR 181.822 MHz), or a Varian Inova NMR 500 (^1H NMR, 499.425 MHz/ 499.683 MHz; $^{13}\text{C}\{^1\text{H}\}$ NMR, 75.424 MHz/ 125.580 MHz; $^{31}\text{P}\{^1\text{H}\}$ NMR, 202.171 MHz; ^{19}F NMR, 469.854 MHz) spectrometer. All spectra were recorded at ambient temperature unless otherwise noted. Chemical shifts are reported in δ /ppm. For ^1H and $^{13}\text{C}\{^1\text{H}\}$ NMR spectra, the residual solvent peak was used as an internal reference.¹⁷² ^{11}B NMR spectra were referenced externally using neat BF_3OEt_2 at $\delta = 0$ ppm, $^{31}\text{P}\{^1\text{H}\}$ NMR spectra were

referenced externally using 85% H₃PO₄ at $\delta = 0$ ppm, and ¹⁹F NMR spectra were referenced externally using 1.0 M CF₃CO₂H in CDCl₃ at $\delta = -78.5$ ppm.

4.4.2 Synthesis of POCS ligands

Synthesis of 404 – A 50 mL culture tube was loaded with 3-hydroxybenzyl alcohol (**403**) (1.38 g, 11.1 mmol), pyridine (1.5 mL, 18.6 mmol) and 30 mL of dichloromethane. The solution was cooled using an ice bath and SOCl₂ (4.0 g, 33.6 mmol) was added dropwise. The solution was stirred for 1 h then 10 mL of H₂O was added (Warning Gas Evolution!). The mixture was transferred to a separatory funnel and washed with additional H₂O (2 × 20 mL). The dichloromethane fraction was reduced *in vacuo* in a Schlenk flask giving a clear oil. The oil was dried *in vacuo* for 6 h then used as is. Yield: 1.41 g (89%). ¹H NMR (CDCl₃): δ 7.23 (t, $J_{\text{H-H}} = 7.9$ Hz, 1H, Ar-*H*), 6.96 (d, $J_{\text{H-H}} = 7.6$ Hz, 1H, Ar-*H*), 6.91 – 6.88 (m, 1H, Ar-*H*), 6.81 (dd, $J_{\text{H-H}} = 8.1, 2.1$ Hz, 1H, Ar-*H*), 6.22 – 5.33 (br s, 1H, Ar-OH), 4.53 (s, 2H, Ar-(CH₂)-Cl). ¹³C{¹H} NMR (CDCl₃): δ 155.6, 139.3, 130.2, 121.1, 115.6, 46.1.

Synthesis of 405 – A 50 mL culture tube was loaded with 3-hydroxybenzyl chloride (**404**) (1.22 g, 8.56 mmol) and 20 mL of THF. NaH (0.250 g, 10.4 mmol) was added as a suspension in THF (Warning Gas Evolution!). The reaction was stirred for 4 h at ambient temperature. As a solution in THF, chlorodi-*tert*-butylphosphine (1.55 g, 8.58 mmol) was added. The tube was sealed, brought out of the glovebox and heated to 65 °C for 24 h. The tube was brought into a glovebox and the mixture was filtered through Celite giving yellow oil which tended to solidified over time. Yield: 1.89 g (78%) ¹H NMR (C₆D₆): δ 7.24-7.23 (m, 1H, Ar-*H*), 7.17 – 7.12 (m, 1H, Ar-*H*), 6.98 (t,

$J_{\text{H-H}} = 7.9$ Hz, 1H, Ar-*H*), 6.72 (d, $J_{\text{H-H}} = 7.6$ Hz, 1H, Ar-*H*), 4.09 (s, 2H, Ar-(CH₂)-Cl), 1.09 (d, $J_{\text{P-H}} = 11.7$ Hz, 18H, Ar-OP^{*t*}Bu₂). ¹³C{¹H} NMR (C₆D₆): δ 160.5 (d, $J_{\text{P-C}} = 9.6$ Hz), 139.4, 129.9, 121.8, 118.72 (d, $J_{\text{P-C}} = 10.3$ Hz), 118.40 (d, $J_{\text{P-C}} = 11.7$ Hz), 46.0, 35.8 (d, $J_{\text{P-C}} = 26.6$ Hz), 27.5 (d, $J_{\text{P-C}} = 15.7$ Hz). ³¹P{¹H} NMR (C₆D₆): δ 153.6.

Synthesis of 406 – A 25 mL Schlenk flask was loaded with 3-hydroxybenzyl chloride (**403**) (3.04 g, 21.3 mmol), 10 mL of diethyl ether, triethylamine (3.2 g, 31.6 mmol) and trimethylsilyl chloride (4.2 g, 27.9 mmol). A white precipitate formed immediately upon addition of trimethylsilyl chloride. The mixture was filtered through Celite and all volatiles were removed *in vacuo* giving clear oil. Yield: 4.90 g (90%). ¹H NMR (CDCl₃): δ 7.21 (t, $J_{\text{H-H}} = 7.9$ Hz, 1H, Ar-*H*), 6.99 – 6.96 (m, 1H, Ar-*H*), 6.91 – 6.89 (m, 1H, Ar-*H*), 6.81 (ddd, $J_{\text{H-H}} = 8.1, 2.5, 1.0$ Hz, 1H, Ar-*H*), 4.54 (s, 2H, Ar-(CH₂)-Cl), 1.01 (t, $J_{\text{H-H}} = 7.9$ Hz, 9H, Ar-OSiEt₃), 0.79 – 0.72 (m, 6H, Ar-OSiEt₃).

Synthesis of 407 – A 50 mL culture tube was loaded with 3-hydroxybenzyl chloride (**404**) (1.22 g, 8.56 mmol) and 20 mL of Et₂O and triethylamine (0.250 g, 10.4 mmol). chlorodiethylphosphine (1.55 g, 8.58 mmol) was added. The mixture was stirred for 12 h at RT. The tube was brought into a glovebox and the mixture was filtered through Celite giving yellow oil which tended to solidified over time. Yield: 1.89 g (78%).

Synthesis of 410 – A 50 mL culture tube was loaded with 1,3-propanedithiol (**408**) (1.38 g, 12.8 mmol) and 30 mL of THF. NaO^{*t*}Bu (2.46 g, 25.6 mmol) was added and the mixture was stirred at 65 °C for 12 h. The white precipitate was collected on a frit, washed with pentane and diethyl ether then dried *in vacuo* overnight. Yield: 1.83 g

(47%). ^1H NMR (CD_3OD): δ 2.55 – 2.48 (t, $J_{\text{H-H}} = 7.8$ Hz, 4H, $\text{SCH}_2\text{CH}_2\text{CH}_2\text{S}$), 1.84 (p, $J_{\text{H-H}} = 7.8$ Hz, 2H, $\text{SCH}_2\text{CH}_2\text{CH}_2\text{S}$). $^{13}\text{C}\{^1\text{H}\}$ NMR (CD_3OD): δ 46.9, 26.2.

Synthesis of 411 – A 50 mL culture tube was loaded with 2-mercaptoethyl ether (**409**) (1.86 g, 13.5 mmol) and 30 mL of THF. NaO^tBu (2.59 g, 27.0 mmol) was added and the mixture was stirred at 65 °C for 12 h. The white precipitate was collected on a frit, washed with pentane and diethyl ether then dried *in vacuo* overnight. Yield: 2.35 g (96%). ^1H NMR (CD_3OD): δ 3.49 (m, 4H), 2.62 (m, 4H). $^{13}\text{C}\{^1\text{H}\}$ NMR (CD_3OD): δ 77.2, 24.9.

Synthesis of 413 – A 50 mL Schlenk flask was loaded with *tert*-butylthiol (**412**) (0.603g, 6.69 mmol) and 20 mL of THF. NaH (0.178 g, 7.42 mmol) was added as a suspension in THF (Warning Gas Evolution!). The mixture was stirred overnight at ambient temperature. Yield: 0.669 g (89%). ^1H NMR (CD_3OD): δ 1.27 (s, 9H). $^{13}\text{C}\{^1\text{H}\}$ NMR (CD_3OD): δ 38.1, 22.0.

Synthesis of 418 – A 50 mL culture tube was loaded with 3-(triethylsilyl(oxy))benzyl chloride (**406**) (2.31 g, 8.99 mmol), 25 mL of acetonitrile and $\text{NaSCH}_2\text{CH}_2\text{CH}_2\text{SNa}$ (**410**) (0.684 g, 4.49 mmol). The reaction was stirred for 24 h at ambient temperature. The mixture was filtered through Celite and all solvent removed *in vacuo* giving yellow oil. Yield: 1.98 g (80%). ^1H NMR (CDCl_3): δ 7.15 (t, $J_{\text{H-H}} = 7.8$ Hz, 2H, Ar-*H*), 6.90 – 6.86 (m, 2H, Ar-*H*), 6.82 (t, $J_{\text{H-H}} = 2.0$ Hz, 2H, Ar-*H*), 6.73 (ddd, $J_{\text{H-H}} = 8.0, 2.4, 0.9$ Hz, 2H, Ar-*H*), 3.62 (s, 4H, Ar-(CH_2)-SR), 2.46 (t, $J_{\text{H-H}} = 7.2$ Hz, 4H, $\text{SCH}_2\text{CH}_2\text{CH}_2\text{S}$), 1.78 (p, $J_{\text{H-H}} = 7.2$ Hz, 2H, $\text{SCH}_2\text{CH}_2\text{CH}_2\text{S}$), 1.00 (t, $J_{\text{H-H}} = 7.9$ Hz,

18H, Ar-OSiEt₃), 0.78 – 0.67 (m, 12H, Ar-OSiEt₃). ¹³C{¹H} NMR (CDCl₃): δ 155.8, 140.0, 129.5, 122.0, 120.6, 118.7, 36.2, 30.2, 28.8, 6.79, 5.16.

Synthesis of 419 – A 50 mL culture tube was loaded with 3-(triethylsilyl(oxy))benzyl chloride (**406**) (2.06 g, 8.02 mmol), 25 mL of acetonitrile and NaSCH₂CH₂OCH₂CH₂SNa (**411**) (0.731 g, 4.01 mmol). The reaction was stirred for 24 h at ambient temperature. The mixture was filtered through Celite and all solvent removed *in vacuo* giving yellow oil. Yield: 1.93 g (83%). ¹H NMR (CDCl₃): δ 7.15 (t, *J*_{H-H} = 7.8 Hz, 2H, Ar-*H*), 6.91 – 6.88 (m, 2H, Ar-*H*), 6.84 – 6.82 (m, 2H, Ar-*H*), 6.73 (ddd, *J*_{H-H} = 8.0, 2.4, 1.0 Hz, 2H, Ar-*H*), 3.69 (s, 4H, Ar-(CH₂)-SR), 3.52 (t, *J*_{H-H} = 6.8 Hz, 4H, SCH₂CH₂OCH₂CH₂S), 2.58 (t, *J*_{H-H} = 6.7 Hz, 4H, SCH₂CH₂OCH₂CH₂S), 0.99 (t, *J*_{H-H} = 7.9 Hz, 18H, Ar-OSiEt₃), 0.78 – 0.70 (m, 12H, Ar-OSiEt₃). ¹³C{¹H} NMR (CDCl₃): δ 155.8, 140.0, 129.5, 122.1, 120.6, 118.7, 70.6, 36.6, 30.7, 6.80, 5.16.

Synthesis of 414 - A 50 mL culture tube was loaded with 3-di-*tert*-butylphosphinitobenzyl chloride (**405**) (1.98 g, 6.90 mmol), 25 mL of acetonitrile and NaSCH₂CH₂CH₂SNa (0.525 g, 3.45 mmol). The reaction was stirred for 24 h at ambient temperature. The mixture was filtered through Celite and all solvent removed *in vacuo* giving yellow oil. Yield: 1.83 g (87%). ¹H NMR (C₆D₆): δ 7.37 (d, *J*_{H-H} = 1.7 Hz, 2H, Ar-*H*), 7.23 – 7.16 (m, 2H, Ar-*H*), 7.06 (t, *J*_{H-H} = 7.8 Hz, 2H, Ar-*H*), 6.87 – 6.77 (m, 2H, Ar-*H*), 3.38 (s, 4H, Ar-(CH₂)-SR), 2.25 (t, *J*_{H-H} = 7.2 Hz, 4H, SCH₂CH₂CH₂S), 1.58 (q, *J*_{H-H} = 7.2 Hz, 2H, SCH₂CH₂CH₂S), 1.13 (d, *J*_{H-H} = 11.7 Hz, 36H, Ar-OP^{*t*}Bu₂). ¹³C{¹H} NMR (C₆D₆): δ 160.5 (d, *J*_{P-C} = 9.6 Hz), 140.8, 129.7, 122.4, 119.2 (d, *J*_{P-C} = 10.6 Hz),

117.2 (d, $J_{P-C} = 11.2$ Hz), 36.2 , 35.7 (d, $J_{P-C} = 26.5$ Hz), 30.4, 29.0, 27.5 (d, $J_{P-C} = 15.7$ Hz). $^{31}P\{^1H\}$ NMR (C_6D_6): δ 153.1.

Synthesis of 415 - A 50 mL culture tube was loaded with 3-di-*tert*-butylphosphinitobenzyl chloride (**405**) (1.12 g, 3.91 mmol), 25 mL of acetonitrile and $NaSCH_2CH_2OCH_2CH_2SNa$ (**411**) (0.356 g, 1.95 mmol). The reaction was stirred for 24 h at ambient temperature. The mixture was filtered through Celite and all solvent removed *in vacuo* giving yellow oil. The ligand was determined to be 82% pure by 1H NMR spectroscopy. Yield: 1.13 g (91%). 1H NMR ($CDCl_3$): δ 7.11 (t, $J_{H-H} = 8.0$ Hz, 2H, Ar-*H*), 7.07 – 7.03 (m, 2H, Ar-*H*), 6.97 (d, $J = 8.2$ Hz, 2H, Ar-*H*), 6.83 (d, $J = 7.5$ Hz, 2H, Ar-*H*), 3.64 (s, 4H, Ar-(CH_2)-SR), 3.46 (t, $J_{H-H} = 6.8$ Hz, 4H, $SCH_2CH_2OCH_2CH_2S$), 2.54 (t, $J = 6.8$ Hz, 4H, $SCH_2CH_2OCH_2CH_2S$), 1.10 (d, $J_{P-H} = 11.8$ Hz, 36H, Ar- OP^tBu_2). $^{31}P\{^1H\}$ NMR ($CDCl_3$): δ 154.4.

Synthesis of 420 - A 50 mL culture tube was loaded with 3-di-*tert*-butylphosphinitobenzyl chloride (**405**) (0.752 g, 2.62 mmol), 15 mL of acetonitrile and $NaSC(CH_3)_3$ (0.296 g, 2.64 mmol). The reaction was stirred for 24 h at ambient temperature. The mixture was filtered through Celite and all solvent removed *in vacuo* giving yellow oil. The ligand was determined to be 89% pure by 1H NMR spectroscopy. Yield: 0.875 g (98%). 1H NMR (C_6D_6): δ 7.50 – 7.44 (m, 1H, Ar-*H*), 7.19 – 7.14 (m, 1H, Ar-*H*), 7.06 (t, $J_{H-H} = 7.8$ Hz, 1H, Ar-*H*), 6.93 (dq, $J_{H-H} = 7.5, 1.0$ Hz, 1H, Ar-*H*), 3.59 (s, 2H, Ar-(CH_2)-SR), 1.19 (s, 9H, Ar-(CH_2)- S^tBu), 1.12 (d, $J_{H-H} = 11.6$ Hz, 18H, Ar- OP^tBu_2). $^{13}C\{^1H\}$ NMR (C_6D_6): δ 160.4 (d, $J_{P-C} = 9.5$ Hz), 141.1 , 129.6 (d, $J_{P-C} = 0.6$ Hz), 122.5 (d, $J_{P-C} = 1.2$ Hz), 119.3 (d, $J_{P-C} = 10.6$ Hz), 117.01 (d, $J_{P-C} = 11.3$ Hz), 42.5 ,

35.7 (d, $J_{P-C} = 26.6$ Hz), 33.8 , 31.1 (d, $J_{P-C} = 8.5$ Hz), 27.8 – 27.3 (m). $^{31}\text{P}\{^1\text{H}\}$ NMR (C_6D_6): δ 152.7.

Synthesis of 421 – A 50 mL culture tube was loaded with anhydrous NiCl_2 (0.666 g, 5.26 mmol), 15 mL of 1,4-dioxane, 2,6-lutidine (0.564 g, 5.27 mmol) and **414** (1.49 g, 2.45 mmol). The mixture was stirred and heated to 100 °C for 24 h. The mixture was filtered through a plug of silica over Celite and solvent was removed *in vacuo* giving a yellow residue. This residue was dissolved in toluene and filtered through a plug of silica over Celite giving yellow solids. The solids were recrystallized from toluene/pentane in a –30 °C freezer. An X-ray quality crystal was grown from a toluene solution of **421** layered with pentane. Yield: 1.48 g (76%). ^1H NMR (C_6D_6): δ 6.85 (t, $J_{H-H} = 7.7$ Hz, 2H, Ar-*H*), 6.61 (d, $J_{H-H} = 7.7$ Hz, 2H, Ar-*H*), 6.46 (d, $J_{H-H} = 7.5$ Hz, 2H, Ar-*H*), 3.66 (s, 4H, Ar-(CH_2)-SR), 2.76 (t, $J_{H-H} = 6.9$ Hz, 4H, $\text{SCH}_2\text{CH}_2\text{CH}_2\text{S}$), 2.49 (p, $J_{H-H} = 7.7$ Hz, 2H, $\text{SCH}_2\text{CH}_2\text{CH}_2\text{S}$), 1.43 (d, $J_{P-H} = 14.3$ Hz, 36H, Ar- OP^tBu_2). $^{13}\text{C}\{^1\text{H}\}$ NMR (C_6D_6): δ 168.4 (d, $J_{P-H} = 10.2$ Hz), 153.0 (d, $J_{P-H} = 2.3$ Hz), 140.4 (d, $J_{P-H} = 25.6$ Hz), 127.1 , 117.9 , 109.0 (d, $J_{P-H} = 13.1$ Hz), 44.7 , 39.5 (d, $J_{P-H} = 14.3$ Hz), 34.6 , 29.3 , 28.1 (d, $J_{P-H} = 4.4$ Hz). $^{13}\text{C}\{^1\text{H}\}$ NMR (C_6D_6): δ 198.1.

Synthesis of 422 – A 50 mL culture tube was loaded with (cod) PdCl_2 (0.164 g, 0.574 mmol), 15 mL of 1,4-dioxane, 2,6-lutidine (0.062 g, 0.579 mmol) and **414** (0.175 g, 0.287 mmol). The mixture was stirred and heated to 100 °C for 24 h. The mixture was filtered through a plug of silica over Celite and solvent was removed *in vacuo* giving a yellow residue. This residue was dissolved in toluene and filtered through a plug of silica over Celite giving yellow solids. The solids were recrystallized from toluene/pentane in

a $-30\text{ }^{\circ}\text{C}$ freezer. Yield: 0.184 g (72%). ^1H NMR (C_6D_6): δ 6.82 (t, $J_{\text{H-H}} = 7.7$ Hz, 2H, Ar-H), 6.71 (d, $J_{\text{H-H}} = 7.9$ Hz, 2H, Ar-H), 6.57 (d, $J_{\text{H-H}} = 7.5$ Hz, 2H, Ar-H), 3.84 (s, 4H, Ar-(CH_2)-SR), 2.86 (s, 4H, $\text{SCH}_2\text{CH}_2\text{CH}_2\text{S}$), 2.55 – 2.43 (m, 2H, $\text{SCH}_2\text{CH}_2\text{CH}_2\text{S}$), 1.33 (d, $J_{\text{P-H}} = 15.3$ Hz, 36H, Ar- OP^iBu_2). $^{31}\text{P}\{^1\text{H}\}$ NMR (C_6D_6): δ 202.0.

Synthesis of 423 – A 25 mL Schlenk flask was loaded with **421** (0.091 g, 0.114 mmol) and 5 mL of dichloromethane. AgOTf (0.065 g, 0.252 mmol) was added and the mixture was stirred in the dark for 1 h at ambient temperature. The mixture was filtered through a plug of silica over Celite and all solvent was removed *in vacuo* giving yellow solids. Yield: 0.107 g (92%). ^1H NMR (C_6D_6): δ 6.73 (td, $J_{\text{H-H}} = 7.9, 0.8$ Hz, 2H, Ar-H), 6.40 (dd, $J_{\text{H-H}} = 7.9, 1.0$ Hz, 2H, Ar-H), 6.29 (d, $J_{\text{H-H}} = 7.6$ Hz, 2H, Ar-H), 3.48 (s, 4H, Ar-(CH_2)-SR), 3.05 (t, $J_{\text{H-H}} = 7.2$ Hz, 4H, $\text{SCH}_2\text{CH}_2\text{CH}_2\text{S}$), 2.48 (p, $J_{\text{H-H}} = 7.7$ Hz, 2H, $\text{SCH}_2\text{CH}_2\text{CH}_2\text{S}$), 1.29 (d, $J_{\text{P-H}} = 14.8$ Hz, 36H, Ar- OP^iBu_2). ^{19}F NMR (C_6D_6): δ -78.2 (s). $^{13}\text{C}\{^1\text{H}\}$ NMR (C_6D_6): δ 168.9 (d, $J = 8.8$ Hz), 154.8, 128.6, 119.0, 109.5 (d, $J = 12.7$ Hz), 41.6, 39.2 (d, $J = 14.0$ Hz), 36.0, 30.0, 27.4 (d, $J = 4.7$ Hz). $^{31}\text{P}\{^1\text{H}\}$ NMR (C_6D_6): δ 196.0.

Synthesis of 425 – A J. Young NMR tube was loaded with $[(\text{cod})\text{IrCl}]_2$ (0.100 g, 0.149 mmol), 1 mL of toluene and pyridine (200 μL , 2.48 mmol). The tube was mixed and **420** (0.101 g, 0.297 mmol) was added. The mixture was heated to $110\text{ }^{\circ}\text{C}$ for 48 h giving a yellow solution. The solution was passed through a short plug of silica over Celite then all solvent was removed *in vacuo* giving yellow-brown solids. A portion of the solids were analyzed by ^1H and $^{31}\text{P}\{^1\text{H}\}$ NMR spectroscopy. The solids were comprised of two isomers in a 75:25 ratio (by comparison of the two observed hydride

signals which have a ratio of 75:25 as well as the two observed ^{31}P resonances having the same 75:25 ratio) and consequently, only the major product could be partially assigned in the ^1H NMR spectrum. Yield: 0.115 g (85%). ^1H NMR (Isomer A, C_6D_6): δ 3.61 (d, $J = 16.2$ Hz, 1H), 3.47 (d, $J = 16.4$ Hz, 1H), 1.51 (d, $J_{\text{P-H}} = 13.9$ Hz, 9H), 1.31 (s, 9H), 1.19 (d, $J_{\text{P-H}} = 14.0$ Hz, 9H), -22.00 (d, $J_{\text{P-H}} = 23.0$ Hz, 1H, 75%). ^1H NMR (Isomer B, C_6D_6): δ -22.10 (d, $J_{\text{P-H}} = 21.2$ Hz, 25%). $^{31}\text{P}\{^1\text{H}\}$ NMR (C_6D_6): δ 151.6 (77%, isomer A), 152.8 (23%, isomer B).

Direct reaction of ligand 420 with $[(\text{cod})\text{IrCl}]_2$ – A J. Young NMR tube was loaded with $[(\text{cod})\text{IrCl}]_2$ (0.107 g, 0.159 mmol), 1 mL of toluene and **420** (0.110 g, 0.323 mmol). The reaction was heated for 36 h at 120 °C. Numerous unidentified products were observed in the $^{31}\text{P}\{^1\text{H}\}$ NMR spectrum.

Synthesis of 426 – A J. Young NMR tube was loaded with $[(\text{cod})\text{IrOAc}]_2$ (0.052 g, 0.072 mmol), 1 mL of toluene and **420** (0.051 g, 0.15 mmol). The solution was heated to 120 °C for 36 h. The solution was passed through a short plug of silica over Celite and all solvent was removed *in vacuo* giving a brown solid. Yield 0.054 g (63%). ^1H NMR (C_6D_6): δ 6.81 – 6.75 (m, 2H, Ar-*H*), 6.51 (t, $J_{\text{H-H}} = 5.1$ Hz, 1H, Ar-*H*), 3.98 (d, $J = 16.6$ Hz, 1H, Ar-(CH_2)-SR), 3.68 (dd, $J = 16.7, 2.3$ Hz, 1H, Ar-(CH_2)-SR), 1.91 (s, 3H, Ir- κ_2 -OAc), 1.38 (d, $J_{\text{P-H}} = 11.5$ Hz, 9H, Ar- OP^tBu_2), 1.33 (d, $J_{\text{P-H}} = 11.2$ Hz, 9H, Ar- OP^iBu_2), 1.12 (s, 9H, Ar-(CH_2)- S^iBu), -28.84 (d, $J_{\text{P-H}} = 19.6$ Hz, 1H, Ir-*H*). $^{31}\text{P}\{^1\text{H}\}$ NMR (C_6D_6): δ 157.4.

Synthesis of 424 – A J. Young NMR tube was loaded with **426** (0.040 g, 0.0676 mmol), cyclohexane (10 μL , 0.10 mmol), 1 mL of C_6D_6 and trimethylsilyl chloride (15

μL , 0.140 mmol). The solution was mixed and analyzed by ^1H and $^{31}\text{P}\{^1\text{H}\}$ NMR spectroscopy. Trimethylsilyl acetate ($\delta = 1.70$ ppm) was observed in the ^1H NMR spectrum. All solvent was removed *in vacuo* giving light brown solids. X-ray quality crystals were grown from a toluene solution layered with pentane. Yield 0.036 g (94%). ^1H NMR (C_6D_6): δ 6.81 – 6.76 (m, 2H), 6.54 (t, $J_{\text{H-H}} = 4.5$ Hz, 1H), 4.43 (d, $J = 15.3$ Hz, 1H), 3.68 (dd, $J = 15.8, 3.2$ Hz, 1H), 1.64 (br d, $J_{\text{P-H}} = 12.3$ Hz, 9H), 1.52 (d, $J_{\text{P-H}} = 14.0$ Hz, 9H), 1.12 (br s, 9H), -27.00 (br m, 1H, Ir-*H*).

Direction reaction of ligand 414 with $[(\text{cod})\text{IrCl}]_2$ or $[(\text{coe})_2\text{IrCl}]_2$ – A J. Young NMR tube was loaded with ligand **414** (0.023 g, 0.0378 mmol), $[(\text{cod})\text{IrCl}]_2$ (0.025 g, 0.0372 mmol) and 1 mL of toluene. A second J. Young NMR tube was loaded with ligand **414** (0.035 g, 0.0575 mmol), $[(\text{coe})_2\text{IrCl}]_2$ (0.053 g, 0.0591 mmol) and 1 mL of toluene. The samples were placed in a 115 °C oil bath for 24 h. In both samples, analysis by ^{31}P NMR spectroscopy revealed numerous products.

Reaction of ligand 414 with $[(\text{cod})\text{IrOAc}]_2$ – A J. Young NMR tube was loaded with ligand **414** (0.022 g, 0.0 mmol), $[(\text{cod})\text{IrOAc}]_2$ (0.027 g, 0.0376 mmol) and 1 mL of C_6D_6 . The sample was placed into a 100 °C oil bath for 36 h. One major product was observed by ^{31}P NMR spectroscopy at 140.0 ppm. The minor product (30%) at 65.2 ppm is in the range of oxidized ligand. Only broad indiscernible signals were observed in the ^1H NMR spectrum. The solution was filtered through a thin plug of silica then all solvent was removed *in vacuo* giving brown solids. While the silica filtration improved purity of the unknown product to $> 90\%$, no discernible signals could be assigned in the ^1H NMR spectrum.

Synthesis of 428 – A 50 mL culture tube was loaded with [(cod)IrCl]₂ (0.078 g, 0.116 mmol), pyridine (1 mL, 12.4 mmol), 15 mL of toluene and ligand **414** (0.141g, 0.232 mmol). The solution was heated to 120 °C for 36 h giving a light yellow solution. All solvent was removed *in vacuo* giving yellow- brown solids. Yield: 0.267 g (94%). The solids were comprised of multiple isomers of **428**.

4.4.3 X-ray crystallography details of **421** and **424**

Crystals of **421** were grown from a solution of toluene layered with pentane. A yellow plate of suitable size and quality (0.36 × 0.36 × 0.05 mm) was selected from a representative sample of crystals of the same habit using an optical microscope, and mounted onto a nylon loop. Low-temperature (150K) X-ray data were obtained on a Bruker APEXII CCD based diffractometer (Mo sealed X-ray tube, K_α = 0.71073 Å). All diffractometer manipulations, including data collection, integration, and scaling were carried out using the Bruker APEX2 software.²³² An absorption correction was applied using SADABS.²³³ The space group was determined on the basis of systematic absences and intensity statistics. The structure was solved by a dual-space algorithm in the monoclinic P2₁/c space group using SHELXT,²³⁴ and refinement was carried out with SHELXL.²³⁵ All non-hydrogen atoms were refined with anisotropic thermal parameters. Hydrogen atoms bound to carbon were placed in idealized positions and refined using a riding model. The structure was brought to convergence by weighted full-matrix least-squares refinement on |F|². A check for missed symmetry was performed with PLATON's ADDSYM facility, finding no apparent higher symmetry.²³⁶ Structure manipulations were performed with the aid of shelXle.²³⁷

Crystals of **424** were grown from a solution of toluene layered with pentane. A brown rod of suitable size and quality ($0.26 \times 0.06 \times 0.05$ mm) was selected from a representative sample of crystals of the same habit using an optical microscope, mounted onto a nylon loop, and placed in a cold stream of nitrogen (150 K). Low-temperature X-ray data were obtained on a Bruker APEXII CCD based diffractometer (Mo sealed X-ray tube, $K_{\alpha} = 0.71073 \text{ \AA}$). All diffractometer manipulations, including data collection, integration, and scaling were carried out using the Bruker APEX2 software. An absorption correction was applied using SADABS. The space group was determined on the basis of systematic absences and intensity statistics. The structure was solved by direct methods in the triclinic P-1 space group using SHELXS.²³⁸ All non-hydrogen atoms were refined with anisotropic thermal parameters. Hydrogen atoms bound to carbon were placed in idealized positions and refined using a riding model. The hydride atom bound to iridium was unobserved in the difference map due to Fourier truncation, but is included in the reported formulae. The structure was brought to convergence by weighted full-matrix least-squares refinement on $|F|^2$. A check for missed symmetry was performed with PLATON's ADDSYM facility, finding no apparent higher symmetry. Structure manipulations were performed with the aid of shelXle.

CHAPTER V
TRIFLYLOXY-SUBSTITUTED CARBORANES AS USEFUL WEAKLY
COORDINATING ANIONS[‡]

5.1 Introduction

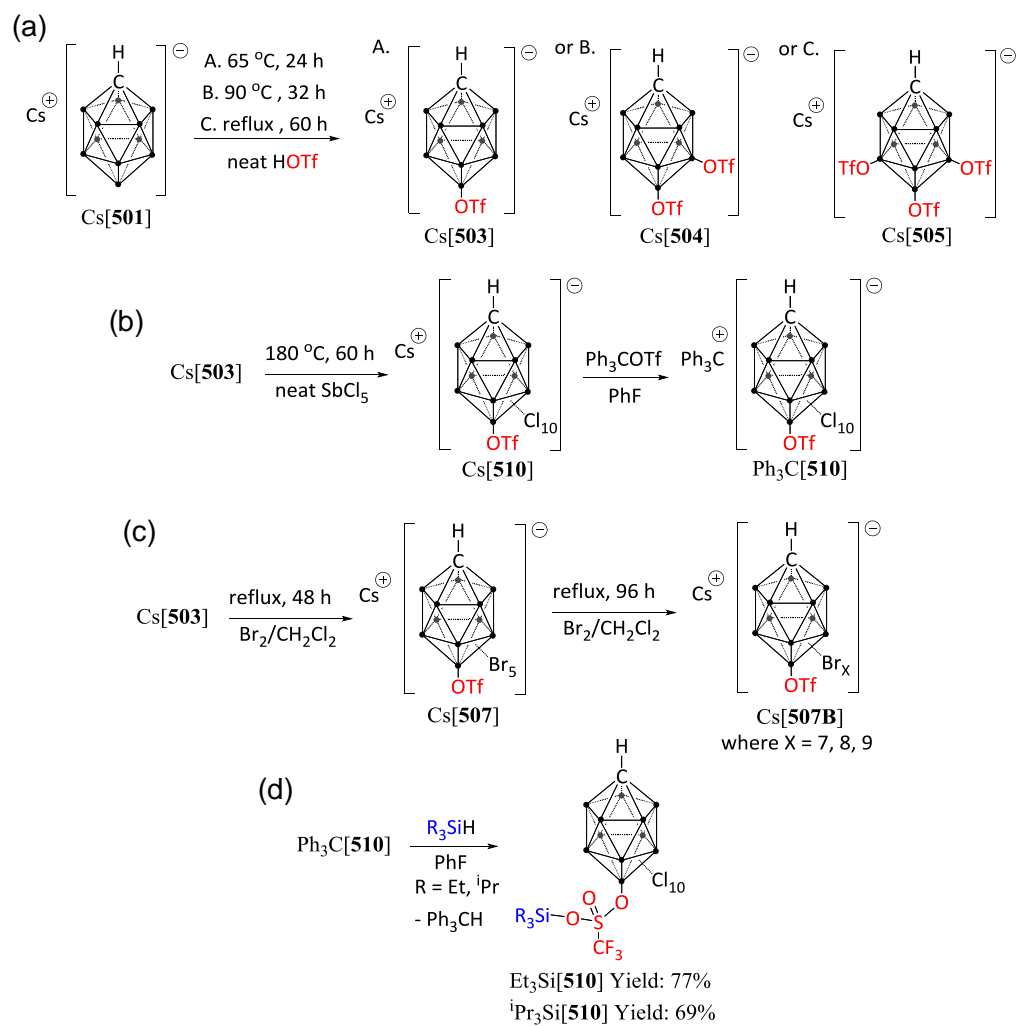
The monocarba-closo-dodecaborate anion $[\text{HCB}_{11}\text{H}_{11}]^-$ (**501**, Figure I-2) is a well-known polyhedral borane that has extraordinary thermal stability²³⁹ yet, as discussed in section 1.7, the B-H bonds of **501** are hydridic and thus susceptible to attack by electrophilic reagents. In addition, the B-H bonds of **501** have also been shown to ligate transition metal complexes.¹¹¹ A common countermeasure to improve the chemical stability of **501** is the substitution of B-H bonds with B-halogen bonds and while the lone pairs of the halogen substituents exhibit some coordinative character,¹¹¹ the benefit of improved chemical stability is well worth the transformation. Reed, Xie et al. previously described the chlorination of **501** using iodine monochloride in neat trifluoromethanesulfonic acid (“triflic acid” or just HOTf) at temperatures exceeding 200 °C for several days.^{240,241} In pursuit to establish reproducible procedures for the synthesis of $[\text{HCB}_{11}\text{Cl}_{11}]^-$ (**502**, Figure I-2) from the parent anion **501**,¹⁴² Weixing Gu of the Ozerov group at one point examined treatment of Cs[**501**] with Cl₂ gas in refluxing triflic acid. In at least one experiment, he observed production of Cs[$\text{HCB}_{11}\text{Cl}_9(\text{OTf})_2$]

[‡] Reproduced in part from “Triflyoxy-Substituted Carboranes as Useful Weakly Coordinating Anions” by Press, L. P.; McCulloch, B. J.; Gu, W.; Chen, C.; Foxman, B. M.; Ozerov, O. V. *Chem. Commun.*, **2015**, 51, 14043, Copyright [2015] by Royal Society of Chemistry.

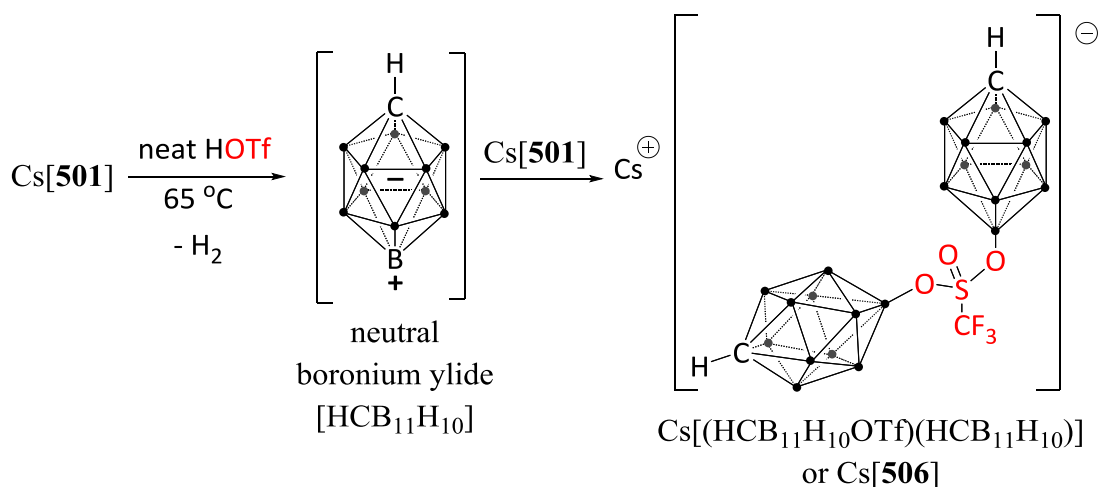
(**511**) as the dominant product with the triflyloxy (triflato) substituents apparently in the 7,12-positions as evidenced from an XRD study on a single crystal (Figure V-1, C). Formation of B-OTf groups from reactions involving triflic acid with **501** is obliquely mentioned in the literature, but rather as a nuisance. For example, methylation of **501** requires a non-nucleophilic base to consume the HOTf by-product lest it react with the B-H bonds of the carborane.^{136–141} In related polyhedral borane chemistry, syntheses of nido-6-OTf-B₁₀H₁₃, nido-6-cyclohexyl-B₁₀H₁₃, nido-5-OTf-B₁₀H₁₃, and MeNB₁₁H₅Me₅OTf have been reported.^{242,243,244,245}

5.2 Results and discussion

We became interested in exploiting OTf as a desirable substituent on the carborane cage and in investigating the behavior of the resultant anions as WCAs in silylium-catalyzed hydrodefluorination^{127–129,246} and toward highly unsaturated transition metal cations.²⁴⁷ We surmised that a B-OTf moiety would still be weakly coordinating and may bring advantages of ¹⁹F NMR spectroscopy and altered solubility. We further surmised that the installation of the OTf groups in our inadvertent synthesis of Cs[**511**] occurred prior to chlorination and set out to examine reactions of Cs[**501**] with HOTf under controlled conditions. All reactions of carborane modification reported here were carried out under dry argon atmosphere.



Scheme V-1. Synthesis of Cs[503], Cs[504], Cs[505], Cs[510], Cs[507], Cs[507B], Ph₃C[510] and R₃Si[510].



Scheme V-2. Side product Cs[506] observed by ¹⁹F NMR spectroscopy and MALDI (–) MS during mono-triflyloxylation of Cs[501] in neat HOTf at 65 °C. The compound was not isolated.

Stirring a mixture of Cs[501] in neat triflic acid (ca. 20:1 molar excess of HOTf) at 65 °C for 24 h resulted in the formation of Cs[503] (Scheme V-1), which was isolated in excellent yields and purity as judged by NMR spectroscopy and MALDI mass spectrometry. We occasionally observed Cs[504] as an impurity in the syntheses of Cs[503], and stirring a mixture of Cs[501] in neat triflic acid (ca. 20:1 molar excess of HOTf) at 90 °C for 32 h gave mostly Cs[504] with some Cs[506] and unidentified side products present. Tris-triflyloxylation to the Cs[HCB₁₁H₁₀-7,9,12-(OTf)₃] (**505**) isomer could be selectively accomplished after refluxing Cs[501] in triflic acid for 60 h (Scheme V-1). The structure was confirmed by an XRD study (Figure V-1, B) and was consistent with solution ¹¹B and ¹⁹F NMR data. During the synthesis of Cs[503] we

observed a minor amount of Cs[**506**] by MALDI(-) mass spectrometry and ^{19}F NMR spectroscopy. This compound presumably forms (Scheme V-2) when a neutral boronium ylide [$\text{HCB}_{11}\text{H}_{10}$], formed via deprotonation of [**501**] $^-$ by HOTf, complexes with Cs[**503**].

Formation of Cs[**511**] under Cl_2/HOTf suggested that the B-OTf moieties can survive harsh halogenation conditions. Indeed, thermolysis of Cs[**503**] in refluxing SbCl_5 for 60 h resulted in the predominant formation of Cs[$\text{HCB}_{11}\text{Cl}_{10}\text{OTf}$] (**510**) (Scheme V-1), by analogy with the synthesis of Cs[**502**]. Bromination of Cs[**503**] with excess Br_2 in refluxing CH_2Cl_2 led to the formation of Cs[$\text{HCB}_{11}\text{H}_5\text{Br}_5\text{OTf}$] (**507**) (Figure V-1, A). Attempts to perbrominate Cs[**503**] by stirring in refluxing $\text{Br}_2/\text{CH}_2\text{Cl}_2$ for 96 h gave mixtures of hepta-, octa- and nona-brominated mono-triflyloxy-substituted carboranes Cs[**507B**] (Scheme V-1). The outcomes of these reactions are analogous to those with a halogen in place of OTf.¹⁴²

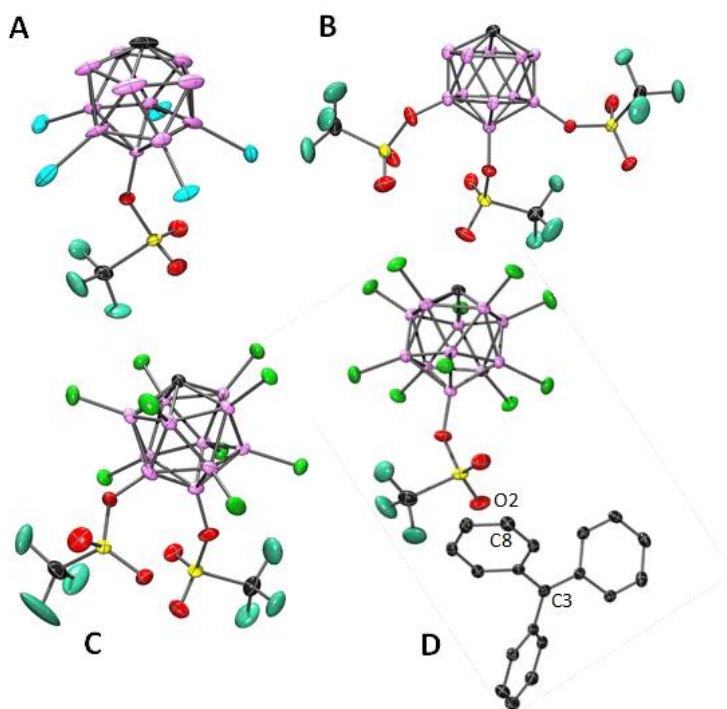


Figure V-1. POV-Ray renditions of the ORTEP drawings¹⁵⁵ of A. Cs[507], B. Cs[505], C. Cs[511] and D. Ph₃C[510] (50% probability ellipsoids) showing selected atom labeling. Omitted for clarity: hydrogen and cesium atoms for all structures, a minor component of cocrystallized Cs[HCB₁₁H₄Br₆OTf] in structure of Cs[507], disorder of one triflyloxy moiety of Cs[511]. All XRD structures were solved by Billy J. McCulloch except C. Cs[511] solved by Bruce Foxman. Anion **511** was synthesized by Weixing Gu.

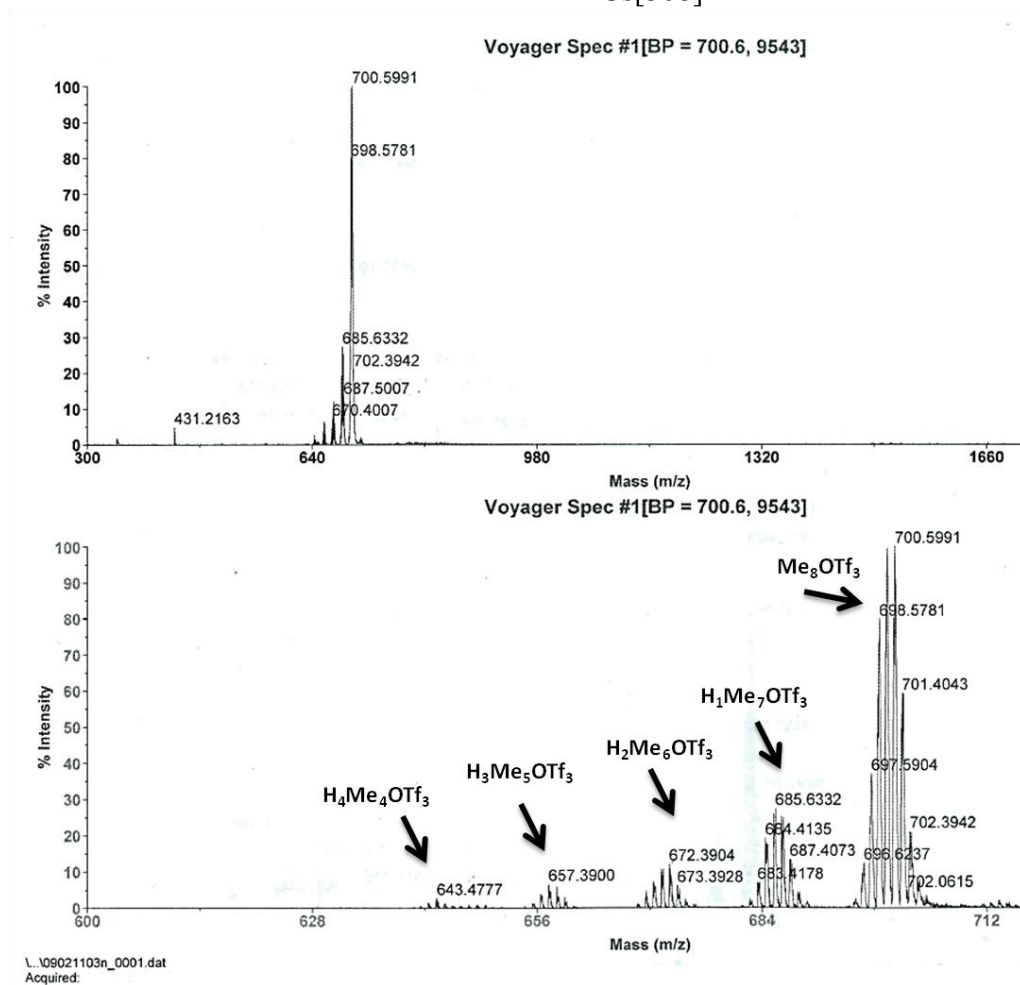
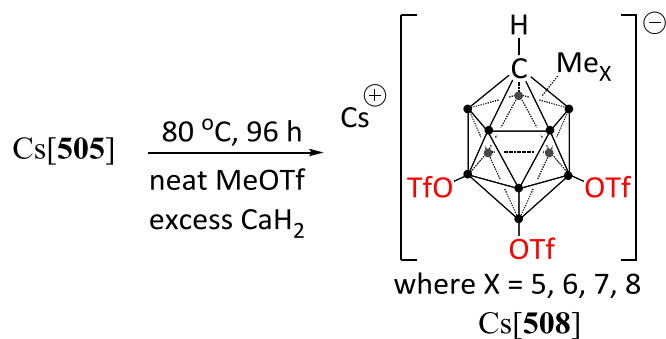


Figure V-2. Attempted permethylation of Cs[505] with neat MeOTf and excess CaH₂.

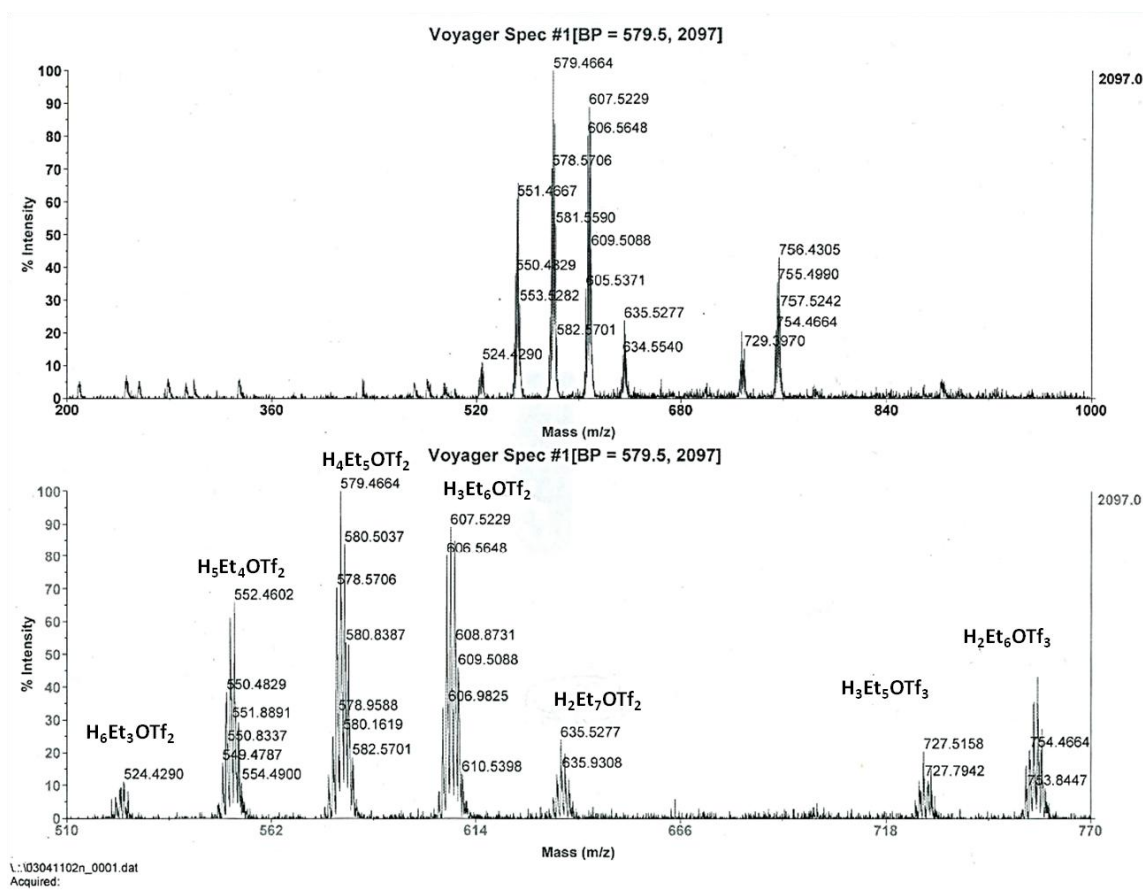
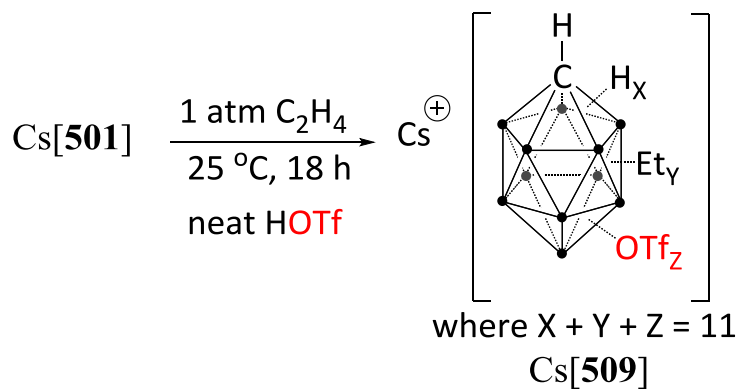


Figure V-3. Attempted ethylation of Cs[501] in neat HOTf and 1 atm of ethylene at 25 °C for 18 h.

The excellent lipophilicity of permethylated carborane derivatives¹³⁷⁻¹³⁹ inspired attempts to permethylate Cs[**505**] by stirring and refluxing in neat MeOTf with excess CaH₂. We sought to exclusively install methyl groups and thus the CaH₂ is required to consume the HOTf byproduct in order to inhibit further triflyloxy substitution. As mentioned in the beginning of this section the use of non-nucleophilic base in the alkylations of **501** as well as its derivatives has precedent in the literature¹¹¹ and other bases besides CaH₂, such as 2,6-di-*tert*-butylpyridine, have been utilized.¹³⁹ After 96 h the reaction gave mixtures of penta-, hexa-, hepta- and octa- methylated tris-triflyloxy-substituted carboranes Cs[**508**] (as observed by MALDI(-) mass spectrometry, Figure V-2) but the reaction was not optimized further. We also found that stirring a mixture of Cs[**501**] in neat triflic acid (ca. 20:1 molar excess of HOTf) in a HI-VAC[®] valve flask backfilled with 1 atm of ethylene at 25 °C for 18 h resulted in the formation of a mixture of ethyl and triflyloxy substituted carboranes Cs[**509**] (as observed by MALDI(-) mass spectrometry, Figure V-3). Cesium salts of the tris-triflyloxy and mono-triflyloxy halogen substituted anions were isolated after workup with Cs₂CO₃ followed by recrystallization. The ¹⁹F NMR resonance of Cs[**503**] ($\delta = -78.1$ ppm, CD₃CN) is sufficiently well resolved from HOTf or CsOTf (both $\delta = -79.6$ ppm, CD₃CN). Halogenation of Cs[**503**] to Cs[**510**] ($\delta = -77.0$, CD₃CN) and Cs[**507**] ($\delta = -77.1$ ppm, CD₃CN) further shifts the ¹⁹F NMR -CF₃ resonance downfield. We previously used [Ph₃C]⁺ salts of [**502**]⁻ and other carborane anions as pre-catalysts for silylium-catalyzed hydrodefluorination (HDF) of sp³ C-F bonds.^{127,128} By analogy, we proceeded to investigate the use of [**510**]⁻ as the partner anion in this reaction. Salt metathesis of

Cs[**510**] with [Ph₃C][OTf] in fluorobenzene resulted in a 95% isolated yield of Ph₃C[**510**] (Scheme V-1). A single crystal XRD study determined the B-OTf moiety does not coordinate to [Ph₃C]⁺; the closest anion-cation distance is approximately 2.74 Å (O2-C8, Figure V-1-D) excluding H atoms. The prowess of Ph₃C[**510**] in HDF of C₆F₅CF₃ and 4-FC₆H₄CF₃ was compared to that of Ph₃C[**502**]^{127,128} (Table V-1).

Table V-1. Catalytic HDF studies^a

#	substrate	$\text{Ar-CF}_3 \xrightarrow[\text{Cat. [Ph}_3\text{C][Anion]}]{\text{Et}_3\text{SiH}} \text{Ar-CH}_3 + \text{Friedel-Crafts products}$		mol% ^c	Si-F conv ^d (%)	C-F conv ^d (%)	TON ^e
		pre-cat. anion ^b					
1	C ₆ F ₅ CF ₃	[510] ⁻		0.05	< 1	< 1	0
2	C ₆ F ₅ CF ₃	[510] ⁻		0.5	20	20	40
3	C ₆ F ₅ CF ₃	[502] ⁻		0.05	69	> 97	2000
4	4-F-C ₆ H ₄ CF ₃	[510] ⁻		0.05	87	85	1700
5 ^f	4-F-C ₆ H ₄ CF ₃	[502] ⁻		0.05	95	> 97	2000

^a All entries were run at 25 °C with 0.30 mL of *o*-C₆H₄Cl₂ as co-solvent and 1.1 mL of Et₃SiH. ^b pre-catalyst is [Ph₃C][carborane], [Ph₃C]⁺ omitted for space. ^c Catalyst loading is expressed per number of C(sp³)-F bonds. ^d Si-F conversion is calculated as fraction of F from the original aliphatic CF bonds, found in the Si-F bonds of R₃SiF and R₂SiF₂ (by ¹⁹F NMR). ^e Turnover numbers (TON) are calculated based on the C-F conversion (by ¹⁹F NMR). ^f All entries were monitored after 24 h while entry 5 was monitored after 1 h.

The [**510**]⁻ anion did support HDF in both cases and gave rise to a high turnover number with the more reactive substrate 4-FC₆H₄CF₃. However, HDF catalysis with [**510**]⁻ was markedly slower. We hypothesized that the reduced rate of the HDF catalysis

was a consequence of greater coordinating ability of **[510]⁻** towards silylium cations compared to **[502]⁻** and set out to independently synthesize trialkylsilylium intermediates partnered with **[510]⁻**. Ph₃C**[510]** reacted smoothly with excess Et₃SiH or ⁱPr₃SiH to give the corresponding trialkylsilylium derivatives Et₃Si**[510]** and ⁱPr₃Si**[510]** in excellent yields (Scheme V-1). The isolated materials were free from trialkylsilane, indicating that **[510]⁻** coordinates to R₃Si⁺ more strongly than R₃SiH. Formation of trialkylsilane adducts of trialkylsilylium cations is common in related syntheses from [Ph₃C]⁺ and R₃SiH, including with the **[502]⁻** anion, and isolation of pure silylium-WCA materials can be challenging.²⁴⁸⁻²⁵⁰

The significantly downfield-shifted ¹⁹F NMR B-OTf resonances of Et₃Si**[510]** (δ = -71.9 ppm, C₆D₅Br) and ⁱPr₃Si**[510]** (δ = -70.4 ppm, C₆D₅Br) suggested coordination of R₃Si⁺ to one of the oxygens of the B-OTf group. The resultant structure is zwitterionic. The cationic portion can be viewed as a siloxy-substituted sulfoxonium or as a triflate bridging between a borenium ylide²⁵¹ and a silylium Lewis acid and is analogous to a triflate bridging two silylium groups in [(Me₃Si)₂OTf][B(C₆F₅)₄] (δ = -74.1 ppm, C₆D₆) reported by Schulz *et. al.*²⁵² and [(Et₃Si)₂OTf][HCB₁₁Cl₁₁] (**518**) (δ = -73.7 ppm, C₆D₅Br). ¹⁹F NMR analysis of the neat reaction solutions from our catalytic HDF experiments revealed a singlet at -72.3 ppm, characteristic of Et₃Si**[510]**. This was confirmed by using a solvent mixture identical to the catalytic experiments with toluene in place of C₆F₅CF₃, Et₃Si[HCB₁₁Cl₁₀OTf] prepared in situ was found to resonate at -72.3 ppm in the ¹⁹F NMR spectrum. No other OTf signals were detectable by ¹⁹F NMR spectroscopy, indicating the anion remains intact. The *para*-B signal in the ¹¹B NMR

spectrum of both silylium adducts broadened relative to the sharper para-B resonances of the cesium and trityl salts, possibly owing to rotational restrictions imposed by the attached R_3Si moieties.

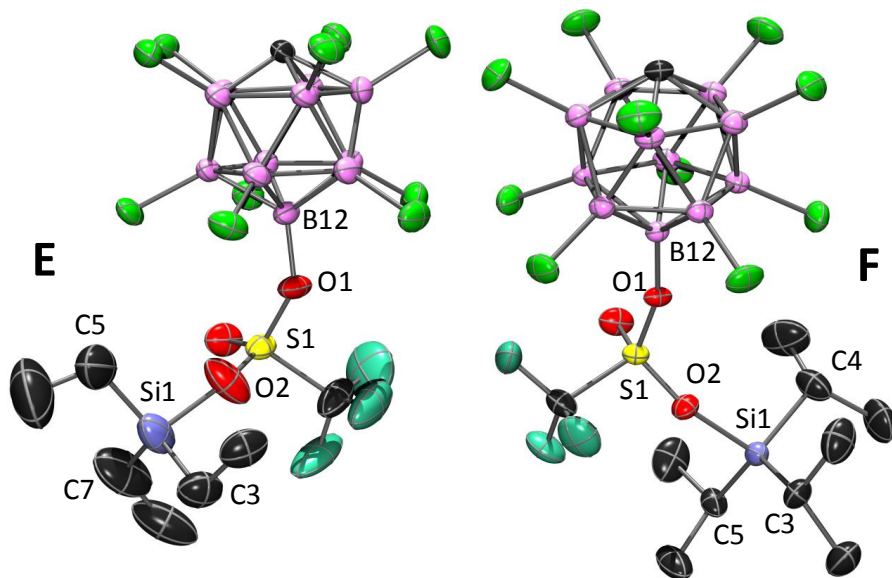
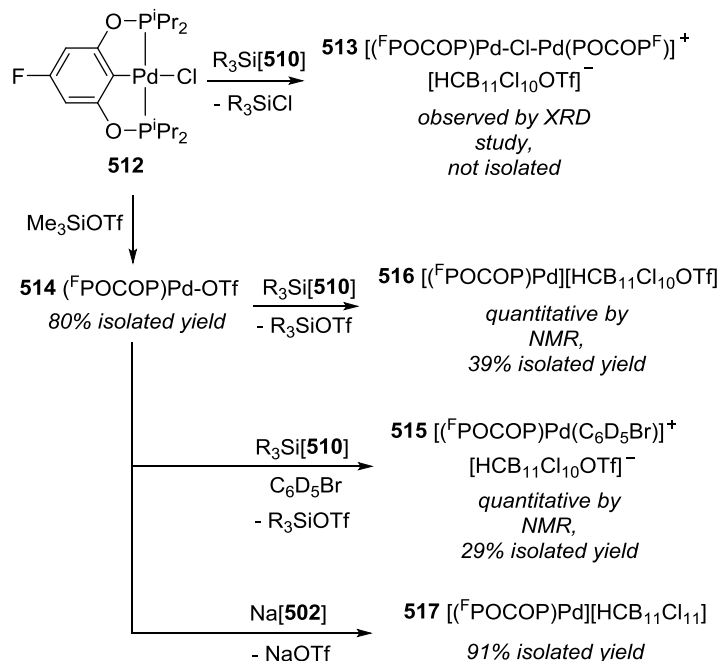


Figure V-4. POV-Ray renditions of the ORTEP¹⁵⁵ drawings of E. $Et_3Si[510]$ and F. ${}^iPr_3Si[510]$ (50% probability ellipsoids) showing selected atom labeling. Omitted for clarity: hydrogen atoms, the second independent molecule in the asymmetric unit of $Et_3Si[510]$, a molecule of fluorobenzene and disorder in the triflyloxy and triisopropylsilyl moieties in ${}^iPr_3Si[510]$. Crystallographic disorder and the presence of two independent molecules in the asymmetric unit of $Et_3Si[510]$ (E) gives rise to multiple metrics that are statistically indistinguishable. All XRD structures were solved by Billy J. McCulloch.

X-ray structural studies (Figure V-4) confirmed the proposed connectivity in $R_3Si[510]$ ($R = Et$ or iPr). The Si-O bond lengths of ca. 1.79-1.82 Å are comparable to those in $[(Me_3Si)_2OTf][B(C_6F_5)_4]$ (ca. 1.82 Å) and $[(Me_3Si)OEt_2][B(C_6F_5)_4]$ (ca. 1.78 Å),²⁵³ but longer than in tBu_3SiOTf (ca. 1.74 Å).²⁵⁴ The modest pyramidalization about the Si centers (sums of C-Si-C angles of 344-346°) is similar to the various weak R_3Si^+ adducts.^{114,128} The ^{29}Si NMR chemical shifts of $R_3Si[510]$ ($\delta = 77.7$ ppm, $R = Et$; $\delta = 74.8$ ppm, $R = ^iPr$; C_6D_5Br) are comparable to those of **518** ($\delta = 75.5$ ppm, C_6D_5Br) and $[(Me_3Si)_2OTf][B(C_6F_5)_4]$ ($\delta = 75.4$ ppm, C_6D_6), and are slightly upfield of $[Et_3Si(toluene)][B(C_6F_5)_4]$ ($\delta = 81.8$ ppm, toluene),²⁵⁵ $[Et_3Si(SO_2)][HCB_{11}Me_5Br_6]$ ($\delta = 85$ ppm, SO_2)²⁴⁸ and $[Me_3Si-H-SiMe_3][502]$ ($\delta = 85.4$ & 82.2 ppm, solid).²⁴⁸



Scheme V-3. Synthesis of palladium compounds.

To examine the affinity of $[510]^-$ towards a softer, transition-metal Lewis acid, preparation of cations derived from abstraction of X^- from $(^F\text{POCOP})\text{Pd-X}$ was targeted (Scheme V-3). Reaction of $(^F\text{POCOP})\text{Pd-Cl}$ (**512**) with $\text{Et}_3\text{Si}[510]$ in C_6D_6 resulted in a mixture with $[(^F\text{POCOP})\text{Pd-Cl-Pd}(\text{POCOP}^F)][\text{HCB}_{11}\text{Cl}_{10}\text{OTf}]$ (**513**) being the major product (Scheme V-3). It did not prove possible to reproducibly isolate **513** in an analytically pure form, but a suitable single crystal was grown for an XRD study (Figure V-5, I). Abstraction of the triflate anion from $(^F\text{POCOP})\text{Pd-OTf}$ (**514**) in $\text{C}_6\text{D}_5\text{Br}$ resulted in $[(^F\text{POCOP})\text{Pd}(\kappa^1\text{-Br-C}_6\text{D}_5\text{Br})][\text{HCB}_{11}\text{Cl}_{10}\text{OTf}]$ (**515**) (XRD evidence, Figure V-5, G) and a B-OTf ^{19}F NMR resonance ($\delta = -76.7$ ppm, C_6D_6) corresponding to free $[510]^-$. On the other hand, abstraction of triflate anion from **514** with $\text{Et}_3\text{Si}[510]$ in C_6D_6 gave complete conversion to $[(^F\text{POCOP})\text{Pd}][\text{HCB}_{11}\text{Cl}_{10}\text{OTf}]$ (**516**). An XRD study of **516** showed $[510]^-$ bound to Pd through one of the distal triflate oxygens (Figure V-5, H). The Pd-O bond distance in it (Pd1-O3, 2.2076(15) Å) is longer than that (2.158(3) Å) in the aquo complex $[(\text{POCOP})\text{Pd}(\text{OH}_2)][\text{PF}_6]$. $^{256}\text{ }^{19}\text{F}$ NMR analysis of **516** revealed a downfield triflyloxy resonance ($\delta = -74.6$ ppm, C_6D_6) and ^{11}B NMR showed a slightly broadened signal for the *para*-B of the anion similar to the silylium adducts. The $[502]^-$ anion also binds to the Pd center in the solid state structure of $[(^F\text{POCOP})\text{Pd}][\text{HCB}_{11}\text{Cl}_{11}]$ (**517**) (Figure V-5, J). Compound **517** was synthesized by reaction of $\text{Na}[502]$ with $(^F\text{POCOP})\text{PdOTf}$ (**514**). $[502]^-$ binds via one of its *meta*-Cl atoms and the corresponding Pd-Cl distance (2.5041(5) Å) is much longer than the Pd-Cl distance in $(\text{POCOP})\text{Pd-Cl}$ (2.371(18) Å)¹⁷³. Thus, although binding to the chlorine on

the carborane cage is possible, even the soft Pd center prefers to bind the B-OTf oxygen in [510]⁻.

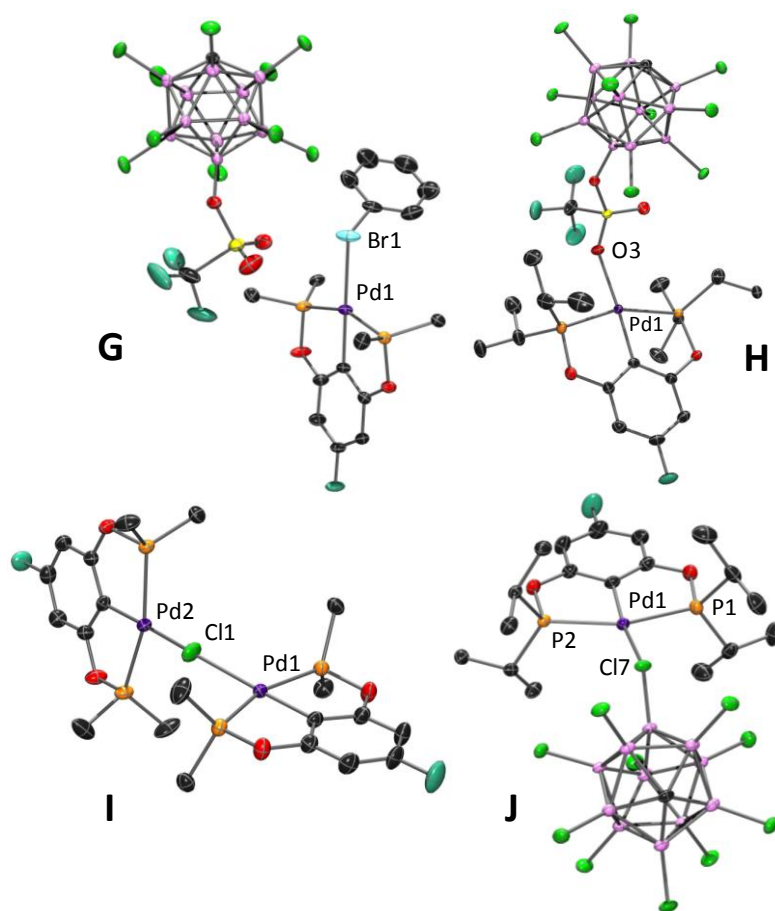


Figure V-5. POV-Ray renditions of the ORTEP drawings¹⁵⁵ of G. **515**, H. **516**, I. **513** and J. **517** (50% probability ellipsoids) showing selected atom labeling. Omitted for clarity: hydrogen atoms, isopropyl methyl carbons of **515**, isopropyl methyl carbons, a second cation within the asymmetric unit and both anions of **513**. All XRD structures were solved by Billy J. McCulloch.

5.3 Conclusion

In summary, we have developed new triflyloxy substituted carboranes for use as weakly coordinating anions. The triflyloxy moiety is chemically robust and highly useful in NMR spectroscopy studies. Catalytic HDF of benzotrifluorides was demonstrated with $\text{Ph}_3\text{C}[\mathbf{510}]$ as precatalyst. The system appears capable of supporting high turnover numbers. However, the activity was diminished compared to the catalyst based on $[\mathbf{502}]^-$ because of the stronger coordination of R_3Si^+ to the anion's distal triflyloxy oxygen, confirmed by XRD and NMR studies of independently synthesized silylium adducts. Partnering $[\mathbf{510}]^-$ with a softer Pd cationic Lewis acid also resulted in coordination via the oxygen atom, which is weak enough to be replaced by coordination to bromobenzene.

5.4 Experimental

5.4.1 General considerations

Unless specified otherwise, all manipulations were performed under an argon atmosphere using standard Schlenk or glovebox techniques. Pentane, diethyl ether, tetrahydrofuran, mesitylene and benzene were dried over sodium benzophenone ketyl, distilled or vacuum transferred and stored over molecular sieves in an Ar-filled glovebox. Methyl *tert*-butyl ether (MTBE) was used as received. 5-fluororesorcinol was prepared according to published procedure.²⁵⁷ $(\text{cod})\text{PdCl}_2$ was prepared according to published procedure.²⁵⁸ Trifluoromethanesulfonic acid (HOTf) was vacuum transferred and stored under an inert atmosphere. Trimethylsilyl trifluoromethanesulfonate (Me_3SiOTf) was vacuum transferred and stored in an argon glovebox free of donor

solvents. Trityl chloride (Ph_3CCl) was recrystallized from toluene and pentane at $-30\text{ }^\circ\text{C}$ in a glovebox free of donor solvents. Triethyl silane (Et_3SiH) and triisopropylsilane (${}^i\text{Pr}_3\text{SiH}$) were stirred over calcium hydride then vacuum transferred and stored in a glovebox free of donor solvents. Antimony pentachloride (SbCl_5) was vacuum transferred and used immediately. 4-fluorobenzotrifluoride ($4\text{-F-C}_6\text{H}_4\text{CF}_3$) and perfluorotoluene ($\text{C}_6\text{F}_5\text{CF}_3$) were stirred over calcium hydride then vacuum transferred and stored in a glovebox free of donor solvents. $[\text{Me}_3\text{NH}][\mathbf{502}]$ was prepared according to published procedures.¹⁴² All other chemicals were used as received from commercial vendors. All NMR spectra were recorded on a Varian iNova 300 spectrometer (${}^1\text{H}$ NMR 299.951 MHz, ${}^{31}\text{P}$ NMR 121.425 MHz, ${}^{13}\text{C}$ NMR 75.413 MHz), Varian Mercury 300 spectrometer (${}^{13}\text{C}$ NMR 75.426 MHz), Varian iNova 400 spectrometer (${}^1\text{H}$ NMR, 399.755 MHz; ${}^{13}\text{C}$ NMR, 100.518 MHz; ${}^{31}\text{P}$ NMR 161.92 MHz; ${}^{11}\text{B}$ NMR 128 MHz, ${}^{29}\text{Si}$ NMR 79.458 MHz), or a Varian iNova NMR 500 (${}^1\text{H}$ NMR, 499.425 MHz/ 499.683 MHz; ${}^{13}\text{C}$ NMR, 75.424 MHz/ 125.580 MHz; ${}^{31}\text{P}$ NMR, 202.171 MHz) spectrometer. Chemical shifts are reported in δ/ppm . For ${}^1\text{H}$ and ${}^{13}\text{C}\{{}^1\text{H}\}$ NMR spectra, the residual solvent peak was used as an internal reference. ${}^1\text{H}$ NMR spectra in $\text{C}_6\text{D}_5\text{Br}$ were referenced 7.30 ppm. For ${}^1\text{H}$ and ${}^{13}\text{C}\{{}^1\text{H}\}$ NMR spectra in 2:1 *o*-difluorobenzene: C_6D_6 the residual benzene solvent peak was used as an internal reference. ${}^{13}\text{C}\{{}^1\text{H}\}$ NMR spectra in $\text{C}_6\text{D}_5\text{Br}$ were referenced by setting the most downfield signal to 130.9 ppm. Et_3SiF and Et_2SiF_2 were identified by ${}^{19}\text{F}$ NMR spectroscopy by comparing to literature values.¹²⁷ ${}^{31}\text{P}$ NMR spectra were referenced externally using 85% H_3PO_4 at δ 0 ppm. ${}^{19}\text{F}$ NMR spectra were referenced externally using 1.0 M $\text{CF}_3\text{CO}_2\text{H}$ in CDCl_3 at δ -78.5

ppm. ^{29}Si NMR spectra were referenced externally to $\delta = 0$ ppm by using Me_4Si . ^{11}B NMR spectra were referenced externally to $\delta = 0$ ppm by using $\text{BF}_3 \cdot \text{Et}_2\text{O}$. Elemental analyses were performed by CALI Labs, Inc. (Parsippany, NJ). All simulated MALDI(-) spectra were generated using a publicly available isotope distribution calculator and mass spectrometry plotter.²⁵⁹

5.4.2 Synthesis of carborane and palladium compounds

Synthesis of Cs[HCB₁₁H₁₀OTf] (503)– A 100 mL Schlenk flask was loaded with Cs[501] (1.58 g, 5.75 mmol) and a PTFE coated stir bar. The flask was evacuated and charged with argon. HOTf (17.4 g, 116 mmol) was added under argon flow. Cs[501] did not immediately dissolve. The flask was placed into a 65 °C oil bath for 24 h under argon flow. All HOTf was then removed *in vacuo* using a short path distillation apparatus and a 60 °C oil bath affording a clear residue. To this residue, 3 mL of 1.0 M Cs_2CO_3 (aq) was added until slightly basic. An additional 20 mL of distilled water was added. All solvent was removed *in vacuo* giving white solid. The product was extracted with MTBE (3 × 75 mL) and filtered through Celite. All solvent was removed *in vacuo* giving a clear resin which was >95% pure Cs[503] via ^1H , ^{11}B and ^{19}F NMR spectroscopy. Isolation of Cs[503] as described was successful on multiple attempts but the protocol was sensitive to minor variations in conditions, particularly temperature. Several impurities were observed in varying amounts (5-20%) via MALDI(-) MS and ^{19}F NMR; of those impurities, only Cs[504] and Cs[506] were identified: ^{19}F NMR (470 MHz, 25 °C, CD_3CN): δ -77.7 (s, 3F), -78.0 (s, 3F). Yield of Cs[503]: 2.39 g (98%). ^1H NMR (400 MHz, 25 °C, CD_3CN): δ 2.47-0.79 (br m, 10H, B-H), 2.32 (br s, 1H, C-H).

^{11}B NMR (128 MHz, 25 °C, CD_3CN): δ 8.5 (s, 1B), -14.1 (d, 5B, $J_{\text{B-H}} = 145$ Hz), -17.8 (d, 5B, $J_{\text{B-H}} = 155$ Hz). $^{13}\text{C}\{^1\text{H}\}$ NMR (101 MHz, 25 °C, CD_3CN): δ 119.3 (q, $J_{\text{C-F}} = 316$ Hz, CF_3), 42.6 (br s, 1C, C-H). ^{19}F NMR (470 MHz, 25 °C, CD_3CN): δ -78.1 (s, 3F).

Synthesis of Cs[HCB₁₁Cl₁₀OTf] (510) – A 250 mL Schlenk flask containing Cs[503] (2.39 g, 5.62 mmol) and a PTFE coated stir bar was charged with freshly distilled SbCl_5 (50 mL, 391 mmol) via glass volumetric pipette under argon flow. The flask was fitted with a reflux condenser and placed into a 180 °C oil bath for 60 h under argon flow. The reaction turned dark brown after several hours of heating. The SbCl_5 was then removed *in vacuo* using a short path distillation apparatus giving a brown residue. To this residue, 3 mL of 1.0 M Cs_2CO_3 (aq) was added until slightly basic. An additional 20 mL of distilled water was added. The mixture was refluxed for 4 h giving cream colored slurry. All solvent was removed *in vacuo* giving a cream colored solid. The product was extracted with MTBE (3 × 150 mL) and filtered through Celite. All solvent was removed *in vacuo* giving a white yellow solid. ^1H and ^{19}F NMR analysis corroborated by MALDI(-) MS revealed the white solid to be 87% pure Cs[510]. The product was purified via recrystallization from boiling water as described below. The solids were loaded into a Schlenk flask with 30 mL of distilled water. The water was brought to a boil and filtered hot (frit and receiving flask were taken out of a 180 °C oven and used immediately). The solvent became yellow and upon cooling a white crystalline solid precipitated out of solution. The solvent was decanted and the solids were washed with 20 mL of distilled water. The recrystallization process was repeated a second time. Residual solvent was removed *in vacuo* at 170 °C for 24 h giving a white

crystalline solid which was >95% pure Cs[**510**] via ^1H , ^{11}B and ^{19}F NMR spectroscopy. Yield 1.98 g (46%). ^1H NMR (500 MHz, 25 °C, CD_3CN): δ 4.16 (br s, 1H, C-H). ^{11}B NMR (128 MHz, 25 °C, CD_3CN): δ -0.40 (s, 1B, *para*-B), -10.9 (s, 5B, *meta*-B), -13.0 (s, 5B, *ortho*-B). $^{13}\text{C}\{^1\text{H}\}$ NMR (101 MHz, 25 °C, CD_3CN): δ 119.2 (q, $J_{\text{C-F}} = 316$ Hz, 1C, CF_3), 46.4 (br s, 1C, C-H). ^{19}F NMR (470 MHz, 25 °C, CD_3CN): δ -77.0 (s, 3F). Anal. Calcd. for Cs[**510**]: C, 3.13; H, 0.13, B, 15.48. Found: C, 3.40 ; H, 0.20, B, 15.06.

Attempt at the synthesis of Cs[HCB₁₁H₉(OTf)₂] (504) – A 25 mL Schlenk flask was loaded with Cs[**501**] (0.105 g, 0.38 mmol)) and a PTFE coated stir bar. The flask was evacuated and charged with argon. HOTf (1.8 g, 12 mmol) was added under argon flow. Cs[**501**] did not immediately dissolve. The flask was placed into a 90 °C oil bath for 32 h under argon flow. An aliquot of the solution was taken and diluted with acetonitrile then the resultant solution was analyzed via MALDI (-) MS. Cs[**504**] was observed as the major product but minor amounts of Cs[**506**] were observed as well as multiple unidentified compounds.

Reaction of Cs[HCB₁₁H₈(OTf)₃] (508) with neat MeOTf in the presence of excess CaH₂ - A 25 mL Schlenk flask was loaded with Cs[**505**] (0.135 g, 0.186 mmol)) and a PTFE coated stir bar. The flask was evacuated and charged with argon. MeOTf (6.0 g, 37 mmol) was added under argon flow. CaH₂ (1.2 g, 29 mmol), freshly powdered via mortar and pestle, was added under argon flow. A condenser was attached and the flask was placed into a 110 °C oil bath for 96 h under argon flow. An aliquot of the solution was taken and diluted with acetonitrile then the resultant solution was analyzed via MALDI (-) MS. A mixture of penta-, hexa-, hepta-, and octa- methylated tris-

triflyloxy substituted carborane products were observed with octa-methyl tris-triflyloxy carborane was the major product (see Figure 5-2)

Reaction of Cs[501] with neat HOTf and 1 atm of ethylene gas - A 500 mL HI-VAC[®] valve flask was loaded with Cs[501] (0.140 g, 0.51 mmol) and a PTFE coated stir bar. The flask was evacuated, charged with argon and HOTf (2.2 g, 15 mmol) was added under argon flow. Cs[501] did not immediately dissolve. The flask was degassed and charged with 1 atm of ethylene. The reaction was stirred for 18 h at ambient temperature giving a yellow liquid. An aliquot of the solution was taken and diluted with acetonitrile then the resultant solution was analyzed via MALDI (-) MS. Various ethyl and triflyloxy substituted carborane products were observed (See Figure 5-3).

Synthesis of Cs[HCB₁₁Cl₉(OTf)₂] (511) - Anion **511** was synthesized by Weixing Gu. A 50 mL three-neck flask was loaded with Cs[501] (0.45 g, 1.63 mmol), a PTFE coated stir bar and HOTf (8 mL, 90.4 mmol). The flask was equipped with a water-cooled condenser and hose adapter connected via Tygon tubing to an inverted filter funnel submerged in a solution of NaOH and Na₂SO₃. Chlorine gas was delivered to the reaction flask from a lecture bottle of chlorine gas with a Monel valve through Tygon tubing and a bubbler with concentrated HCl solution. The third neck was equipped with a glass stopper. Chlorine gas was slowly added into the flask and the reaction mixture was heated to 160 °C for 50 h. The flow of chlorine gas was ceased and reaction mixture was allowed to cool down to room temperature. All volatiles were removed *in vacuo* and the resulting white powder was washed with hexanes then dried *in vacuo* for 3 h. The products were dissolved in acetonitrile and identified as Cs[511] on

the basis of ^{19}F NMR spectroscopy, and MALDI(-) MS. ^{19}F NMR (470 MHz, 25 °C, CD_3CN): δ -76.6 (s, 3F), -76.7 (s, 3F).

Synthesis of Cs[HCB₁₁H₅Br₅OTf] (507) - A 50 mL Schlenk flask was loaded with Cs[501] (0.283 g, 1.03 mmol) and a PTFE coated stir bar. The flask was evacuated and charged with argon. HOTf (3.40 g, 22.6 mmol) was added under argon flow. The flask was placed into a 65 °C oil bath for 24 hours under argon flow. The HOTf was then removed *in vacuo* using a short path distillation apparatus and a 60 °C oil bath affording a clear residue. To this residue, 3 mL of 1.0 M Cs_2CO_3 (aq) was added until slightly basic. All solvent was removed *in vacuo* giving white solid. The product was extracted with MTBE (3 × 25 mL) and filtered through Celite. All solvent was removed *in vacuo* giving Cs[503] as a clear resin. Under argon flow the flask was charged with 20 mL of dichloromethane followed by Br_2 (9 mL, 175 mmol). The flask was fitted with a reflux condenser cooled to 0 °C and placed into a 60 °C oil bath for 48 h under argon flow. All volatiles were removed *in vacuo* giving tan powder. This powder was dissolved in a minimum of boiling water and filtered hot. Upon cooling tan solid precipitated from solution. This was washed with water and dried *in vacuo* at 170 °C. An X-ray quality crystal was obtained by slow evaporation of a dichloromethane solution of Cs[507]. MALDI(-) MS and ^{19}F NMR revealed approximately 5% hexa-brominated product Cs[HCB₁₁H₄Br₆OTf]. The compound was purified further by dissolving Cs[507] in MTBE/toluene and layering with hexane affording colorless crystals. Yield: 521 mg (62%). ^1H NMR (400 MHz, 25 °C, CD_3CN): δ 2.82 (br s, 1H, C-H), 2.43-1.60 (br m, 5H, B-H). ^{11}B NMR (128 MHz, 25 °C, CD_3CN): δ 3.26 (s, 1B), -11.4 (s, 5B), -20.6 (d,

$J_{B-H} = 166$ Hz, 5B). $^{13}\text{C}\{^1\text{H}\}$ NMR (101 MHz, 25 °C, CD_3CN): δ 119.4 (q, $J_{C-F} = 320$ Hz, 1C, CF_3), 40.2 (br s, 1C, C-H). ^{19}F NMR (376 MHz, 25 °C, CD_3CN): -77.1 (s, 3F). Anal. Calcd. for $\text{Cs}[\mathbf{507}]$: C, 2.94; H, 0.74, B, 14.53. Found: C, 3.16 ; H, 0.99, B, 14.28.

Synthesis of $\text{Cs}[\text{HCB}_{11}\text{H}_8(\text{OTf})_3]$ (505**)** - A 50 mL Schlenk flask was loaded with $\text{Cs}[\mathbf{501}]$ (0.326 g, 1.19 mmol) and a PTFE coated stir bar. The flask was evacuated and charged with argon. HOTf (5.88 g, 39.2 mmol) was added under argon flow. The flask was fitted with a reflux condenser and placed into a 170 °C oil bath for 60 hours under argon flow. The HOTf was removed *in vacuo* using a short path distillation apparatus affording a tan residue. To this residue, 3 mL of 1.0 M Cs_2CO_3 (aq) was added until slightly basic. The tan residue did not fully dissolve. An additional 20 mL of distilled water was added and the mixture was brought to a boil at which point the tan residue dissolved. Upon cooling a white solid precipitated from solution. The solvent was decanted and the white solid was washed with 20 mL of water. All solvent was removed *in vacuo* giving a white solid. ^1H ^{11}B , and ^{19}F NMR corroborated by MALDI(-) MS revealed the white solid to be >95% pure $\text{Cs}[\mathbf{505}]$. The compound was further purified via recrystallization from acetone and water. Yield: 772 mg (90 %). ^1H NMR (400 MHz, 25 °C, CD_3CN): δ 2.57 (br s, 1H, C-H), 2.72-0.83 (br m, 8H, B-H). $^{11}\text{B}\{^1\text{H}\}$ NMR (128 MHz, 25 °C, CD_3CN): δ 4.0 (s, 1B), -0.28 (s, 2B), -16.05 (s, 1B), -16.6 (s, 2B), -21.3 (s, 2B), -23.1 (s, 2B), -23.8 (s, 1B). $^{13}\text{C}\{^1\text{H}\}$ NMR (101 MHz, 25 °C, CD_3CN): δ 119.4 (q, $J_{C-F} = 318$ Hz, 2C, CF_3), 119.3 (q, $J_{C-F} = 320$ Hz, 1C, CF_3), 39.5 (s, 1C, C-H). ^{19}F NMR (376 MHz, 25 °C, CD_3CN): -77.43 (s, 6F), -77.75 (s, 3F). Anal. Calcd. for $\text{Cs}[\mathbf{505}]$: C, 6.67; H, 1.26, B, 16.51. Found: C, 6.93 ; H, 0.91, B, 16.29.

Synthesis of Ph₃C[OTf] – A 50 mL Schlenk flask was loaded with Ph₃CCl (0.524 g, 1.88 mmol) and dissolved in 6 mL of benzene. Via syringe, Me₃SiOTf (1.22 mL, 6.76 mmol) was added giving a bright orange solution. The reaction was stirred for 2 h at room temperature and solvent was removed *in vacuo* giving orange powder. The orange powder was washed with pentane (2 × 15 mL). All solvent was decanted and the solids were dried *in vacuo*. Yield: 715 mg (97 %). ¹H NMR (500 MHz, 25 °C, CDCl₃): δ 8.24 (apparent t, *J*_{H-H} = 7.3 Hz, 3H, [Ph₃C]⁺), 7.89 (apparent t, *J*_{H-H} = 7.4 Hz, 6H, [Ph₃C]⁺), 7.70 (d, *J*_{H-H} = 7.7 Hz, 6H, [Ph₃C]⁺). ¹³C{¹H} NMR (101 MHz, 25 °C, CDCl₃): δ 210.7 (s, 1C, [Ph₃C]⁺), 143.4 (s, [Ph₃C]⁺), 142.7 (s, [Ph₃C]⁺), 139.9 (s, [Ph₃C]⁺), 130.7 (s, [Ph₃C]⁺), 120.7 (q, *J*_{C-F} = 321 Hz, 1C, CF₃), . ¹⁹F NMR (376 MHz, 25 °C, CDCl₃): δ –79.0 (s, 3F).

Previously, **Ph₃C[OTf]** was synthesized by Martin and co-workers^{260,261} from Ph₃CCl and trifluoroacetyl triflate and by Bosnich and co-workers²⁶² from Ph₃CCl and AgOTf. In the latter work, no yield was reported and the purity of **Ph₃C[OTf]** was only ~80% due to Ph₃COH formation. Literature NMR data follows: ¹H NMR (CF₃CO₂H) δ 8.26 (tt, *J* = 7.5 and 1 Hz, 3H), 7.90 (tt, *J* = 7.5 and 1 Hz, 6H), 7.78 (tt, *J* = 7.5 and 1 Hz, 6H); ¹H NMR (CH₃NO₂) δ 7.87 (m, 12), 8.33 (m, 3H); ¹⁹F NMR (CH₃NO₂) δ –78.1 (s); ¹H NMR (CD₂Cl₂) δ 8.30 (br s, 3H), 7.92 (br s, 6H), 7.70 (br s, 6H).

Synthesis of Ph₃C[510] – A 50 mL Schlenk flask was loaded with Cs[510] (0.195 g, 0.254 mmol) and Ph₃C[OTf] (0.0998 g, 0.254 mmol). 8 mL of fluorobenzene was added and the mixture was stirred for 12 h. The mixture was filtered and solvent removed *in vacuo* giving yellow residue. Washing with pentane (3 × 10 mL), decanting

and removing all volatiles *in vacuo* gave a bright yellow powder. Surprisingly Ph₃C[510] was poorly soluble in common solvents such as CD₃CN and CDCl₃ giving broad indiscernible resonances in the ¹H NMR spectrum. The compound had excellent solubility in C₆D₅Br. Yield: 212 mg (95 %). ¹H NMR (500 MHz, 25 °C, C₆D₅Br): δ 7.76 (apparent t, *J*_{H-H} = 7.2 Hz, 3H, [Ph₃C]⁺), 7.43 (apparent t, *J*_{H-H} = 7.8 Hz, 6H, [Ph₃C]⁺), 7.15 (d, *J*_{H-H} = 7.5 Hz, 6H, [Ph₃C]⁺), 2.78 (br s, 1H, C-H). ¹¹B NMR (128 MHz, 25 °C, C₆D₅Br): δ -0.98 (s, 1B), -11.43 (s, 5B), -13.77 (s, 5B). ¹³C{¹H} NMR (101 MHz, 25 °C, C₆D₅Br): δ 209.2 (s, 1C, [Ph₃C]⁺), 143.0 (s, [Ph₃C]⁺), 142.2 (s, [Ph₃C]⁺), 139.1 (s, [Ph₃C]⁺), 130.2 (s, [Ph₃C]⁺), 118.5 (q, *J*_{C-F} = 318 Hz, 1C, CF₃), 45.8 (br s, 1C, [HCB₁₁Cl₁₀OTf]⁻). ¹⁹F NMR (470 MHz, 25 °C, C₆D₅Br): δ -76.38. Anal. Calcd. for Ph₃C[510]: C, 28.70; H, 1.84, B, 13.53. Found: C, 28.67 ; H, 1.72, B, 13.27.

Synthesis of Na[502] – A 250 mL Schlenk flask was loaded with Me₃NH[502] (1.0927 g, 1.877 mmol), Na₂CO₃ (0.263 g, 1.877 mmol), 100 mL of MeOH, 20 mL of H₂O and a PTFE coated stirbar. The mixture was heated to reflux for 2 h followed by removal of all solvent *in vacuo*. The resultant off white solid was dried *in vacuo* over night at 200 °C then brought into a glovebox. The solid was suspended in fluorobenzene and filtered. The frit was washed with additional fluorobenzene until the entire product was washed through. All solvent was removed *in vacuo* and the resultant white solid was dried for 12 h at 200 °C. The product was used without further purification and found to be >95% pure Na[502] via ¹H and ¹¹B NMR spectroscopy. Yield: 0.620 g (61%). ¹H NMR (300 MHz, 25 °C, CD₃CN): δ 4.10 (br s, 1H, C-H).

Synthesis of Ph₃C[502]¹¹⁵ – A 50 mL culture tube was loaded with Na[502] (0.540 g, 0.991 mmol), Ph₃CCl (0.278 g, 0.997 mmol), and 15 mL of fluorobenzene. The mixture was stirred for 6 h then filtered and all solvent was removed *in vacuo* giving a bright yellow solid. This was washed with pentane (2 × 20 mL) and dried *in vacuo*. The product was used without further purification and found to be >95% pure Ph₃C[502] via ¹H and ¹¹B NMR spectroscopy. Yield: 0.654 g (86%). ¹H NMR (400 MHz, 25 °C, C₆D₅Br): δ 7.72 (br s, 3H, [Ph₃C]⁺), 7.41 (br s, 6H, [Ph₃C]⁺), 7.13 (br s, 6H, [Ph₃C]⁺), 2.84 (br s, 1H, [HCB₁₁Cl₁₁][−]). ¹¹B NMR (128 MHz, 25 °C, C₆D₅Br): δ −2.58 (br s, 1B), −10.18 (br s, 5B), −13.39 (br s, 5B). ¹³C{¹H} NMR (101 MHz, 25 °C, C₆D₅Br): δ 209.1 (br s, 1C, [Ph₃C]⁺), 142.9 (s, [Ph₃C]⁺), 142.3 (s, [Ph₃C]⁺), 139.2 (s, [Ph₃C]⁺), 130.2 (s, [Ph₃C]⁺), 46.7 (br s, 1C, [HCB₁₁Cl₁₁][−]).

Comparison of Ph₃C[510] with other [Ph₃C][WCA] NMR signals – Three J. Young NMR tubes were loaded with Ph₃C[510] (0.062 g, 0.071 mmol), Ph₃C[502] (0.058 g, 0.076 mmol), and Ph₃C[B(C₆F₅)₄] (0.079 g, 0.086 mmol), respectively. 800 μL of C₆D₅Br was added to each NMR tube giving intense yellow orange solutions. Each sample was analyzed by ¹H, ¹³C{¹H} and ¹⁹F NMR spectroscopy (Figure V-6, Table V-2 and Table V-3). Surprisingly, compound Ph₃C[OTf] was poorly soluble in C₆D₅Br and no useful NMR signals could be obtained.

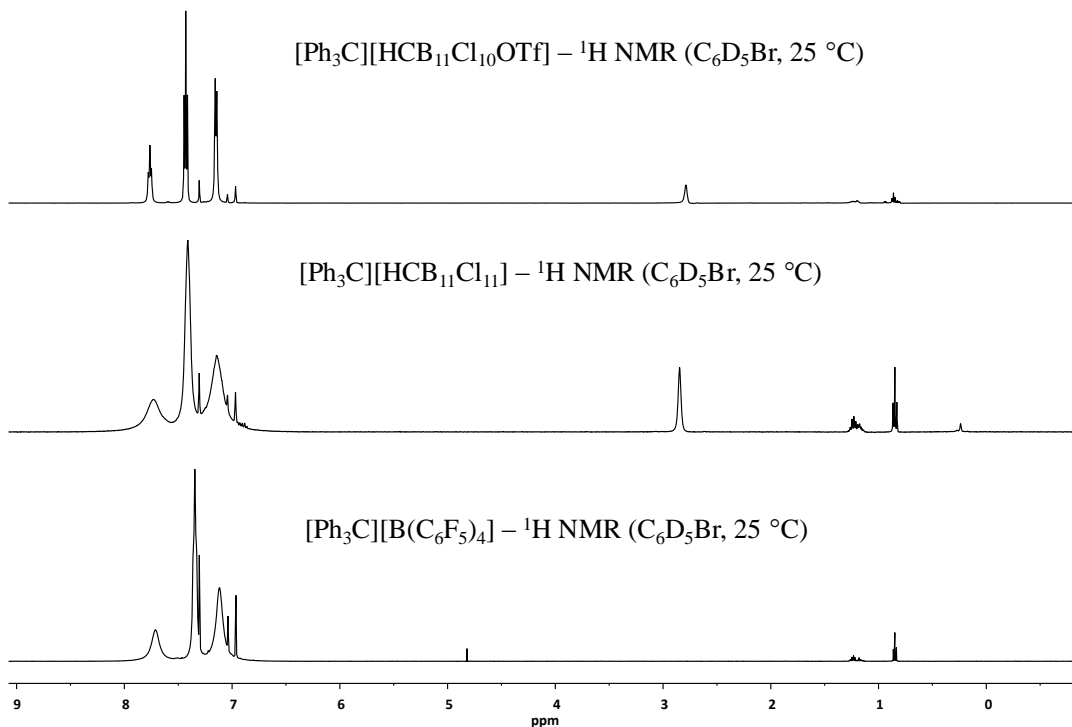


Figure V-6. Comparison of ^1H NMR spectra of various [trityl][WCA] in $\text{C}_6\text{D}_5\text{Br}$.

Table V-2. Comparison of ^1H NMR resonances of various $\text{Ph}_3\text{C}[\text{WCA}]$ salts in $\text{C}_6\text{D}_5\text{Br}$

$[\text{Ph}_3\text{C}][\text{WCA}]$	<i>ortho</i> C-H (δ , m)	<i>meta</i> C-H (δ , m) ^a	<i>para</i> C-H (δ , m) ^a	carborane C-H (δ , m)
$\text{Ph}_3\text{C}[\mathbf{510}]$	7.14, br d	7.43, br at	7.76, br at	2.78, br s
$\text{Ph}_3\text{C}[\mathbf{502}]$	7.13, br s	7.41, br s	7.72, br s	2.84, br s
$\text{Ph}_3\text{C}[\text{B}(\text{C}_6\text{F}_5)_4]$	7.11, br s	7.34, br at	7.71, br s	n/a

a. at = apparent triplet

Table V-3. Comparison of $^{13}\text{C}\{^1\text{H}\}$ NMR resonances of various $\text{Ph}_3\text{C}[\text{WCA}]$ salts in $\text{C}_6\text{D}_5\text{Br}$

$\text{Ph}_3\text{C}[\text{WCA}]$	Ph_3C^+ (δ , m)
$\text{Ph}_3\text{C}[\mathbf{510}]$	209.2, s
$\text{Ph}_3\text{C}[\mathbf{502}]$	209.1, br s
$\text{Ph}_3\text{C}[\text{B}(\text{C}_6\text{F}_5)_4]$	209.4, s

Synthesis of $\text{Et}_3\text{Si}[\mathbf{510}]$ – A 10 mL PTFE capped glass vial was charged with $\text{Ph}_3\text{C}[\mathbf{510}]$ (0.216 g, 0.246 mmol), fluorobenzene (1 mL) and triethylsilane (1.5 g, 9.3 mmol) resulting in a colorless solution. All solvent was removed *in vacuo* and the white solid was washed with pentane, dried *in vacuo*, collected and stored in a $-30\text{ }^\circ\text{C}$ glovebox freezer. The white solid was determined to be >95% pure $\text{Et}_3\text{Si}[\mathbf{510}]$ via ^1H , ^{11}B , $^{13}\text{C}\{^1\text{H}\}$, ^{19}F and $^{29}\text{Si}\{^1\text{H}\}$ NMR. Yield: 143 mg (77%). An X-Ray quality crystal was grown by charging a 10 mL PTFE capped glass vial with $\text{Ph}_3\text{C}[\mathbf{510}]$ and triethylsilane in an analogous fashion as described above then adding fluorobenzene until all solids dissolved. Aliquots of the solution were layered with additional fluorobenzene placed into a pentane chamber affording clear colorless block crystals. ^1H NMR (500 MHz, $25\text{ }^\circ\text{C}$, $\text{C}_6\text{D}_5\text{Br}$): δ 2.70 (br s, 1H, C-H), 0.76-0.71 (m, 15H, Et_3Si). ^{11}B NMR (128 MHz, $25\text{ }^\circ\text{C}$, $\text{C}_6\text{D}_5\text{Br}$): δ -0.26 (br s, 1B), -12.23 (s, 5B), -13.78 (s, 5B). $^{13}\text{C}\{^1\text{H}\}$ NMR (126 MHz, $25\text{ }^\circ\text{C}$, $\text{C}_6\text{D}_5\text{Br}$): δ 117.6 (q, $J_{\text{C-F}} = 324\text{ Hz}$, 1C, CF_3), 48.2 (br s, 1C, $[\text{HCB}_{11}\text{Cl}_{10}(\text{OSO}_2\text{CF}_3)]^-$), 5.21 (s, 3C, Et_3Si), 5.18 (s, 3C, Et_3Si). ^{19}F NMR (470

MHz, 25 °C, C₆D₅Br): δ -71.9 (s, 3F). ²⁹Si NMR (79.5 MHz, 25 °C, C₆D₅Br): δ 77.7 (s, 1Si).

Synthesis of ¹Pr₃Si[510] - A 10 mL PTFE capped glass vial was charged with Ph₃C[510] (0.141 g, 0.160 mmol), fluorobenzene (1 mL) and triisopropylsilane (1.6 g, 10.1 mmol) resulting in a colorless solution. All solvent was removed *in vacuo* and the white solid was washed with pentane, dried *in vacuo*, collected and stored in a -30 °C glovebox freezer. The white solid was determined to be >95% pure ¹Pr₃Si[510] via ¹H, ¹¹B ¹³C{¹H}, ¹⁹F and ²⁹Si{¹H} NMR. Yield: 0.088 g (69%). An X-Ray quality crystal was grown by charging a 10 mL PTFE capped glass vial with Ph₃C[510] and triisopropylsilane as described above then adding fluorobenzene until all solids dissolved. Aliquots of the solution were then layered with additional fluorobenzene and placed into a pentane chamber affording colorless needle crystals. ¹H NMR (500 MHz, 25 °C, C₆D₅Br): δ 2.71 (br s, 1H, [HCB₁₁Cl₁₀OTf]⁻), 1.21-1.12 (m, 3H, Si(CH(CH₃)₂)₃), 0.87-0.85 (m, 18H, Si(CH(CH₃)₂)₃). ¹¹B NMR (128 MHz, 25 °C, C₆D₅Br): δ -0.53 (br s, 1B), -12.26 (s, 5H), -13.75 (s, 5H). ¹³C{¹H} NMR (126 MHz, 25 °C, C₆D₅Br): δ -OTf carbon not observed, 48.2 (br s, 1C, [HCB₁₁Cl₁₀OTf]⁻), 16.3 (s, Si(CH(CH₃)₂)₃), 16.2 (s, Si(CH(CH₃)₂)₃), 12.9 (s, Si(CH(CH₃)₂)₃). ¹⁹F NMR (470 MHz, 25 °C, C₆D₅Br): δ -70.4 (s, 3F). ²⁹Si NMR (79.5 MHz, 25 °C, C₆D₅Br): δ 74.8 (s).

Synthesis of (*p*-F-P⁰C⁰PⁱPr)Pd(Cl) (512) - A Hi-Vac valve round bottom flask was loaded with a stirbar, 5-fluororesorcinol (0.630 g, 4.92 mmol), NEt₃ (2.83 mL, 20.3 mmol), ClPⁱPr₂ (1.62 mL, 10.2 mmol) and 50 mL of THF. This was brought out of the glovebox and heated to 80 °C for 1 h and NEt₃HCl was observed. The flask was brought

back into the glovebox and the flask was loaded with (cod)PdCl₂ (1.48 g, 5.18 mmol). The reaction mixture was heated to 80 °C for 24 h and then brought back in a glovebox. The mixture was filtered through a plug of silica and the resultant light yellow solution was concentrated, layered with pentane and placed in a -30 °C freezer overnight. Solvent was decanted, the white-yellow precipitate was washed with pentane and the solids were dried *in vacuo*. Yield: 1.28 g (52%). ¹H NMR (500 MHz, 25 °C, C₆D₆): δ 6.43 (d, *J*_{H-F} = 9.7 Hz 2H, Ar-*H*), 2.13-2.04 (m, 4H, P-CH(CH₃)₂), 1.24 (dvt, *J*_{H-H} = 9.5 Hz, *J*_{P-H} = 8.5 Hz, 12H, P-CH(CH₃)₂), 1.03 (dvt, *J*_{H-H} = 8.5 Hz, *J*_{P-H} = 7.0 Hz, 12H, P-CH(CH₃)₂). ¹³C{¹H} NMR (101 MHz, 25 °C, C₆D₆): δ 166.4 (dt, *J*_{C-F} = 14.4 Hz, *J*_{C-P} = 7.0 Hz, 2C, Ar C-OPR₂), 163.9 (d, *J*_{C-F} = 241 Hz, 1C, Ar *p*-C-F), 125.3 (m, *J* = 3.1 Hz, 1C, Ar C-Pd), 94.9 (dt, *J*_{C-F} = 26.1 Hz, *J*_{C-P} = 7.6 Hz, 2C, Ar C-H), 29.0 (vt, *J*_{C-P} = 11.3 Hz, P-CH(CH₃)₂, 4C), 17.2 (vt, *J*_{C-P} = 3.7 Hz, 4C, P-CH(CH₃)₂), 16.6 (s, 4C, P-CH(CH₃)₂). ¹⁹F NMR (376 MHz, 25 °C, C₆D₆): δ -114.8 (t, *J*_{H-F} = 9.7 Hz, 1F, Ar *p*-F). ³¹P{¹H} NMR (202 MHz, 25 °C, C₆D₆): δ 190.2 (s). Anal. Calcd. for **512**: C, 43.13; H, 6.03. Found: C, 43.15 ; H, 6.15.

Synthesis of [(*p*-F-P^OC^OP^{iPr})₂Pd₂(Cl)] [HCB₁₁Cl₁₀OTf] (513**) *in situ* – A J. Young tube was loaded with **512** (0.0133 g, 0.0265 mmol) and C₆D₆. Et₃Si[**510**] (0.020 g, 0.0266 mmol) was added. The J. Young tube was sealed and shaken. Immediately white precipitate began to form and via ¹H NMR analysis, Et₃SiCl was observed. The white precipitate was collected on a frit, washed with benzene and pentane, then allowed to dry. The white precipitate was dissolved in fluorobenzene and aliquots of the solution**

were placed into vials then layered with fluorobenzene and put into a pentane chamber. X-Ray quality crystals of **513** formed after several days.

Synthesis of (*p*-F-P^OC^OP^{iPr})Pd(OTf) (514**)** – A 50 mL Schlenk flask was loaded with **512** (0.758 g, 1.51 mmol) and 10 mL of benzene. Via syringe, Me₃SiOTf (2.75 mL, 15.2 mmol) was added and the reaction was stirred at room temperature for 20 minutes. The solvent was removed *in vacuo* giving a white solid. The product was recrystallized by dissolving in a minimum of toluene, layering with pentane and placed in a –30 °C glovebox freezer overnight. The white solid recovered was dried *in vacuo*. Yield: 0.742 g (80%). ¹H NMR (500 MHz, 25 °C, C₆D₆): δ 6.28 (d, *J*_{H-F} = 9.7 Hz, 2H, Ar-*H*), 2.24–2.15 (m, *J* = 7.0 Hz, 4H, P–CH(CH₃)₂), 1.19 (dvt, *J*_{H-H} = 10.0 Hz, *J*_{P-H} = 8.5 Hz, 12H, P–CH(CH₃)₂), 0.94 (dvt, *J*_{H-H} = 8.3 Hz, *J*_{P-H} = 7.2 Hz, 12H, P–CH(CH₃)₂). ¹³C{¹H} NMR (126 MHz, 25 °C, C₆D₆): δ 166.8 (dt, *J*_{C-F} = 14.5 Hz, *J*_{C-P} = 6.3 Hz, 2C, Ar C–OPR₂), 164.3 (d, *J*_{C-F} = 243 Hz, 1C, Ar *p*-C–F), 120.8 (q, *J*_{C-F} = 318 Hz, 1C, –CF₃), 116.5 (m, 1C, Ar C–Pd), 95.5 (dt, *J*_{C-F} = 26.2 Hz, *J*_{C-P} = 7.6 Hz, 2C, Ar C–H), 29.1 (vt, *J*_{C-P} = 11.3 Hz, 4C, P–CH(CH₃)₂), 17.1(vt, *J*_{C-P} = 3.8 Hz, 4C, P–CH(CH₃)₂), 16.4 (s, 4C, P–CH(CH₃)₂). ¹⁹F NMR (470 MHz, 25 °C, C₆D₆): δ –77.7 (s, 3F, –CF₃), –112.8 (t, *J*_{F-H} = 9.7 Hz, 1F, Ar-*F*). ³¹P{¹H} NMR (202 MHz, 25 °C, C₆D₆): δ 192.8 (s). Anal. Calcd. for **514**: C, 37.12; H, 4.92. Found: C, 37.22; H, 5.02.

Synthesis of [(*p*-F-P^OC^OP^{iPr})Pd(BrC₆D₅)] [HCB₁₁Cl₁₀OTf] (515**)** – A J. Young tube was charged with **514** (0.0681 g, 0.111 mmol) which was dissolved in C₆D₅Br then ⁱPr₃Si[**510**] (0.088 g, 0.111 mmol) was added. The reaction was mixed then analyzed by ¹H, ¹⁹F and ³¹P{¹H} NMR. The formation of one equivalent of ⁱPr₃SiOTf was observed

via ^1H NMR as well as a new organometallic product assumed to be >95% **515** via ^1H , ^{19}F , $^{31}\text{P}\{^1\text{H}\}$ NMR analysis. The solution was poured into a vial then layered with pentane giving white yellow solids. The solids were repeatedly washed with hexane, dried *in vacuo* and analyzed via ^1H , ^{11}B , $^{13}\text{C}\{^1\text{H}\}$, ^{19}F , $^{31}\text{P}\{^1\text{H}\}$ NMR spectroscopy. X-ray quality crystals were grown by slow diffusion of pentane into a $\text{C}_6\text{D}_5\text{Br}$ solution of **515**. Yield: 0.040 g (29%). ^1H NMR (400 MHz, 25 °C, $\text{C}_6\text{D}_5\text{Br}$): δ 6.35 (d, $J_{\text{H-F}} = 9.3$ Hz, 2H, Ar-*H*), 2.81 (br s, 1H, $[\text{HCB}_{11}\text{Cl}_{10}(\text{OSO}_2\text{CF}_3)]^-$), 1.87 (m, 4H, P-*CH*(CH_3)₂), 1.05-0.95 (m, 24H, P-*CH*(CH_3)₂). $^{13}\text{C}\{^1\text{H}\}$ NMR (101 MHz, 25 °C, $\text{C}_6\text{D}_5\text{Br}$): δ 165.2 (dt, $J_{\text{C-F}} = 14$ Hz, $J_{\text{C-P}} = 5$ Hz, 2C, Ar C-*OPR*₂), 164.2 (d, $J_{\text{C-F}} = 246$ Hz, 1C, Ar *p*-C-F), 120.6 (br m, 1C, Ar C-Pd), 118.6 (q, $J_{\text{C-F}} = 316$ Hz, 1C, $[\text{HCB}_{11}\text{Cl}_{10}(\text{OSO}_2\text{CF}_3)]^-$), 96.1 (m, 2C, Ar C-H), 46.0 (br s, 1C, $[\text{HCB}_{11}\text{Cl}_{10}(\text{OSO}_2\text{CF}_3)]^-$), 29.3 (m, 4C, P-*CH*(CH_3)₂), 17.0 (br, 4C, P-*CH*(CH_3)₂), 16.3 (br, 4C, P-*CH*(CH_3)₂). ^{19}F NMR (470 MHz, 25 °C, $\text{C}_6\text{D}_5\text{Br}$): δ -76.7 (s, 3F, $[\text{HCB}_{11}\text{Cl}_{10}(\text{OSO}_2\text{CF}_3)]^-$), -108.5 (br s, 1F, Ar *p*-F). $^{31}\text{P}\{^1\text{H}\}$ NMR (162 MHz, 25 °C, $\text{C}_6\text{D}_5\text{Br}$): δ 194.2. ^{11}B NMR (128 MHz, 25 °C, $\text{C}_6\text{D}_5\text{Br}$): δ -1.07 (br s, 1B), -11.6 (br s, 5B), -13.9 (br s, 5B). Anal. Calcd. for **515**: C, 24.72; H, 3.27; B, 9.41. Found: C, 24.55; H, 2.99; B, 9.24.

Synthesis of $[(p\text{-F-P}^{\text{O}}\text{C}^{\text{O}}\text{P}^{\text{iPr}})\text{Pd}][\text{HCB}_{11}\text{Cl}_{10}\text{OTf}]$ (516**) *in situ*** – A J. Young tube was charged with **514** (0.0232 g, 0.0377 mmol), 10 μL of C_6F_6 , 10 μL of mesitylene, C_6D_6 , then $\text{Et}_3\text{Si}[\text{510}]$ (0.0285 g, 0.0380 mmol) was added. The reaction was mixed then analyzed by ^1H , ^{11}B , ^{19}F and $^{31}\text{P}\{^1\text{H}\}$ NMR. Quantitative formation of **516** and concomitant formation of Et_3SiOTf was observed by ^1H and ^{19}F NMR analysis.

Synthesis of [(*p*-F-P^OC^OP^{iPr})Pd][HCB₁₁Cl₁₀OTf] (516) - A 10 mL PTFE capped glass vial was charged **514** (0.0413 g, 0.0672 mmol) and fluorobenzene (1 mL). Et₃Si[**510**] (0.0505 g, 0.0673 mmol) was added and the solution was stirred for 5 minutes then all solvent was removed *in vacuo* giving white solid. Recrystallization from toluene and pentane gave white colorless crystals. X-ray quality crystals of **516** were grown from an *o*-difluorobenzene solution layered with pentane at room temperature. Yield: 0.029 g (39%). ¹H NMR (500 MHz, 25 °C, C₆D₆): δ 6.12 (d, *J*_{H-F} = 9.4 Hz, 2H, Ar-*H*), 2.33 (br s, 1H, [HCB₁₁Cl₁₀(OSO₂CF₃)][−]), 1.94 (m, 4H, P-CH(CH₃)₂), 0.98 (br dvt, *J*_{H-H} = 9.5 Hz, *J*_{P-H} = 9.2 Hz, 12H, P-CH(CH₃)₂), 0.80 (br dvt, *J*_{H-H} = 7.7 Hz, *J*_{P-H} = 7.5 Hz, 12H, P-CH(CH₃)₂). ¹¹B NMR (128 MHz, 25 °C, C₆D₆): δ −0.46 (br s, 1B), −11.31 (s, 5B), −13.20 (s 5B). ¹³C{¹H} NMR (126 MHz, 25 °C, C₆D₆): δ 166.2 (dt, *J*_{C-F} = 14 Hz, *J*_{C-P} = 6.3 Hz, 2C, Ar *C*-OPR₂), 164.6 (d, *J*_{C-F} = 247 Hz, 1C, Ar *p*-*C*-F), 118.6 (q, *J*_{C-F} = 320 Hz, 1C, [HCB₁₁Cl₁₀(OSO₂CF₃)][−]), 112.9 (m, 1C, Ar *C*-Pd), 96.1 (dt, *J*_{C-F} = 26.5 Hz, *J*_{C-P} = 7.6 Hz, 2C, Ar *C*-H), 47.1 (br s, 1C, [HCB₁₁Cl₁₀(OSO₂CF₃)][−]), 29.5 (vt, *J*_{C-P} = 11.5 Hz, 4C, P-CH(CH₃)₂), 17.3 (vt, *J*_{C-P} = 3.3 Hz, 4C, P-CH(CH₃)₂), 16.3 (s, 4C, P-CH(CH₃)₂). ¹⁹F NMR (470 MHz, 25 °C, C₆D₆): δ −74.6 (s, 3F, [HCB₁₁Cl₁₀(OSO₂CF₃)][−]), −110.5 (br m, 1F, Ar-*p*-F). ³¹P{¹H} NMR (202 MHz, 25 °C, C₆D₆): δ 193.9. Anal. Calcd. for **516**: C, 21.81; H, 2.84; B, 10.80. Found: C, 21.94; H, 2.73; B, 10.54.

Synthesis of [(*p*-F-P^OC^OP^{iPr})Pd][HCB₁₁Cl₁₁] (517) – A J. Young NMR tube was charged with **514** (0.0721 g, 0.060 mmol), Na[**502**] (0.064 g, 0.0609 mmol) and a 2:1 *o*-difluorobenzene:C₆D₆ solvent mixture. The mixture was agitated for 24 h at room

temperature then filtered through a plug of celite. All solvent was removed *in vacuo* resulting in a white solid. X-ray quality crystals of **517** were grown from fluorobenzene solution layered with hexanes at room temperature. Yield: 0.105 g (91%). ^1H NMR (400 MHz, 25 °C, 2:1 ODFB: C_6D_6): δ 6.17 (d, $J_{\text{H-F}} = 9.5$ Hz, 2H, Ar-*H*), 2.63 (br s, 1H, [$\text{HCB}_{11}\text{Cl}_{11}$] $^-$), 1.97 (br m, 4H, P- $\text{CH}(\text{CH}_3)_2$), 1.05-0.99 (br m, 24H, P- $\text{CH}(\text{CH}_3)_2$). ^{11}B NMR (128 MHz, 25 °C, 2:1 ODFB: C_6D_6): δ -2.22 (br s, 1B), -9.69 (br s, 5B), -12.83 (br s, 5B). $^{13}\text{C}\{^1\text{H}\}$ NMR (101 MHz, 25 °C, 2:1 ODFB: C_6D_6): δ 165.7 (m, 2C, Ar C- OPR_2), 164.8 (d, $J_{\text{C-F}} = 247$ Hz, 1C, Ar *p*-C-F), Ar C-Pd signal could not be identified, 95.9 (dt, $J_{\text{C-F}} = 26.5$ Hz, $J_{\text{C-P}} = 7.8$ Hz, 2C, Ar C-H), 47.7 (br s, 1C, [$\text{HCB}_{11}\text{Cl}_{11}$] $^-$), 30.1 (br vt, $J_{\text{C-P}} = 10.4$ Hz, 4C, P- $\text{CH}(\text{CH}_3)_2$), 17.5 (br s, 4C, P- $\text{CH}(\text{CH}_3)_2$), 16.2 (s, 4C, P- $\text{CH}(\text{CH}_3)_2$). δ ^{19}F NMR (376 MHz, 25 °C, 2:1 ODFB: C_6D_6): δ -110.2 (br s, Ar-*p*-F). $^{31}\text{P}\{^1\text{H}\}$ NMR (162 MHz, 25 °C, 2:1 ODFB: C_6D_6): δ 193.9. Anal. Calcd. for **517**: C, 23.11; H, 3.16; B, 12.04. Found: C, 23.20; H, 3.06; B, 11.96.

Synthesis of [(Et₃Si)₂OTf][HCB₁₁Cl₁₁] (518) – A vial was loaded with Ph₃C[**502**] (0.116 g, 0.152 mmol), a PTFE stir bar and 2 mL of PhF. Me₃SiOTf (136 mg, 0.612 mmol) and Et₃SiH (80 mg, 0.688 mmol) were added and the solution went colorless. The reaction was stirred for 1 h at room temperature then all solvent was removed *in vacuo* giving yellow oil determined to be >95% pure **518** via ^1H , ^{11}B , $^{13}\text{C}\{^1\text{H}\}$, ^{19}F and $^{29}\text{Si}\{^1\text{H}\}$ NMR. The use of Et₃SiOTf in place of Me₃SiOTf gave the same product, **518**. Yield: 0.109 g (80%). ^1H NMR (400 MHz, 25 °C, C₆D₅Br): δ 2.88 (br s, 1H, [$\text{HCB}_{11}\text{Cl}_{11}$] $^-$), 0.85–0.71 (m, 30H, [(Et₃Si)₂OTf]). ^{11}B NMR (128 MHz, 25 °C, C₆D₅Br): δ -2.54 (s, 1B), -10.09 (s, 5B), -13.23 (s, 5B). $^{13}\text{C}\{^1\text{H}\}$ NMR (126 MHz, 25

°C, C₆D₅Br): δ 117.4 (q, J_{C-F} = 323 Hz, 1C, [(Et₃Si)₂OTf]⁺), 47.0 (s, 1C, [HCB₁₁Cl₁₁]), 5.52-5.04 (m, 3H, [(Et₃Si)₂OTf]⁺), 5.12 (s, 3H, [(Et₃Si)₂OTf]⁺). ¹⁹F NMR (376 MHz, 25 °C, C₆D₅Br): δ -73.7. ²⁹Si NMR (79.5 MHz, 25 °C, C₆D₅Br): δ 75.5 (s).

5.4.3 Catalytic hydrodefluorination studies

CAUTION – *In certain cases, C-F activation reactions may proceed very rapidly, self-accelerating and releasing dangerous amounts of heat. In addition, these reactions may generate hydrogen and possibly even other gases. Great care and preliminary testing of safe conditions are necessary for performing reactions in closed vessels. All reactions were done in 20 mL polypropylene vials pierced with a 20 gauge 1.5” needle to allow gas to escape. Entries 1-5 refer to Table V-1.*

Entry 1 – A 20 mL polypropylene vial was loaded with Ph₃C[**510**] (2.9 mg, 3.3 μ mol), C₆F₆ (20 μ L, 0.17 mmol), o-dichlorobenzene (0.3 mL), C₆F₅CF₃ (0.30 mL, 2.1 mmol), and a PTFE coated stirbar. Et₃SiH (1.1 mL, 6.9 mmol) was added slowly and the mixture was allowed to stir for 24 h at room temperature. The mixture was taken up into a J. Young tube, sealed, taken out of the glovebox and analyzed via ¹⁹F NMR spectroscopy. A trace amount (<1%) of Et₃SiF (δ = -177.5 ppm) was observed.

Entry 2 – A 20 mL polypropylene vial was loaded with Ph₃C[**510**] (29 mg, 33 μ mol), C₆F₆ (20 μ L, 0.17 mmol), o-dichlorobenzene (0.3 mL), C₆F₅CF₃ (0.30 mL, 2.1 mmol), and a PTFE coated stirbar. Et₃SiH (1.1 mL, 6.9 mmol) was added slowly and the mixture was allowed to stir for 24 h at room temperature. The mixture was taken up into a J. Young tube, sealed, taken out of the glovebox and analyzed via ¹⁹F NMR

spectroscopy. After 24 h, 20% of the $C_6F_5CF_3$ had been consumed. Et_3SiF (s, $\delta = -177.5$ ppm) was observed in a 20% yield.

Entry 3 – A 20 mL polypropylene vial was loaded with $Ph_3C[502]$ (2.5 mg, 3.3 μ mol), C_6F_6 (20 μ L, 0.17 mmol), o-dichlorobenzene (0.3 mL), $C_6F_5CF_3$ (0.30 mL, 2.1 mmol), and a PTFE coated stirbar. Et_3SiH (1.1 mL, 6.9 mmol) was added slowly and the mixture was allowed to stir for 24 h at room temperature. The mixture was taken up into a J. Young tube, sealed, taken out of the glovebox and analyzed via ^{19}F NMR spectroscopy. After 24 h, all $C_6F_5CF_3$ had been consumed. Et_3SiF (s, $\delta = -177.5$ ppm) and Et_2SiF_2 (br s, $\delta = -145.3$ ppm) were observed in a 59% and 10% yield, respectively.

Entry 4 – A 20 mL polypropylene vial was loaded with $Ph_3C[510]$ (2.9 mg, 3.3 μ mol), C_6F_6 (20 μ L, 0.17 mmol), o-dichlorobenzene (0.3 mL), 4-F- $C_6H_4CF_3$ (0.30 mL, 2.4 mmol), and a PTFE coated stirbar. Et_3SiH (1.1 mL, 6.9 mmol) was added slowly and the mixture was allowed to stir for 24 h at room temperature. The mixture was taken up into a J. Young tube, sealed, taken out of the glovebox and analyzed via ^{19}F NMR spectroscopy. After 24 h, 85% of the 4-F- $C_6H_4CF_3$ had been consumed. Et_3SiF (s, $\delta = -177.5$ ppm) was observed in an 87% yield.

Entry 5 – A 20 mL polypropylene vial was loaded with $Ph_3C[502]$ (2.5 mg, 3.3 μ mol), C_6F_6 (20 μ L, 0.17 mmol), o-dichlorobenzene (0.3 mL), 4-fluorobenzotrifluoride (0.30 mL, 2.4 mmol), and a PTFE coated stirbar. Et_3SiH (1.1 mL, 6.9 mmol) was added slowly and gas evolved violently. The solution turned dark brown. The mixture was allowed to stir for 1 h at room temperature. The mixture was taken up into a J. Young tube, sealed, taken out of the glovebox and analyzed via ^{19}F NMR spectroscopy. After 1

h, all 4-F-C₆H₄CF₃ had been consumed. Et₃SiF (s, $\delta = -177.5$ ppm) was observed in a 95% yield.

5.4.4 X-ray crystallography

Crystals of [(^FPOCOP)Pd][HCB₁₁Cl₁₁] were grown from a solution of fluorobenzene layered with hexanes. A colorless block of suitable size and quality (0.27 × 0.15 × 0.08 mm) was selected from a representative sample of crystals of the same habit using an optical microscope, mounted onto a nylon loop, and placed in a cold stream of nitrogen (110 K). Low-temperature X-ray data were obtained on a Bruker APEXII CCD based diffractometer (Mo sealed X-ray tube, $K_{\alpha} = 0.71073$ Å). All diffractometer manipulations, including data collection, integration, and scaling were carried out using the Bruker APEX2 software.²³² An absorption correction was applied using SADABS.²³³ The space group was determined on the basis of systematic absences and intensity statistics. The structure was solved by direct methods in the triclinic P1 space group using SHELXS,²³⁸ then converted to the centrosymmetric P-1 space group with PLATON's ADDSYM facility.²³⁶ All non-hydrogen atoms were refined with anisotropic thermal parameters. Hydrogen atoms bound to carbon were placed in idealized positions and refined using a riding model. The structure was brought to convergence by weighted full-matrix least-squares refinement on $|F|^2$. PLATON's SQUEEZE feature was utilized to account for partial occupancy and disorder of solvent in the crystal structure, which appeared to be fluorobenzene based on the difference map (total void volume 353 Å³, 85 e⁻). Structure manipulations were performed with the aid of shelXle.²³⁷

Crystals of [$^{\text{F}}\text{POCOP}$] Pd][$\text{HCB}_{11}\text{Cl}_{10}\text{OTf}$] were grown from a solution of *ortho*-difluorobenzene layered with pentane. A clear colorless block of suitable size and quality ($0.34 \times 0.32 \times 0.08$ mm) was selected from a representative sample of crystals of the same habit using an optical microscope, mounted onto a nylon loop, and placed in a cold stream of nitrogen (110 K). Low-temperature X-ray data were obtained on a Bruker APEXII CCD based diffractometer (Mo sealed X-ray tube, $K_{\alpha} = 0.71073$ Å). All diffractometer manipulations, including data collection, integration, and scaling were carried out using the Bruker APEX2 software.²³² An absorption correction was applied using SADABS.²³³ The space group was determined on the basis of systematic absences and intensity statistics. The structure was solved by direct methods in the triclinic P-1 space group using SHELXS.²³⁸ All non-hydrogen atoms were refined with anisotropic thermal parameters. Hydrogen atoms bound to carbon were placed in idealized positions and refined using a riding model. The structure was brought to convergence by weighted full-matrix least-squares refinement on $|F|^2$. A check for missed symmetry was performed with PLATON's ADDSYM facility, finding no apparent higher symmetry.²³⁶ Structure manipulations were performed with the aid of shelXle.²³⁷

Crystals of [$^{\text{F}}\text{POCOP}^{\text{iPr}}$] $\text{Pd}(\text{BrC}_6\text{D}_5)$][$\text{HCB}_{11}\text{Cl}_{10}\text{OTf}$] were grown from a solution of bromobenzene- d_5 by vapor diffusion of pentane. A colorless block of suitable size and quality ($0.33 \times 0.21 \times 0.06$ mm) was selected from a representative sample of crystals of the same habit using an optical microscope, mounted onto a nylon loop, and placed in a cold stream of nitrogen (150 K). Low-temperature X-ray data were obtained on a Bruker APEXII CCD based diffractometer (Mo sealed X-ray tube,

$K_{\alpha} = 0.71073 \text{ \AA}$). All diffractometer manipulations, including data collection, integration, and scaling were carried out using the Bruker APEX2 software.²³² An absorption correction was applied using SADABS.²³³ The space group was determined on the basis of systematic absences and intensity statistics. The structure was solved by direct methods in the monoclinic $P2_1/n$ space group using SHELXS.²³⁸ All non-hydrogen atoms were refined with anisotropic thermal parameters. Hydrogen atoms bound to carbon were placed in idealized positions and refined using a riding model. The structure was brought to convergence by weighted full-matrix least-squares refinement on $|F|^2$. Structure manipulations were performed with the aid of shelXle.²³⁷ A check for missed symmetry was run using the ADDSYM program within PLATON,²³⁶ revealing no apparent higher symmetry.

Crystals of $[\text{Ph}_3\text{C}][\text{HCB}_{11}\text{Cl}_{10}\text{OTf}] \cdot \text{C}_6\text{H}_5\text{F}$ were grown from a fluorobenzene solution layered with pentane. A clear yellow block of suitable size and quality (0.27 x 0.19 x 0.11 mm) was selected from a representative sample of crystals of the same habit using an optical microscope, mounted onto a nylon loop, and placed in a cold stream of nitrogen (150 K). Low-temperature X-ray data were obtained on a Bruker APEXII CCD based diffractometer (Mo sealed X-ray tube, $K_{\alpha} = 0.71073 \text{ \AA}$). All diffractometer manipulations, including data collection, integration, and scaling were carried out using the Bruker APEX2 software.²³² An absorption correction was applied using SADABS.²³³ The space group was determined on the basis of systematic absences and intensity statistics. The structure was solved by direct methods in the orthorhombic $Pbca$ space group using SHELXS.²³⁸ All non-hydrogen atoms were refined with anisotropic thermal

parameters. Hydrogen atoms bound to carbon were placed in idealized positions and refined using a riding model. The structure was brought to convergence by weighted full-matrix least-squares refinement on $|F|^2$. Structure manipulations were performed with the aid of shelXle.²³⁷ A check for missed symmetry was run using the ADDSYM program within PLATON, revealing no apparent higher symmetry.²³⁶

A solvent molecule consistent with fluorobenzene was identified in the electron difference map, but was unable to be satisfactorily modeled, due to an apparent 6-fold rotational disorder. The solvent electron density was therefore accounted for with SQUEEZE, which revealed four voids in the unit cell (292 \AA^3 , $104 e^-$), consistent with one fluorobenzene solvent molecule ($50 e^-$) per asymmetric unit. Our model is therefore inconsistent with the checkCIF calculated values of moiety/sum formulae, formula weight (Mr), density (Dx), absorption coefficient (μ), and F000, which accounts for all checkCIF alerts level A–C.

Crystals of $[i\text{Pr}_3\text{Si}][\text{HCB}_{11}\text{Cl}_{10}\text{OTf}] \cdot \text{C}_6\text{H}_5\text{F}$ were grown from a solution of approximately equal parts fluorobenzene and triisopropylsilane by vapor diffusion of pentane. A colorless rod of suitable size and quality ($0.54 \times 0.14 \times 0.13 \text{ mm}$) was selected from a representative sample of crystals of the same habit using an optical microscope, mounted onto a nylon loop, and placed in a cold stream of nitrogen (150 K). Low-temperature X-ray data were obtained on a Bruker APEXII CCD based diffractometer (Mo sealed X-ray tube, $K_\alpha = 0.71073 \text{ \AA}$). All diffractometer manipulations, including data collection, integration, and scaling were carried out using the Bruker APEX2 software.²³² An absorption correction was applied using SADABS.²³³

The space group was determined on the basis of systematic absences and intensity statistics. The structure was solved by direct methods in the monoclinic $P2_1/c$ space group using SHELXS.²³⁸ All non-hydrogen atoms were refined with anisotropic thermal parameters. Hydrogen atoms bound to carbon were placed in idealized positions and refined using a riding model. The structure was brought to convergence by weighted full-matrix least-squares refinement on $|F|^2$. Structure manipulations were performed with the aid of shelXle.²³⁷ A check for missed symmetry was run using the ADDSYM program within PLATON, revealing no apparent higher symmetry.²³⁶ Similarity restraints were applied to the triflyloxy and triisopropylsilyl moieties to handle the refinement of the disorder.

Crystals of **[Et₃Si][HCB₁₁Cl₁₀OTf]** were grown from a fluorobenzene solution by vapor diffusion of pentane. A colorless block of suitable size and quality (0.28 x 0.17 x 0.16 mm) was selected from a representative sample of crystals of the same habit using an optical microscope, mounted onto a nylon loop, and placed in a cold stream of nitrogen (150 K). Low-temperature X-ray data were obtained on a Bruker APEXII CCD based diffractometer (Mo sealed X-ray tube, $K_{\alpha} = 0.710\ 73\ \text{\AA}$). All diffractometer manipulations, including data collection, integration, and scaling were carried out using the Bruker APEX2 software.²³² An absorption correction was applied using SADABS.²³³ The space group was determined on the basis of systematic absences and intensity statistics. The structure was solved by direct methods in the monoclinic $P2_1/n$ space group using XS²³⁸ (incorporated in SHELXTL). All non-hydrogen atoms were refined with anisotropic thermal parameters. Hydrogen atoms bound to carbon were placed in

idealized positions and refined using a riding model. The structure was brought to convergence by weighted full-matrix least-squares refinement on $|F|^2$. A check for missed symmetry was run using the ADDSYM program within PLATON,²³⁶ revealing no apparent higher symmetry. Similarity restraints were applied to the triflyloxy and silylium moieties to handle the refinement of the disorder. The checkCIF report yielded three moderate-level alerts attributed to the disordered alkyl chains of the triethylsilyl moieties, specifically identifying the prolate nature of the disordered carbons, and the resultant imprecision of C–C bond lengths. High residual density ($1.49 \text{ e}^- \text{ \AA}^{-3}$) was found near one of the disordered silicon centers (Si1_5 – 0.04 Å), and a hole in the residual density ($-0.99 \text{ e}^- \text{ \AA}^{-3}$) was also observed near the same atom (Si1_5 – 0.65 Å); this is attributed to imperfect modeling of the disorder. Large X–O–Y angles ($>140^\circ$) were observed, as expected in light of previously reported triflate-bridged trimethylsilylium cations.

Crystals of $[(p\text{-F-P}^{\text{O}}\text{C}^{\text{O}}\text{P}^{\text{iPr}})\text{Pd}]_2\text{Cl}[\text{HCB}_{11}\text{Cl}_{10}\text{OTf}]$ were grown from a solution of fluorobenzene by vapor diffusion of pentane. A colorless block of suitable size and quality (0.207 x 0.174 x 0.087 mm) was selected from a representative sample of crystals of the same habit using an optical microscope, mounted onto a nylon loop, and placed in a cold stream of nitrogen (150 K). Low-temperature X-ray data were obtained on a Bruker APEXII CCD based diffractometer (Mo sealed X-ray tube, $K_\alpha = 0.71073 \text{ \AA}$). All diffractometer manipulations, including data collection, integration, and scaling were carried out using the Bruker APEX2 software.²³² An absorption correction was applied using SADABS.²³³ The space group was determined on the basis of

systematic absences and intensity statistics. The structure was solved by direct methods in the monoclinic $P2_1/n$ space group using SHELXS.²³⁸ All non-hydrogen atoms were refined with anisotropic thermal parameters. Hydrogen atoms bound to carbon were placed in idealized positions and refined using a riding model. The structure was brought to convergence by weighted full-matrix least-squares refinement on $|F|^2$. Structure manipulations were performed with the aid of shelXle.²³⁷ A check for missed symmetry was run using the ADDSYM program within PLATON, revealing no apparent higher symmetry.²³⁶ Similarity restraints were applied to the triflyloxy moieties to handle the refinement of the disorder.

Crystals of **Cs[HCB₁₁H₅Br₅OTf]** were grown from a solution of dichloromethane by slow evaporation of solvent. A colorless sheet of suitable size and quality (0.20 x 0.12 x 0.08 mm) was selected from a representative sample of crystals of the same habit using an optical microscope, mounted onto a nylon loop, and placed in a cold stream of nitrogen (150 K). Low-temperature X-ray data were obtained on a Bruker APEXII CCD based diffractometer (Mo sealed X-ray tube, $K_\alpha = 0.71073 \text{ \AA}$). All diffractometer manipulations, including data collection, integration, and scaling were carried out using the Bruker APEX2 software.²³² An absorption correction was applied using SADABS.²³³ The space group was determined on the basis of systematic absences and intensity statistics. The structure was solved by the direct methods in the orthorhombic $Pbcn$ space group using SHELXS.²³⁸ All non-hydrogen atoms were refined with anisotropic thermal parameters. Hydrogen atoms bound to carbon and boron were placed in idealized positions and refined using a riding model. The structure was brought

to convergence by weighted full-matrix least-squares refinement on $|F|^2$. Structure manipulations were performed with the aid of shelXle.²³⁵ A check for missed symmetry was run using the ADDSYM program within PLATON, revealing no apparent higher symmetry.²³⁶ **Cs[HCB₁₁H₄Br₆OTf]** co-crystallizes as a minor component (~6%), and is satisfactorily modeled as a substitutional disorder, replacing a hydrogen atom on the *ortho* belt with a bromine atom. This is agreement with the ~5% of **Cs[HCB₁₁H₄Br₆OTf]** observed by MALDI MS.

Crystals of **Cs[HCB₁₁H₈(OTf)₃]** were grown from a solution of dichloromethane by slow evaporation of solvent. A colorless block of suitable size and quality (0.55 x 0.20 x 0.10 mm) was selected from a representative sample of crystals of the same habit using an optical microscope, mounted onto a nylon loop, and placed in a cold stream of nitrogen (150 K). Low-temperature X-ray data were obtained on a Bruker APEXII CCD based diffractometer (Mo sealed X-ray tube, $K_{\alpha} = 0.71073 \text{ \AA}$). All diffractometer manipulations, including data collection, integration, and scaling were carried out using the Bruker APEX2 software.²³² An absorption correction was applied using SADABS.²³³ The space group was determined on the basis of systematic absences and intensity statistics. The structure was solved by the Patterson method in the monoclinic $P2_1/c$ space group using SHELXS.²³⁸ All non-hydrogen atoms were refined with anisotropic thermal parameters. Hydrogen atoms bound to carbon and boron were placed in idealized positions and refined using a riding model. The structure was brought to convergence by weighted full-matrix least-squares refinement on $|F|^2$. Structure manipulations were performed with the aid of shelXle. A check for missed symmetry

was run using the ADDSYM program within PLATON, revealing no apparent higher symmetry.²³⁶

Crystals of **Cs[HCB₁₁Cl₉(OTf)₂]** were grown from a solution of acetonitrile by slow evaporation of solvent. A colorless plate of suitable size and quality (0.42 x 0.14 x 0.05 mm) was selected from a representative sample of crystals of the same habit using an optical microscope. All operations were performed on a Bruker-Nonius Kappa Apex2 diffractometer, using graphite-monochromated MoK α radiation. All diffractometer manipulations, including data collection, integration, scaling, and absorption corrections were carried out using the Bruker Apex2 software.²³² Preliminary cell constants were obtained from three sets of 12 frames. Data collection was carried out at 120 K, using a frame time of 30 sec and a detector distance of 60 mm. The optimized strategy used for data collection consisted of two phi and seven omega scan sets, with 0.5° steps in phi or omega; completeness was 99.8%. A total of 2234 frames were collected. Final cell constants were obtained from the xyz centroids of 9002 reflections after integration.

From the systematic absences, the observed metric constants and intensity statistics, space group *Pbca* was chosen initially; subsequent solution and refinement confirmed the correctness of the initial choice. The structures were solved using SIR-92,²⁶³ and refined (full-matrix-least squares) using the Oxford University *Crystals for Windows* program.²⁶⁴ All ordered non-hydrogen atoms were refined using anisotropic displacement parameters; the hydrogen atoms attached to the carborane C atom was fixed at a calculated geometric position 0.95 Å from C(1) and refined as a riding atom. Compound **Cs[HCB₁₁Cl₉(OTf)₂]** contained significant disorder, which was resolved (in

part) successfully. The resolvable disorder involved the sulfonate oxygen atoms of the triflyloxy moiety attached to B(7); modeling of the disorder of the CF₃ group was not successful. The two-component disorder (major: O4/O5/O6; minor: O41/O51/O61) was described with a constraint such that the occupancies of the major (anisotropic displacement parameters, occupancy 0.777(9)) and minor components (isotropic displacement parameters) sum to 1.0. It appears that the disorder is caused by two positions for the CB₁₁ cage, related by a small rotation approximately about the B5-B8 axis. It was not possible to model the lower level of disorder in the other triflyloxy moiety. The final least-squares refinement converged to $R_1 = 0.0326$ ($I > 2\sigma(I)$, 5328 data) and $wR_2 = 0.0870$ (F^2 , 7782 data, 356 parameters).

CHAPTER VI

CONCLUSION

The catalytic C-H borylation of arenes with HBpin using POCOP-type pincer complexes of Ir has been demonstrated, with turnover numbers exceeding 10,000 in some cases. The selectivity of C-H activation was based on steric preferences and largely mirrored that found in other Ir borylation catalysts. Catalysis in the (POCOP)Ir system depends on the presence of stoichiometric quantities of sacrificial olefin, which is hydrogenated to consume the H₂ equivalents generated in the borylation of C-H bonds with HBpin. Smaller olefins such as ethylene or 1-hexene were more advantageous to catalysis than a sterically encumbered *tert*-butylethylene. Olefin hydroboration is a competing side reaction, the synthesis and isolation of multiple complexes potentially relevant to catalysis permitted examination of several key elementary reactions. Insight from these experiments indicated that the C-H activation step in catalysis ostensibly involves oxidative addition of an aromatic C-H bond to the three-coordinate (POCOP)Ir species. The olefin is mechanistically critical to gain access to this 14-electron, monovalent Ir intermediate. C-H activation at Ir(I) here is in contrast to the olefin-free catalysis with state-of-the-art Ir complexes supported by neutral bidentate ligands, where the C-H activating step is understood to involve trivalent Ir-boryl intermediates. Our studies indicate Ir pincer complexes hold great promise for catalytic C-H borylation-type chemistries. In order to be competitive with the current state-of-the-art Ir borylation catalyst,^{47,61} the next generation of Ir pincer catalysts ideally should try and meet the

following criteria: (a) Eliminate the requirement of excess arene (as solvent) and give high yields of borylated product while utilizing near 1:1 HBpin:arene ratios. (b) The capability to achieve borylations at, or near, room temperature; allowing borylations of temperature sensitive substrates. (c) Achieve high catalytic activity without the need of H₂ acceptor. (d) High functional group tolerance including C-halogen bonds, pyridines, nitriles and other reactive or coordinating groups. (e) Utilize ligand modifications similar to those investigated by Kanai⁷² and Itami⁷³ et al. to improve site specific selectivity.

These criteria will likely not be met by one catalyst but the extensive array of available pincer ligands²²⁴ to the synthetic chemist calls for broad screening studies to identify systems which meet as many of the aforementioned criteria as possible. Additionally, various boranes beyond HBpin could be investigated and one could also envision expanding the scope to include the catalytic formation of C-Si bonds in what is known as C-H bond silylation.²⁶⁵

A (POCOP)Ir(Bpin)₂ compound was investigated for the activation of small molecules. The deoxygenation of CO₂ to give an (POCOP)Ir(CO) compound was demonstrated. The 1,2-diboration of ethylene was observed. Selective protonation of a boryl ligand within (POCOP)Ir(Bpin)₂ was observed and serves as a means for the synthesis of (POCOP)Ir(HBpin). High turnovers were observed in the catalytic hydrogenolysis of B₂pin₂ using (POCOP)Ir(H)(Cl). The system is on par with the state-of-the-art diborane hydrogenolysis catalyst found within the literature. In the presence of substrates such as DMAP and methyl benzoate, (POCOP)Ir(Bpin)₂ first borylated the benzene solvent. The (POCOP)Ir fragment then reacted with the substrates to give Ir(I)

and Ir(III) compounds, respectively. Future studies with these diboryl pincer complexes should undoubtedly focus on boryl ligands beyond Bpin and their subsequent reactivity with various substrates. The substituents on boryl ligands can have dramatic effects in terms of boryl ligand reactivity and many studies have been limited to Bpin or Bpin-type ligands.^{47,202}

The synthesis and characterization of several POCS type ligands was accomplished. The modular nature of the POCS ligand design allows access to a variety of monomeric and bridging POCS ligands. This followed with the synthesis and characterization of several (POCS)Ni and Pd compounds containing a C₃ bridge. Halide ligand substitution (chloride to triflate) was demonstrated for a bridging (POCS)Ni complex. A binuclear (POCS)Ni compound containing a C₃ bridge was characterized by an XRD study. A six-coordinate monomeric (POCS)Ir(H)(Cl)(py) (two isomers) species was synthesized in a manner reminiscent of (POCOP)Ir species. Efforts to readily obtain (POCS)Ir(H)(Cl) were less straightforward and required the use of [(cod)IrOAc]₂ to give (POCS)Ir(H)(OAc) followed by ligand exchange. A (POCS)Ir(H)(Cl) compound was characterized by NMR spectroscopy and XRD studies. As discussed in the introduction of Chapter 4, the combination of the theme of pincer ligands with bridging binuclear species (or even polynuclear systems) is an emerging area of interest with fascinating possibilities. In the immediate future, straightforward synthetic methods are required for the synthesis of discrete bridging binuclear complexes containing metal centers other than those of group 10. The investigation of (POCS)Ir(H)(Cl) type complexes for catalytic C-H functionalization studies would also be of interest.

The selective installation of triflyloxy groups has been demonstrated with the mono-carba-closocarborane anion $[\text{HCB}_{11}\text{H}_{11}]^-$. These triflyloxy substituted carboranes were further functionalized by halogen substituents (including chlorine and bromine) and investigated for use as weakly coordinating anions. The triflyloxy moiety is chemically robust and survives the harsh conditions of halogenation. The triflyloxy moiety is also highly useful in NMR spectroscopy studies. The ^{19}F NMR chemical shift of the triflyloxy group was observed to be highly sensitive to the nature of coordinating species. Preliminary results regarding the alkylation and triflyloxylation of $[\text{HCB}_{11}\text{H}_{11}]^-$ hold promising results but further optimization is required to able discrete compounds. The HDF of benzotrifluorides was demonstrated with $\text{Ph}_3\text{C}[\text{HCB}_{11}\text{Cl}_{10}\text{OTf}]$ as precatalyst and compared to the state-of-the-art HDF catalysts. Two examples of $[\text{silylium}][\text{HCB}_{11}\text{Cl}_{10}\text{OTf}]$ were studied by XRD and NMR spectroscopy. These compounds were observed by NMR spectroscopy in the catalytic mixtures during HDF studies.

Future work regarding triflyloxy-substituted carboranes could be the further investigation of the permethylation (Figure V-2) and ethylation (Figure V-3) or other alkylation reactions to try and form single, pure compounds. These alkylated and triflyloxyated carboranes would likely be lipophilic in nature and would have the added benefit of ^{19}F NMR handles. Alternatives to triflic acid, such as perfluorooctanoic acid could also be used to functionalize the B vertices.

REFERENCES

- (1) Hartwig, J. F. *J. Am. Chem. Soc.* **2016**, *138*, 2.
- (2) Crabtree, R. H. *J. Chem. Soc. Dalton Trans.* **2001**, No. 17, 2437.
- (3) Wencel-Delord, J.; Dröge, T.; Liu, F.; Glorius, F. *Chem. Soc. Rev.* **2011**, *40*, 4740.
- (4) Balcells, D.; Clot, E.; Eisenstein, O. *Chem. Rev.* **2010**, *110*, 749.
- (5) Zimmermann, H.; Walzl, R. In *Ullmann's Encyclopedia of Industrial Chemistry*; Wiley-VCH Verlag GmbH & Co. KGaA, 2000.
- (6) Rossberg, M.; Lendle, W.; Pfeleiderer, G.; Tögel, A.; Torkelson, T. R.; Beutel, K. K. In *Ullmann's Encyclopedia of Industrial Chemistry*; Wiley-VCH Verlag GmbH & Co. KGaA, 2000.
- (7) Röper, M.; Gehrler, E.; Narbeshuber, T.; Siegel, W. In *Ullmann's Encyclopedia of Industrial Chemistry*; Wiley-VCH Verlag GmbH & Co. KGaA, 2000.
- (8) Labinger, J. A.; Bercaw, J. E. *Nature* **2002**, *417*, 507.
- (9) Engle, K. M.; Mei, T.-S.; Wasa, M.; Yu, J.-Q. *Acc. Chem. Res.* **2012**, *45*, 788.
- (10) Hartwig, J. F.; Larsen, M. A. *ACS Cent. Sci.* **2016**.
- (11) BrÜckl, T.; Baxter, R. D.; Ishihara, Y.; Baran, P. S. *Acc. Chem. Res.* **2012**, *45*, 826.
- (12) Shilov, A. E.; Shul'pin, G. B. *Chem. Rev.* **1997**, *97*, 2879.
- (13) Parshall, G. W. *Acc. Chem. Res.* **1970**, *3*, 139.
- (14) Bennett, M. A.; Milner, D. L. *J. Am. Chem. Soc.* **1969**, *91*, 6983.
- (15) Moritanl, I.; Fujiwara, Y. *Tetrahedron Lett.* **1967**, *8*, 1119.

- (16) Fujiwara, Y.; Moritani, I.; Matsuda, M.; Teranishi, S. *Tetrahedron Lett.* **1968**, *9*, 633.
- (17) Fujiwara, Y.; Noritani, I.; Danno, S.; Asano, R.; Teranishi, S. *J. Am. Chem. Soc.* **1969**, *91*, 7166.
- (18) Crabtree, R. H.; Mihelcic, J. M.; Quirk, J. M. *J. Am. Chem. Soc.* **1979**, *101*, 7738.
- (19) Baudry, D.; Ephritikhine, M.; Felkin, H.; Holmes-Smith, R. *J. Chem. Soc. Chem. Commun.* **1983**, No. 14, 788.
- (20) Felkin, H.; Fillebeen-Khan, T.; Gault, Y.; Holmes-Smith, R.; Zakrzewski, J. *Tetrahedron Lett.* **1984**, *25*, 1279.
- (21) Felkin, H.; Fillebeen-khan, T.; Holmes-Smith, R.; Yingrui, L. *Tetrahedron Lett.* **1985**, *26*, 1999.
- (22) Burk, M. J.; Crabtree, R. H. *J. Am. Chem. Soc.* **1987**, *109*, 8025.
- (23) Crabtree, R. H. *Chem. Rev.* **1985**, *85*, 245.
- (24) Janowicz, A. H.; Bergman, R. G. *J. Am. Chem. Soc.* **1982**, *104*, 352.
- (25) Hoyano, J. K.; Graham, W. A. G. *J. Am. Chem. Soc.* **1982**, *104*, 3723.
- (26) Maguire, J. A.; Petrillo, A.; Goldman, A. S. *J. Am. Chem. Soc.* **1992**, *114*, 9492.
- (27) Bergman, R. G. *Science* **1984**, *223*, 902.
- (28) Arndtsen, B. A.; Bergman, R. G.; Mobley, T. A.; Peterson, T. H. *Acc. Chem. Res.* **1995**, *28*, 154.
- (29) Niu, S.; Hall, M. B. *Chem. Rev.* **2000**, *100*, 353.
- (30) Torrent, M.; Solà, M.; Frenking, G. *Chem. Rev.* **2000**, *100*, 439.

- (31) Ritleng, V.; Sirlin, C.; Pfeffer, M. *Chem. Rev.* **2002**, *102*, 1731.
- (32) Murai, S.; Kakiuchi, F.; Sekine, S.; Tanaka, Y.; Kamatani, A.; Sonoda, M.; Chatani, N. *Nature* **1993**, *366*, 529.
- (33) Lenges, C. P.; Brookhart, M. *J. Am. Chem. Soc.* **1999**, *121*, 6616.
- (34) Jia, C.; Piao, D.; Oyamada, J.; Lu, W.; Kitamura, T.; Fujiwara, Y. *Science* **2000**, *287*, 1992.
- (35) Jia, C.; Kitamura, T.; Fujiwara, Y. *Acc. Chem. Res.* **2001**, *34*, 633.
- (36) Dick, A. R.; Hull, K. L.; Sanford, M. S. *J. Am. Chem. Soc.* **2004**, *126*, 2300.
- (37) Lyons, T. W.; Sanford, M. S. *Chem. Rev.* **2010**, *110*, 1147.
- (38) Powers, D. C.; Ritter, T. *Nat. Chem.* **2009**, *1*, 302.
- (39) Powers, D. C.; Geibel, M. A. L.; Klein, J. E. M. N.; Ritter, T. *J. Am. Chem. Soc.* **2009**, *131*, 17050.
- (40) Daugulis, O.; Do, H.-Q.; Shabashov, D. *Acc. Chem. Res.* **2009**, *42*, 1074.
- (41) Daugulis, O. In *C-H Activation*; Yu, J.-Q., Shi, Z., Eds.; Topics in Current Chemistry; Springer Berlin Heidelberg, 2009; pp 57–84.
- (42) Lewis, J. C.; Bergman, R. G.; Ellman, J. A. *Acc. Chem. Res.* **2008**, *41*, 1013.
- (43) Liu, W.; Ackermann, L. *ACS Catal.* **2016**, 3743.
- (44) Huang, X.; Bergsten, T. M.; Groves, J. T. *J. Am. Chem. Soc.* **2015**, *137*, 5300.
- (45) Paradine, S. M.; White, M. C. *J. Am. Chem. Soc.* **2012**, *134*, 2036.
- (46) Ishiyama, T.; Takagi, J.; Ishida, K.; Miyaura, N.; Anastasi, N. R.; Hartwig, J. F. *J. Am. Chem. Soc.* **2002**, *124*, 390.

- (47) Mkhaliid, I. A. I.; Barnard, J. H.; Marder, T. B.; Murphy, J. M.; Hartwig, J. F. *Chem. Rev.* **2010**, *110*, 890.
- (48) Hartwig, J. F. *Acc. Chem. Res.* **2012**, *45*, 864.
- (49) Hartwig, J. F. *Chem. Soc. Rev.* **2011**, *40*, 1992.
- (50) Cho, J.-Y.; Tse, M. K.; Holmes, D.; Maleczka, R. E.; Smith, M. R. *Science* **2002**, *295*, 305.
- (51) Nguyen, P.; Blom, H. P.; Westcott, S. A.; Taylor, N. J.; Marder, T. B. *J. Am. Chem. Soc.* **1993**, *115*, 9329.
- (52) *Boronic Acids: Preparation and Applications in Organic Synthesis, Medicine and Materials*; Hall, D. G., Ed.; Wiley-VCH Verlag GmbH & Co. KGaA: Weinheim, Germany, 2011.
- (53) Murphy, J. M.; Lawrence, J. D.; Kawamura, K.; Incarvito, C.; Hartwig, J. F. *J. Am. Chem. Soc.* **2006**, *128*, 13684.
- (54) Chen, H. *Science* **2000**, *287*, 1995.
- (55) Chen, H.; Hartwig, J. F. *Angew. Chem. Int. Ed.* **1999**, *38*, 3391.
- (56) Mazzacano, T. J.; Mankad, N. P. *J. Am. Chem. Soc.* **2013**, *135*, 17258.
- (57) Obligacion, J. V.; Semproni, S. P.; Chirik, P. J. *J. Am. Chem. Soc.* **2014**, *136*, 4133.
- (58) Schaefer, B. A.; Margulieux, G. W.; Small, B. L.; Chirik, P. J. *Organometallics* **2015**, *34*, 1307.
- (59) Furukawa, T.; Tobisu, M.; Chatani, N. *J. Am. Chem. Soc.* **2015**, *137*, 12211.

- (60) Légaré, M.-A.; Courtemanche, M.-A.; Rochette, É.; Fontaine, F.-G. *Science* **2015**, *349*, 513.
- (61) Preshlock, S. M.; Ghaffari, B.; Maligres, P. E.; Krska, S. W.; Maleczka, R. E.; Smith, M. R. *J. Am. Chem. Soc.* **2013**, *135*, 7572.
- (62) Boller, T. M.; Murphy, J. M.; Hapke, M.; Ishiyama, T.; Miyaura, N.; Hartwig, J. F. *J. Am. Chem. Soc.* **2005**, *127*, 14263.
- (63) Britt A. Vanchura, I. I.; Preshlock, S. M.; Roosen, P. C.; Kallepalli, V. A.; Staples, R. J.; Robert E. Maleczka, J.; Singleton, D. A.; Milton R. Smith, I. I. *Chem. Commun.* **2010**, *46*, 7724.
- (64) Ghaffari, B.; Vanchura, B. A.; Chotana, G. A.; Staples, R. J.; Holmes, D.; Maleczka, R. E.; Smith, M. R. *Organometallics* **2015**, *34*, 4732.
- (65) Boebel, T. A.; Hartwig, J. F. *J. Am. Chem. Soc.* **2008**, *130*, 7534.
- (66) Ghaffari, B.; Preshlock, S. M.; Plattner, D. L.; Staples, R. J.; Maligres, P. E.; Krska, S. W.; Maleczka, R. E.; Smith, M. R. *J. Am. Chem. Soc.* **2014**, *136*, 14345.
- (67) Wang, G.; Xu, L.; Li, P. *J. Am. Chem. Soc.* **2015**, *137*, 8058.
- (68) Ishiyama, T.; Isou, H.; Kikuchi, T.; Miyaura, N. *Chem Commun* **2010**, *46*, 159.
- (69) Kawamorita, S.; Ohmiya, H.; Hara, K.; Fukuoka, A.; Sawamura, M. *J. Am. Chem. Soc.* **2009**, *131*, 5058.
- (70) Miyaura, N. *Bull. Chem. Soc. Jpn.* **2008**, *81*, 1535.
- (71) Chotana, G. A.; Rak, M. A.; Smith, M. R. *J. Am. Chem. Soc.* **2005**, *127*, 10539.
- (72) Kuninobu, Y.; Ida, H.; Nishi, M.; Kanai, M. *Nat. Chem.* **2015**, *7*, 712.

- (73) Saito, Y.; Segawa, Y.; Itami, K. *J. Am. Chem. Soc.* **2015**, *137*, 5193.
- (74) Hammer, G.; Lübcke, T.; Kettner, R.; Pillarella, M. R.; Recknagel, H.; Commichau, A.; Neumann, H.-J.; Paczynska-Lahme, B. In *Ullmann's Encyclopedia of Industrial Chemistry*; Wiley-VCH Verlag GmbH & Co. KGaA, Ed.; Wiley-VCH Verlag GmbH & Co. KGaA: Weinheim, Germany, 2006.
- (75) Cavaliere, V. N.; Mindiola, D. J. *Chem. Sci.* **2012**, *3*, 3356.
- (76) Cook, A. K.; Schimler, S. D.; Matzger, A. J.; Sanford, M. S. *Science* **2016**, *351*, 1421.
- (77) Smith, K. T.; Berritt, S.; Gonzalez-Moreiras, M.; Ahn, S.; Smith, M. R.; Baik, M.-H.; Mindiola, D. J. *Science* **2016**, *351*, 1424.
- (78) Schmidt, R.; Griesbaum, K.; Behr, A.; Biedenkapp, D.; Voges, H.-W.; Garbe, D.; Paetz, C.; Collin, G.; Mayer, D.; Höke, H. In *Ullmann's Encyclopedia of Industrial Chemistry*; Wiley-VCH Verlag GmbH & Co. KGaA, Ed.; Wiley-VCH Verlag GmbH & Co. KGaA: Weinheim, Germany, 2014; pp 1–74.
- (79) Sanfilippo, D.; Rylander, P. N. In *Ullmann's Encyclopedia of Industrial Chemistry*; Wiley-VCH Verlag GmbH & Co. KGaA, Ed.; Wiley-VCH Verlag GmbH & Co. KGaA: Weinheim, Germany, 2009.
- (80) Choi, J.; MacArthur, A. H. R.; Brookhart, M.; Goldman, A. S. *Chem. Rev.* **2011**, *111*, 1761.
- (81) Dobereiner, G. E.; Crabtree, R. H. *Chem. Rev.* **2010**, *110*, 681.
- (82) Gupta, M.; Hagen, C.; Flesher, R. J.; Kaska, W. C.; Jensen, C. M. *Chem Commun* **1996**, No. 17, 2083.

- (83) Xu, W.; Rosini, G. P.; Krogh-Jespersen, K.; Goldman, A. S.; Gupta, M.; Jensen, C. M.; Kaska, W. C. *Chem. Commun.* **1997**, No. 23, 2273.
- (84) Jensen, C. M. *Chem. Commun.* **1999**, No. 24, 2443.
- (85) Liu, F.; Goldman, A. S. *Chem. Commun.* **1999**, No. 7, 655.
- (86) Zhu, K.; Achord, P. D.; Zhang, X.; Krogh-Jespersen, K.; Goldman, A. S. *J. Am. Chem. Soc.* **2004**, *126*, 13044.
- (87) Haenel, M. W.; Oevers, S.; Angermund, K.; Kaska, W. C.; Fan, H.-J.; Hall, M. B. *Angew. Chem. Int. Ed.* **2001**, *40*, 3596.
- (88) Romero, P. E.; Whited, M. T.; Grubbs, R. H. *Organometallics* **2008**, *27*, 3422.
- (89) Punji, B.; Emge, T. J.; Goldman, A. S. *Organometallics* **2010**, *29*, 2702.
- (90) Göttker-Schnetmann, I.; White, P.; Brookhart, M. *J. Am. Chem. Soc.* **2004**, *126*, 1804.
- (91) Morales-Morales, D.; Redón, R.; Yung, C.; Jensen, C. M. *Inorganica Chim. Acta* **2004**, *357*, 2953.
- (92) Werkmeister, S.; Neumann, J.; Junge, K.; Beller, M. *Chem. - Eur. J.* **2015**, *21*, 12226.
- (93) Azerraf, C.; Gelman, D. *Chem. - Eur. J.* **2008**, *14*, 10364.
- (94) Bézier, D.; Brookhart, M. *ACS Catal.* **2014**, *4*, 3411.
- (95) Gupta, M.; Kaska, W. C.; Jensen, C. M. *Chem. Commun.* **1997**, No. 5, 461.
- (96) Lyons, T. W.; Bézier, D.; Brookhart, M. *Organometallics* **2015**, *34*, 4058.
- (97) Yao, W.; Zhang, Y.; Jia, X.; Huang, Z. *Angew. Chem. Int. Ed.* **2014**, *53*, 1390.
- (98) Jia, X.; Huang, Z. *Nat. Chem.* **2016**, *8*, 157.

- (99) Tondreau, A. M.; Atienza, C. C. H.; Weller, K. J.; Nye, S. A.; Lewis, K. M.; Delis, J. G. P.; Chirik, P. J. *Science* **2012**, *335*, 567.
- (100) Kumar, A.; Zhou, T.; Emge, T. J.; Mironov, O.; Saxton, R. J.; Krogh-Jespersen, K.; Goldman, A. S. *J. Am. Chem. Soc.* **2015**, *137*, 9894.
- (101) Adams, J. J.; Lau, A.; Arulsamy, N.; Roddick, D. M. *Organometallics* **2011**, *30*, 689.
- (102) Ito, J.; Shiomi, T.; Nishiyama, H. *Adv. Synth. Catal.* **2006**, *348*, 1235.
- (103) Allen, K. E.; Heinekey, D. M.; Goldman, A. S.; Goldberg, K. I. *Organometallics* **2013**, *32*, 1579.
- (104) Tanoue, K.; Yamashita, M. *Organometallics* **2015**, *34*, 4011.
- (105) Goldman, A. S. *Science* **2006**, *312*, 257.
- (106) Haibach, M. C.; Kundu, S.; Brookhart, M.; Goldman, A. S. *Acc. Chem. Res.* **2012**, *45*, 947.
- (107) Bailey, B. C.; Schrock, R. R.; Kundu, S.; Goldman, A. S.; Huang, Z.; Brookhart, M. *Organometallics* **2009**, *28*, 355.
- (108) Ahuja, R.; Punji, B.; Findlater, M.; Supplee, C.; Schinski, W.; Brookhart, M.; Goldman, A. S. *Nat. Chem.* **2011**, *3*, 167.
- (109) Hartwig, J. *Organotransition Metal Chemistry: From Bonding to Catalysis*, 1 edition.; University Science Books: Sausalito, Calif, 2009.
- (110) van Leeuwen, P. W. N. M.; Chadwick, J. C. *Homogeneous Catalysts: Activity - Stability - Deactivation*; Wiley-VCH Verlag GmbH & Co. KGaA: Weinheim, Germany, 2011.

- (111) Douvris, C.; Michl, J. *Chem. Rev.* **2013**, *113*, PR179.
- (112) Krossing, I.; Raabe, I. *Angew. Chem. Int. Ed.* **2004**, *43*, 2066.
- (113) Yang, J.; Brookhart, M. *J. Am. Chem. Soc.* **2007**, *129*, 12656.
- (114) Reed, C. A. *Acc. Chem. Res.* **1998**, *31*, 325.
- (115) Reed, C. A. *Acc. Chem. Res.* **2010**, *43*, 121.
- (116) Strauss, S. H. *Chem. Rev.* **1993**, *93*, 927.
- (117) Krossing, I.; Reisinger, A. *Coord. Chem. Rev.* **2006**, *250*, 2721.
- (118) Ramírez-Contreras, R.; Bhuvanesh, N.; Zhou, J.; Ozerov, O. V. *Angew. Chem. Int. Ed.* **2013**, *52*, 10313.
- (119) Kato, T.; Reed, C. A. *Angew. Chem. Int. Ed.* **2004**, *43*, 2908.
- (120) Kim, K.-C.; Reed, C. A.; Elliott, D. W.; Mueller, L. J.; Tham, F.; Lin, L.; Lambert, J. B. *Science* **2002**, *297*, 825.
- (121) Duttwyler, S.; Douvris, C.; Fackler, N. L. P.; Tham, F. S.; Reed, C. A.; Baldrige, K. K.; Siegel, J. S. *Angew. Chem. Int. Ed.* **2010**, *49*, 7519.
- (122) Reed, C. A. *Chem. Commun.* **2005**, No. 13, 1669.
- (123) Kato, T.; Stoyanov, E.; Geier, J.; Grützmacher, H.; Reed, C. A. *J. Am. Chem. Soc.* **2004**, *126*, 12451.
- (124) Nava, M.; Stoyanova, I. V.; Cummings, S.; Stoyanov, E. S.; Reed, C. A. *Angew. Chem.* **2014**, *126*, 1149.
- (125) Stoyanov, E. S.; Hoffmann, S. P.; Juhasz, M.; Reed, C. A. *J. Am. Chem. Soc.* **2006**, *128*, 3160.
- (126) Schleyer, P. von R.; Najafian, K. *Inorg. Chem.* **1998**, *37*, 3454.

- (127) Douvris, C.; Ozerov, O. V. *Science* **2008**, *321*, 1188.
- (128) Douvris, C.; Nagaraja, C. M.; Chen, C.-H.; Foxman, B. M.; Ozerov, O. V. *J. Am. Chem. Soc.* **2010**, *132*, 4946.
- (129) Allemann, O.; Duttwyler, S.; Romanato, P.; Baldrige, K. K.; Siegel, J. S. *Science* **2011**, *332*, 574.
- (130) Nava, M. J.; Reed, C. A. *Inorg. Chem.* **2010**, *49*, 4726.
- (131) Ramírez-Contreras, R.; Ozerov, O. V. *Dalton Trans* **2012**, *41*, 7842.
- (132) Estrada, J.; Woen, D. H.; Tham, F. S.; Miyake, G. M.; Lavallo, V. *Inorg. Chem.* **2015**, *54*, 5142.
- (133) El-Hellani, A.; Kefalidis, C. E.; Tham, F. S.; Maron, L.; Lavallo, V. *Organometallics* **2013**, *32*, 6887.
- (134) Lavallo, V.; Wright, J. H.; Tham, F. S.; Quinlivan, S. *Angew. Chem. Int. Ed.* **2013**, *52*, 3172.
- (135) El-Hellani, A.; Lavallo, V. *Angew. Chem. Int. Ed.* **2014**, *53*, 4489.
- (136) King, B. T.; Noll, B. C.; McKinley, A. J.; Michl, J. *J. Am. Chem. Soc.* **1996**, *118*, 10902.
- (137) Valášek, M.; Štursa, J.; Pohl, R.; Michl, J. *Inorg. Chem.* **2010**, *49*, 10255.
- (138) In *Inorganic Syntheses*; Rauchfuss, T. B., Ed.; John Wiley & Sons, Inc.: Hoboken, NJ, USA, 2010; pp 56–66.
- (139) King, B. T.; Körbe, S.; Schreiber, P. J.; Clayton, J.; Němcová, A.; Havlas, Z.; Vyakaranam, K.; Fete, M. G.; Zharov, I.; Ceremuga, J.; Michl, J. *J. Am. Chem. Soc.* **2007**, *129*, 12960.

- (140) Zharov, I.; Havlas, Z.; Orendt, A. M.; Barich, D. H.; Grant, D. M.; Fete, M. G.; Michl, J. *J. Am. Chem. Soc.* **2006**, *128*, 6089.
- (141) Valášek, M.; Štursa, J.; Pohl, R.; Michl, J. *Inorg. Chem.* **2010**, *49*, 10247.
- (142) Gu, W.; McCulloch, B. J.; Reibenspies, J. H.; Ozerov, O. V. *Chem. Commun.* **2010**, *46*, 2820.
- (143) Fang, H.; Choe, Y.-K.; Li, Y.; Shimada, S. *Chem. – Asian J.* **2011**, *6*, 2512.
- (144) Brück, A.; Gallego, D.; Wang, W.; Irran, E.; Driess, M.; Hartwig, J. F. *Angew. Chem. Int. Ed.* **2012**, *51*, 11478.
- (145) Palmer, W. N.; Obligacion, J. V.; Pappas, I.; Chirik, P. J. *J. Am. Chem. Soc.* **2016**, *138*, 766.
- (146) Anaby, A.; Butschke, B.; Ben-David, Y.; Shimon, L. J. W.; Leitius, G.; Feller, M.; Milstein, D. *Organometallics* **2014**, *33*, 3716.
- (147) Lee, C.-I.; Zhou, J.; Ozerov, O. V. *J. Am. Chem. Soc.* **2013**, *135*, 3560.
- (148) Lee, C.-I.; DeMott, J. C.; Pell, C. J.; Christopher, A.; Zhou, J.; Bhuvanesh, N.; Ozerov, O. V. *Chem. Sci.* **2015**, *6*, 6572.
- (149) Pell, C. J.; Ozerov, O. V. *Inorg Chem Front* **2015**, *2*, 720.
- (150) Timpa, S. D.; Fafard, C. M.; Herbert, D. E.; Ozerov, O. V. *Dalton Trans.* **2011**, *40*, 5426.
- (151) Pell, C. J.; Ozerov, O. V. *ACS Catal.* **2014**, *4*, 3470.
- (152) Mucha, N. T.; Waterman, R. *Organometallics* **2015**, *34*, 3865.
- (153) Mucha, N. T.; Waterman, R. *Organometallics* **2015**, *34*, 5682.

- (154) Arunachalampillai, A.; Olsson, D.; Wendt, O. F. *Dalton Trans.* **2009**, No. 40, 8626.
- (155) Farrugia, L. J. *J. Appl. Crystallogr.* **1997**, *30*, 565.
- (156) Lyons, T. W.; Guironnet, D.; Findlater, M.; Brookhart, M. *J. Am. Chem. Soc.* **2012**, *134*, 15708.
- (157) Cho, J.-Y.; Iverson, C. N.; Smith, M. R. *J. Am. Chem. Soc.* **2000**, *122*, 12868.
- (158) Ishiyama, T.; Ishida, K.; Takagi, J.; Miyaura, N. *Chem. Lett.* **2001**, No. 11, 1082.
- (159) Boebel, T. A.; Hartwig, J. F. *Organometallics* **2008**, *27*, 6013.
- (160) Larsen, M. A.; Wilson, C. V.; Hartwig, J. F. *J. Am. Chem. Soc.* **2015**, *137*, 8633.
- (161) Ishiyama, T.; Takagi, J.; Hartwig, J. F.; Miyaura, N. *Angew. Chem. Int. Ed.* **2002**, *41*, 3056.
- (162) Göttker-Schnetmann, I.; White, P. S.; Brookhart, M. *Organometallics* **2004**, *23*, 1766.
- (163) Kanzelberger, M.; Singh, B.; Czerw, M.; Krogh-Jespersen, K.; Goldman, A. S. *J. Am. Chem. Soc.* **2000**, *122*, 11017.
- (164) Zhu, Y.; Smith, D. A.; Herbert, D. E.; Gatard, S.; Ozerov, O. V. *Chem. Commun.* **2011**, *48*, 218.
- (165) Clot, E.; Mégret, C.; Eisenstein, O.; Perutz, R. N. *J. Am. Chem. Soc.* **2009**, *131*, 7817.
- (166) Hebden, T. J.; Denney, M. C.; Pons, V.; Piccoli, P. M. B.; Koetzle, T. F.; Schultz, A. J.; Kaminsky, W.; Goldberg, K. I.; Heinekey, D. M. *J. Am. Chem. Soc.* **2008**, *130*, 10812.

- (167) Kleeberg, C.; Crawford, A. G.; Batsanov, A. S.; Hodgkinson, P.; Apperley, D. C.; Cheung, M. S.; Lin, Z.; Marder, T. B. *J. Org. Chem.* **2012**, *77*, 785.
- (168) Göttker-Schnetmann, I.; Heinekey, D. M.; Brookhart, M. *J. Am. Chem. Soc.* **2006**, *128*, 17114.
- (169) Bose, S. K.; Deißberger, A.; Eichhorn, A.; Steel, P. G.; Lin, Z.; Marder, T. B. *Angew. Chem. Int. Ed.* **2015**, *54*, 11843.
- (170) Herde, J. L.; Lambert, J. C.; Senoff, C. V.; Cushing, M. A. In *Inorganic Syntheses*; Parshall, G. W., Ed.; John Wiley & Sons, Inc.: Hoboken, NJ, USA, 2007; pp 18–20.
- (171) Kelley, M. R.; Rohde, J.-U. *Dalton Trans.* **2013**, *43*, 527.
- (172) Fulmer, G. R.; Miller, A. J. M.; Sherden, N. H.; Gottlieb, H. E.; Nudelman, A.; Stoltz, B. M.; Bercaw, J. E.; Goldberg, K. I. *Organometallics* **2010**, *29*, 2176.
- (173) Morales-Morales, D.; Grause, C.; Kasaoka, K.; Redón, R.; Cramer, R. E.; Jensen, C. M. *Inorganica Chim. Acta* **2000**, *300–302*, 958.
- (174) Vabre, B.; Spasyuk, D. M.; Zargarian, D. *Organometallics* **2012**, *31*, 8561.
- (175) Bedford, R. B.; Betham, M.; Blake, M. E.; Coles, S. J.; Draper, S. M.; Hursthouse, M. B.; Scully, P. N. *Inorganica Chim. Acta* **2006**, *359*, 1870.
- (176) Takaya, J.; Ito, S.; Nomoto, H.; Saito, N.; Kirai, N.; Iwasawa, N. *Chem. Commun.* **2015**, *51*, 17662.
- (177) Hoffman, B. M.; Lukoyanov, D.; Yang, Z.-Y.; Dean, D. R.; Seefeldt, L. C. *Chem. Rev.* **2014**, *114*, 4041.

- (178) Appl, M. In *Ullmann's Encyclopedia of Industrial Chemistry*; Wiley-VCH Verlag GmbH & Co. KGaA, 2000.
- (179) Kaneko, T.; Derbyshire, F.; Makino, E.; Gray, D.; Tamura, M.; Li, K. In *Ullmann's Encyclopedia of Industrial Chemistry*; Wiley-VCH Verlag GmbH & Co. KGaA, 2000.
- (180) Bahrmann, H.; Bach, H.; Frey, G. D. In *Ullmann's Encyclopedia of Industrial Chemistry*; Wiley-VCH Verlag GmbH & Co. KGaA, 2000.
- (181) Aresta, M.; Dibenedetto, A.; Angelini, A. *Chem. Rev.* **2014**, *114*, 1709.
- (182) Laitar, D. S.; Müller, P.; Sadighi, J. P. *J. Am. Chem. Soc.* **2005**, *127*, 17196.
- (183) Palit, C. M.; Graham, D. J.; Chen, C.-H.; Foxman, B. M.; Ozerov, O. V. *Chem. Commun.* **2014**, *50*, 12840.
- (184) Scheuermann, M. L.; Semproni, S. P.; Pappas, I.; Chirik, P. J. *Inorg. Chem.* **2014**, *53*, 9463.
- (185) Ríos, P.; Curado, N.; López-Serrano, J.; Rodríguez, A. *Chem Commun* **2016**, *52*, 2114.
- (186) Courtemanche, M.-A.; Légaré, M.-A.; Maron, L.; Fontaine, F.-G. *J. Am. Chem. Soc.* **2013**, *135*, 9326.
- (187) Chen, J.; Falivene, L.; Caporaso, L.; Cavallo, L.; Chen, E. Y.-X. *J. Am. Chem. Soc.* **2016**, *138*, 5321.
- (188) Tanaka, R.; Yamashita, M.; Nozaki, K. *J. Am. Chem. Soc.* **2009**, *131*, 14168.
- (189) Yang, J.; White, P. S.; Brookhart, M. *J. Am. Chem. Soc.* **2008**, *130*, 17509.
- (190) Park, S.; Bézier, D.; Brookhart, M. *J. Am. Chem. Soc.* **2012**, *134*, 11404.

- (191) Cheng, C.; Brookhart, M. *J. Am. Chem. Soc.* **2012**, *134*, 11304.
- (192) Park, S.; Brookhart, M. *J. Am. Chem. Soc.* **2012**, *134*, 640.
- (193) Park, S.; Kim, B. G.; Göttker-Schnetmann, I.; Brookhart, M. *ACS Catal.* **2012**, *2*, 307.
- (194) Park, S.; Brookhart, M. *Organometallics* **2010**, *29*, 6057.
- (195) Haibach, M. C.; Guan, C.; Wang, D. Y.; Li, B.; Lease, N.; Steffens, A. M.; Krogh-Jespersen, K.; Goldman, A. S. *J. Am. Chem. Soc.* **2013**, *135*, 15062.
- (196) Ahmed Foskey, T. J.; Heinekey, D. M.; Goldberg, K. I. *ACS Catal.* **2012**, *2*, 1285.
- (197) Lao, D. B.; Owens, A. C. E.; Heinekey, D. M.; Goldberg, K. I. *ACS Catal.* **2013**, *3*, 2391.
- (198) Kundu, S.; Choliy, Y.; Zhuo, G.; Ahuja, R.; Emge, T. J.; Warmuth, R.; Brookhart, M.; Krogh-Jespersen, K.; Goldman, A. S. *Organometallics* **2009**, *28*, 5432.
- (199) Nawara-Hultzsich, A. J.; Hackenberg, J. D.; Punji, B.; Supplee, C.; Emge, T. J.; Bailey, B. C.; Schrock, R. R.; Brookhart, M.; Goldman, A. S. *ACS Catal.* **2013**, *3*, 2505.
- (200) Goldberg, J. M.; Wong, G. W.; Brastow, K. E.; Kaminsky, W.; Goldberg, K. I.; Heinekey, D. M. *Organometallics* **2015**, *34*, 753.
- (201) Huang, Z.; White, P. S.; Brookhart, M. *Nature* **2010**, *465*, 598.
- (202) Dang, L.; Lin, Z.; Marder, T. B. *Chem. Commun.* **2009**, No. 27, 3987.
- (203) Burgess, K.; Ohlmeyer, M. J. *Chem. Rev.* **1991**, *91*, 1179.

- (204) *Contemporary Metal Boron Chemistry I*; Marder, T. B., Lin, Z., Eds.; Structure and Bonding; Springer Berlin Heidelberg: Berlin, Heidelberg, 2008; Vol. 130.
- (205) Toribatake, K.; Nishiyama, H. *Angew. Chem. Int. Ed.* **2013**, *52*, 11011.
- (206) Lee, C.-I.; Shih, W.-C.; Zhou, J.; Reibenspies, J. H.; Ozerov, O. V. *Angew. Chem. Int. Ed.* **2015**, *54*, 14003.
- (207) Zhang, X.; Wang, D. Y.; Emge, T. J.; Goldman, A. S. *Inorganica Chim. Acta* **2011**, *369*, 253.
- (208) Zhang, X.; Kanzelberger, M.; Emge, T. J.; Goldman, A. S. *J. Am. Chem. Soc.* **2004**, *126*, 13192.
- (209) Fan, L.; Parkin, S.; Ozerov, O. V. *J. Am. Chem. Soc.* **2005**, *127*, 16772.
- (210) Puri, M.; Gatard, S.; Smith, D. A.; Ozerov, O. V. *Organometallics* **2011**, *30*, 2472.
- (211) Sadler, S. A.; Tajuddin, H.; Mkhaliid, I. A. I.; Batsanov, A. S.; Albesa-Jove, D.; Cheung, M. S.; Maxwell, A. C.; Shukla, L.; Roberts, B.; Blakemore, D. C.; Lin, Z.; Marder, T. B.; Steel, P. G. *Org. Biomol. Chem.* **2014**, *12*, 7318.
- (212) Braunschweig, H.; Guethlein, F.; Mailänder, L.; Marder, T. B. *Chem. – Eur. J.* **2013**, *19*, 14831.
- (213) Wei, C. S.; Jiménez-Hoyos, C. A.; Videa, M. F.; Hartwig, J. F.; Hall, M. B. *J. Am. Chem. Soc.* **2010**, *132*, 3078.
- (214) Bontemps, S.; Vendier, L.; Sabo-Etienne, S. *Angew. Chem. Int. Ed.* **2012**, *51*, 1671.
- (215) Abu Ali, H.; Goldberg, I.; Srebnik, M. *Organometallics* **2001**, *20*, 3962.

- (216) Arrowsmith, M.; Hadlington, T. J.; Hill, M. S.; Kociok-Köhn, G. *Chem. Commun.* **2012**, 48, 4567.
- (217) Creutz, C.; Taube, H. *J. Am. Chem. Soc.* **1969**, 91, 3988.
- (218) Henry Taube - Nobel Lecture: Electron Transfer between Metal Complexes - Retrospective
http://www.nobelprize.org/nobel_prizes/chemistry/laureates/1983/taube-lecture.html (accessed May 6, 2016).
- (219) Buchanan, R. M.; Mashuta, M. S.; Oberhausen, K. J.; Richardson, J. F.; Li, Q.; Hendrickson, D. N. *J. Am. Chem. Soc.* **1989**, 111, 4497.
- (220) Lu, Y.; Yeung, N.; Sieracki, N.; Marshall, N. M. *Nature* **2009**, 460, 855.
- (221) Casey, C. P.; Audett, J. D. *Chem. Rev.* **1986**, 86, 339.
- (222) D'Elia, V.; Dong, H.; Rossini, A. J.; Widdifield, C. M.; Vummaleti, S. V. C.; Minenkov, Y.; Poater, A.; Abou-Hamad, E.; Pelletier, J. D. A.; Cavallo, L.; Emsley, L.; Basset, J.-M. *J. Am. Chem. Soc.* **2015**, 137, 7728.
- (223) Mankad, N. P. *Chem. – Eur. J.* **2016**, 22, 5822.
- (224) Dupont, J.; Consorti, C. S.; Spencer, J. In *The Chemistry of Pincer Compounds*; Elsevier, 2007; pp 1–24.
- (225) Herbert, D. E.; Ozerov, O. V. *Organometallics* **2011**, 30, 6641.
- (226) Gagliardo, M.; Selander, N.; Mehendale, N. C.; van Koten, G.; Klein Gebbink, R. J. M.; Szabó, K. J. *Chem. – Eur. J.* **2008**, 14, 4800.
- (227) Li, J.; Siegler, M.; Lutz, M.; Spek, A. L.; Klein Gebbink, R. J. M.; van Koten, G. *Adv. Synth. Catal.* **2010**, 352, 2474.

- (228) Breschi, M. C.; Calderone, V.; Digiacomo, M.; Macchia, M.; Martelli, A.; Martinotti, E.; Minutolo, F.; Rapposelli, S.; Rossello, A.; Testai, L.; Balsamo, A. *J. Med. Chem.* **2006**, *49*, 2628.
- (229) Chakraborty, S.; Krause, J. A.; Guan, H. *Organometallics* **2009**, *28*, 582.
- (230) Polukeev, A. V.; Kuklin, S. A.; Petrovskii, P. V.; Peregudova, S. M.; Smol'yakov, A. F.; Dolgushin, F. M.; Koridze, A. A. *Dalton Trans.* **2011**, *40*, 7201.
- (231) Titova, E. M.; Silant'ev, G. A.; Filippov, O. A.; Gulyaeva, E. S.; Gutsul, E. I.; Dolgushin, F. M.; Belkova, N. V. *Eur. J. Inorg. Chem.* **2016**, *2016*, 56.
- (232) APEX2; Bruker AXS Inc.: Madison, WI, 2013.
- (233) SADABS; Bruker AXS Inc.: Madison, WI, 2008.
- (234) Sheldrick, G. M. *Acta Crystallogr. Sect. A* **2015**, *71*, 3.
- (235) Sheldrick, G. M. *Acta Crystallogr. Sect. C* **2015**, *71*, 3.
- (236) Spek, A. L. *J. Appl. Crystallogr.* **2003**, *36*, 7.
- (237) Hübschle, C. B.; Sheldrick, G. M.; Dittrich, B. *J. Appl. Crystallogr.* **2011**, *44*, 1281.
- (238) Sheldrick, G. M. *Acta Crystallogr. Sect. A* **2008**, *64*, 112.
- (239) Romerosa, A. M. *Thermochim. Acta* **1993**, *217*, 123.
- (240) Xie, Z.; Tsang, C.-W.; Sze, E. T.-P.; Yang, Q.; Chan, D. T. W.; Mak, T. C. W. *Inorg. Chem.* **1998**, *37*, 6444.
- (241) Juhasz, M.; Hoffmann, S.; Stoyanov, E.; Kim, K.-C.; Reed, C. A. *Angew. Chem. Int. Ed.* **2004**, *43*, 5352.

- (242) Bondarev, O.; Sevryugina, Y. V.; Jalisatgi, S. S.; Hawthorne, M. F. *Inorg. Chem.* **2012**, *51*, 9935.
- (243) Hawthorne, M. F.; Mavunkal, I. J.; Knobler, C. B. *J. Am. Chem. Soc.* **1992**, *114*, 4427.
- (244) Berkeley, E. R.; Ewing, W. C.; Carroll, P. J.; Sneddon, L. G. *Inorg. Chem.* **2014**, *53*, 5348.
- (245) Lomme, P.; Roth, M.; Englert, U.; Paetzold, P. *Chem. Ber.* **1996**, *129*, 1227.
- (246) Douvris, C.; Stoyanov, E. S.; Tham, F. S.; Reed, C. A. *Chem. Commun.* **2007**, No. 11, 1145.
- (247) Douvris, C.; Reed, C. A. *Organometallics* **2008**, *27*, 807.
- (248) Hoffmann, S. P.; Kato, T.; Tham, F. S.; Reed, C. A. *Chem. Commun.* **2006**, No. 7, 767.
- (249) Nava, M.; Reed, C. A. *Organometallics* **2011**, *30*, 4798.
- (250) Connelly, S. J.; Kaminsky, W.; Heinekey, D. M. *Organometallics* **2013**, *32*, 7478.
- (251) Volkis, V.; Douvris, C.; Michl, J. *J. Am. Chem. Soc.* **2011**, *133*, 7801.
- (252) Schulz, A.; Thomas, J.; Villinger, A. *Chem. Commun.* **2010**, *46*, 3696.
- (253) Driess, M.; Barmeyer, R.; Monsé, C.; Merz, K. *Angew. Chem. Int. Ed.* **2001**, *40*, 2308.
- (254) Lerner, H.W.; Bolte, M.; Noth, H.; Knizek, J. *Z Naturforsch B J Chem Sci* **2002**, *57*, 177.
- (255) Lambert, J. B.; Zhang, S. *J. Chem. Soc. Chem. Commun.* **1993**, No. 4, 383.

- (256) Ogo, S.; Takebe, Y.; Uehara, K.; Yamazaki, T.; Nakai, H.; Watanabe, Y.; Fukuzumi, S. *Organometallics* **2006**, *25*, 331.
- (257) Sun, W.-C.; Gee, K. R.; Klaubert, D. H.; Haugland, R. P. *J. Org. Chem.* **1997**, *62*, 6469.
- (258) Drew, D.; Doyle, J. R.; Shaver, A. G. In *Inorganic Syntheses*; Angelici, R. J., Ed.; John Wiley & Sons, Inc.: Hoboken, NJ, USA, 1990; Vol. 28, pp 346–349.
- (259) *Isotope Distribution Calculator and Mass Spec Plotter*, <http://www.sisweb.com/mstools/isotope.htm>, (accessed July 2015).
- (260) Forbus, T. R.; Martin, J. C. *J. Org. Chem.* **1979**, *44*, 313.
- (261) Forbus, T. R.; Taylor, S. L.; Martin, J. C. *J. Org. Chem.* **1987**, *52*, 4156.
- (262) Hollis, T. K.; Bosnich, B. *J. Am. Chem. Soc.* **1995**, *117*, 4570.
- (263) Altomare, A.; Cascarano, G.; Giacovazzo, C.; Guagliardi, A.; Burla, M. C.; Polidori, G.; Camalli, M. *J. Appl. Crystallogr.* **1994**, *27*, 435.
- (264) Betteridge, P. W.; Carruthers, J. R.; Cooper, R. I.; Prout, K.; Watkin, D. J. *J. Appl. Crystallogr.* **2003**, *36*, 1487.
- (265) Cheng, C.; Hartwig, J. F. *Chem. Rev.* **2015**, *115*, 8946.